

Development and application of a SWAT hydropower routine for flow, sediment, and energy management

By

Jayandra Prasad Shrestha

A Thesis Submitted to the Department of Civil and
Natural Resources Engineering, University of Canterbury,
Christchurch, New Zealand

In Partial Fulfilment of the Requirements for the Degree
of Doctor of Philosophy in Civil Engineering

August 2021

ACKNOWLEDGEMENTS

At the very first, I would like to thank the Goddess Saraswati for providing me blessings, courage, and means throughout the journey of my PhD.

I sincerely acknowledge my senior supervisor, Dr. Markus Pahlow, for giving me the opportunity to venture into this work and for his incredibly valuable mentorship and guidance to successfully complete this thesis. Furthermore, I would like to extend my thanks and gratitude to my co-supervisor Prof. Dr. Thomas A. Cochrane for his constructive and encouraging suggestions, regarding the research and leading me towards the goal of the thesis. Both supervisors have always encouraged me to carry out the research fairly. I thank them for spending time to meticulously reviewing my manuscripts and providing insightful and valuable feedbacks. Their down-to-earth nature and motivating words have allowed me to sail through the difficult phases.

I would like to thank the University of Canterbury, New Zealand, for providing financial support to conduct this research through the College of Engineering PhD Scholarship. I would also like to thank all the technical and administrative staffs and members of the Hydro-Eco Group at the Department of Civil and Natural Resources Engineering. Again, I would like to thank Olive Dalton, System Manager for her support for providing the necessary softwares, a laptop, and quick solutions to IT-related problems.

I would like to thank my PhD fellows, especially Anh Nguyen, with whom I shared the moments of joy and woe. I also take this opportunity to thank a former PhD fellow, Dr. Bikesh Shrestha, for providing me all the input data and the calibrated SWAT model.

Special thanks to Dr. Narayan K. Shrestha, an old fellow of mine, who has been very helpful during my learning stage of SWAT software and his expertise in handling this tool and in-depth knowledge of hydrology has been vital in various stages of my research work.

I am very happy to acknowledge Dr. Netra Timalina and Dr. Ram Acharya for their suggestion and encouragement to initiate this study.

I would also have high sense of appreciation to my Nepali friends and families in Christchurch for creating homely atmosphere in New Zealand.

I am very grateful to my family members, especially my brothers and sister, for their inspiration and blessing during my PhD. I am grateful to my wife Manisha who is part of this journey from the beginning to the end. Her love and constant encouragement made this journey easier and enjoyable. I would like to express my gratitude to my brothers Niroj and Bijendra and bhauju Sanita for their support and cooperation towards my household responsibilities in my absence.

Last but not least; I would like to dedicate this thesis to my beloved parents late Narayan and Indira. I am always grateful for their blessings.

Jayandra Prasad Shrestha
(जयन्द्र प्रसाद श्रेष्ठ)

ABSTRACT

Current assessment of hydropower reservoir management entails three key steps: flow and sediment estimation with a hydrological model (e.g. SWAT - Soil and Water Assessment Tool), reservoir operation modelling (e.g. HEC-ResSim - Hydrologic Engineering Center Reservoir System Simulation) and sediment management modelling (e.g. SedSim - Sediment Simulation Screening). This approach, however, is time-consuming to set up and leads to challenges regarding simulating the impacts of interrelated processes such as climatic conditions, land use changes and operational policies on the flows, sediment and hydropower production. Moreover, multiple reservoirs in a catchment and their dependencies add complexity to flow and sediment management. Therefore, a single model that can simulate hydrological processes, reservoir operations and sediment management at the river basin scale is warranted. Hence, the main objectives of this study are: 1) to develop and evaluate a hydropower reservoir operation routine for the spatially distributed physically-based SWAT hydrological model; 2) to develop and evaluate a sediment management routine for SWAT; 3) to assess the impacts of climate change and reservoir operational policies on hydropower production and downstream flow regime; and 4) to assess reservoir sedimentation and to develop a better understanding of sediment management in a complex reservoir system.

A new SWAT modelling routine called Reservoir Operation and Sediment Management (ROSMAN), was developed that has two sub-routines, HYDropower Reservoir Operations Routine (HydROR) and REServoir Sediment MANagement routine (ResSMan). HydROR simulates hydropower reservoir operations under imposed operational policies. It was successfully validated in a case study comparison with HEC-ResSim, where $R^2 > 0.99$ for outflow, power generation and water level. Similarly, ResSMan has functions to estimate sediment accumulation in multi-reservoir systems, and its impacts on the storage capacity and

hydropower production under user-specified operational policies. It allows to compute the restoration of storage capacity due to the removal of sediment by flushing and sluicing. ResSMan was validated through a comparison with the SedSim model, with R^2 values exceeding 0.99 for simulations including flushing and sluicing.

The developed routine was applied in the 3S basin (Sekong, Sesan and Srepok river basins) of the lower Mekong. The Mekong basin is one of the biodiversity hotspots in the world, yet hydropower reservoirs are being planned and developed at a rapid pace. HydrOR was applied to assess hydrological alterations due to the combined impacts of climate change and reservoir operations of 38 hydropower dams in the 3S basin. Hydropower production will vary from -1.6% to 2.3% under different climate change scenarios. Hydropower production will decrease up to 13% if the operational policy changes from maximizing energy production to maintaining ecological flows. The calculation of hydrological alteration indices revealed that the natural flow regime at the 3S basin outlet could be altered by more than 113% due to the combined impacts of climate change and reservoir operations. Alterations were significant within the basin, and, as expected, were larger for high-head and small-river reservoirs. These alterations will adversely affect ecological dynamics, in particular, habitat availability.

Subsequently, ResSMan was applied to assess and manage reservoir sedimentation in a complex system of 19 reservoirs in the Sesan and Srepok (2S) basin for the time period 2021-2120. The unregulated mean annual sediment yield at the outlet of the 2S basin was estimated as 7.24 million tonnes/year (Mt/y) and it will be reduced to 0.11 Mt/y due to the operation of the 19 reservoirs. In total 924 Mt of sediment will accumulate in these 19 reservoirs over 100 years, resulting in an average trapping efficiency of 74% (ranging from 11% to 97%). System-wide sediment management coordination simulations demonstrated that bi-annually and 5-

yearly flushing of alternate reservoirs are effective options for efficiently releasing sediment in the 2S basin.

ROSMAN expands the functionalities of SWAT to allow for comprehensive assessment of the operation of complex reservoir systems under land use and climate change. In this study, the new tool helped to improve the scientific understanding of the impact of individual reservoirs and complex reservoir systems on the hydrologic and sediment regimes in the 3S basin. The development and implementation of ROSMAN in SWAT provide new opportunities for decision-makers to make better informed decisions regarding the planning of future hydropower reservoirs, the optimisation of their integration in reservoir systems and long-term sustainable management.

Deputy Vice-Chancellor's Office
Postgraduate Research Office

Co-Authorship Form

This form is to accompany the submission of any thesis that contains research reported in co-authored work that has been published, accepted for publication, or submitted for publication. A copy of this form should be included for each co-authored work that is included in the thesis. Completed forms should be included at the front (after the thesis abstract) of each copy of the thesis submitted for examination and library deposit.

Please indicate the chapter/section/pages of this thesis that are extracted from co-authored work and provide details of the publication or submission from the extract comes:

Chapter 2:

Shrestha, J. P., Pahlow, M., and Cochrane, T. A. (2020). "Development of a SWAT Hydropower Operation Routine and Its Application to Assessing Hydrological Alterations in the Mekong." Water, 12(8), 2193.

Shrestha, J. P., Pahlow, M., and Cochrane, T. A. (under review). "Managing Reservoir Sedimentation through Coordinated Operation of Transboundary Reservoirs in the Mekong." Manuscript submitted for publication to Journal of Hydro-environment Research and under review.

Chapter 3:

Shrestha, J. P., Pahlow, M., and Cochrane, T. A. (2020). "Development of a SWAT Hydropower Operation Routine and Its Application to Assessing Hydrological Alterations in the Mekong." Water, 12(8), 2193.

Chapter 4:

Shrestha, J. P., Pahlow, M., and Cochrane, T. A. (under review). "Managing Reservoir Sedimentation through Coordinated Operation of Transboundary Reservoirs in the Mekong." Manuscript submitted for publication to Journal of Hydro-environment Research and under review.

Please detail the nature and extent (%) of contribution by the candidate:

The candidate developed methodologies (80%), data analyses (100%), carried out model simulations (100%), and led manuscripts' writing (80%). Overall, the candidate's contribution was 90%. Co-authors were involved mainly in developing methodologies and proofreading manuscripts.

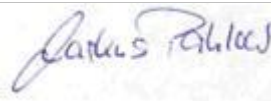
Certification by Co-authors:

If there is more than one co-author then a single co-author can sign on behalf of all

The undersigned certifies that:

- The above statement correctly reflects the nature and extent of the Doctoral candidate's contribution to this co-authored work
- In cases where the candidate was the lead author of the co-authored work he or she wrote the text

Name: *Markus Pahlow* Signature:



Date: *22 February 2021*

ACRONYM

| | |
|----------------|---|
| 2S | Sesan and Srepok |
| 3S | Sekong, Sesan and Srepok |
| AET | Actual Evapotranspiration |
| ASCII | American Standard Code for International Interchange |
| BOOT | Build, Own, Operate and Transfer |
| DEM | Digital Elevation Model |
| FSL | Full Supply Level |
| GCM | General Circulation Model |
| GFDL | Geophysical Fluid Dynamics Laboratory Climate model |
| GISS | Goddard Institute for Space Studies Model |
| HA | Hydrological Alteration |
| HEC-ResSim | Hydrological Engineering Center Reservoir Simulation Model |
| HydROR | Hydropower Reservoir Operation Routine |
| ICOLD | International Commission on Large Dams |
| IHA | Indicators of Hydrological Alternation |
| IPCC | Intergovernmental Panel on Climate Change |
| IPSL | Institute Pierre-Simon Laplace Coupled Model |
| LSP 3 | Lower Srepok 3 |
| LSP 4 | Lower Srepok 4 |
| LSS 2 | Lower Sesan 2 + Lower Srepok |
| LSS 3 | Lower Sesan 3 |
| m.a.s.l | meters above sea level |
| MOL | Minimum Operating Level |
| MRC | Mekong River Commission |
| Mt | Million metric tonne |
| MUSLE | Modified Universal Soil Loss Equation |
| NSE | Nash Sutcliffe Efficiency |
| PBIAS | Percent Bias |
| PERC | Percolation from upper zone to lower zone |
| PET | Potential Evapotranspiration |
| R ² | Correlation coefficient |
| RCP | Representative Concentration Pathways |
| RESCON | REServoir CONservation model |
| ResSMan | REServoir Sediment MANagement Routine |
| ROSMAN | Reservoir Operation and Sediment MANagement Routine |
| RSR | Ratio of Standard deviation of Observations to Root Mean Square Error |
| SedSim | Sediment Simulation Screening model |
| SP 3 | Srepok 3 |
| SP 4 | Srepok 4 |
| SS 3 | Sesan 3 |

| | |
|-------|--------------------------------------|
| SS 3A | Sesan 3A |
| SS 4 | Sesan 4 |
| SS 4A | Sesan 4A |
| SV | Seasonal Variation |
| SWAT | Soil and Water Assessment Tool |
| TE | Trap efficiency |
| USLE | Universal Soil Loss Equation |
| VIC | Variable Infiltration Capacity |
| WEAP | Water Evaluation and Planning System |
| WRAP | Water Rights Analysis Package |

TABLE OF CONTENTS

| | |
|---|-------------|
| ACKNOWLEDGEMENTS..... | I |
| ABSTRACT | III |
| ACRONYM..... | VIII |
| TABLE OF CONTENTS..... | X |
| LIST OF FIGURES | XIII |
| LIST OF TABLES | XVI |
| CHAPTER 1. INTRODUCTION | 1-1 |
| 1.1 BACKGROUND | 1-1 |
| 1.2 PROBLEM STATEMENT AND OBJECTIVES | 1-4 |
| 1.3 LITERATURE REVIEW | 1-7 |
| 1.3.1 Reservoir sedimentation..... | 1-7 |
| 1.3.2 Reservoir sediment management techniques..... | 1-8 |
| 1.3.3 Reservoir operation..... | 1-15 |
| 1.3.4 Climate change..... | 1-17 |
| 1.3.5 Land use/land cover (LULC) change | 1-18 |
| 1.3.6 Hydrological models | 1-19 |
| 1.3.7 Reservoir simulation models | 1-23 |
| 1.3.8 Reservoir sediment management models | 1-25 |
| 1.3.9 Summary of literature review | 1-26 |
| 1.4 THESIS OUTLINE | 1-27 |
| 1.5 REFERENCES | 1-28 |
| CHAPTER 2. DEVELOPMENT OF A SWAT HYDROPOWER ROUTINE | 2-1 |
| 2.1 INTRODUCTION..... | 2-1 |
| 2.1 METHODOLOGY..... | 2-3 |
| 2.1.1 SWAT Model..... | 2-3 |
| 2.1.2 Reservoir Operation and Sediment Management (ROSMAN) routine | 2-6 |
| 2.1.3 Hydropower Reservoir Operation Routine (HydROR) | 2-7 |
| 2.1.4 Evaluation of the HydROR..... | 2-10 |

| | | |
|--|---|------------|
| 2.1.5 | <i>SWAT with HydROR and HEC-ResSim Model Simulation</i> | 2-11 |
| 2.1.6 | <i>Performance Criteria</i> | 2-12 |
| 2.1.7 | <i>Reservoir Sediment Management routine (ResSMan)</i> | 2-13 |
| 2.1.8 | <i>Evaluation of the ResSMan</i> | 2-19 |
| 2.2 | RESULTS AND DISCUSSIONS | 2-20 |
| 2.2.1 | <i>Performance of HydROR</i> | 2-20 |
| 2.2.2 | <i>Performance of the ResSMan</i> | 2-23 |
| 2.3 | CONCLUSIONS | 2-25 |
| 2.4 | REFERENCES | 2-27 |
| CHAPTER 3. APPLICATION OF THE HYDROR TO ASSESSING | | |
| HYDROLOGICAL ALTERATIONS | | 3-1 |
| 3.1 | INTRODUCTION..... | 3-1 |
| 3.2 | METHODOLOGY..... | 3-2 |
| 3.2.1 | <i>Study Area</i> | 3-2 |
| 3.2.2 | <i>Hydrological Modelling</i> | 3-3 |
| 3.2.3 | <i>Hydropower Reservoir Simulation</i> | 3-6 |
| 3.2.4 | <i>Climate Change Scenarios</i> | 3-6 |
| 3.2.5 | <i>Analysing Changes Using Indicators of Hydrological Alternation (IHA Method)</i> 3-7 | |
| 3.2.6 | <i>Scenarios</i> | 3-9 |
| 3.3 | RESULTS..... | 3-11 |
| 3.3.1 | <i>Climate Change Impacts on Precipitation and Flow</i> | 3-11 |
| 3.3.2 | <i>Impacts of Operation Rules and Climate Change on Hydropower Production</i> | 3-13 |
| 3.3.3 | <i>HA Due to Reservoir Operation and Climate Change</i> | 3-19 |
| 3.3.4 | <i>Predictors for Alteration</i> | 3-22 |
| 3.4 | DISCUSSION..... | 3-24 |
| 3.4.1 | <i>Impacts of Climate Change on Hydropower Production</i> | 3-24 |
| 3.4.2 | <i>HA Due to Reservoir Operations and Climate Change</i> | 3-26 |
| 3.4.3 | <i>Possible Ecohydrological Consequences</i> | 3-30 |
| 3.5 | CONCLUSIONS | 3-31 |
| 3.6 | REFERENCES | 3-33 |

| | |
|--|------------|
| CHAPTER 4. MANAGING RESERVOIR SEDIMENTATION THROUGH COORDINATED OPERATIONS | 4-1 |
| 4.1 INTRODUCTION..... | 4-1 |
| 4.2 METHODOLOGY..... | 4-3 |
| 4.2.1 Study area..... | 4-3 |
| 4.2.2 Hydrological modelling..... | 4-4 |
| 4.2.3 Sediment management simulation..... | 4-4 |
| 4.2.4 Scenarios | 4-6 |
| 4.3 RESULTS AND DISCUSSION..... | 4-10 |
| 4.3.1 Sediment load and reservoir sedimentation | 4-10 |
| 4.3.2 Sediment management simulation..... | 4-13 |
| 4.3.3 Possible consequences on the sediment regime | 4-23 |
| 4.4 CONCLUSIONS | 4-26 |
| 4.5 REFERENCES | 4-30 |
| CHAPTER 5. CONCLUSIONS AND RECOMMENDATIONS | 5-1 |
| 5.1 CONCLUSIONS | 5-1 |
| 5.1.1 Development of a SWAT hydropower routine..... | 5-1 |
| 5.1.2 Assessing the impacts of climate change and reservoir operational policies on hydropower production and downstream hydrological regime | 5-1 |
| 5.1.3 Assessing reservoir sedimentation and managing sedimentation through coordinated operation in a complex multi-reservoir system..... | 5-2 |
| 5.2 LIMITATIONS | 5-3 |
| 5.3 RECOMMENDATIONS | 5-5 |
| 5.3.1 Future development of the routine | 5-5 |
| 5.3.2 Future research..... | 5-6 |
| 5.3.3 Recommendations to the developers and stakeholders | 5-7 |
| APPENDICES | |
| APPENDIX – 1 | |
| APPENDIX – 2 | |
| APPENDIX – 3 | |
| APPENDIX – 4 | |

LIST OF FIGURES

| | |
|---|------|
| Figure 1-1: a) Current approach of simulating reservoir operations by externally linking with a reservoir operation model and a sediment management model, and b) an integrative approach to manage flow, sediment and energy for hydropower reservoirs. | 1-6 |
| Figure 1-2: Check dams to trap sediment upstream of the reservoir | 1-10 |
| Figure 1-3: Sediment bypass though the diversion tunnel. | 1-11 |
| Figure 1-4: Sediment passing by the partial drawdown sluicing. | 1-12 |
| Figure 1-5: Sediment removal due to full drawdown flushing. | 1-13 |
| Figure 1-6: Schematic diagram of the hydrologic process in SWAT (Neitsch et al. 2011).. | 1-20 |
| Figure 1-7: Components of typical reservoir in SWAT model (Source: (Neitsch et al. 2011)) | 1-21 |
| Figure 2-1: Framework of the reservoir operation and sediment management routine (ROSMAN) | 2-7 |
| Figure 2-2: The HydROR operation framework. | 2-10 |
| Figure 2-3: Typical reservoir features and dam components in the ResSMan routine | 2-16 |
| Figure 2-4: Comparison of (a) outflow from the reservoir, (b) power production and (c) reservoir water level of the Yali hydropower scheme, as determined using HydROR and HEC-ResSim. | 2-21 |
| Figure 2-5: Scatter plots of (a) outflow, (b) power generation and (c) water level for HydROR (vertical axes) and HEC-ResSim (horizontal axes)..... | 2-22 |
| Figure 2-6: Comparison of the ResSMan routine with SedSim Model for sediment outflow (Million ton) and reservoir outflow from the reservoir due to a) and b) flushing and due to c) and d) sluicing simulation respectively. | 2-24 |
| Figure 3-1: Location map showing the river network, energy production and storage capacity of each existing, proposed and under construction hydropower reservoir in the Sesan, Srepok, and Sekong (3S) river basins..... | 3-3 |
| Figure 3-2: a) Average (T_{ave}), minimum (T_{min}) and maximum (T_{max}) annual temperature and b) average monthly temperature for 3S basin for 1985-2005..... | 3-4 |
| Figure 3-3: Subbasin-wise mean annual, wet seasonal and dry seasonal precipitation of the 3S basin for 1986-2005. | 3-5 |

| | |
|--|------|
| Figure 3-4: Percentage (%) change in annual precipitation under three emissions scenarios (L—low, M—medium and H—high emissions) for GCMs: (a) GISS model, (b) IPSL model and (c) GFDL model for 2051–2070 compared to the base line climate for period 1986–2005 and location of XeKaman 3, Yali and LSP 4 for analysis of climate change impacts. | 3-13 |
| Figure 3-5: Percentage (%) change in average annual flow under three emissions scenarios (L—low, M—medium and H—high emissions) for the GISS, GFDL and IPSL models with respect to the baseline climate (BL) scenario at the 3S outlet. | 3-13 |
| Figure 3-6: Average daily energy generation using the seasonal variation rule curve (SV rule) and full supply rule (FSL rule) curve for the baseline climate (BL-R) scenario and for each emissions scenario (L—low, M—medium and H—high emissions) of the GISS, GFDL and IPSL models due to operation of reservoirs (R—reservoir operations). | 3-13 |
| Figure 3-7: Percentage change in energy production under each emissions scenario for the GISS, GFDL and IPSL models with respect to the BL-R scenario under SV rule across the 3S basin and per country. | 3-15 |
| Figure 3-8: Mean monthly inflow (left), and percentage change in average annual inflow and average energy production (right) for baseline and higher emissions climate change scenarios under SV rule curves for a)Xekaman 3, b) Yali and c) LSP 4. | 3-17 |
| Figure 3-9: Daily water level variation for 20 years simulation period for baseline, high emissions climate change scenarios and SV-Rule curve for a)Xekaman 3, b) Yali and c) LSP 4. | 3-18 |
| Figure 3-10: (a) Overall HA (%) and (b) HA for each IHA statistics group (% in log scale) due to operation of hydropower reservoirs at downstream of each reservoir, and (c) HA per gigawatt-hour of hydropower reservoirs under the seasonal variation and full supply level rule curve (denoted by SV and FSL respectively) for the baseline climate (BL-R) scenarios. ... | 3-20 |
| Figure 3-11: Percentage changes in overall HA due to operation of hydropower reservoirs under seasonal variation rule curves with respect to operation of reservoirs under full supply level rule curves for the baseline climate (BL-R) scenario. | 3-22 |
| Figure 3-12: Comparison between mean HA across all reservoirs of the baseline climate using the seasonal variation rule curve (BL-R-SV scenario) and the full supply rule curve (BL-R-FSL scenario), for GFDL, GISS and IPSL models under high emissions scenarios using the seasonal variation rule (denoted as GFDL-H-R, GISS-H-R and IPSL-H-R) for overall HA and the five HA groups considered. | 3-22 |

| | |
|---|------|
| Figure 4-1: Location map of selected hydropower reservoirs (showing the river network, energy production and storage capacity of existing, proposed and under construction) in the Sesan and Srepok river basins (reproduced from Shrestha et al. (2020)). | 4-4 |
| Figure 4-2: Distance (x-axis) of reservoirs from the most upstream reservoir and their full supply level (FSL on the y-axis) and storage capacity (denoted by the circle size in Mm^3) for a) Sesan cascade and b) Srepok cascade. | 4-9 |
| Figure 4-3: Mean annual sediment load in million ton/year (Mt/y) at the inlet of each of the reservoirs considered for the Unregulated scenario and mean annual sediment load (Mt/y) inflow and outflow for the Regulated scenario: assuming reservoirs are operating under SV rule curve but no sediment management techniques have been applied. The change in percentage between unregulated sediment load and regulated sediment outflow are shown in percentage (%) values. | 4-12 |
| Figure 4-4: Initial storage capacity loss due to sediment deposition after 100 years of operation and average trapping efficiency of the reservoirs under the SV rule curve. | 4-12 |
| Figure 4-5: Percent (%) deposition of flushed sediment loads (x-axis) due to flushing of the upstream reservoir (y-axis) in the a) Sesan and b) Srepok cascade | 4-14 |
| Figure 4-6: Reservoir storage capacity, expressed as a percentage of reservoir storage capacity at the full supply level, for the set of considered reservoirs over a 100-year simulation period (shown are only the first 50 years here) under the Regulated-SV (Regulated scenario under the SV rule), Regulated-FSL (Regulated scenario under the FSL rule), IF-5 (Individual reservoir 5-yearly flushing), MF-1 (Multiple reservoirs annually flushing), MF-2 (Multiple reservoirs bi-annually flushing), MF-5 (Multiple reservoirs 5-yearly flushing), and MS-P (sluicing reservoirs during extreme flood period) scenarios. | 4-23 |
| Figure 4-7: Mean monthly sediment load outflows in million tonnes at the outlet of LSS 2 over a 100-year simulation period under the Unregulated, the Regulated-SV (Regulated scenario under the SV rule), MF-1 (Multiple reservoirs annually flushing), MF-2 (Multiple reservoirs bi-annually flushing with alternate reservoirs in alternate years), MF-5 (Multiple reservoirs 5-yearly flushing with alternate reservoirs in alternate years), and MS-P (sluicing reservoirs during extreme flood periods) scenarios. The error bars represent one standard deviation of the mean. | 4-24 |

LIST OF TABLES

| | |
|---|------|
| Table 1-1: Summary on highlighting the strength and weakness of different sediment management techniques | 1-15 |
| Table 1-2: Summary on hydrological models | 1-23 |
| Table 1-3: Summary on the strength and weakness of reservoir simulation models | 1-25 |
| Table 1-4: Summary on the strength and weakness of reservoir sediment management models | 1-26 |
| Table 3-1: Summary of temperature and precipitation of 3S basin | 3-5 |
| Table 3-2: The 33 indicators of hydrologic alteration (IHAs) adapted from IHA Manual V7 (Richter et al. 1996; Shi et al. 2019; Timpe and Kaplan 2017; Xue et al. 2017). | 3-8 |
| Table 3-3: Description of scenarios to assess impacts of climate change on hydropower production (where, R- simulation with reservoirs, L—low, M—medium and H—high emissions scenarios). | 3-10 |
| Table 3-4: Pearson correlation R values for overall HA and individual IHA parameter groups (Group 1–5 IHA parameters are denoted as Gr1–5) among logarithmic predictor values for features (Energy: annual energy production; Installed: installed capacity; Storage: reservoir storage capacity at full supply level; Area: reservoir surface area at FSL; Act Ht: active storage height; FSL: full supply level; Head: design head of the scheme; Qmean: mean annual flow of the river and Qdesign: design discharge of the scheme) for the 3S basin under the SV-rule curve and FSL-rule curve (green and red indicate positive and negative correlations, bold values represent $p < 0.05$). | 3-23 |
| Table 3-5: Pearson correlation R values for overall HA and IHA parameter groups (Group 1–5 IHA parameters are denoted as Gr1–5), between logarithmic predictor values for features (all notations are described in the caption of Table 3-3) for the (a) Sekong, (b) Sesan and (c) Srepok subbasin under the SV-rule curve and FSL-rule curve (green and red indicate positive and negative correlations, bold values represent $p < 0.05$). | 3-24 |
| Table 4-1: Percentage (%) change in total energy production over the 100-year simulation period due to different sediment management scenarios (IF-1 and IF-5: individual reservoir flushing annually and 5-yearly respectively, MF-1, MF-2 and MF-5: multiple reservoir flushing annually, bi-annually and 5-yearly respectively and MS-P: multiple reservoir sluicing during specified threshold peak flood periods). | 4-16 |

| | |
|--|------|
| Table 4-2: Storage capacity (Mm^3) at the full supply level, mean annual inflow (m^3/s) for the Regulated-SV scenario and capacity-inflow ratio (CIR) for the considered reservoirs for sediment management | 4-16 |
|--|------|

CHAPTER 1. INTRODUCTION

1.1 Background

Water is an indispensable component of everyday life for human beings. However, increased population, climate change, drought and other factors can cause a scarcity of adequate fresh water and hence there is a need for water storage systems. Reservoirs are constructed to store the water for various purposes like drinking water, flood control, irrigation and hydropower. These play an important role in society and the economy (ICOLD 2009).

For the last 100 years reservoirs have been used for power generation (Tigrek and Aras 2011). Currently, hydropower is one of the largest renewable electricity generation sources in the world (IHA 2018). Yet it must be noted that regardless of an adequate availability of surface water runoff, numerous hydropower plants have not been yielding expected output primarily due to reservoir sedimentation problems (Sangroula 2009; Shrestha 2012). Dam operators have to manage several challenges, whereby sediment deposition is one of the most critical challenges. Reservoir capacities decrease over time due to sediment deposition and result in wear and tear of turbines due to the highly sediment-laden flow. Annual rate of reduction of global water storage volumes vary from 0.5% to 1% due to reservoir sedimentation (Mahmood 1987; Morris 2014; White 2001). The rate of reservoir sedimentation is about 0.8 percent per year worldwide (or approximately 45 km³ per year) and the sedimentation rate is much higher in the Asian region (ICOLD 2009). With growing demands for water storage, and fewer technically feasible and economically viable sites available for new reservoirs, loss of capacity in the existing reservoirs threatens the sustainability of the water supply (Annandale 2013). Furthermore, if reservoir sedimentation further increases, the production of valuable hydropower peak energy is at risk (Schleiss and De Cesare 2010).

Sedimentation not only reduces storage capacity of reservoirs, but also negatively affects the downstream sediment regime, the viability of aquatic life, river health, and the recreational value of reservoirs (Arias et al. 2014; Jager and Smith 2008; Juracek 2015; Kondolf 1997; Smith et al. 2013). The trapping of the sediments in the upstream reservoir has negative consequences in terms of river morphology and ecology (Juracek 2015; Kummu et al. 2010). These negative changes in river morphology influence water quality and the ecosystem by decreasing aquatic lives and riparian habitats with consequences for water quality (Kondolf 1997; Merz et al. 2006). Moreover, dams also trap nutrients which are attached to the sediments. Therefore, the lack in nutrients in the water downstream of reservoirs may jeopardize the equilibrium of the downstream ecosystem (Sumi and Hirose 2009).

Furthermore, the excess of sediments in reservoirs causes abrasion of outlet structures such as spillways, canals, and tunnels, and erosion of mechanical components like turbines and outlet valves (Faghihirad et al. 2017; Palmieri et al. 2003). The outlet structures may be clogged depending on the amount of sediment accumulation. More specifically, excess sediment not only reduces the efficiency and life of hydropower turbines, but also causes problems in operation and maintenance (Neopane et al. 2011). Hence, abrasion of hydraulic structures, reducing their efficiency and increasing the maintenance costs, is a possible consequence of excess of sediments in a reservoir (Schleiss et al. 2016).

Soil erosion within the catchment is a major contributor to reservoir sedimentation. Surface runoff and soil erosion in a catchment are, in part, driven by the climate system; thus, climate change can have a significant impact on the variability of water flow and soil erosion (Yu et al. 2017). Changes in temperature and precipitation trends are associated with climate change. Consequently, climate change is expected to change sediment loads, and may exacerbate reservoir sedimentation and thereby challenging the management of reservoir operations (Laura et al. 2017; Lu et al. 2013; Yasarer and Sturm 2016). Thus, changes in

sediment loads due to climate change in the future can have huge implications for planned reservoirs and related sediment management techniques (Shrestha et al. 2013).

Land use/land cover (LULC) changes alter surface runoff generation, result in changes in water demand and supply, and affect basin hydrological processes including soil infiltration capacity, groundwater recharge and discharge (Shrestha et al. 2018; Wijesekara et al. 2012). Therefore, the uncertainties of climate and land use changes can directly impact the inflows into reservoirs and their operations (Prasanchum and Kangrang 2018). Further, LULC change can alter sediment transport and influence the geomorphological processes within the river bed (Kondolf et al. 2002). Thus, changes in land use alter sediment yield and consequently, alter the reservoir sedimentation.

Sediment management techniques in reservoirs are broadly classified as: (1) reducing sediment inflow from upstream, (2) passing sediment through the reservoir to minimize sediment trapping, and (3) removal of deposit sediment (Annandale 2013; Morris 2014; Sumi and Kantoush 2011). These sediment management techniques have been implemented in the Sediment Simulation Screening (SedSim) model (Wild and Loucks 2012) to simulate sedimentation and hydropower production from reservoirs. A hydrological model that has a basic built-in reservoir routine is the Soil and Water Assessment Tool (SWAT) (Arnold et al. 1998). The SWAT model has the ability to simulate inflow to and sediment yields in reservoirs for various climatic conditions and LULCs. Even though the SWAT model has been successfully applied in many studies for different purposes such as for predicting sediment yields, assessing climate change impacts on surface runoff, and simulating hydrology in different catchments (Arnold et al. 2012; Hallouz et al. 2018; Joorabian Shooshtari et al. 2017; Sohoulane Djebou 2018), sediment management techniques and reservoir operation methods have not yet been implemented within the framework of the SWAT model. More specifically, the SWAT model does not have capabilities to simulate sediment management techniques such

as flushing, sluicing, dredging, and bypassing, and reservoir operations, and hence their effects on the hydropower energy production cannot be predicted. Therefore, a single simulation model with capabilities to simulate hydrological process, sediment yield and hydropower production at a river basin level is needed to:

- predict the effects of flow and sediment on reservoir operations and hydropower production;
- predict the impacts of climate change and LULC change on flow and sedimentation;
- improve the management of hydropower schemes to avoid loss in productivity due to sediment deposition.

Clearly, research is necessary to develop flow and sediment management routines integrated within the framework of the SWAT model to quantify the impacts of climate change and LULC change, and to minimize the productivity loss using specific sediment management techniques for hydropower reservoirs.

1.2 Problem Statement and Objectives

The importance of developing a reliable tool to simulate, predict and support management of flows and sediment in hydropower plants has long been recognized by hydropower developers as a requirement for better operation of hydropower plants. Hydrological models are widely used for design and management of water resource projects. These models are used to predict reliable quantity and sediment transport rates from land surface into streams, rivers and reservoirs, to identify erosion problem areas within a catchment, and to propose the best management practices to reduce erosion impact (Yesuf et al. 2015). The SWAT is a physically-based hydrological model which can basically estimates flow and sediment yields in large and complex catchments with varying soils, LULCs, climatic

conditions and management conditions (Arnold and Fohrer 2005; Arnold et al. 2012; Arnold et al. 1998; Gassman et al. 2007). The reservoir component of SWAT has ability to compute the mass balance of water and sediment of a reservoir (Neitsch et al. 2011). Nevertheless, the SWAT model has limited capabilities for reservoir operations. Currently, the SWAT model does not have complex reservoir operation routines for the prediction of flows, sediment and energy production as influences on the operation of a hydropower system. In contrast, available reservoir management models such as HEC-ResSim (USACE 2007) and SedSim have the ability to simulate reservoir operations and to predict the energy production. However, these models do not have the capability to simulate flows and sediment transport under the impact of LULC and climate change in complex catchments. Climatic conditions, soil types and LULC types are closely interrelated with hydrological processes of the river basin, which eventually affects reservoir operations. The current approach (Figure 1-1a) of externally linking (‘soft-coupling’) a hydrological model (SWAT) with a reservoir operation model (HEC-ResSim) and a sediment management model (SedSim) is complex to set up, time-consuming and does not allow for simulations under various climate conditions and LULC change scenarios simultaneously. Such a soft-coupling approach also does not allow for investigation of hydrological systems, such as numerous hydropower reservoirs in a given catchment, which are best operated and managed in a coordinated manner. Therefore, a new functionality in the SWAT model is needed to provide the capability to simulate reservoir operations, sedimentation processes and to enhance reservoir management. There is thus a clear need to develop flow and sediment management routines integrated within the framework of the SWAT model (Figure 1-1b).

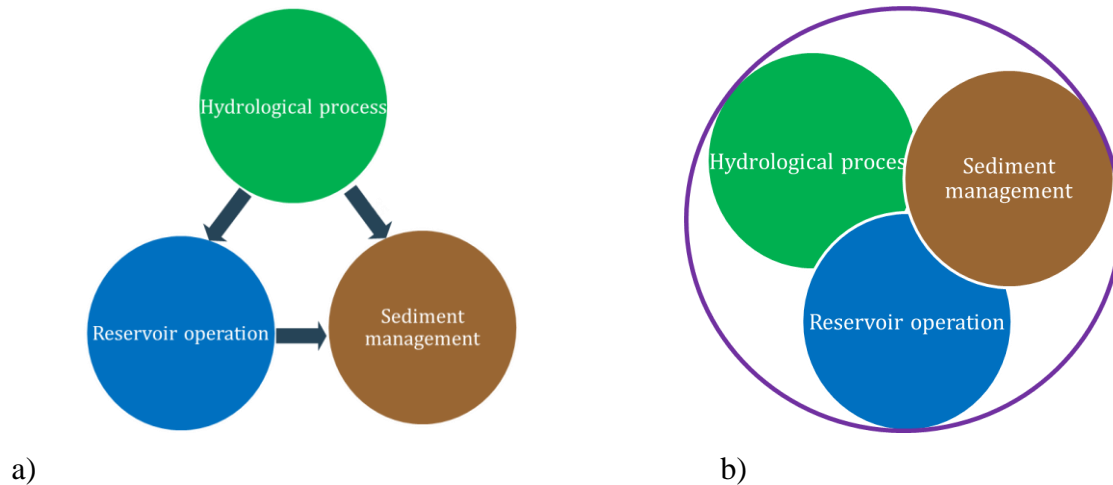


Figure 1-1: a) Current approach of simulating reservoir operations by externally linking with a reservoir operation model and a sediment management model, and b) an integrative approach to manage flow, sediment and energy for hydropower reservoirs.

The main aim of this study is to develop an integrative approach to quantify changes to river flow and sediment regime in a river system due to the operation of a hydropower system. More specifically, the objectives of this study are:

- 1) to develop and test a hydropower reservoir routine within the SWAT modelling framework to simulate flows and energy generation for hydropower reservoir operations;
- 2) to develop, test and evaluate sediment management routines within the framework of SWAT;
- 3) to assess the impacts of climate change and reservoir operation policies on hydropower production and downstream flow regime in a complex multi-reservoir system; and
- 4) to assess the impacts of sedimentation on hydropower reservoirs, and to develop a better understanding of sediment management in a complex multi-reservoir system.

1.3 Literature review

1.3.1 Reservoir sedimentation

Sediment deposition is the principal problem affecting the useful life of reservoirs, increasing evaporation losses, backwater flooding, and damage to hydropower stations (Annandale et al. 2016; Morris 2020). According to figures that have been kept since 1987, 0.5–1% of the annual global storage volume is reducing due to sedimentation (Basson 2009; Mahmood 1987). For example, the Mekong basin has been rapidly developing in the context of hydropower reservoirs. Once all planned reservoirs are built, about 96% of sediment load of the pre-dam period would be trapped (Kondolf et al. 2014; Manh et al. 2014; Pokhrel et al. 2018).

Sediment entering into reservoirs originates mainly from the products of soil and stream bed erosion (Hrissanthou 2014). The sediments erosion, transportation, and deposition processes can be classified in three main general processes: (1) sediment production, including erosion and unchannelled conveyance of sediments in the upper areas of the river basins due to weathering, snow avalanches and glaciers, rill and gully erosion, river bank failure, landslides and debris flows; (2) sediment transport, along the channel network and into reservoirs and lakes; and (3) sediment deposition, in the flat areas, lakes and delta deposits (Kondolf et al. 2014). The rate of sediment deposition varies significantly between sites of reservoirs, depending on discharge rates and sediment loads of the rivers, which are flowing into the reservoirs and the trapping efficiencies of the reservoirs (Wurbs 2005). During floods, the sediment transport increases and at the time of occurrence of these events the reservoir sedimentation also varies greatly. A remarkable example of 85.3 million m³ (Mm³) sediment deposition was observed at Kulekhani Hydropower Reservoir in Nepal (Galay et al. 1995). The Kulekhani catchment was affected by a heavy rainfall resulting in slope failures throughout the

entire catchment surface area. It was estimated that the majority of all transported sediment originated due to the slope failures within the catchment. Hence, the impacts of sediment deposition, over the life of the reservoir, must be considered in project planning and operation.

Moreover, reservoir construction and operation can have a substantial effect on the stability of the river channel downstream from the dam (Kantoush and Sumi 2010). The trapping of sediment in a reservoir, accompanied by sediment-free water releases from the dam, upsets the regime or state of quasi-equilibrium of the downstream river channel (Hotchkiss 1990). This unstable condition of the downstream river channel causes the degradation of the river channel bed and banks. The degradation process moves progressively downstream until it reaches a point where the sediment being transported results in a stable channel or equilibrium (Strand and Pemberton 1982).

1.3.2 Reservoir sediment management techniques

There are different techniques available to successfully manage reservoir sedimentation, whereby suitable techniques for sustainable use of the reservoir are selected (Palmieri et al. 2003). These techniques for reservoirs sediment management can be broadly classified as reducing sediment inflow from upstream, minimizing sediment deposition, and removal of reservoir sediment after it has been deposited (Morris 2014; Morris 2020).

1.3.2.1 Reducing sediment inflows

In this technique, the sediment delivery to the reservoir from upstream sub-catchments is minimized by different catchment management strategies and trapping the upstream eroded sediment by constructing check dams.

i) Catchment management

Catchment management is the process of organizing and guiding land, water, and other natural resources in a catchment to provide the appropriate goods and services while mitigating the impact on the soil and catchment resources (Wang et al. 2016). Catchment management is one of the increasingly utilized techniques to reduce soil erosion and consequently to decrease reservoir sediment deposition (Amare 2005; Paskett 1982; Tamene et al. 2006; Wolancho 2012). The main source of reservoir sediment is soil erosion from the upstream catchment and this can be controlled and reduced by adequate catchment management methods. The soil erosion rates can be reduced by different methods such as forestation, prevention of erosion by vegetation and tillage management, sediment deposits and change in land usage patterns (Tigrek and Aras 2011). Agronomic management methods, which include crop and vegetation management, crop rotation, shifting cultivation, and grazing land management, can reduce the impact of the erosion and sedimentation processes (Alemu 2016).

Previous study has shown that intensive conservation efforts are needed over several decades to reduce sediment production by 10-20% for catchments over 1,000 km² (Dixon and Hufschmidt 1986). Furthermore, in very large catchments conservation measures are often, from a reservoir sedimentation management point of view, considered to be ineffective because of the large time lag between implementation of erosion control measures and realization of their effect in reducing sediment load into rivers (Palmieri et al. 2003).

ii) Upstream sediment trapping

A check dam can be defined as a structural measure established within rivers or gullies to trap sediment (Mekonnen et al. 2015). It is a fixed structure built upstream of the reservoir, constructed from timber, sandbags, loose rock, masonry or concrete, to control concentrated water flow and trap sediment in an erodible channel and is an effective strategy for reducing sediment loss (Figure 1-2). Check dams are likely the most emblematic civil engineering

structures used in soil conservation projects (Piton et al. 2017). They can be built on one or more tributaries upstream of a reservoir and sediments should be periodically removed. Ease of access to remove sediment from the check dams and the potential to re-use sediments make the application of check dams potentially feasible. In the absence of these conditions, life of a check dam is likely to be short and its effectiveness is limited (Palmieri et al. 2003). According to results presented by Ran et al. (2008), the most effective method to rapidly reduce the amount of coarse sediment entering the Yellow River is sediment reduction by the check dams. The high stream flow velocity during flood events has high capacity to channel erosion and sediment transport. The installation of check dams can significantly reduce the stream power and thereby decreasing sediment transport and channel erosion (Liu 1992). However, check dams are not cost-effective to limit sediment yields in semi-arid conditions (Rooseboom and Basson 1997).

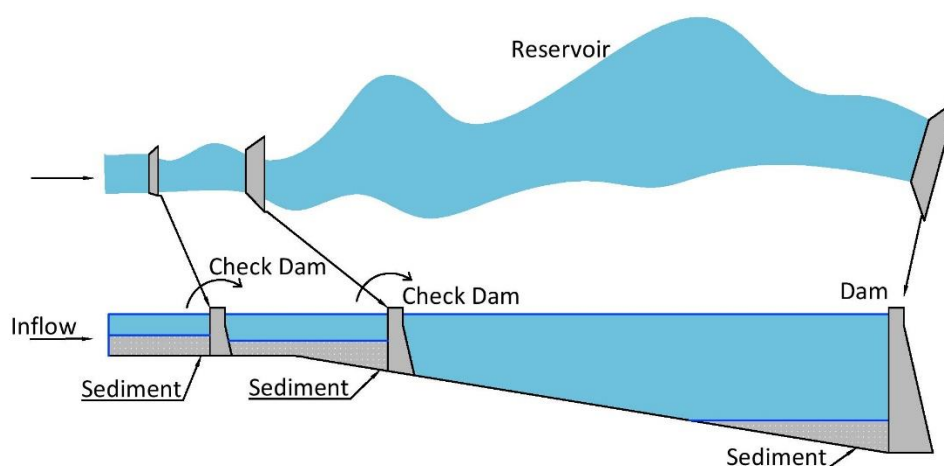


Figure 1-2: Check dams to trap sediment upstream of the reservoir

1.3.2.2 Minimizing sediment deposition

Sediment deposition in reservoirs can be minimized by sediment routing that includes any method to manipulate reservoir hydraulics, geometry, or both, to pass sediment through or around storage or intake areas while minimizing objectionable deposition (Morris and Fan 1998).

1. Reservoir bypass

Sediment bypass may be accomplished by constructing an offstream or off-channel reservoir, diverting water having low sediment concentration into storage by either gravity or pumping while allowing large sediment-laden floods to bypass the storage pool (Morris 2014). In this technique, a weir or check dam upstream of the reservoir diverts sediment-laden flows during peak flows and high sediment loads, through a diversion tunnel/channel that conveys the sediment-laden flows downstream of the dam (Figure 1-3).

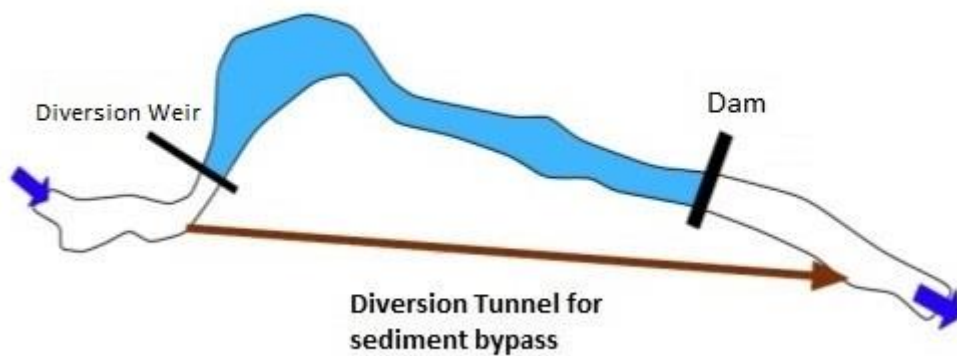


Figure 1-3: Sediment bypass through the diversion tunnel.

Again, river flow is allowed into the reservoir after it has decreased sediment concentration in the flow. The sediment bypassing technique is most suitable for steep rivers with sharp bends. A sharp bend between the location of sediment diversion and the location of sediment discharges reduces the length of the conveyance tunnel/channel and the steeper gradient between these two-locations contributes to transport sediment through the diversion tunnel/channel with gravity flow of sediment-laden water. If this kind of ideal condition is not given, then the technique is applicable for a reservoir of relatively short length, so that the diversion tunnel/channel can attain sufficient gradient to drive the transport of sediment through the diversion devices (Kondolf et al., 2014).

2. Sluicing

Sediment sluicing, also known as sediment pass-through, is another way of bypassing sediment before suspended sediment solids have settled down in the reservoirs (Figure 1-4). In this method, the reservoir water level is drawn down during a flood season and allowed to flow through the sluice gates to maintain the incoming sediment in suspension (Tigrek and Aras 2011). The reservoir can behave like a river during high flood when all the floodgates are fully opened so that the high velocity of the flood can minimize the deposition of fine sediments. Hence, opening the reservoir's gates at the flood event allows the sediment-laden flood to pass at high velocity, and closing the gates to refill the recession part of impoundment after the flood event. This method is most suitable for narrow, elongated-shaped reservoirs as well as small to medium-size reservoirs (Batuca and Jordaan Jr 2000).

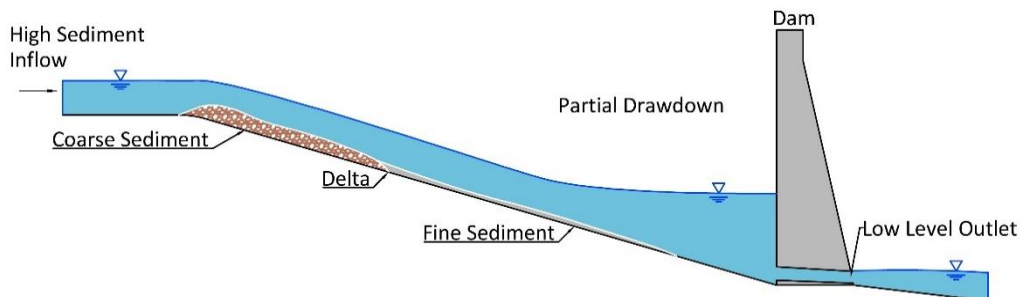


Figure 1-4: Sediment passing by the partial drawdown sluicing.

1.3.2.3 Removal of reservoir sediment

Accumulated sediment in reservoirs can be removed by one of the following removal methods: flushing, dredging and hydrosuction systems.

i) Flushing

Sediment flushing is defined as the removal of deposited sediment from a reservoir by passing water and sediment through low level outlets (Figure 1-5). Sediment flushing increases storage capacity by 1) completely scouring deposited sediment in the vicinity of the flush gates

and 2) lowering the general level of deposits upstream. This technique is effective under certain favourable conditions and so is not universally applicable (Atkinson 1996). However, flushing has proven to be greatly effective at some sites. For example, at the Mangahao reservoir in New Zealand, 59% of the operational storage capacity had been lost by 1958, 34 years after the first impoundment. The reservoir was flushed in 1969 and 75% of the deposited sediment was removed in a month (Jowett 1984). In order to create favourable conditions for flushing, it is essential to establish river-like flow conditions through the reservoir upstream of the dam. This can best be achieved given the following: narrow valleys with steep sides; steep longitudinal slopes; river discharge maintained above the threshold to mobilize and transport sediment; and low-level gates installed in the dam (Morris and Fan 1998).

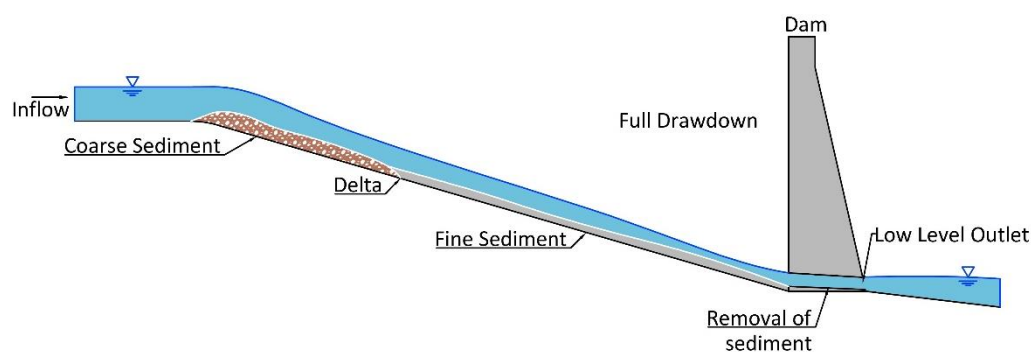


Figure 1-5: Sediment removal due to full drawdown flushing.

There are two approaches to remove sediment by flushing: 1) complete drawdown flushing and 2) partial drawdown flushing (Palmieri et al. 2003). The complete drawdown flushing method is achieved by emptying the reservoir during flood season and routing water inflow from upstream by providing riverine conditions. Partial drawdown flushing occurs when the reservoir level is drawn down only partially and the sediment flows through the low level outlets by keeping the reservoir water level high. Flushing with partial drawdown may be used to clear more live storage space and locate the sediment in a more favourable position for future complete drawdown flushing.

ii) Dredging

The mechanical process of excavating deposited sediments from under water is termed dredging (Palmieri et al. 2003). If a dredging equipment can be transported towards a reservoir, it may be possible to dredge. This is quite an extensive operation since a dredging unit is usually of a considerable size and the location of reservoirs is most of the time situated in a mountainous and remote environment (Bronsvort 2013). Another difficulty with dredging is to find a suitable area for dumping the excavated sediments. Therefore, the cost of disposal land is an important item in the calculation of dredging costs. Thus, dredging is more expensive than other methods, so it is most often used to remove sediment from specific areas such as near dam intakes (Kondolf et al. 2014).

iii) Hydrosuction Removal System (HSRS)

Hydrosuction Sediment Removal System (HSRS) is one of the methods of sediment flushing that uses the hydraulic head available at the dam as energy to remove sediment (Shrestha 2012). So, where there is sufficient head available, the operating costs are substantially lower than those of traditional dredging (Palmieri et al. 2003). The HSRS consists of a sediment removal pipe and valves to control the discharge. The inlet of the pipe is located where sediment removal is desired upstream of the reservoir it extends downstream either over the dam or through low level outlets. The hydraulic potential energy thus stored drives water and sediment into sediment removal pipes. Whether an HSRS is feasible for a reservoir sediment management plan depends on hydraulic, environmental, and operational factors (Hotchkiss and Huang 1995).

Table 1-1: Summary on highlighting the strength and weakness of different sediment management techniques

| Sediment management technique | Strength | Weakness |
|--------------------------------------|---|---|
| Catchment management | <ul style="list-style-type: none"> • reduce soil erosion and consequently to decrease reservoir sediment deposition. | <ul style="list-style-type: none"> • does not address the issue of sediment starvation downstream. • considered to be ineffective in very large catchments. |
| Upstream sediment trapping | <ul style="list-style-type: none"> • the most effective method to rapidly reduce the amount of coarse sediment. | <ul style="list-style-type: none"> • should be accessible to remove sediment from the check dams and have the potential to re-use sediments. |
| Reservoir bypass | <ul style="list-style-type: none"> • the most suitable for steep rivers with sharp bends. • bed load can be excluded from the reservoir. | <ul style="list-style-type: none"> • technical and economic feasibility of this option is a function of location. |
| Sluicing | <ul style="list-style-type: none"> • finer sediments can be more effectively transported through the reservoir. • address the issue of sediment starvation downstream in some extent. | <ul style="list-style-type: none"> • effective for narrow, elongated-shaped reservoirs as well as small to medium-size reservoirs |
| Flushing | <ul style="list-style-type: none"> • removes previously deposited sediment. | <ul style="list-style-type: none"> • sediment deposited from flushing can have significant environmental impacts. • favourable at narrow valleys with steep sides, steep longitudinal slopes, river discharge maintained above the threshold. |
| Dredging | <ul style="list-style-type: none"> • is useful to remove sediment from specific areas such as near dam intakes | <ul style="list-style-type: none"> • not suitable for very large reservoirs and situated in remote mountainous sites. • should have suitable area for dumping the excavated sediments. |
| HSRS | <ul style="list-style-type: none"> • flexibility in sediment release management and cost-effectiveness. | <ul style="list-style-type: none"> • only able to remove a smaller volume of sediment in a specific period of time. |

1.3.3 Reservoir operation

Reservoirs can be operated by either applying the normal operation method or by optimizing the operation. The normal operation applies the runoff regulation theory and the hydroelectricity energy computation method to determine the reservoir storage-draft process satisfying the task defined by the reservoir operation policy (Chen and Chen 2015). Whereas,

an optimum reservoir operation is accomplished by finding an optimum solution, which depends on an objective function and constraints (Ginting et al. 2017; Heydari et al. 2015). Furthermore, in the case of multipurpose reservoirs, the reservoirs are often operated considering a number of conflicting objectives (such as different water uses) related to environmental, economic, and public services (Chu et al. 2015). Therefore, reservoirs have to be operated under various operational constraints and design restrictions such as hydropower, municipal, industrial and irrigation demands, flood control and navigation, and environmental flows for fish and aquatic lives, recreational needs, and downstream flow regulation (Shrestha et al. 1996). These constraints and restrictions are translated into a set of rules for determining the capacities of water to be stored and to be released or extracted from a reservoir or system of multiple reservoirs under various conditions (Khan et al. 2012; Wurbs 1994).

Most reservoir systems are managed based on fixed predefined operational rules. The comprehensive negotiations and subsequent agreements with stakeholders is one of the main reasons to operate a reservoir system on fixed predefined rules. The predefined operating rules are often evaluated using simulation models but before they can be simulated, these rules must be defined (Wafae et al. 2016). Optimization models can help to determine the predefined rules, rules that satisfy various operational constraints, while minimizing spills or maximizing energy production or minimizing expected future undesired deviations from various water release, storage capacity and/or energy production targets (Oliveira and Loucks 1997).

However, in the region where rivers are characterized by large sediment load, the reservoir operations in the regions are not sustainable unless sedimentation can be controlled, and reservoirs may represent the most important class of non-sustainable infrastructure (Wang and Yang 2014). Moreover, the reservoir operational rules which affect the sedimentation in the reservoir and the application of sediment control techniques should be worked out in view of the needs of the various users of the storage (Bruk 1985). In this study, predefined operational

rules for hydropower reservoirs considering the point of view of reservoir sediment management and maximizing hydropower production will be implemented.

1.3.4 Climate change

Climate change as defined by the Intergovernmental Panel on Climate Change (IPCC) is a change in the state of the climate that can be recognized by variations in the average and/or the variability of its characteristics and that persists for a projected long period of time (Bernstein et al. 2007). According to climate change models, an increase in air temperature is expected during the 21st century (IPCC 2018). The evidence of observed climate change has been linked to changes in large scale hydrological cycles such as: precipitation patterns, melting of snow and ice, and affecting water resources in terms of quantity and quality (Akter et al. 2019; Bates et al. 2008; Jiménez Cisneros et al. 2014; Xu and Luo 2015). Furthermore, it has been shown that climate change can alter the flow regimes of rivers (Arnell and Gosling 2013; Bhatta et al. 2019; Döll and Zhang 2010; Evers and Pathirana 2018; Timalisina et al. 2015) and change the timing and magnitude of floods (Kopytkovskiy et al. 2015; Wagena et al. 2016).

Hydropower reservoir operators are more concerned with climate change because changes in the period and magnitude of flows will affect the production of energy (Haguma et al. 2017; Meng et al. 2020; Qin et al. 2020; Shu et al. 2018). Therefore, reservoir owners will have to modify the reservoir operating policies to adapt to the impacts of climate change and to minimize the negative impacts (Ahmadi et al. 2015; Chang et al. 2018; Ehsani et al. 2017; Eum and Simonovic 2010; Hidalgo et al. 2020; Zhong et al. 2020). Climatic change has potentially important implications for the operation of the reservoir system (Burn and Simonovic 1996). Furthermore, climate change impacts the rate of soil erosion (Michael et al. 2005; O'Neal et al. 2005; Pruski and Nearing 2002; Wagena et al. 2016) and increase of sediment yield (Azim et al. 2016; Shrestha et al. 2013; Syvitski et al. 2005; Xu 2003; Zhu et al. 2008). This increase in

sediment yield also affects the reservoir sedimentation and ultimately the reservoir sediment management.

1.3.5 Land use/land cover (LULC) change

The increase in demand for food and energy causes increasing deforestation or removal of native bush to clear land for agricultural production and also for new urban areas (FAO 2016). LULC change can play an important role with regard to the alteration of the hydrologic cycle, including rainfall, evapotranspiration, and land-surface temperature (Dwarakish and Ganasri 2015; Lørup et al. 1998; McColl and Aggett 2007; Wang et al. 2014). The type of LULC that is found in a specific area determines the amount of evaporation, and therefore affects the total surface runoff (Jackson et al. 2005; Piao et al. 2007). Hence the change in this specific type of LULC will have an impact on the stream flow in that area. Furthermore, a significant part of the changes in runoff cannot be related to changes in precipitation, and but can be explained by changes in evapotranspiration, i.e., LULC change (Costa et al. 2003).

The characteristics of soil, LULC, climatic conditions and topography of land are the main factors affecting soil erosion (Wischmeier and Smith 1978). More specifically, improper LULC patterns can cause severe soil and nutrient losses, and further land degradation (Costa et al. 2003). Eventually, soil erosion contributes to an increase in reservoir sedimentation. Soil erosion is greatly controlled by the presence of protective LULC, whereas sediment transport to rivers is determined by on-site sediment production and the connectivity of sediment sources and rivers (Bakker et al. 2008). Sediment transport is also a function of LULC, since the sediment transport capacity varies depending on LULC (Van Oost et al. 2000). In summary, the impacts of LULC change on runoff and sediment yield will further affect the sediment deposition in reservoirs and hydropower production (de Oliveira Serrão et al. 2020; Dorber et al. 2018; Harden 1993; Shrestha et al. 2018; Welde and Gebremariam 2017).

1.3.6 Hydrological models

Hydrologic models are simplified, conceptual representations of a part of or the entire hydrologic cycle (Jana and Majumder 2010). They are used for hydrologic prediction and for understanding hydrologic processes. Moreover, hydrological models are widely used for design and management of water resources projects. Simulated series of river flows are used for example in the design and operation of multipurpose reservoirs and to evaluate the risks and benefits of LULC change over time. Some well-known hydrological models are SWAT (Arnold et al. 1998), VIC (Hamman et al. 2018; Liang et al. 1994), TOPMODEL (Beven and Kirkby 1979), and HBV (Bergström and Forsman 1973). Among them, SWAT and VIC models have a reservoir simulation component within their modelling framework and their capabilities and applicability will be briefly described in the next sections.

1.3.6.1 SWAT model

Soil and Water Assessment Tool (SWAT) (Arnold et al. 1998) was developed in the early 1990's by the U.S. Department of Agriculture, Agricultural Research Service (USDA-ARS). SWAT is a physically-based model that operates on a daily time step and can predict the impact of land management practices on water, sediment, and agricultural chemical yields (nutrient loss) in large and complex catchments with varying soils, LULCs and management conditions over a long period of time (Neitsch et al. 2011). SWAT has been applied to an extensive array of water resource problems such as impacts of impoundments, best management practices, climate change, or LULC change on streamflow and/or pollutant transport (Gassman and Wang 2015). SWAT is meanwhile used in many countries all over the world due to its flexibility to be used under a wide range of different environmental conditions (Arnold and Fohrer 2005).

The hydrologic components considered in SWAT are shown in Figure 1-6. Stream processes considered in SWAT include channel flood routing, channel sediment routing, and nutrient and pesticide routing and transformation. The ponds and reservoirs component contains water balance, routing, sediment settling, and simplified nutrient and pesticide transformation routines. Moreover, the built-in reservoir routine in SWAT has the ability to determine water diversions for irrigation and other purposes and flood flows into and out of the reservoirs (Xie et al. 2011). The representation of a dam in SWAT includes an emergency spillway to control emergency flood and a principal spillway for normal flood control (Figure 1-7).

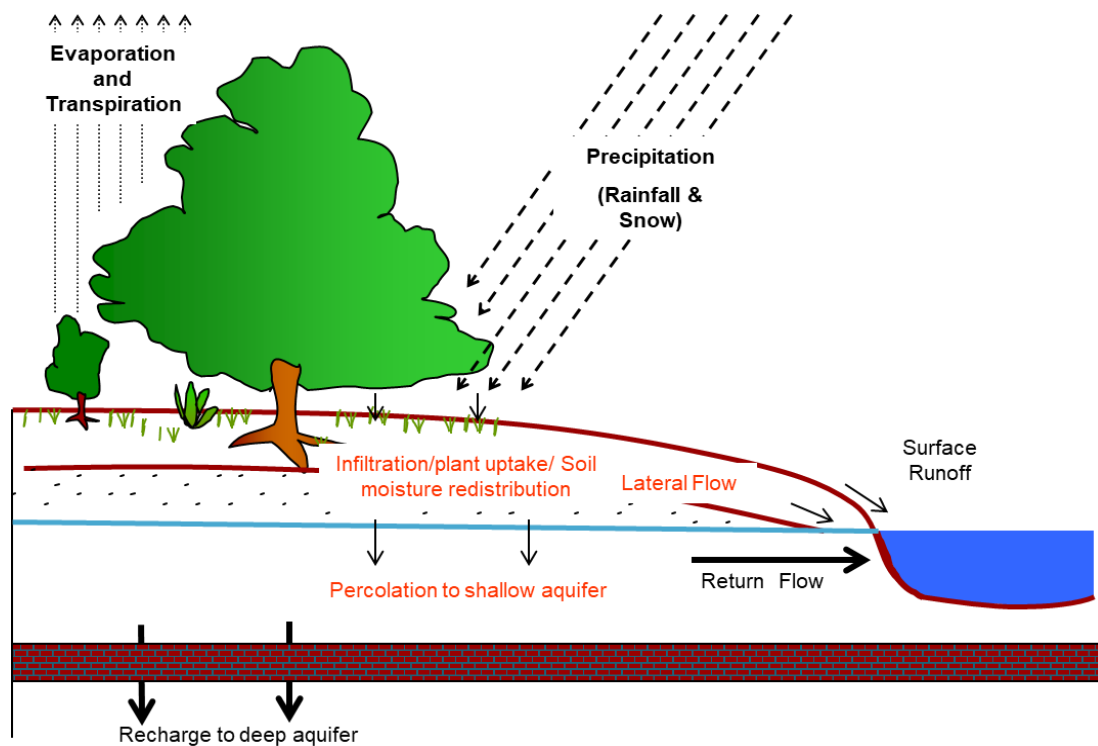


Figure 1-6: Schematic diagram of the hydrologic process in SWAT (Neitsch et al. 2011).

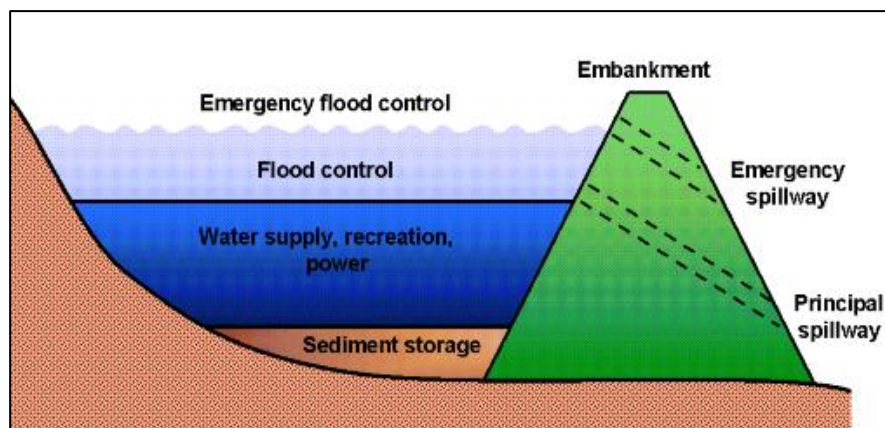


Figure 1-7: Components of typical reservoir in SWAT model (Source: (Neitsch et al. 2011))

In previous studies, the built-in reservoir routine in SWAT was used to assess the impact of reservoir parameters on runoff (Liu et al. 2019); the influence of a reservoir on the hydrological situation of Lhasa River (Yasir et al. 2020); influence of reservoir operation in the Yangtze River (Zhang et al. 2012); and similarly, to model and account for the effects of reservoirs in SWAT modelling (Kirsch et al. 2002; Wang et al. 2016). Furthermore, SWAT was used to estimate discharge and sediment yields to the reservoir by various researchers (Betrie et al. 2011; Bieger et al. 2015; Hallouz et al. 2018; Kumar et al. 2015; Schmalz et al. 2015; Sohoulane Djebou 2018; Yesuf et al. 2015). Jalowska and Yuan (2019) evaluated different SWAT reservoir routing methods to improve the model calibration by incorporating impoundments in the modelling setup. Some researchers have also modified the existing SWAT reservoir routine to improve the performance of reservoir routing and solve the specific problems such as seasonal flood routing (Lv et al. 2016; Wang and Xia 2010; Zhang et al. 2012). However, SWAT still does not have the functionality to simulate reservoirs under the influence of hydropower operations, thus researchers are using either reservoir simulation models externally or have to compute separately to assess hydropower production (Bhatta et al. 2019; Chiogna et al. 2018; Hasan and Wyseure 2018; Kaura et al. 2019; Phiri and Mulungu 2019; Trung et al. 2020).

1.3.6.2 Variable Infiltration Capacity (VIC) model

VIC is a large-scale, semi-distributed grid based hydrological model developed and maintained by the University of Washington (Hamman et al. 2018; Liang et al. 1994). The VIC model contains two main components, specifically a rainfall-runoff and routing module that can be applied to multi-spatial scales and different temporal resolutions. Using climate forcings input data such as precipitation, temperature, and wind, the rainfall-runoff module simulates water balance and energy fluxes, which govern the hydrological process (Dang et al. 2020). Other additional input data are required for the VIC model are: land use, soil maps, and a Digital Elevation Model (DEM). The VIC model divides each grid cell into one vegetation layer and two (or three) soil layers, for each grid the module independently computes evaporation, infiltration, runoff and base flow (Dang et al. 2020). Then, these cell variables are simulated by the separate routing model for discharge throughout the river network (Lohmann et al. 1996). However, the VIC model is applicable only for large scale catchments (i.e. grid cell >1km to ~2° resolution) (Hiep et al. 2018).

Haddeland et al. (2006) and Haddeland et al. (2006) developed and implemented a simple reservoir module and irrigation scheme in the VIC model to assess the effects of reservoir operations on surface water flows. This reservoir module calculates water release according to reservoir inflow, storage capacity and irrigation or hydropower water demands. The main limitation of this reservoir module is that it cannot simulate simultaneous multiple reservoirs operations simultaneously in a river basin and water demands are estimated on a monthly basis and if possible, the monthly release is kept constant (Gao et al. 2010; Haddeland et al. 2006).

Table 1-2: Summary on hydrological models

| Model | Strength | Weakness |
|-------|--|--|
| SWAT | <ul style="list-style-type: none"> • applied extensively for a broad range of water quantity and quality problems worldwide. • a semi-distributed structure which is capable of modelling water quantity and quality. • a flexible framework which allows to assess various catchment management options. | <ul style="list-style-type: none"> • intensive input data required. • requires calibration of numerous parameters • non-spatial portrayal of hydraulic response unit (HRU) is a key limitation. |
| VIC | <ul style="list-style-type: none"> • is a water and energy balance, semi-distributed gridded model. • capable of integrating point- and grid-meteorological inputs. • ability to perform studies on a continental scale. | <ul style="list-style-type: none"> • each grid cell is treated independently except for routing. • not applicable for small catchments. |

1.3.7 Reservoir simulation models

1.3.7.1 Hydrological Engineering Center Reservoir Simulation Model (HEC-ResSim)

HEC-ResSim was developed by the US Army Corps of Engineers, Hydrologic Engineering Center and is used to simulate reservoir operations at one or more reservoirs for various operational goals and constraints (USACE 2007). The model simulation can be used for reservoir flood management, low flow augmentation and water supply for planning studies, detailed reservoir regulation plan investigations, and real-time decision support (Lara et al. 2014). Several studies have been carried out in the field of water resources planning and management due to wider applicability of HEC-ResSim. Piman et al. (2013) and Piman et al. (2016) applied the HEC-ResSim model to assess flow changes due to hydropower reservoir operations and to assess the effects of planned large dams on hydropower production in the Sekong, Sesan and Srepok Rivers of the Mekong Basin because of the model's greater ability and versatility. Similarly, Shrestha et al. (2021) used HEC-ResSim to assess the impact of climate change on the Kulekhani hydropower reservoir in Nepal. However, the major limitations of HEC-ResSim are that it does not have the capabilities to simulate hydrological

processes such as flow, sediment production, transportation and the impacts of sediment accumulation in the reservoirs. Therefore, researchers generally use hydrological models, such as SWAT, to predict flows and sediment yields from the catchment and enter them as the main input into the HEC-ResSim for reservoir simulations.

1.3.7.2 MODSIM

MODSIM is a generic river basin management system originally conceived in 1978 at Colorado State University, making it the longest continuously maintained river basin management software package currently available from an open source Shafer and Labadie (1978). MODSIM has the capability to simulate reservoir operations and hydropower generation. In hydropower reservoir operation, reservoir balancing routines are included allowing division of reservoir storage into several operational zones for controlling the spatial distribution of available storage in a river basin (Labadie et al. 2000). Hydropower generation capacity and energy production are based on power plant efficiencies varying with discharge and head. MODSIM can be used as a decision support system for water allocation optimization (Chhuon et al. 2016). However, MODSIM model does not consider the influence of sediment in the reservoir and its management techniques.

1.3.7.3 Water Rights Analysis Package (WRAP) modelling system

The WRAP was designed for long-term, monthly time-step modelling assessments of hydrologic and institutional water availability and reliability for water supply diversions, environmental flow requirements, hydropower energy generation and reservoir storage (Wurbs 2005).

Table 1-3: Summary on the strength and weakness of reservoir simulation models

| Model | Strength | Weakness |
|------------|---|--|
| HEC-ResSim | <ul style="list-style-type: none"> • can simulate reservoir operation, data management capabilities, and graphics and reporting features. • multipurpose, multi-reservoir systems can be simulated. • has ability to simulate flood in short durations up to 15 minutes. | <ul style="list-style-type: none"> • not an optimization model • does not have the capabilities to simulate sediment production, transport and the impacts of sediment accumulation in reservoirs. |
| MODSIM | <ul style="list-style-type: none"> • linear programming model to simulate reservoirs. • has also capability to simulate salinity and conjunctive use of surface water and groundwater. | <ul style="list-style-type: none"> • does not have the capabilities to simulate sediment production, transport and the impacts of sediment accumulation in the reservoirs. • the minimum computational time step is one day. |
| WRAP | <ul style="list-style-type: none"> • is designed for efficient modeling and analysis of large complex datasets with many hundreds of reservoirs and water users. • has capability of reliability and frequency analyses, economic evaluations, water quality, and surface/groundwater interactions. | <ul style="list-style-type: none"> • does not have the capabilities to simulate sediment production, transport and the impacts of sediment accumulation in the reservoirs. • The minimum computational time step is one day. |

1.3.8 Reservoir sediment management models

1.3.8.1 RERservoir CONservation (RESCON) Model

The RESCON model (Kawashima et al. 2003; Palmieri et al. 2003) (a revised version is RESCON2; (Efthymiou et al. 2017)) is a pre-feasibility sediment management tool, which has the capability to evaluate the technical feasibility and economic viability of specific sediment management techniques at the considered reservoir sites. RESCON includes flushing, hydrosuction, traditional dredging and trucking techniques to remove sediments. The model performs economic optimization for each of the sediment management techniques in separate subprograms to determine the optimum option. The limitation of RESCON is that it is not a simulation model and unable to consider multiple dam operations.

Table 1-4: Summary on the strength and weakness of reservoir sediment management models

| Model | Strength | Weakness |
|--------------|--|---|
| RESCON | <ul style="list-style-type: none"> • has the capability to evaluate the technical feasibility and economic viability of specific. | <ul style="list-style-type: none"> • it is not a simulation model and unable to consider multiple dam operations. |
| SedSim | <ul style="list-style-type: none"> • simulates sediment production, transport and accumulation in multiple reservoirs. • has capability to simulate multiple reservoir sediment management techniques. | <ul style="list-style-type: none"> • does not have the capabilities to simulate hydrological process such as impacts of climate change and land use change on flows and sediment. • does not have capability to simulate overland sediment production and transportation. |

1.3.8.2 Sediment Simulation Screening (SedSim) Model

The SedSim model simulates a sediment mass balance as affected by hydropower operations in a daily time-step. This model predicts the spatial accumulation and depletion of sediment in river reaches and in reservoirs under different reservoir operations and sediment management policies (Wild and Loucks 2014). The model is intended for use in estimating sediment transport in a river basin that has experienced extensive reservoir development. The SedSim model conducts a sediment mass balance, which allows the model to track the effect of sediment accumulation on both the reservoir storage capacity and water surface level for a given storage capacity (Wild and Loucks 2012). However, the SedSim model does not have the capability to determine which sediment management techniques are technically feasible and economically viable for a particular reservoir.

1.3.9 Summary of literature review

This section provided a literature review to contextualize the problem and methodology used in this thesis. The above sections described the state of the knowledge on the problems and challenges which are being faced by hydropower dam operators and the capabilities and limitations

of techniques and models available for reservoir management. As mentioned above, there are some models that have the capability to simulate the flow and sediment yields of reservoirs, however, a model that can simulate flow and sediment management techniques within the framework of a hydrological model to operate hydropower reservoirs is missing. Hence, there is a clear need to develop new functionality in a hydrological model to allow for simultaneous simulation of hydropower generation and sediment transport, plus the development of efficient sediment management strategies, under LULC change and climate change. For the current study, SWAT2012 (Rev. 670) has been selected as a fundamental hydrological model for embedding a new reservoir routine because SWAT has been widely applied across the world in water resources studies due to its versatility and availability of the source code and documentation.

1.4 Thesis outline

This thesis contains five chapters. Chapter 1 is the introduction and literature review. Chapter 2 presents a review of capabilities and limitations of the currently available models to model hydrology, hydropower and sediment, the development of a new hydropower and sediment management routine within the modelling framework of the SWAT, and testing and evaluation of the performance of the developed routine. Chapter 3 describes a comprehensive approach to implementing the new SWAT hydropower routine for assessing hydrological alterations due to reservoir operations and climate change in a complex multi-reservoir system. Chapter 4 presents the application of the SWAT sediment management routine to quantify the impacts of reservoir sedimentation and the implications of sediment management techniques in order to establish coordinated management operations in a complex multi-reservoir system. Finally, Chapter 5 is comprised of the key conclusions, limitations and recommendations for further development of the routine in particular and potential future research in general.

1.5 References

- Ahmadi, M., Haddad, O. B., and Loáiciga, H. A. (2015). "Adaptive Reservoir Operation Rules Under Climatic Change." *Water Resources Management*, 29(4), 1247-1266.
- Akter, S., Howladar, M. F., Ahmed, Z., and Chowdhury, T. R. (2019). "The rainfall and discharge trends of Surma River area in North-eastern part of Bangladesh: an approach for understanding the impacts of climatic change." *Environmental Systems Research*, 8(1), 28.
- Alemu, M. M. (2016). "Integrated Watershed Management and Sedimentation." *Journal of Environmental Protection*, Vol.07No.04, 5.
- Amare, A. (2005). "Study of sediment yield from the Watershed of Angereb reservoir." *Master's Thesis, Department of Agricultural Engineering, Alemaya University, Ethiopia*.
- Annandale, G. (2013). *Quenching the thirst: sustainable water supply and climate change*, CreateSpace Independent Publishing Platform North Charleston, SC.
- Annandale, G. W., Morris, G. L., and Karki, P. (2016). *Extending the life of reservoirs: sustainable sediment management for dams and run-of-river hydropower*, The World Bank.
- Arias, M. E., Cochrane, T. A., Kumm, M., Lauri, H., Holtgrieve, G. W., Koponen, J., and Piman, T. (2014). "Impacts of hydropower and climate change on drivers of ecological productivity of Southeast Asia's most important wetland." *Ecological Modelling*, 272, 252-263.
- Arnell, N. W., and Gosling, S. N. (2013). "The impacts of climate change on river flow regimes at the global scale." *Journal of Hydrology*, 486, 351-364.
- Arnold, J. G., and Fohrer, N. (2005). "SWAT2000: current capabilities and research opportunities in applied watershed modelling." *Hydrological Processes*, 19(3), 563-572.
- Arnold, J. G., Moriasi, D. N., Gassman, P. W., Abbaspour, K. C., White, M. J., Srinivasan, R., Santhi, C., Harmel, R., Van Griensven, A., and Van Liew, M. W. (2012). "SWAT: Model use, calibration, and validation." *Transactions of the ASABE*, 55(4), 1491-1508.
- Arnold, J. G., Srinivasan, R., Muttiah, R. S., and Williams, J. R. (1998). "Large area hydrologic modeling and assessment part I: model development." *JAWRA Journal of the American Water Resources Association*, 34(1), 73-89.
- Atkinson, E. (1996). "The feasibility of flushing sediment from reservoirs." *TDR Project R5839, Report 0D137, HR Wallingford, UK*.
- Azim, F., Shakir, A. S., Habib ur, R., and Kanwal, A. (2016). "Impact of climate change on sediment yield for Naran watershed, Pakistan." *International Journal of Sediment Research*, 31(3), 212-219.

- Bakker, M. M., Govers, G., van Doorn, A., Quetier, F., Chouvardas, D., and Rounsevell, M. (2008). "The response of soil erosion and sediment export to land-use change in four areas of Europe: The importance of landscape pattern." *Geomorphology*, 98(3-4), 213-226.
- Basson, G. "Management of siltation in existing and new reservoirs. General Report Q. 89." *Proc., 23rd Congress of the CIGB-ICOLD, Brasilia, Brazil*.
- Bates, B., Kundzewicz, Z. W., Wu, S., and Palutikof, J. (2008). "Climate change and water technical paper of the intergovernmental panel on climate change (Geneva: IPCC Secretariat)." *Climate Change*, 95, 96.
- Batuca, D. G., and Jordaan Jr, J. (2000). *Silting and desilting of reservoirs*, CRC Press.
- Bergström, S., and Forsman, A. (1973). "Development of a conceptual deterministic rainfall-runoff model." *Hydrology Research*, 4(3), 147-170.
- Bernstein, L., Bosch, P., Canziani, O., Chen, Z., Christ, R., Davidson, O., Hare, W., Huq, S., Karoly, D., and Kattsov, V. (2007). "Climate Change 2007: Synthesis Report: Intergovernmental Panel on Climate Change." *Valencia, Spain*.
- Betrie, G. D., Mohamed, Y. A., van Griensven, A., and Srinivasan, R. (2011). "Sediment management modelling in the Blue Nile Basin using SWAT model." *Hydrology and Earth System Sciences*, 15(3), 807.
- Beven, K. J., and Kirkby, M. J. (1979). "A physically based, variable contributing area model of basin hydrology / Un modèle à base physique de zone d'appel variable de l'hydrologie du bassin versant." *Hydrological Sciences Bulletin*, 24(1), 43-69.
- Bhatta, B., Shrestha, S., Shrestha, P. K., and Talchabhadel, R. (2019). "Evaluation and application of a SWAT model to assess the climate change impact on the hydrology of the Himalayan River Basin." *CATENA*, 181, 104082.
- Bieger, K., Hörmann, G., and Fohrer, N. (2015). "Detailed spatial analysis of SWAT-simulated surface runoff and sediment yield in a mountainous watershed in China." *Hydrological Sciences Journal*, 60(5), 784-800.
- Bronsvoort, K. (2013). *Sedimentation in reservoirs: Investigating reservoir preservation options and the possibility of implementing water Injection dredging in reservoirs*.
- Bruk, S. (1985). *Methods of Computing Sedimentation in Lakes and Reservoirs. IHP-II Project A. 2.6. 1*, Unesco.
- Burn, D. H., and Simonovic, S. P. (1996). "Sensitivity of reservoir operation performance to climatic change." *Water Resources Management*, 10(6), 463-478.
- Chang, J., Wang, X., Li, Y., Wang, Y., and Zhang, H. (2018). "Hydropower plant operation rules optimization response to climate change." *Energy*, 160, 886-897.
- Chen, S.-H., and Chen, M. (2015). *Hydraulic structures*, Springer.

- Chhuon, K., Herrera, E., and Nadaoka, K. (2016). "Application of Integrated Hydrologic and River Basin Management Modeling for the Optimal Development of a Multi-Purpose Reservoir Project." *Water Resources Management*, 30(9), 3143-3157.
- Chiogna, G., Marcolini, G., Liu, W., Pérez Ciria, T., and Tuo, Y. (2018). "Coupling hydrological modeling and support vector regression to model hydropeaking in alpine catchments." *Science of The Total Environment*, 633, 220-229.
- Chu, J., Zhang, C., Fu, G., Li, Y., and Zhou, H. (2015). "Improving multi-objective reservoir operation optimization with sensitivity-informed dimension reduction."
- Costa, M. H., Botta, A., and Cardille, J. A. (2003). "Effects of large-scale changes in land cover on the discharge of the Tocantins River, Southeastern Amazonia." *Journal of Hydrology*, 283(1-4), 206-217.
- Dang, T. D., Chowdhury, A. F. M. K., and Galelli, S. (2020). "On the representation of water reservoir storage and operations in large-scale hydrological models: implications on model parameterization and climate change impact assessments." *Hydrol. Earth Syst. Sci.*, 24(1), 397-416.
- Dang, T. D., Vu, D. T., Chowdhury, A. F. M. K., and Galelli, S. (2020). "A software package for the representation and optimization of water reservoir operations in the VIC hydrologic model." *Environmental Modelling & Software*, 126, 104673.
- de Oliveira Serrão, E. A., Silva, M. T., Ferreira, T. R., de Paulo Rodrigues da Silva, V., de Salviano de Sousa, F., de Lima, A. M. M., de Ataíde, L. C. P., and Wanzeler, R. T. S. (2020). "Land use change scenarios and their effects on hydropower energy in the Amazon." *Science of The Total Environment*, 744, 140981.
- Dixon, J. A., and Hufschmidt, M. M. (1986). "Economic evaluation techniques for the environment."
- Döll, P., and Zhang, J. (2010). "Impact of climate change on freshwater ecosystems: a global-scale analysis of ecologically relevant river flow alterations." *Hydrol. Earth Syst. Sci.*, 14(5), 783-799.
- Dorber, M., May, R., and Verones, F. (2018). "Modeling Net Land Occupation of Hydropower Reservoirs in Norway for Use in Life Cycle Assessment." *Environmental science & technology*, 52(4), 2375-2384.
- Dwarakish, G. S., and Ganasri, B. P. (2015). "Impact of land use change on hydrological systems: A review of current modeling approaches." *Cogent Geoscience*, 1(1), 1115691.
- Efthymiou, N., Palt, S., Annandale, G., and Karki, P. (2017). "Rapid Assessment Tool for Sustainable Sediment Management (RESCON2): User Manual." *World Bank: Washington, DC, USA*.
- Ehsani, N., Vörösmarty, C. J., Fekete, B. M., and Stakhiv, E. Z. (2017). "Reservoir operations under climate change: storage capacity options to mitigate risk." *Journal of Hydrology*, 555, 435-446.

- Eum, H.-I., and Simonovic, S. P. (2010). "Integrated Reservoir Management System for Adaptation to Climate Change: The Nakdong River Basin in Korea." *Water Resources Management*, 24(13), 3397-3417.
- Evers, J., and Pathirana, A. (2018). "Adaptation to climate change in the Mekong River Basin: introduction to the special issue." *Climatic Change*, 149(1), 1-11.
- Faghihirad, S., Lin, B., and Falconer, R. A. (2017). "3D Layer-Integrated Modelling of Morphodynamic Processes Near River Regulated Structures." *Water Resources Management*, 31(1), 443-460.
- FAO (2016). "State of the World's Forests 2016. Forests and agriculture: Land-use challenges and opportunities." Food and Agriculture Organization of the United Nations, Rome, Italy.
- Galay, V., Okaji, T., and Ntshino, K. (1995). "Erosion from the Kulekhani Watershed, Nepal during the July 1993 Ftainstorm."
- Gao, H., Tang, Q., Shi, X., Zhu, C., Bohn, T., Su, F., Pan, M., Sheffield, J., Lettenmaier, D., and Wood, E. (2010). "Water budget record from Variable Infiltration Capacity (VIC) model."
- Gassman, P. W., Reyes, M. R., Green, C. H., and Arnold, J. G. (2007). "The soil and water assessment tool: historical development, applications, and future research directions." *Transactions of the ASABE*, 50(4), 1211-1250.
- Gassman, P. W., and Wang, Y. K. (2015). "IJABE SWAT Special Issue: Innovative modeling solutions for water resource problems." *International Journal of Agricultural and Biological Engineering*, 15(3), 1-8.
- Ginting, B. M., Harlan, D., Taufik, A., and Ginting, H. (2017). "Optimization of reservoir operation using linear program, case study of Riam Jerawi Reservoir, Indonesia." *International Journal of River Basin Management*, 15(2), 187-198.
- Haddeland, I., Lettenmaier, D. P., and Skaugen, T. (2006). "Effects of irrigation on the water and energy balances of the Colorado and Mekong river basins." *Journal of Hydrology*, 324(1), 210-223.
- Haddeland, I., Skaugen, T., and Lettenmaier, D. P. (2006). "Anthropogenic impacts on continental surface water fluxes." *Geophysical Research Letters*, 33(8).
- Haguma, D., Leconte, R., and Krau, S. (2017). "Hydropower plant adaptation strategies for climate change impacts on hydrological regime." *Canadian Journal of Civil Engineering*, 44(11), 962-970.
- Hallouz, F., Meddi, M., Mahé, G., Alirahmani, S., and Keddar, A. (2018). "Modeling of discharge and sediment transport through the SWAT model in the basin of Harraza (Northwest of Algeria)." *Water Science*, 32(1), 79-88.
- Hamman, J. J., Nijssen, B., Bohn, T. J., Gergel, D. R., and Mao, Y. (2018). "The Variable Infiltration Capacity model version 5 (VIC-5): infrastructure improvements for new applications and reproducibility." *Geosci. Model Dev.*, 11(8), 3481-3496.

- Harden, C. P. (1993). "Land Use, Soil Erosion, and Reservoir Sedimentation in an Andean Drainage Basin in Ecuador." *Mountain Research and Development*, 13(2), 177-184.
- Hasan, M. M., and Wyseure, G. (2018). "Impact of climate change on hydropower generation in Rio Jubones Basin, Ecuador." *Water Science and Engineering*, 11(2), 157-166.
- Heydari, M., Othman, F., and Qaderi, K. (2015). "Developing Optimal Reservoir Operation for Multiple and Multipurpose Reservoirs Using Mathematical Programming." *Mathematical Problems in Engineering*, 2015, 435752.
- Hidalgo, I. G., Paredes-Arquiola, J., Andreu, J., Lerma-Elvira, N., Lopes, J. E. G., and Cioffi, F. (2020). "Hydropower generation in future climate scenarios." *Energy for Sustainable Development*, 59, 180-188.
- Hiep, N. H., Luong, N. D., Viet Nga, T. T., Hieu, B. T., Thuy Ha, U. T., Du Duong, B., Long, V. D., Hossain, F., and Lee, H. (2018). "Hydrological model using ground- and satellite-based data for river flow simulation towards supporting water resource management in the Red River Basin, Vietnam." *Journal of Environmental Management*, 217, 346-355.
- Hotchkiss, R. H. (1990). "Reservoir sedimentation and sediment sluicing: Experimental and numerical analysis."
- Hotchkiss, R. H., and Huang, X. (1995). "Hydrosuction sediment-removal systems (HSRS): principles and field test." *Journal of Hydraulic Engineering*, 121(6), 479-489.
- Hrissanthou, V. (2014). "Case studies of reservoir sedimentation as a consequence of soil erosion." *Browse's Introduction to the Symptoms & Signs of Surgical Disease*, 71.
- ICOLD (2009). "Sedimentation and Sustainable Use of Reservoirs and River Systems." *Draft ICOLD Bulletin, Sedimentation Committee, ICOLD, Paris*. .
- IHA (2018). "2018 Hydropower Status Report." *International Hydropower Association: London, UK*.
- IPCC (2018). "Special Report on the impacts of global warming of 1.5 C above pre-industrial levels and related global greenhouse gas emission pathways, in the context of strengthening the global response to the threat of climate change, sustainable development, and efforts to eradicate poverty. ." *Intergovernmental Panel on Climate Change*.
- Jackson, R. B., Jobbágy, E. G., Avissar, R., Roy, S. B., Barrett, D. J., Cook, C. W., Farley, K. A., Le Maitre, D. C., McCarl, B. A., and Murray, B. C. (2005). "Trading water for carbon with biological carbon sequestration." *science*, 310(5756), 1944-1947.
- Jager, H. I., and Smith, B. T. (2008). "Sustainable reservoir operation: can we generate hydropower and preserve ecosystem values?" *River Research and Applications*, 24(3), 340-352.
- Jalowska, A. M., and Yuan, Y. (2019). "Evaluation of SWAT Impoundment Modeling Methods in Water and Sediment Simulations." *JAWRA Journal of the American Water Resources Association*, 55(1), 209-227.

- Jana, B. K., and Majumder, M. (2010). *Impact of climate change on natural resource management*, Springer Science & Business Media.
- Jiménez Cisneros, B., Oki, T., Arnell, N., Benito, G., Cogley, J., Döll, P., Jiang, T., and Mwakalila, S. (2014). "Climate change 2014: impacts, adaptation, and vulnerability. Part A: global and sectoral aspects. Contribution of working group II to the fifth assessment report of the intergovernmental panel on climate change." Cambridge University Press Cambridge, UK and New York, NY, 229-269.
- Joorabian Shooshtari, S., Shayesteh, K., Gholamalifard, M., Azari, M., Serrano-Notivol, R., and López-Moreno, J. I. (2017). "Impacts of future land cover and climate change on the water balance in northern Iran." *Hydrological Sciences Journal*, 62(16), 2655-2673.
- Jowett, I. (1984). "Sedimentation in New Zealand Hydroelectric Schemes." *Water International*, 9(4), 172-176.
- Juracek, K. E. (2015). "The aging of America's reservoirs: in-reservoir and downstream physical changes and habitat implications." *JAWRA Journal of the American Water Resources Association*, 51(1), 168-184.
- Kantoush, S. A., and Sumi, T. (2010). "River morphology and sediment management strategies for sustainable reservoir in Japan and European Alps."
- Kaura, M., Arias, M. E., Benjamin, J. A., Ourng, C., and Cochrane, T. A. (2019). "Benefits of forest conservation on riverine sediment and hydropower in the Tonle Sap Basin, Cambodia." *Ecosystem Services*, 39, 101003.
- Kawashima, S., Johndrow, T., Annandale, G., and Shah, F. (2003). "Reservoir conservation, vol. II: RESCON model and user manual." *World Bank, Washington, DC*.
- Khan, N. M., Babel, M. S., Tingsanchali, T., Clemente, R. S., and Luong, H. T. (2012). "Reservoir Optimization-Simulation with a Sediment Evacuation Model to Minimize Irrigation Deficits." *Water Resources Management*, 26(11), 3173-3193.
- Kirsch, K., Kirsch, A., and G. Arnold, J. (2002). "PREDICTING SEDIMENT AND PHOSPHORUS LOADS IN THE ROCK RIVER BASIN USING SWAT." *Transactions of the ASAE*, 45(6), 1757.
- Kondolf, G. (1997). "Hungry water: effects of dams and gravel mining on river channels. Department of landscape architecture and environmental planning." *University of California, Berkeley, California*, 94720, 533-551.
- Kondolf, G. M., Gao, Y., Annandale, G. W., Morris, G. L., Jiang, E., Zhang, J., Cao, Y., Carling, P., Fu, K., and Guo, Q. (2014). "Sustainable sediment management in reservoirs and regulated rivers: Experiences from five continents." *Earth's Future*, 2(5), 256-280.
- Kondolf, G. M., Piégay, H., and Landon, N. (2002). "Channel response to increased and decreased bedload supply from land use change: contrasts between two catchments." *Geomorphology*, 45(1), 35-51.

- Kondolf, G. M., Rubin, Z. K., and Minear, J. T. (2014). "Dams on the Mekong: Cumulative sediment starvation." *Water Resources Research*, 50(6), 5158-5169.
- Kopytkovskiy, M., Geza, M., and McCray, J. E. (2015). "Climate-change impacts on water resources and hydropower potential in the Upper Colorado River Basin." *Journal of Hydrology: Regional Studies*, 3, 473-493.
- Kumar, S., Raghuwanshi, N. S., and Mishra, A. (2015). "Identification and management of critical erosion watersheds for improving reservoir life using hydrological modeling." *Sustainable Water Resources Management*, 1(1), 57-70.
- Kummu, M., Lu, X., Wang, J., and Varis, O. (2010). "Basin-wide sediment trapping efficiency of emerging reservoirs along the Mekong." *Geomorphology*, 119(3-4), 181-197.
- Labadie, J., Baldo, M., and Larson, R. (2000). "MODSIM: Decision support system for river basin management: Documentation and user manual." *Colorado State University and US Bureau of Reclamation, Ft Collins, CO, USA*.
- Lara, P. G., Lopes, J. D., Luz, G. M., and Bonuma, N. B. (2014). "RESERVOIR OPERATION EMPLOYING HEC-RESSIM: CASE STUDY OF TUCURUÍ DAM, BRAZIL."
- Laura, M., Tartari, G., Salerno, F., Valsecchi, L., Bravi, C., Lorenzi, E., Genoni, P., and Guzzella, L. (2017). "Climate change impacts on sediment quality of Subalpine reservoirs: Implications on management." *Water*, 9(9), 680.
- Liang, X., Lettenmaier, D. P., Wood, E. F., and Burges, S. J. (1994). "A simple hydrologically based model of land surface water and energy fluxes for general circulation models." *Journal of Geophysical Research: Atmospheres*, 99(D7), 14415-14428.
- Liu, C.-M. (1992). "The effectiveness of check dams in controlling upstream channel stability in northeastern Taiwan." *Erosion, Debris Flows and Environment in Mountain Regions. IAHS Publication*, 209, 423-428.
- Liu, X., Yang, M., Meng, X., Wen, F., and Sun, G. (2019). "Assessing the Impact of Reservoir Parameters on Runoff in the Yalong River Basin using the SWAT Model." *Water*, 11(4), 643.
- Lohmann, D., NOLTE-HOLUBE, R., and RASCHKE, E. (1996). "A large-scale horizontal routing model to be coupled to land surface parametrization schemes." *Tellus A*, 48(5), 708-721.
- Lørup, J. K., Refsgaard, J. C., and Mazvimavi, D. (1998). "Assessing the effect of land use change on catchment runoff by combined use of statistical tests and hydrological modelling: Case studies from Zimbabwe." *Journal of Hydrology*, 205(3), 147-163.
- Lu, X. X., Ran, L. S., Liu, S., Jiang, T., Zhang, S. R., and Wang, J. J. (2013). "Sediment loads response to climate change: A preliminary study of eight large Chinese rivers." *International Journal of Sediment Research*, 28(1), 1-14.
- Lv, M., Hao, Z., Lin, Z., Ma, Z., Lv, M., and Wang, J. (2016). "Reservoir Operation with Feedback in a Coupled Land Surface and Hydrologic Model: A Case Study of the Huai

- River Basin, China." *JAWRA Journal of the American Water Resources Association*, 52(1), 168-183.
- Mahmood, K. (1987). "Reservoir sedimentation: impact, extent, and mitigation. Technical Report No. 5." International Bank for Reconstruction and Development, Washington, DC (USA).
- Manh, N. V., Dung, N. V., Hung, N. N., Merz, B., and Apel, H. (2014). "Large-scale suspended sediment transport and sediment deposition in the Mekong Delta." *Hydrol. Earth Syst. Sci.*, 18(8), 3033-3053.
- McColl, C., and Aggett, G. (2007). "Land-use forecasting and hydrologic model integration for improved land-use decision support." *Journal of Environmental Management*, 84(4), 494-512.
- Mekonnen, M., Keesstra, S. D., Stroosnijder, L., Baartman, J. E. M., and Maroulis, J. (2015). "Soil Conservation Through Sediment Trapping: A Review." *Land Degradation & Development*, 26(6), 544-556.
- Meng, Y., Liu, J., Leduc, S., Mesfun, S., Kraxner, F., Mao, G., Qi, W., and Wang, Z. (2020). "Hydropower Production Benefits More From 1.5 °C than 2 °C Climate Scenario." *Water Resources Research*, 56(5), e2019WR025519.
- Merz, J. E., Pasternack, G. B., and Wheaton, J. M. (2006). "Sediment budget for salmonid spawning habitat rehabilitation in a regulated river." *Geomorphology*, 76(1-2), 207-228.
- Michael, A., Schmidt, J., Enke, W., Deutschlander, T., and Malitz, G. (2005). "Impact of expected increase in precipitation intensities on soil loss - results of comparative model simulations." *Catena*, 61(2-3), 155-164.
- Morris, G. L. (2014). "Sediment Management and Sustainable Use of Reservoirs." *Modern Water Resources Engineering*, L. K. Wang, and C. T. Yang, eds., Humana Press, Totowa, NJ, 279-337.
- Morris, G. L. (2020). "Classification of Management Alternatives to Combat Reservoir Sedimentation." *Water*, 12(3), 861.
- Morris, G. L., and Fan, J. (1998). *Reservoir sedimentation handbook; design and management of dams, reservoirs, and watersheds for sustainable use*, McGraw-Hill, New York.
- Neitsch, S. L., Arnold, J. G., Kiniry, J. R., and Williams, J. R. (2011). "Soil and water assessment tool theoretical documentation version 2009." Texas Water Resources Institute.
- Neopane, H. P., Dahlhaug, O. G., and Cervantes, M. (2011). "Sediment erosion in hydraulic turbines." *Global J. of researches in Engineering, Mechanical and Mechanics engineering*, 11(6).
- O'Neal, M. R., Nearing, M. A., Vining, R. C., Southworth, J., and Pfeifer, R. A. (2005). "Climate change impacts on soil erosion in Midwest United States with changes in crop management." *Catena*, 61(2-3), 165-184.

- Oliveira, R., and Loucks, D. P. (1997). "Operating rules for multireservoir systems." *Water resources research*, 33(4), 839-852.
- Palmieri, A., Shah, F., Annandale, G., and Dinar, A. (2003). "Reservoir conservation volume I: the RESCON approach." *Washington, DC: World Bank*.
- Paskett, C. J. (1982). "Watershed Management—A Method of Decreasing Reservoir Sediment Accumulation." *Water International*, 7(2), 59-63.
- Phiri, T. L. C., and Mulungu, D. M. M. (2019). "Simulation modelling for integration of hydropower, irrigation water and water supply potentials of Lweya Basin, Malawi." *International Journal of River Basin Management*, 1-15.
- Piao, S., Friedlingstein, P., Ciais, P., de Noblet-Ducoudré, N., Labat, D., and Zaehle, S. (2007). "Changes in climate and land use have a larger direct impact than rising CO₂ on global river runoff trends." *Proceedings of the National academy of Sciences*, 104(39), 15242-15247.
- Piman, T., Cochrane, T., Arias, M., Green, A., and Dat, N. (2013). "Assessment of flow changes from hydropower development and operations in Sekong, Sesan, and Srepok rivers of the Mekong basin." *Journal of Water Resources Planning and Management*, 139(6), 723-732.
- Piman, T., Cochrane, T. A., and Arias, M. E. (2016). "Effect of Proposed Large Dams on Water Flows and Hydropower Production in the Sekong, Sesan and Srepok Rivers of the Mekong Basin." *River Research and Applications*, 32(10), 2095-2108.
- Piton, G., Carlados, S., Recking, A., Tacnet, J. M., Liébault, F., Kuss, D., Quefféléan, Y., and Marco, O. (2017). "Why do we build check dams in Alpine streams? An historical perspective from the French experience." *Earth Surface Processes and Landforms*, 42(1), 91-108.
- Pokhrel, Y., Burbano, M., Roush, J., Kang, H., Sridhar, V., and Hyndman, D. W. (2018). "A Review of the Integrated Effects of Changing Climate, Land Use, and Dams on Mekong River Hydrology." *Water*, 10(3), 266.
- Prasanchum, H., and Kangrang, A. (2018). "Optimal reservoir rule curves under climatic and land use changes for Lampao Dam using Genetic Algorithm." *KSCE Journal of Civil Engineering*, 22(1), 351-364.
- Pruski, F. F., and Nearing, M. A. (2002). "Climate-induced changes in erosion during the 21st century for eight U.S. locations." *Water Resources Research*, 38(12), 1298.
- Qin, P., Xu, H., Liu, M., Du, L., Xiao, C., Liu, L., and Tarroja, B. (2020). "Climate change impacts on Three Gorges Reservoir impoundment and hydropower generation." *Journal of Hydrology*, 580, 123922.
- Rooseboom, and Basson, G. (1997). "Dealing with reservoir sedimentation." *Water Resources Commission report*(91/97).
- Sangroula, D. P. (2009). "Hydropower development and its sustainability with respect to sedimentation in Nepal." *Journal of the Institute of Engineering*, 7(1), 56-64.

- Schleiss, A., and De Cesare, G. (2010). "Physical model experiments on reservoir sedimentation." *Journal of Hydraulic Research*, 48(EPFL-ARTICLE-151611), 54-57.
- Schleiss, A. J., Franca, M. J., Juez, C., and De Cesare, G. (2016). "Reservoir sedimentation." *Journal of Hydraulic Research*, 54(6), 595-614.
- Schmalz, B., Zhang, Q., Kuemmerlen, M., Cai, Q., Jähnig, S. C., and Fohrer, N. (2015). "Modelling spatial distribution of surface runoff and sediment yield in a Chinese river basin without continuous sediment monitoring." *Hydrological Sciences Journal*, 60(5), 801-824.
- Shafer, J. M., and Labadie, J. W. (1978). *Synthesis and calibration of a river basin water management model*, Colorado Water Resources Research Institute.
- Shrestha, A., Shrestha, S., Tingsanchali, T., Budhathoki, A., and Ninsawat, S. (2021). "Adapting hydropower production to climate change: A case study of Kulekhani Hydropower Project in Nepal." *Journal of Cleaner Production*, 279, 123483.
- Shrestha, B., Babel, M. S., Maskey, S., Griensven, A. v., Uhlenbrook, S., Green, A., and Akkharath, I. (2013). "Impact of climate change on sediment yield in the Mekong River basin: a case study of the Nam Ou basin, Lao PDR." *Hydrology and Earth System Sciences*, 17(1), 1-20.
- Shrestha, B., Babel, M. S., Maskey, S., Van Griensven, A., Uhlenbrook, S., Green, A., and Akkharath, I. (2013). "Impact of climate change on sediment yield in the Mekong River basin: A case study of the Nam Ou basin, Lao PDR." *Hydrology and Earth System Sciences*, 17(1), 1-20.
- Shrestha, B., Cochrane, T. A., Caruso, B. S., and Arias, M. E. (2018). "Land use change uncertainty impacts on streamflow and sediment projections in areas undergoing rapid development: A case study in the Mekong Basin." *Land degradation & development*, 29(3), 835-848.
- Shrestha, B. P., Duckstein, L., and Stakhiv, E. Z. (1996). "Fuzzy rule-based modeling of reservoir operation." *Journal of water resources planning and management*, 122(4), 262-269.
- Shrestha, H. S. (2012). "Application of Hydrosuction Sediment Removal System (HSRS) on Peaking Ponds." *Hydro Nepal: Journal of Water, Energy and Environment*, 11, 43-48.
- Shrestha, H. S. (2012). "Sedimentation and sediment handling in Himalayan reservoirs." PhD Thesis, Norwegian University of Science and Technology (NTNU), Trondheim, Norway.
- Shu, J., Qu, J. J., Motha, R., Xu, J. C., and Dong, D. F. (2018). "Impacts of climate change on hydropower development and sustainability: a review." *IOP Conference Series: Earth and Environmental Science*, 163, 012126.
- Smith, C., Williams, J., Nejadhashemi, A. P., Woznicki, S., and Leatherman, J. (2013). "Cropland management versus dredging: An economic analysis of reservoir sediment management." *Lake and Reservoir Management*, 29(3), 151-164.

- Sohoulande Djebou, D. C. (2018). "Assessment of sediment inflow to a reservoir using the SWAT model under undammed conditions: A case study for the Somerville reservoir, Texas, USA." *International Soil and Water Conservation Research*.
- Strand, R. I., and Pemberton, E. L. (1982). "Reservoir sedimentation technical guidelines for Bureau of Reclamation." *US Bureau of Reclamation, Denver, Colorado*, 48.
- Sumi, T., and Hirose, T. (2009). "Accumulation of sediment in reservoirs." *Water storage, transport and distribution*, 224-252.
- Sumi, T., and Kantoush, S. "Sediment management strategies for sustainable reservoir." *Proc.), Xx icold annual meeting, dams and reservoirs under changing challenges*, 353-362.
- Syvitski, J. P. M., Kettner, A. J., Peckham, S. D., and Kao, S. J. (2005). "Predicting the flux of sediment to the coastal zone: Application to the Lanyang Watershed, Northern Taiwan." *Journal of Coastal Research*, 21(3), 580-587.
- Tamene, L., Park, S., Dikau, R., and Vlek, P. (2006). "Analysis of factors determining sediment yield variability in the highlands of northern Ethiopia." *Geomorphology*, 76(1-2), 76-91.
- Tigrek, S., and Aras, T. (2011). *Reservoir sediment management*, CRC Press.
- Timalsina, N. P., Alfredsen, K. T., and Killingtveit, Å. (2015). "Impact of climate change on ice regime in a river regulated for hydropower." *Canadian Journal of Civil Engineering*, 42(9), 634-644.
- Trung, L. D., Duc, N. A., Nguyen, L. T., Thai, T. H., Khan, A., Rautenstrauch, K., and Schmidt, C. (2020). "Assessing cumulative impacts of the proposed Lower Mekong Basin hydropower cascade on the Mekong River floodplains and Delta – Overview of integrated modeling methods and results." *Journal of Hydrology*, 581, 122511.
- USACE, U. S. A. C. o. E. (2007). "HEC-ResSim reservoir system simulation user's manual version 3.0." *Institute for Water Resources, Hydrologic Engineering Center, USACE, Davis, CA*, 512.
- Van Oost, K., Govers, G., and Desmet, P. J. J. (2000). "Evaluating the effects of changes in landscape structure on soil erosion by water and tillage." *Landsc. Ecol* 15, 579-591.
- Wafae, E. H., Driss, O., Bouziane, A., and Hasnaoui, M. D. "Genetic Algorithm applied to reservoir operation optimization with emphasis on the Moroccan context." *Proc., 2016 3rd International Conference on Logistics Operations Management (GOL)*, 1-4.
- Wagena, M. B., Sommerlot, A., Abiy, A. Z., Collick, A. S., Langan, S., Fuka, D. R., and Easton, Z. M. (2016). "Climate change in the Blue Nile Basin Ethiopia: implications for water resources and sediment transport." *Climatic Change*, 139(2), 229-243.
- Wang, G., Huicai Yang, Lijing Wang, Zongxue Xu, and Xue, B. (2014). "Using the SWAT model to assess impacts of land use changes on runoff generation in headwaters." *Hydrological Processes*, 28(3), 1032-1042.

- Wang, G., Jager, H. I., Baskaran, L. M., Baker, T. F., and Brandt, C. C. (2016). "SWAT modeling of water quantity and quality in the Tennessee river basin: spatiotemporal calibration and validation." *Hydrology and Earth System Sciences Discussions*, 1-33.
- Wang, G., Mang, S., Cai, H., Liu, S., Zhang, Z., Wang, L., and Innes, J. L. (2016). "Integrated watershed management: evolution, development and emerging trends." *Journal of Forestry Research*, 27(5), 967-994.
- Wang, G., and Xia, J. (2010). "Improvement of SWAT2000 modelling to assess the impact of dams and sluices on streamflow in the Huai River basin of China." *Hydrological Processes: An International Journal*, 24(11), 1455-1471.
- Wang, L. K., and Yang, C. T. (2014). *Modern water resources engineering*, Springer Science & Business Media.
- Welde, K., and Gebremariam, B. (2017). "Effect of land use land cover dynamics on hydrological response of watershed: Case study of Tekeze Dam watershed, northern Ethiopia." *International Soil and Water Conservation Research*, 5(1), 1-16.
- White, R. (2001). *Evacuation of sediments from reservoirs*, Thomas Telford.
- Wijesekara, G. N., Gupta, A., Valeo, C., Hasbani, J. G., Qiao, Y., Delaney, P., and Marceau, D. J. (2012). "Assessing the impact of future land-use changes on hydrological processes in the Elbow River watershed in southern Alberta, Canada." *Journal of Hydrology*, 412-413, 220-232.
- Wild, T., and Loucks, D. (2012). "SedSim model: a simulation model for the preliminary screening of sediment transport and management in river basins, version 3.0: documentation and users manual." *Department of Civil and Environmental Engineering, Cornell University, Ithaca, NY USA*
- Wild, T. B., and Loucks, D. P. (2014). "Managing flow, sediment, and hydropower regimes in the Sre Pok, Se San, and Se Kong Rivers of the Mekong basin." *Water Resources Research*, 50(6), 5141-5157.
- Wischmeier, W. H., and Smith, D. D. (1978). *Predicting rainfall-erosion losses - a guide to conservation planning*, USDA Forest Service, Washington, D.C.
- Wolanco, K. W. (2012). "Watershed Management: An option to sustain dam and reservoir Function in Ethiopia." *Journal of Environmental Science and Technology*, 5(5), 262-273.2012.
- Wurbs, R. A. (1994). "Computer models for water resources planning and management." ARMY ENGINEER INST FOR WATER RESOURCES FORT BELVOIR VA.
- Wurbs, R. A. (2005). "Comparative evaluation of generalized river/reservoir system models." Texas Water Resources Institute.
- Wurbs, R. A. (2005). "Modeling river/reservoir system management, water allocation, and supply reliability." *Journal of Hydrology*, 300(1-4), 100-113.

- Xie, H., Nkonya, E., and Wielgosz, B. (2011). "Technical Note: Assessing the Risks of Soil Erosion and Small Reservoir Siltation in a Tropical River Basin in Mali Using the SWAT Model under Limited Data Condition." *Journal of Agricultural Safety and Health*, 27(6), 895.
- Xu, H., and Luo, Y. (2015). "Climate change and its impacts on river discharge in two climate regions in China." *Hydrol. Earth Syst. Sci.*, 19(11), 4609-4618.
- Xu, J. X. (2003). "Sediment flux to the sea as influenced by changing human activities and precipitation: Example of the Yellow River, China." *Environmental Management*, 31(3), 328-341.
- Yasarer, L. M. W., and Sturm, B. S. M. (2016). "Potential impacts of climate change on reservoir services and management approaches." *Lake and Reservoir Management*, 32(1), 13-26.
- Yasir, M., Hu, T., and Abdul Hakeem, S. (2020). "Simulating Reservoir Induced Lhasa Streamflow Variability Using ArcSWAT." *Water*, 12(5), 1370.
- Yesuf, H. M., Assen, M., Alamirew, T., and Melesse, A. M. (2015). "Modeling of sediment yield in Maybar gauged watershed using SWAT, northeast Ethiopia." *Catena*, 127, 191-205.
- Yu, X., Xie, X., and Meng, S. (2017). "Modeling the Responses of Water and Sediment Discharge to Climate Change in the Upper Yellow River Basin, China." *Journal of Hydrologic Engineering*, 22(12), 05017026.
- Zhang, N., He, H. M., Zhang, S. F., Jiang, X. H., Xia, Z. Q., and Huang, F. (2012). "Influence of Reservoir Operation in the Upper Reaches of the Yangtze River (China) on the Inflow and Outflow Regime of the TGR-based on the Improved SWAT Model." *Water Resources Management*, 26(3), 691-705.
- Zhong, W., Guo, J., Chen, L., Zhou, J., Zhang, J., and Wang, D. (2020). "Future hydropower generation prediction of large-scale reservoirs in the upper Yangtze River basin under climate change." *Journal of Hydrology*, 588, 125013.
- Zhu, Y.-M., Lu, X. X., and Zhou, Y. (2008). "Sediment flux sensitivity to climate change: A case study in the Longchuanjiang catchment of the upper Yangtze River, China." *Global and Planetary Change*, 60(3-4), 429-442.

CHAPTER 2. DEVELOPMENT OF A SWAT HYDROPOWER ROUTINE

2.1 Introduction

Hydropower reservoirs generate benefits by producing renewable energy that plays an essential role in the reduction of greenhouse gas emissions (Berga 2016; Kumar et al. 2011). Hydropower is generated by converting potential energy into electricity. The water balance of a catchment determines the water inflows into a reservoir, and consequently affects the hydropower generation (Yu et al. 2014). On the other hand, operations of hydropower reservoirs may alter the hydrologic regimes of rivers by shifting the seasonal flow patterns (Ngo et al. 2016; Räsänen et al. 2015), by trapping sediments upstream of dams and by increasing the sediment transport capacity downstream of dams (Kondolf et al. 2014). Therefore, accurate simulation of catchment hydrology is essential for optimal management and operation of a reservoir. A hydrological model mimics the real world system and is mainly used for predicting system behaviour and for simulations of various hydrological processes (Sorooshian et al. 2008). Nowadays, hydrological models are considered essential tools for water resource management (Devi et al. 2015). Hence, the complex interaction of reservoir operations and natural hydrological processes must be captured by a modelling system that is used to support management of catchments that include hydropower reservoirs.

As described in Chapter 1, widely used hydrological models such as SWAT and VIC have limited capability to simulate reservoir operations. The reservoir operating algorithms in these models are simple and are able to represent seasonal and inter-annual variation using monthly basis operating rules only (Zhao et al. 2016). In contrast, some examples of models that are specifically developed for reservoir operation simulations based on complex operational policies include HEC-ResSim, MODSIM and WRAP. These models have the capability to simulate multipurpose multi-reservoir operations for various water resource design

and management studies. But, reservoir sediment management models that can be used to simulate sediment inflow, accumulation and removal/passing by different management techniques are very rare and one model is the SedSim model. SedSim model is a deterministic model that predicts the temporal accumulation and depletion of sediment in hydropower reservoirs under different reservoir operations and sediment management policies (Wild and Loucks 2014). Although the SedSim model is capable of simulating reservoir operations and sediment management techniques for multiple reservoirs, it cannot simulate catchment hydrology and hence must be externally linked with a hydrological model for more comprehensive catchment management studies. Despite the existence of models for the simulation of hydropower reservoirs, these current models have limited applicability in complex catchments to concurrently simulate flows, the water balance and sediment transport for changing climate and land use. This is particularly relevant as land management, climate and land use change impact surface runoff, shift seasonal flow patterns, alter dry and wet periods and change sediment loads, which eventually affects reservoir operation (Haguma et al. 2017; Kopytkovskiy et al. 2015; Shrestha et al. 2013; Timalina et al. 2015; Wang et al. 2014; Zhang et al. 2014).

SWAT is a physically-based hydrological model initially developed to assess stream flows, sediment yield, chemical yield and nutrient processes in large catchments (Arnold et al. 1998). SWAT is extensively used around the world and it has been used to various levels of success in catchments in which hydropower development is ongoing (Chhuon et al. 2016; MRC 2011; Piman et al. 2016; Shrestha et al. 2018; Trung et al. 2020). However, SWAT lacks the capability to model complex hydropower reservoir operations and energy generation. To better understand the complex effects of hydropower operations on downstream flows, current applications in catchments have focused on externally linking SWAT with models such as HEC-ResSim and SedSim. This linked approach, however, is complex to set up and does not

allow for simulating climate change and land use change impacts on reservoir operations and sediment management simultaneously.

This chapter introduces the development, testing and implementation of a new SWAT hydropower reservoir operation and sediment management (ROSMAN) routine to simulate hydropower reservoir operation, power generation, and sediment management techniques.

2.1 Methodology

2.1.1 SWAT Model

The SWAT model is one of the ecohydrological models for the river basin scale which was developed in the early 1990s (Gassman and Wang 2015; Krysanova and White 2015). Since then, SWAT has been continuously improved, capabilities have been added and it has been applied worldwide in water resources. The model was chosen for this work due to its versatility and the fact that the source code and extensive documentation are available in the public domain.

SWAT is a physically based distributed model that operates on a daily time step (Neitsch et al. 2011). Major components of the model are weather, hydrology, sedimentation, soil temperature, crop growth, nutrients, pesticides, bacteria and algae land management practices (Arnold et al. 2013; Neitsch et al. 2011). In the SWAT model, a river basin is divided into subbasins, which are then further subdivided into hydrologic response units (HRUs) consisting of unique combinations of land use and soil characteristics based on topography. Various routines can be used to compute the relative impacts of land use, soil and weather within each HRU. More specifically, SWAT computes hydrologic processes and soil erosion and sediment yield at each HRU using the following water balance and Modified Universal Soil Loss Equation (MUSLE) (Williams 1975) equations:

$$SW_t = SW_0 + \sum_{i=1}^n (R_{day} - Q_{surf} - E_a - W_{seep} - Q_{gw}) \quad (2-1)$$

$$SY_t = 11.8 \times (Q_{surf} \times q_p \times A)^{0.56} \times K \times LS \times C \times P \quad (2-2)$$

Where, SW_t is soil water content (mm), SW_0 is initial soil water content (mm), R_{day} is daily precipitation (mm), Q_{surf} is surface runoff (mm), E_a is evapotranspiration (mm), W_{seep} is percolation (mm), and Q_{gw} is groundwater flow (mm) and; SY_t is sediment yield(metric ton/ha), q_p is peak flow rate (m^3/s), A is the area of HRU (ha), K is the soil erodibility factor (0.013 metric ton m^2 hr/(m^3 metric ton cm)), LS is the slope length and gradient factor, C is the cropping management factor, P is the erosion control practice factor.

The flow routing in the stream channels is calculated using the variable storage coefficient method (Williams 1969) or Muskingum method (Chow 1959). Additionally, sediment transport in the stream channels is given by a function of degradation and aggradation (Neitsch et al. 2011). SWAT uses the simplified version of Bagnold equation (Bagnold 1977) for sediment routing in the stream channel. The maximum load of sediment that can be transported from a channel segment is determined by the peak channel velocity (Neitsch et al. 2011).

2.1.1.1 Existing Reservoir Routine in SWAT

In SWAT, a reservoir, either man-made or naturally occurring, is an impoundment located on the main channel of the river system (Neitsch et al. 2011). SWAT provides functions to account for the mass balance of water and sediment transported into and out of a reservoir (Xie et al. 2011). A typical reservoir has an emergency spillway to control large floods safely and a principal spillway for frequent flood control. The reservoir outflow is determined based on the reservoir water balance:

$$V = V_{stored} + V_{flowin} - V_{outflow} + V_{pcp} - V_{evap} - V_{seep} \quad (2-3)$$

$$sed_{res} = sed_i + sed_{flowin} - sed_{stl} - sed_{outflow} \quad (2-4)$$

where V is the volume of water in the reservoir at the end of the simulation step (m^3), V_{stored} is the volume of water stored in the reservoir at the beginning of the simulation step (m^3), V_{flowin} is volume of water entering in the reservoir (m^3), $V_{outflow}$ is volume of water flowing out of the reservoir (m^3), V_{pep} is volume of precipitation falling on the reservoir (m^3), V_{evap} is volume of evaporated water from the reservoir (m^3) and V_{seep} is volume of water lost from the reservoir by seepage (m^3), sed_{res} is amount of sediment in the reservoir at end of the simulation step (metric tons), sed_i is amount of sediment in the reservoir (metric tons), sed_{flowin} is amount of sediment inflow to the reservoir (metric tons), sed_{stl} is amount of sediment settled (metric tons), and $sed_{outflow}$ is amount of sediment transported out of the reservoir with water outflow (metric tons).

The SWAT reservoir routine allows the user to determine $V_{outflow}$ with one of four different methods: measured daily outflow, measured monthly outflow, average annual release rate for uncontrolled reservoir and controlled outflow with target release (Figure A2-1) (Neitsch et al. 2011). In the measured daily or monthly outflow method, the reservoir outflow ($V_{outflow}$) is determined using time series data of daily or monthly outflow rate provided by the user. Contrarily, in the average annual release rate method, the reservoir releases water whenever the reservoir volume exceeds the principal spillway volume of the reservoir. In the target release method, the reservoir releases water as a function of the target storage and defined non-flood season (Jalowska and Yuan 2019). In this way, the existing SWAT reservoir routine was primarily developed for those reservoirs which have adequate measured outflow data. In addition, SWAT allows one to simulate flood control reservoirs just accounting two flood limit levels and monthly flood storage, and it is especially suitable only for small reservoirs. Thus, the applicability of SWAT for highly-regulated, large-scale reservoirs with hydropower generation capacity is limited. In order to address this limitation, we developed a new algorithm

for the SWAT reservoir routine to simulate hydropower reservoirs under predefined complex operational rules.

Furthermore, the SWAT reservoir sediment routine assumes that the suspended solid sediment settles only when the sediment concentration in the reservoir exceeds the equilibrium sediment concentration specified by the user (Neitsch et al. 2011). The amount of sediment outflow is determined based on the volume of water outflow and concentration of sediment in the reservoir. This method of calculating trap efficiency in the SWAT model is specifically formulated to model the sediment behaviour in small ponds and lakes (Haan et al. 1994).

2.1.2 Reservoir Operation and Sediment Management (ROSMAN) routine

Reservoir Operation and Sediment Management (ROSMAN) routine (explained in detail in the Appendix–1: A ROSMAN User’s Manual) is a new reservoir routine integrated in the SWAT. The routine has fundamentally two subroutines: 1) hydropower reservoir operations without considering sedimentation (HydROR) and 2) accumulation and removal of sediment under hydropower reservoir operations and sediment management techniques (ResSMan) (Figure 2-1). Thus, the user has an option to choose the simulation option between HydROR and ResSMan. The HydROR predicts energy generation and impacts on the hydrologic regime of the river due to operation of hydropower reservoirs under different policies at the river basin scale. However, the HydROR neglects the effect of sedimentation on storage capacity of reservoirs and computes the reservoir routing using the Modified Puls Method. The HydROR uses the existing sediment routing method of the SWAT to compute sediment in and out from the reservoir. In addition, the HydROR calculates water balance of a reservoir and energy generation of a hydropower plant using the predefined rule curves and plant efficiency. On the other hand, the ResSMan has the capability to estimate the accumulation of sediment and its impact on reservoir storage capacity. The ResSMan predicts the accumulation of trapped sediment using the Brune Curve (Brune 1953) method, its impacts on the storage capacity of a

reservoir, and losses in hydropower generation under user-specified operation policies. Furthermore, it allows to compute the restoration of storage capacity due to the removal of sediment by flushing and sluicing.

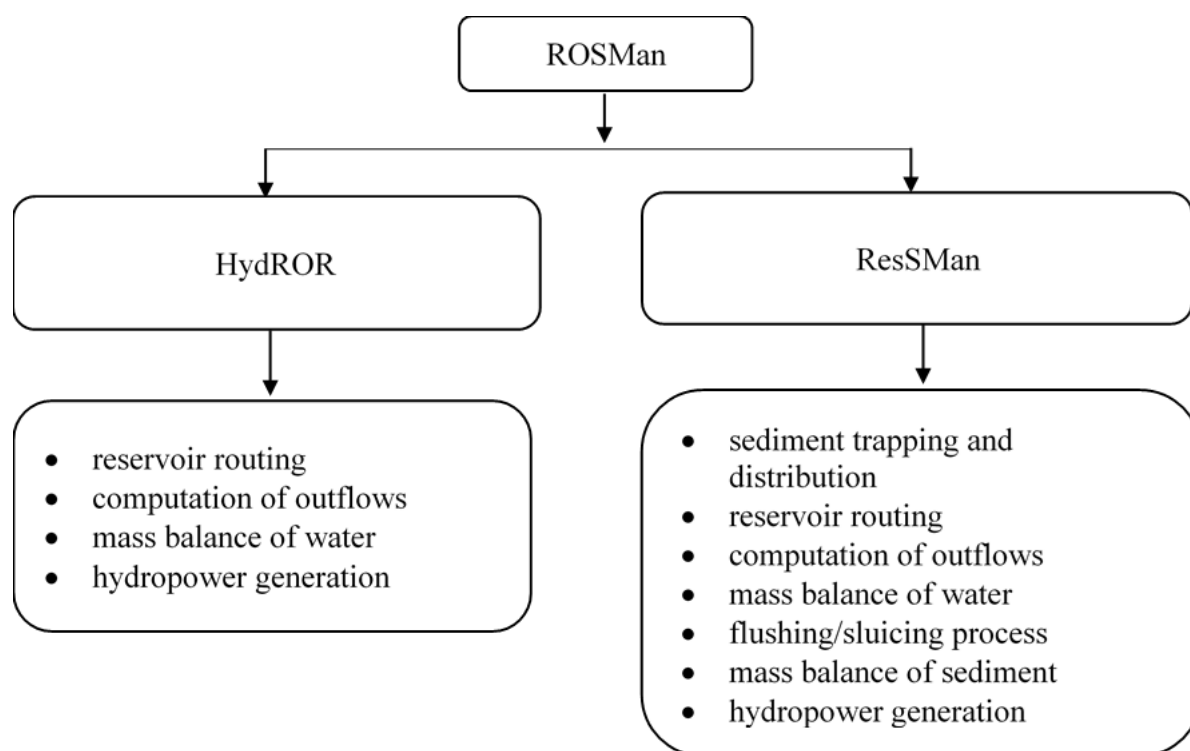


Figure 2-1: Framework of the reservoir operation and sediment management routine (ROSMan)

2.1.3 Hydropower Reservoir Operation Routine (HydROR)

A new hydropower reservoir operation routine (HydROR) was developed and integrated into SWAT. In the HydROR, the reservoir considered is a manmade structure and specifically used to generate hydropower and it replaces the existing simplified reservoir routine of the SWAT model. HydROR calculates the water balance of a reservoir and the energy generation of a hydropower plant using predefined rule curves and plant efficiency. Inflow to the reservoir, precipitation on the reservoir water surface, seepage loss and potential evapotranspiration from the reservoir are computed using existing SWAT routines.

In addition to data required for SWAT, area-elevation, volume-elevation curve, maximum/minimum operating levels, rule curves, outlet capacity curves, plant efficiency,

installed capacity, headloss coefficient and design flow of the hydropower scheme must be provided by the user. These data are readily available from hydropower scheme operators. The main function computes outflows of a reservoir using reservoir routing and rule curves. The water balance equation (Equation (2-3)) is applied to calculate the water volume of the reservoir.

In step 1 (Figure 2-2), reservoir routing is calculated using the level pool routing method (modified Puls method), which estimates the maximum outflow capacity ($V_{outflow}$) of the reservoir by solving the continuity equation (Chow 1964). The $V_{outflow}$ includes outflows from all the outlets at the simulation step. The relationship between reservoir volume, water level and outflow is established as a lookup table, combining an outflow rating curve and volume-elevation curve of the reservoir. This relationship table is used to estimate the maximum outflow capacity of the reservoir. Thus, the volume-elevation curve and the outflow rating curve (spillway rating curve) data of a reservoir must be provided for each reservoir in the basin considered. The relationship between water level and reservoir volume can be derived using topographic information of the reservoir. The outflow rating curve of a spillway is derived from hydraulic equations relating discharge and head of the spillways.

In step 2 (Figure 2-2), the final outflow (Equation (2-5) to (2-8)) of the reservoir is determined based on the operating policy using a user-defined rule curve of the reservoir because reservoirs have to be operated under various operational constraints and design restrictions. These constraints and restrictions are translated into a set of rule curves for the guidance of reservoir operators (Khan et al. 2012). In HydROR, the rule curve is defined by specifying a target water level for the first day of each month and the routine calculates daily target water levels by linear interpolation.

$$V_{check} = V_{stored} + V_{flowin} + V_{pcp} - V_{evap} - V_{seep} - V_{rule} \quad (2-5)$$

$$IF (V_{check} \leq 0), then V_{final_outflow} = 0 \quad (2-6)$$

$$IF (V_{check} \leq V_{outflow}), then V_{final_outflow} = V_{check} \quad (2-7)$$

$$IF (V_{check} > V_{outflow}), then V_{final_outflow} = V_{outflow} \quad (2-8)$$

where V_{rule} is volume of the reservoir as indicated by the rule curve for a simulation time step and V_{check} is the difference in total water volume (V) and V_{rule} . $V_{final_outflow}$ is the final outflow from the reservoir. This final outflow includes the outflows from different outlets of a reservoir:

$$V_{final_outflow} = V_{spill} + V_{tur} \quad (2-9)$$

where $V_{final_outflow}$ is the final total outflow in terms of volume of water during the day (m^3), V_{spill} is the volume of water spilling from spillway in a day (m^3) and V_{tur} is the volume of water through turbine for power generation (m^3). The discharge through a spillway is allocated using the outflow rating curve of the spillway. The turbine flow for hydropower generation depends on the design discharge for hydropower plants and operation rules.

In step 3 (Figure 2-2), power generation from the hydropower plant for every time step of simulation is calculated as in Equation (2-10) and (2-11).

$$P = \frac{\eta \times \gamma \times Q_{tur} \times H_{net}}{1000} \quad (2-10)$$

$$E = \frac{P \times \Delta t}{1000} \quad (2-11)$$

where Q_{tur} is the flow through turbine in m^3/s , η is the efficiency of power plant, γ is the specific gravity of water in KN/m^3 , H_{net} is net head for power plant in m, Δt is time step in hour, P is power production in MW and E is energy generation in GWh. The net head is calculated by taking the difference between reservoir water level and the tailrace level/turbine level of the power plant, which should be entered by a user.

In step 4 (Figure 2-2), the HydrOR updates reservoir water volume using the mass balance equation and updates water level and surface area from the volume-area-elevation curve

of the reservoir. Finally, in step 5 (Figure 2-2) the outputs (reservoir volume, level, outflow and power generation) are written to an output file.

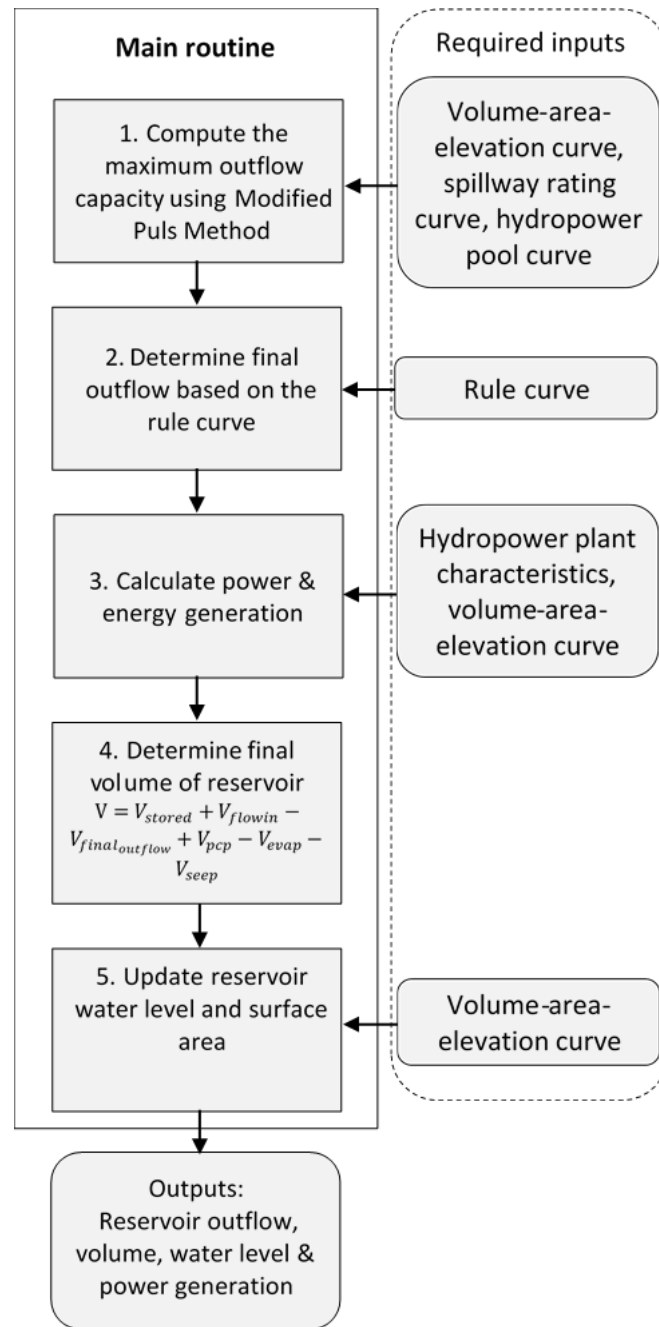


Figure 2-2: The HydROR operation framework.

2.1.4 Evaluation of the HydROR

In order to test the performance of HydROR, the HEC-ResSim model (USACE 2007), which was specifically designed by the U.S. Army Corps of Engineers Hydrologic Engineering Center to simulate multipurpose reservoirs, was used as a benchmark model for comparison

and set up utilizing the same runoff data generated by the SWAT model. The Yali reservoir (one of the oldest reservoirs in the 3S basin) was selected to compare HydrOR with HEC-ResSim for the time period between 1986 and 2008. Yali is located in a tributary of the Sesan River in Vietnam, about 70 km upstream of the border with Cambodia (Figure A2-2). The total catchment area at the Yali reservoir is 7445 km² and the dam operates between 515 m.a.s.l. to 490 m.a.s.l., with a maximum power generating capacity of 720 MW.

2.1.5 SWAT with HydrOR and HEC-ResSim Model Simulation

The SWAT model of the Yali reservoir consists of one subbasin and one HRU to illustrate a simple model setup and output analysis. The input data for the SWAT model includes one land use type, one soil layer, topography (digital elevation map) and daily weather data. Additional data which are essential for the application of SWAT with HydrOR and HEC-ResSim include the volume-area-elevation curve, hydroplant pool curve, spillway rating curve, rule curve and hydropower plant characteristics (design discharge, minimum operating level, full supply level, installed capacity, tailwater/turbine level, plant efficiency, headloss coefficient) (Figure A2-3 and Table A2-1).

In addition to input flow from SWAT, the operation of a reservoir is primarily determined by the rule curve. Both HydrOR and HEC-ResSim always attempt to bring the level of the reservoir as close as possible to the rule curve by obeying the operation rules.

The rule curve used for both HydrOR and HEC-ResSim (Figure A2-3d) is typical of tropical seasonal systems, with the ability to store water in the wet season by reducing spillage and release water to generate energy during the dry season. When the reservoir level is below the level of 490 m.a.s.l. in the month of June, the hydropower station stops producing energy, and when the water level is greater than 515 m.a.s.l., the reservoir starts spilling all the excess volume of water (Calvo Gobbetti 2018). Thus, the main objective of this rule curve is to

maximize energy production. Furthermore, selection of other types of rule curves and their purposes are described in the chapter 3 and 4.

2.1.6 Performance Criteria

The criteria of goodness for fit of the model were evaluated by comparing the outputs of the HydrOR routine and the HEC-ResSim model with respect to outflow, reservoir water level and power generation. Nash–Sutcliffe efficiency (NSE) (Nash and Sutcliffe 1970), which has been widely used in water resources to assess the performance of a hydrological model (Jain and Sudheer 2008), was used to evaluate the performance and is given by:

$$NSE = 1 - \frac{\sum(Q_h - Q_s)^2}{\sum(Q_h - \bar{Q}_h)^2} \quad (2-12)$$

Where, Q_h , Q_s and \bar{Q}_h are the outflow from HEC-ResSim model, outflow from HydrOR and average outflow from HEC-ResSim model in m³/s respectively. The NSE can vary from $-\infty$ to 1, whereby 1 is the perfect performance the model. NSE was recommended for two major reasons: it is very commonly used, which provides extensive information on reported values and the second reason is that Servat and Dezetter (1991) found NSE to be the best objective function for reflecting the overall fit of a hydrograph.

Moreover, the performance of HydrOR was evaluated by the RMSE-observations standard deviation ratio (RSR). RSR standardizes RMSE using the observations standard deviation, and it combines both an error index and the additional information recommended by Legates and McCabe Jr. (1999). RSR incorporates the benefits of error index statistics and includes a scaling/normalization factor, so that the resulting statistic and reported values can apply to various constituents.

$$RSR = \frac{\sqrt{\sum(Q_h - Q_s)^2}}{\sqrt{\sum(Q_h - \overline{Q_h})^2}} \quad (2-13)$$

The RSR varies from 0, which is the optimal value, to a large positive value (Moriassi et al. 2007).

The percent bias (PBIAS), a method to measure the average tendency of the simulated values to be larger or smaller than their observed values (Gupta et al. 1999), was used as well. PBIAS was selected for recommendation for several reasons: a) percent deviation of flow volume is commonly used to quantify water balance errors, b) its use can easily be extended to load errors, and c) PBIAS has the ability to clearly indicate poor model performance.

$$PBIAS = \frac{\sum(Q_h - Q_s)}{\sum(Q_h)} \times 100 \quad (2-14)$$

2.1.7 Reservoir Sediment Management routine (ResSMan)

A Reservoir Sediment Management routine (ResSMan) for hydropower reservoirs was developed and implemented into SWAT. The ResSMan is a tool to analyse the impacts of sediment deposition in the reservoir and to manage sedimentation at the project planning phase. The ResSMan has capabilities to predict the accumulation of trapped sediment, its impacts on the storage-capacity of a reservoir, and losses in hydropower generation under user-specified operation policies. Furthermore, it allows to simulate flushing and sluicing techniques and computes the restoration of storage volume due to the removal of sediment by these techniques.

Trap efficiency (TE) of a reservoir is the capacity to collect or trap sediment. The sediment deposition process and sediment distribution pattern within the reservoir is a very complex phenomenon. The TE of a reservoir depends on a number of factors such as reservoir inflow, sediment inflow, characteristics of sediment, shape and size of the reservoir, operation policy and turbidity current (Ghomeshi 1995). In ResSMan, TE is estimated using available empirical trap efficiency curves, such as the Brune curve (Brune 1953) and Churchill curve

(Churchill 1948). Brune (1953) developed a trap efficiency curve related to reservoir capacity-inflow ratio by using data of 40 normally ponded reservoirs and 4 other types of reservoirs in the USA. The Brune curve is still extensively used to estimate the trap efficiency of reservoirs and can be used for large reservoir with limited input data. The Brune curve has been shown to provide adequate long-term reservoir TE estimates for ponded reservoirs throughout the world (Morris and Fan 1998). The Brune curve, which equates “capacity to inflow ratio”, requires little input data, is simple to apply, and has been widely adopted to estimate reservoir TE (Lewis et al. 2013). The recent study by Tan et al. (2019) showed that the average error (~8%) between the calculated TEs and measured TEs were relatively small by using the Brune curve method. Therefore, Brune curve was implemented in ResSMan to estimate TE. The algebraic best fit equations to the three Brune curves as proposed by Gill (1979) for coarse-grained, medium and fine-grained sediments:

$$TE_{coarse} = \frac{\Delta t^2}{(0.994701 \times \Delta t^2 + 0.006297 \times \Delta t + 0.3 \times 10^{-5})} \quad (2-15)$$

$$TE_{medium} = \frac{\Delta t}{(0.012 + 1.02 \times \Delta t)} \quad (2-16)$$

$$TE_{fine} = \frac{\Delta t^3}{(1.02655 \times \Delta t^3 + 0.02621 \times \Delta t^2 - 0.133 \times 10^{-3} \times \Delta t + 0.1 \times 10^{-5})} \quad (2-17)$$

$$\Delta t = \frac{V}{I} \quad (2-18)$$

Where, TE is trap efficiency (for coarse, medium, and fine grained sediment), Δt is the residence time in years, V is storage capacity of the reservoir in m^3 , I is mean annual inflow volume in m^3/year .

Churchill developed a TE equation using a sedimentation index (SI), which is a ratio of the resident time to the average velocity of the river discharge.

$$SI = \frac{(V/I)^2}{L} \quad (2-19)$$

$$TE = 112 - 800 \times (0.3048 \times SI)^{-0.2} \quad (2-20)$$

Where, SI is Sedimentation Index, V is storage capacity of the reservoir (m^3), I is average daily inflow in m^3/s , L is the length of the reservoir measured from the dam wall to the most upstream impounded water at dam storage capacity (m).

The Churchill method considers only retention time and mean velocity to compute trapping efficiency, omitting other parameters affecting reservoir sedimentation. Notwithstanding its simplicity, previous studies indicate that the Churchill method appears to produce more realistic estimates of trapped sediment when compared with results obtain using Brune's approach (Borland 1971; Revel et al. 2014; Trimble and Carey 1990). Although the use of the Churchill curves may give a better prediction of TE than the Brune curves, one must first obtain the input data for calculating the sedimentation index. This is probably the reason why Brune's approach is used so extensively as opposed to that of Churchill (Verstraeten and Poesen 2000). In ResSMan, TE is estimated by the Churchill curve only during the sluicing period. During the reservoir draw down process, reservoirs are hydrologically smaller than during normal operations (Wild and Loucks 2012). Therefore, the Churchill curve can approximate more accurately passing of sediments for this condition than the Brune curve method.

Furthermore, in ResSMan, the volume of settled sediment is distributed linearly throughout the depth of the reservoir with proportion to the volume-area-elevation curve of the reservoir. ResSMan assumes that sediment is deposited equally in the reservoir at all elevations. For example, if a reservoir's total water volume is stored over 100 m of depth, when sediment is deposited ResSMan will reduce the available water storage capacity at each of the depths (i.e. reduce the cumulative water storage volume value for each elevation) in proportion to the fraction each depth represents out of the total 100 m differential. The storage capacity of the reservoir reduces accordingly due to the deposition of sediment and the reduction of storage

capacity is considered by updating the volume-area-elevation curve of the reservoir. Similarly, when flushing is simulated, deposited sediment is assumed to be removed equally from all elevations from the reservoir. For flushing, this assumption is particularly appropriate because the flushing channel extends from the upstream end of the reservoir (at the highest elevation) to the base of the dam (the lowest elevation). Thus, when flushing occurs, some sediment is likely removed from every elevation in the reservoir's profile. It is assumed that the reservoir is full of sediment when sediment is deposited up to full supply level (FSL) of the reservoir (Figure 2-3).

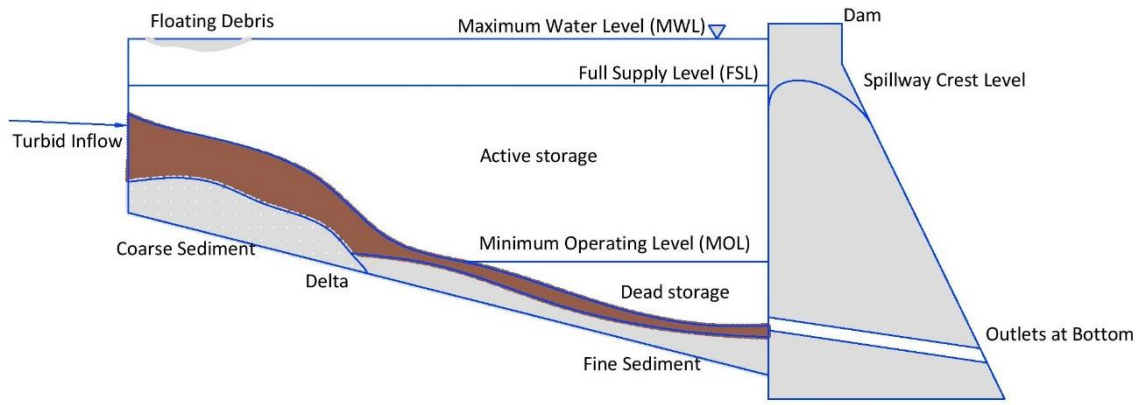


Figure 2-3: Typical reservoir features and dam components in the ResSMan routine

Once the trap efficiency has been estimated, the amount of sediment settled and outflow from the reservoir will be calculated using following equations.

$$sed_{stl} = sed_{flowin} \times TE \quad (2-21)$$

$$conc_{sed,f} = \frac{(conc_{sed,i} \times V_{stored} + sed_{flowin} - sed_{stl})}{(V_{stored} + V_{flowin})} \quad (2-22)$$

$$sed_{outflow} = (conc_{sed,f}) \times V_{outflow} \quad (2-23)$$

Where, $conc_{sed,f}$ is final sediment concentration of suspended solids (ton/m³), $conc_{sed,i}$ is initial sediment concentration of suspended solids (ton/m³), and other symbols are as described above. Finally, the mass balance equation of sediment (Equation 2-4) is used to calculate the amount of sediment (sed_{res}) in a reservoir.

2.1.7.1 Flushing Process

There are two approaches to remove sediment by flushing: 1) complete drawdown flushing and 2) partial drawdown flushing (Atkinson 1996; Palmieri et al. 2003), in this study, the complete drawdown method has been adopted because this method can remove deposited sediment more effectively than the partial drawdown method. The complete drawdown flushing method is achieved by emptying the reservoir during flood season and routing water inflow from upstream by achieving river-like flow. The process of flushing in the ResSMan comprises three phases: drawdown of water surface level, removal of sediment due to occurrence of the flushing, and refilling the reservoir (Figure A2-4). The drawdown initiates on or after the user specified initiation date of drawdown and meets the criterion of minimum reservoir inflow (Figure A2-5). The low level outlets, usually which are installed at the bottom of a dam, are opened at their full capacity to achieve the complete drawdown of the reservoir. The routine assumes the gates are opened as soon as the initiation of drawdown is initiated and closed once flushing is completed. The operation policy of reservoir routing during the drawdown phase is to achieve the river-like flow emptying the reservoir. The total water release from the reservoir is decided based on reservoir inflow, water storage during drawdown, the maximum drawdown capacity and the sum of the release capacity of all opened outlets.

It is assumed that all the sediment entering the reservoir will remain in suspension during the flushing process. This approach also has been adopted by SedSim to simplify computation. The main aim of drawdown flushing focuses on remobilizing, scouring and re-suspending deposited sediment and transporting it downstream. When low level outlets in a

dam are opened, high flow velocities are produced in the immediate vicinity of the outlet. Sediment deposits are thus scoured from a region close to the outlets. When complete drawdown is accomplished, the reservoir behaves like a river channel and at that time, the volume of the reservoir is approximately zero. Therefore, the model assumes all the entering sediment in suspension for simplification of calculations but still, in reality, some amount of sediments is being settled. Hence, there is no trapping of sediment and the concentration of the suspension sediment rises. Thus, flow with high sediment concentration is passed during release of water through the outlets. However, previously settled sediment mass cannot be removed until criteria for occurrence of flushing have been satisfied (Wild and Loucks 2012), which are

- 1) the water surface level should not exceed the maximum flushing water surface elevation and
- 2) the water release from low level outlets should be greater than the required minimum flushing flow as specified by the user.

The first criterion suggests to maintain the water surface level as low as possible to achieve the river-like open channel flow in order to increase the efficiency of the flushing (Lai and Shen 1996; Wen Shen 1999). After the complete drawdown of the reservoir, the outflow through the low level outlets should equal the river runoff, which depends on the hydrological condition of the catchment and time of operation of the flushing. Thus, the model user can define the required minimum flushing flow by analysing the historical hydrological data of the river flow. Once both criteria are met, flushing is initiated. The amount of sediment removal during the drawdown phase is equal to the concentration of sediment multiplied by the volume of water outflow. During the flushing phase, deposited sediment is assumed to be removed from portions of the volume-area-elevation curve in the same way in which the distribution of sediment deposition in the reservoir was assumed. The routine assumes that uniformly deposited sediment within the reservoir cross-sectional area can be removed only when the flushing channel attains its long term capacity ratio (LTCR). LTCR is

the ratio of the storage capacity of a reservoir that can be sustained due to flushing in the long term to the original capacity of a reservoir (Atkinson 1996).

The ResSMan has adopted the approach proposed by Atkinson (1996) and Wild et al. (2019) to compute the amount of sediment removal due to flushing (detailed in Appendix -1). During the flushing process, there is no energy generation from the hydropower plants. Once flushing has taken place for a specified duration, the flushing phase is completed, the low level outlets are closed and refilling of the reservoir begins. Once the reservoir water level rises above the minimum operating level (MOL), the reservoir operates in the normal operating policy using the specified rule curve.

2.1.7.2 *Sluicing Process*

Sluicing is the process of passing sediment by drawn downing the reservoir water level during the flood season periods and high sediment load, thereby increasing the velocity of flow while reducing residence time and trapping efficiency (Annandale et al. 2016). In ResSMan, the drawdown for sluicing initiates either on the user specified initiation date of drawdown or when the criterion of minimum reservoir inflow is met. The maximum drawdown per day can be restricted by defining the maximum drawdown rate. The minimum reservoir inflow criterion is fixed by analysing hydrology of the river. Once drawdown is initiated, the routine will try to achieve and keep the reservoir water level at target sluicing level releasing sediment-laden flow through the low level outlets. The routine assumes that the removal of sediment during sluicing is only suspended solid sediment and does not scour and remove deposited sediment. Finally, the drawdown ends either on the user specified end date of drawdown or when the criterion of minimum reservoir inflow is met.

2.1.8 Evaluation of the ResSMan

In order to test the performance of the ResSMan, the SedSim model (Wild and Loucks 2012; Wild and Loucks 2014; Wild et al. 2015), which was specifically designed to simulate

sediment transport and trapping, as well as removal of sediment from the reservoir under various sediment management techniques for hydropower reservoirs, was used as a benchmark model for evaluation of the performance of the ResSMan. In addition to three performance criteria described in the section 2.1.6, the determination of coefficient (R^2) was computed, which is a measure of the usefulness of a regression equation in the sense of comparing two models (Barrett 1974; Cheng et al. 2014). A case study application of the ResSMan was carried out for the Nam Kong 3 reservoir with a capacity of 28 MW within the Sekong River basin in Lao PDR (Figure A2-6). The simulation of flushing and sluicing was carried out on the specified date. To compare for reservoir outflow and sediment outflow from ResSMan and SedSim, ResSMan was run independently from SWAT, since SedSim cannot simulate hydrological processes and these processes may have an effect on the simulation results. Runoff and sediment inflow generated from the SWAT model were fed as input data to setup both models. Additional data which are essential for the application with ResSMan as well as for the SedSim include a volume-area-elevation curve, hydroplant pool curve, spillway rating curve, flushing gate rating curve, rule curve, and hydropower plant characteristics (design discharge, minimum operating level, full supply level, installed capacity, tailwater/turbine level, plant efficiency, headloss coefficient), flushing and sluicing specifications (Table A2-2, A2-3 and A2-4).

2.2 Results and discussions

2.2.1 Performance of HydROR

A comparison of simulated outflows from the Yali hydropower reservoir between HydROR and HEC-ResSim models shows an excellent fit for outflows, power production and water levels with NSE and R^2 values exceeding 0.99, and RSR and PBIAS values lower than 0.01 (Figure 2-4 and Figure 2-5), confirming that the new routine reproduces the HEC-ResSim results. The disagreement in some instances stems from the different interpolation methods used

by the two models. HydrOR and HEC-ResSim reproduce the operation of the reservoir equally well, as shown in Figure 2-4c when simulated water levels are compared to a given input rule curve. In this study, we have set the HEC-ResSim as a benchmark model to evaluate the capability of the HydrOR, because previous studies (Calvo Gobbetti 2018; Jebbo and Awchi 2016; Lara et al. 2014; Minville et al. 2010; Piman et al. 2013) have shown that the HEC-ResSim can simulate hydropower reservoirs according to imposed operating rule curves, predefined constraints and goals. The HydrOR, like HEC-ResSim, requires the user to enter physical properties of hydropower plants, outlet capacities, reservoir geometry and operation policies (rule curves) to realistically simulate power generation and water releases.

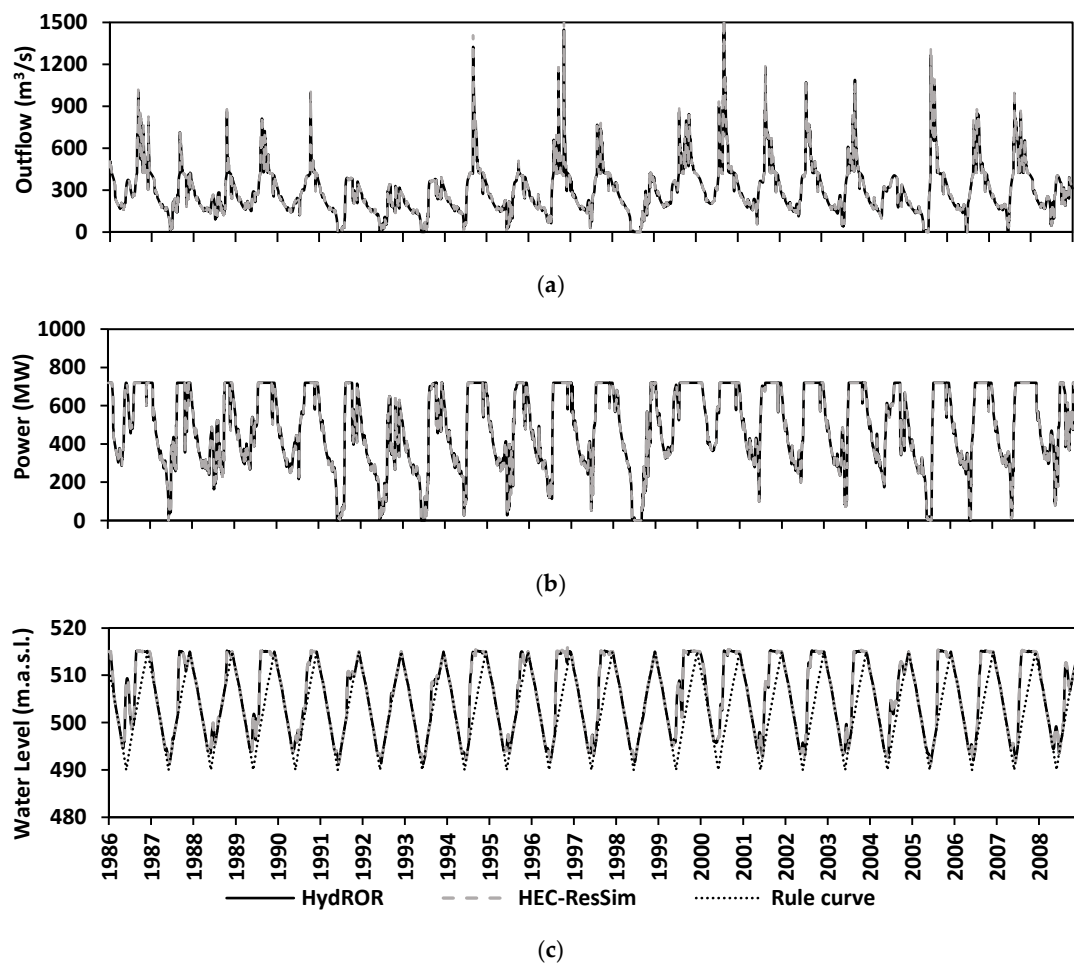


Figure 2-4: Comparison of (a) outflow from the reservoir, (b) power production and (c) reservoir water level of the Yali hydropower scheme, as determined using HydrOR and HEC-ResSim.

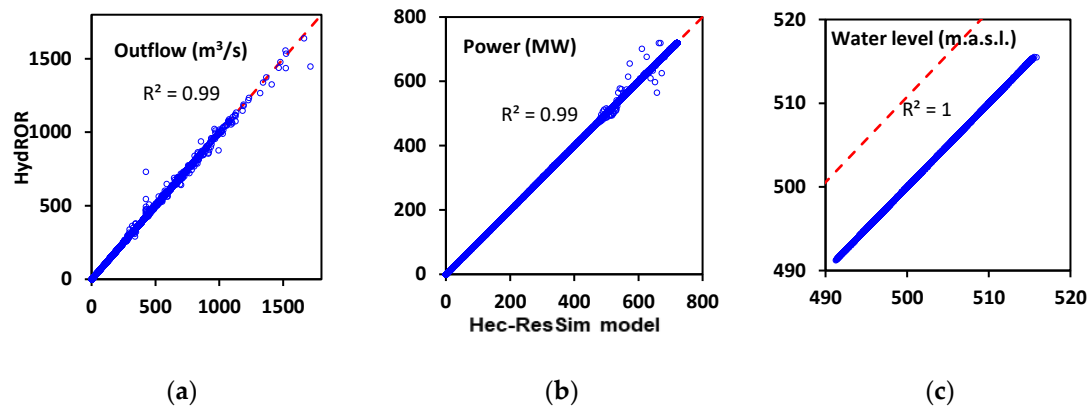


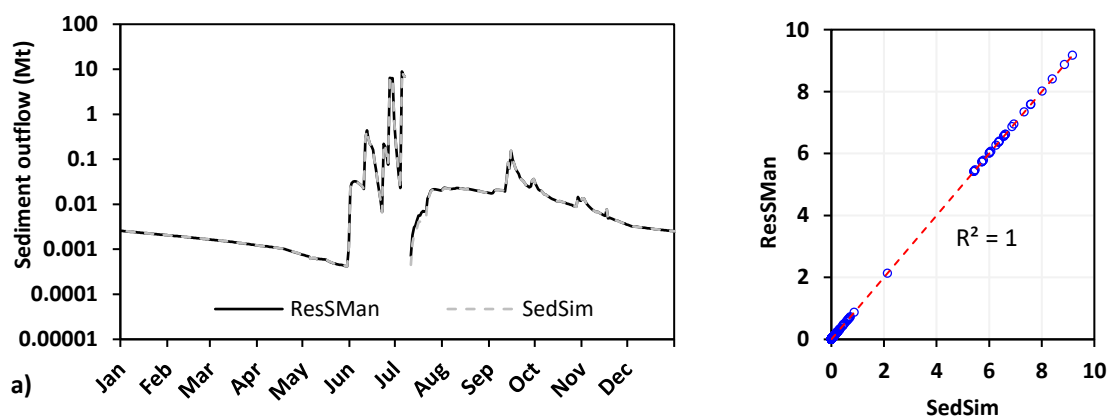
Figure 2-5: Scatter plots of (a) outflow, (b) power generation and (c) water level for HydrOR (vertical axes) and HEC-ResSim (horizontal axes).

The addition of the HydrOR to SWAT allows users to establish an integrative approach to manage hydropower production in complex reservoir systems under changing conditions, such as land use, climate change and policy. However, the HydrOR has some limitations and assumptions that simplify the computation of flows, which allow it to be applied when extensive data are not available for a basin scale level analysis. For example, the routine restricts the release of water through hydropower plant intakes and top-level spillways only and does not allow simulation of other diversion outlets (e.g., irrigation, water supply) and alternative controlled/uncontrolled outlets at various levels. The routine simulates hydropower plants assuming a constant hydropower plant efficiency and tailwater water level, and it is only able to simulate daily time steps. Moreover, sediment transportation and deposition in the reservoir are not currently simulated. Trapping of sediment reduces storage capacity of the reservoir, ultimately affects the water release capacity of the reservoir and imbalances the downstream sediment regime. Hence, future developments will focus on the addition of various level outlets and a reservoir sediment routing scheme to the routine, thereby including added functionalities to simulate different sediment management techniques (e.g., flushing and sluicing).

2.2.2 Performance of the ResSMan

The performance of the ResSMan routine was assessed by comparing results to the SedSim model for the Nam Kong 3 reservoir. The ResSMan routine and SedSim model showed a good correlation (NSE and $R^2 > 0.99$, $PBIAS$ and $RSR < 0.003$) for sediment outflow dynamics (Figure 2-6a and c) and reservoir water outflow (Figure 2-6b and d) while simulating with flushing and sluicing techniques.

The drawdown for flushing was initiated during the pre-flood period and lasted for about a month (Figure 2-6a). The reservoir was successfully restored to its original storage capacity after the application of flushing with ResSMan. Note that the actual flushing operation began only after meeting the stipulated two criteria (keeping the water level as low as maximum flushing water level and reservoir outflow should be larger than the required minimum flushing flow) and it took six days to remove the deposited sediment. In the case of sluicing, the drawdown for sluicing was initiated on 1st July for 60 days every year. Thus, during the sluicing process, the water level was maintained at the target sluicing level and a large amounts of suspended sediment load were transported by releasing high floods during flood season.



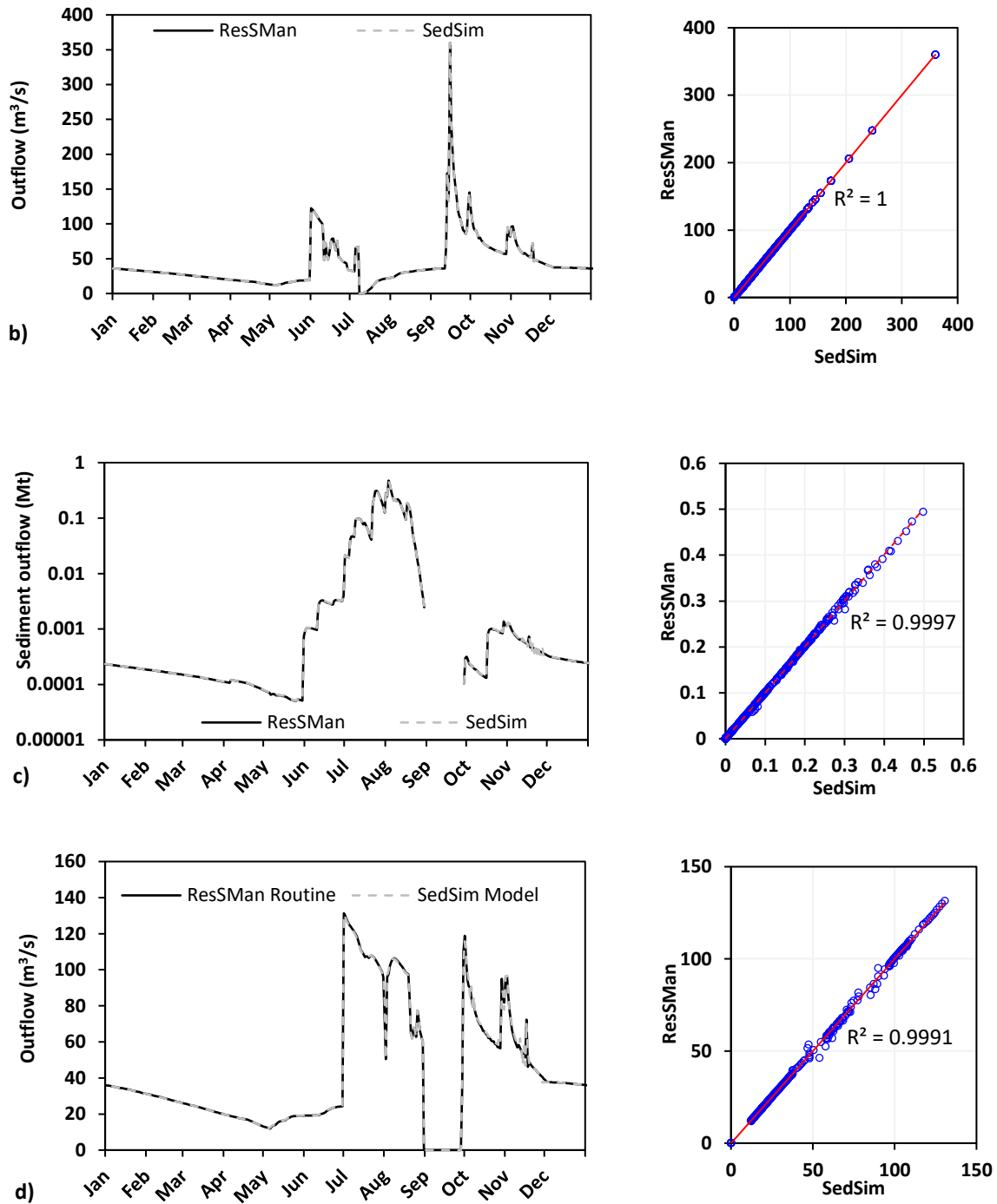


Figure 2-6: Comparison of the ResSMan routine with SedSim Model for sediment outflow (Million ton) and reservoir outflow from the reservoir due to a) and b) flushing and due to c) and d) sluicing simulation respectively.

The ResSMan fulfils the some limitations of the HydrOR by adding the capabilities to simulate various level outlets, sediment transportation and deposition in the reservoir and sediment management techniques. However, the ResSMan can be further improve by implementing various other sediment management techniques such as dredging, bypassing,

hydrosuction and density current venting. Furthermore, it has been identified that the inclusion of an optimization module will enhance to manage sedimentation effectively and maximize energy production.

2.3 Conclusions

In this chapter, a new hydropower reservoir routine was developed and integrated into the SWAT model. SWAT is used to simulate hydrological processes under different climatic conditions and land use scenarios, yet to date it has limited capabilities for reservoir operations. A new reservoir operation routine (ROSMAN), further sub-divided into the HyDROR and ResSMan, was therefore developed to simulate hydropower reservoir operations within the SWAT modelling framework.

A verification of the new routine to simulated outflow, energy production and water level of a reservoir using the HyDROR was carried out, thereby using the HEC-ResSim model to evaluate the functionality of the HyDROR. The strong agreement of outputs of the HyDROR and the HEC-ResSim model confirms that the developed model is capable of simulating operations of hydropower reservoirs under predefined rule curves.

Similarly, the performance of the ResSMan was evaluated by comparing the simulated sediment outflow due to flushing and sluicing between the ResSMan and SedSim models. The perfect correlation of the ResSMan and the SedSim model corroborates that the ResSMan has the capability to simulate sediment management techniques under user-specified inputs.

The integration of the new routine into the SWAT will allow to carry out a comprehensive application to investigate alterations in the hydrologic and sediment regime due to reservoir operations. This application will demonstrate some of the benefits of integrating the new routine in the SWAT. However, it is important to note that the developed routine is a reservoir simulation and management model. The performance of the developed routine solely

depends on user-defined physical properties of hydropower plants, outlet capacities, reservoir geometry, sediment size and density and operation policies such as rule curves. Therefore, the results of the model depend on the accuracy of the input values provided.

2.4 References

- Annandale, G. W., Morris, G. L., and Karki, P. (2016). *Extending the Life of Reservoirs*, Washington, DC: World Bank.
- Arnold, J., Kiniry, J., Srinivasan, R., Williams, J., Haney, E., and Neitsch, S. (2013). "SWAT 2012 Input/Output Documentation." Texas Water Resources Institute.
- Arnold, J. G., Srinivasan, R., Muttiah, R. S., and Williams, J. R. (1998). "Large area hydrologic modeling and assessment part I: model development." *JAWRA Journal of the American Water Resources Association*, 34(1), 73-89.
- Atkinson, E. (1996). "The feasibility of flushing sediment from reservoirs." *TDR Project R5839*, Report 0D137, HR Wallingford, UK.
- Bagnold, R. A. (1977). "Bed load transport by natural rivers." *Water Resources Research*, 13(2), 303-312.
- Barrett, J. P. (1974). "The coefficient of determination—some limitations." *The American Statistician*, 28(1), 19-20.
- Berga, L. (2016). "The Role of Hydropower in Climate Change Mitigation and Adaptation: A Review." *Engineering*, 2(3), 313-318.
- Borland, W. M. (1971). "Reservoir sedimentation." *River mechanics*, 2, 29.21-29.38.
- Brune, G. M. (1953). "Trap efficiency of reservoirs." *Eos, Transactions American Geophysical Union*, 34(3), 407-418.
- Calvo Gobbetti, L. E. (2018). "Application of HEC-ResSim® in the study of new water sources in the Panama Canal." *Journal of Applied Water Engineering and Research*, 6(3), 236-250.
- Cheng, C. L., Shalabh, and Garg, G. (2014). "Coefficient of determination for multiple measurement error models." *Journal of Multivariate Analysis*, 126, 137-152.
- Chhuon, K., Herrera, E., and Nadaoka, K. (2016). "Application of Integrated Hydrologic and River Basin Management Modeling for the Optimal Development of a Multi-Purpose Reservoir Project." *Water Resources Management*, 30(9), 3143-3157.
- Chow, V. (1959). "T. 1959 Open-Channel Hydraulics." *MCGraw Hiu*.
- Chow, V. T. (1964). *Handbook of Applied Hydrology*, McGraw-Hill, New York, N.Y.
- Churchill, M. "Discussion of "Analysis and use of reservoir sedimentation data"." *Proc., Proceedings of the Federal Interagency Sedimentation Conference. Bureau of Reclamation, US Department of the Interior, Washington, DC*, 139-140.
- Devi, G. K., Ganasri, B. P., and Dwarakish, G. S. (2015). "A review on hydrological models." *Aquatic Procedia*, 4, 1001-1007.

- Gassman, P. W., and Wang, Y. K. (2015). "IJABE SWAT Special Issue: Innovative modeling solutions for water resource problems." *International Journal of Agricultural and Biological Engineering*, 15(3), 1-8.
- Ghomeshi, M. (1995). "Reservoir sedimentation modelling." Doctor of Philosophy, University of Wollongong.
- Gill, M. A. (1979). "Sedimentation and useful life of reservoirs." *Journal of Hydrology*, 44(1), 89-95.
- Gupta, H. V., Sorooshian, S., and Yapo, P. O. (1999). "Status of Automatic Calibration for Hydrologic Models: Comparison with Multilevel Expert Calibration." *Journal of Hydrologic Engineering*, 4(2), 135-143.
- Haan, C. T., Barfield, B. J., and Hayes, J. C. (1994). *Design hydrology and sedimentology for small catchments*, Elsevier.
- Haguma, D., Leconte, R., and Krau, S. (2017). "Hydropower plant adaptation strategies for climate change impacts on hydrological regime." *Canadian Journal of Civil Engineering*, 44(11), 962-970.
- Jain, S. K., and Sudheer, K. (2008). "Fitting of hydrologic models: a close look at the Nash–Sutcliffe index." *Journal of hydrologic engineering*, 13(10), 981-986.
- Jalowska, A. M., and Yuan, Y. (2019). "Evaluation of SWAT Impoundment Modeling Methods in Water and Sediment Simulations." *JAWRA Journal of the American Water Resources Association*, 55(1), 209-227.
- Jebbo, B. E., and Awchi, T. A. (2016). "Simulation Model for Mosul Dam Reservoir Using HEC-ResSim 3.0 Package." *ZANCO Journal of Pure and Applied Sciences*, 28(2).
- Khan, N. M., Babel, M. S., Tingsanchali, T., Clemente, R. S., and Luong, H. T. (2012). "Reservoir Optimization-Simulation with a Sediment Evacuation Model to Minimize Irrigation Deficits." *Water Resources Management*, 26(11), 3173-3193.
- Kondolf, G. M., Gao, Y., Annandale, G. W., Morris, G. L., Jiang, E., Zhang, J., Cao, Y., Carling, P., Fu, K., and Guo, Q. (2014). "Sustainable sediment management in reservoirs and regulated rivers: Experiences from five continents." *Earth's Future*, 2(5), 256-280.
- Kopytkovskiy, M., Geza, M., and McCray, J. E. (2015). "Climate-change impacts on water resources and hydropower potential in the Upper Colorado River Basin." *Journal of Hydrology: Regional Studies*, 3, 473-493.
- Krysanova, V., and White, M. (2015). "Advances in water resources assessment with SWAT—an overview." *Hydrological Sciences Journal*, 60(5), 771-783.
- Kumar, A., Schei, T., Ahenkorah, A., Rodriguez, R. C., Devernay, J.-M., Freitas, M., Hall, D., Killingtveit, Å., and Liu, Z. (2011). "Hydropower." *IPCC special report on renewable energy sources and climate change mitigation*, 437-496.

- Lara, P. G., Lopes, J. D., Luz, G. M., and Bonuma, N. B. (2014). "RESERVOIR OPERATION EMPLOYING HEC-RESSIM: CASE STUDY OF TUCURUÍ DAM, BRAZIL."
- Legates, D. R., and McCabe Jr., G. J. (1999). "Evaluating the use of "goodness-of-fit" Measures in hydrologic and hydroclimatic model validation." *Water Resources Research*, 35(1), 233-241.
- Lewis, S. E., Bainbridge, Z. T., Kuhnert, P. M., Sherman, B. S., Henderson, B., Dougall, C., Cooper, M., and Brodie, J. E. (2013). "Calculating sediment trapping efficiencies for reservoirs in tropical settings: a case study from the Burdekin Falls Dam, NE Australia." *Water Resources Research*, 49(2), 1017-1029.
- Minville, M., Brissette, F., and Leconte, R. (2010). "Impacts and Uncertainty of Climate Change on Water Resource Management of the Peribonka River System (Canada)." *Journal of Water Resources Planning and Management*, 136(3), 376-385.
- Moriasi, D. N., Arnold, J. G., Van Liew, M. W., Bingner, R. L., Harmel, R. D., and Veith, T. L. (2007). "Model evaluation guidelines for systematic quantification of accuracy in watershed simulations." *Transactions of the ASABE*, 50(3), 885-900.
- Morris, G. L., and Fan, J. (1998). *Reservoir sedimentation handbook; design and management of dams, reservoirs, and watersheds for sustainable use*, McGraw-Hill, New York.
- MRC (2011). "Application of MRC modelling tools in the 3S basin." Mekong River Commission, Phnom Penh, Cambodia.
- Nash, J. E., and Sutcliffe, J. V. (1970). "River flow forecasting through conceptual models part I—A discussion of principles." *Journal of hydrology*, 10(3), 282-290.
- Neitsch, S. L., Arnold, J. G., Kiniry, J. R., and Williams, J. R. (2011). "Soil and water assessment tool theoretical documentation version 2009." Texas Water Resources Institute.
- Ngo, L. A., Masih, I., Jiang, Y., and Douven, W. (2016). "Impact of reservoir operation and climate change on the hydrological regime of the Sesan and Srepok Rivers in the Lower Mekong Basin." *Climatic Change*.
- Palmieri, A., Shah, F., Annandale, G., and Dinar, A. (2003). "Reservoir conservation volume I: the RESCON approach." *Washington, DC: World Bank*.
- Piman, T., Cochrane, T., Arias, M., Green, A., and Dat, N. (2013). "Assessment of flow changes from hydropower development and operations in Sekong, Sesan, and Srepok rivers of the Mekong basin." *Journal of Water Resources Planning and Management*, 139(6), 723-732.
- Piman, T., Cochrane, T. A., and Arias, M. E. (2016). "Effect of Proposed Large Dams on Water Flows and Hydropower Production in the Sekong, Sesan and Srepok Rivers of the Mekong Basin." *River Research and Applications*, 32(10), 2095-2108.
- Räsänen, T. A., Joffre, O. M., Someth, P., Thanh, C. T., Keskinen, M., and Kumm, M. (2015). "Model-Based Assessment of Water, Food, and Energy Trade-Offs in a Cascade of

- Multipurpose Reservoirs: Case Study of the Sesan Tributary of the Mekong River." *Journal of Water Resources Planning and Management*, 141(1), 05014007.
- Revel, N., Ranasiri, L., Rathnayake, R., and Pathirana, K. (2014). "Experimental Investigation of Sediment Trap Efficiency in Reservoirs." *Engineer: Journal of the Institution of Engineers, Sri Lanka*, 47(2).
- Servat, E., and Dezetter, A. (1991). "Selection of calibration objective fonctions in the context of rainfall-runoff modelling in a Sudanese savannah area." *Hydrological Sciences Journal*, 36(4), 307-330.
- Shrestha, B., Babel, M. S., Maskey, S., Griensven, A. v., Uhlenbrook, S., Green, A., and Akkharath, I. (2013). "Impact of climate change on sediment yield in the Mekong River basin: a case study of the Nam Ou basin, Lao PDR." *Hydrology and Earth System Sciences*, 17(1), 1-20.
- Shrestha, B., Maskey, S., Babel, M. S., van Griensven, A., and Uhlenbrook, S. (2018). "Sediment related impacts of climate change and reservoir development in the Lower Mekong River Basin: a case study of the Nam Ou Basin, Lao PDR." *Climatic Change*, 149(1), 13-27.
- Sorooshian, S., Hsu, K.-l., Coppola, E., Tomassetti, B., Verdecchia, M., and Visconti, G. (2008). *Hydrological modelling and the water cycle: coupling the atmospheric and hydrological models*, Springer Science & Business Media.
- Tan, G., Chen, P., Deng, J., Xu, Q., Tang, R., Feng, Z., and Yi, R. (2019). "Review and improvement of conventional models for reservoir sediment trapping efficiency." *Heliyon*, 5(9), e02458.
- Timalsina, N. P., Alfredsen, K. T., and Killingtveit, Å. (2015). "Impact of climate change on ice regime in a river regulated for hydropower." *Canadian Journal of Civil Engineering*, 42(9), 634-644.
- Trimble, S., and Carey, W. (1990). "A comparison of the Brune and Churchill methods for computing sediment yields applied to a reservoir system." *USGS Water Supply Paper*, 2340, 195-202.
- Trung, L. D., Duc, N. A., Nguyen, L. T., Thai, T. H., Khan, A., Rautenstrauch, K., and Schmidt, C. (2020). "Assessing cumulative impacts of the proposed Lower Mekong Basin hydropower cascade on the Mekong River floodplains and Delta – Overview of integrated modeling methods and results." *Journal of Hydrology*, 581, 122511.
- USACE, U. S. A. C. o. E. (2007). "HEC-ResSim reservoir system simulation user's manual version 3.0." *Institute for Water Resources, Hydrologic Engineering Center, USACE, Davis, CA*, 512.
- Verstraeten, G., and Poesen, J. (2000). "Estimating trap efficiency of small reservoirs and ponds: methods and implications for the assessment of sediment yield." *Progress in Physical Geography*, 24(2), 219-251.

- Wang, G., Huicai Yang, Lijing Wang, Zongxue Xu, and Xue, B. (2014). "Using the SWAT model to assess impacts of land use changes on runoff generation in headwaters." *Hydrological Processes*, 28(3), 1032-1042.
- Wild, T., and Loucks, D. (2012). "SedSim model: a simulation model for the preliminary screening of sediment transport and management in river basins, version 3.0: documentation and users manual." *Department of Civil and Environmental Engineering, Cornell University, Ithaca, NY USA*
- Wild, T. B., and Loucks, D. P. (2014). "Managing flow, sediment, and hydropower regimes in the Sre Pok, Se San, and Se Kong Rivers of the Mekong basin." *Water Resources Research*, 50(6), 5141-5157.
- Wild, T. B., Loucks, D. P., and Annandale, G. W. (2019). "SedSim: A River Basin Simulation Screening Model for Reservoir Management of Sediment, Water, and Hydropower." *Journal of Open Research Software*, 7(1).
- Wild, T. B., Loucks, D. P., Annandale, G. W., and Kaini, P. (2015). "Maintaining sediment flows through hydropower dams in the Mekong River Basin." *Journal of Water Resources Planning and Management*, 142(1), 05015004.
- Williams, J. (1975). "Sediment-Yield Prediction with Universal Equation Using Runoff."
- Williams, J. R. (1969). "Flood Routing With Variable Travel Time or Variable Storage Coefficients." *Transactions of the ASAE*, 12(1), 100-0103.
- Xie, H., Nkonya, E., and Wielgosz, B. (2011). "Technical Note: Assessing the Risks of Soil Erosion and Small Reservoir Siltation in a Tropical River Basin in Mali Using the SWAT Model under Limited Data Condition." *Journal of Agricultural Safety and Health*, 27(6), 895.
- Yu, P.-S., Yang, T.-C., Kuo, C.-M., Chou, J.-C., and Tseng, H.-W. (2014). "Climate change impacts on reservoir inflows and subsequent hydroelectric power generation for cascaded hydropower plants." *Hydrological Sciences Journal*, 59(6), 1196-1212.
- Zhang, C., Zhu, X., Fu, G., Zhou, H., and Wang, H. (2014). "The impacts of climate change on water diversion strategies for a water deficit reservoir." *Journal of Hydroinformatics*, 16(4), 872-889.
- Zhao, G., Gao, H., Naz, B. S., Kao, S.-C., and Voisin, N. (2016). "Integrating a reservoir regulation scheme into a spatially distributed hydrological model." *Advances in Water Resources*, 98, 16-31.

CHAPTER 3. APPLICATION OF THE HydROR TO ASSESSING HYDROLOGICAL ALTERATIONS

3.1 Introduction

Reservoir operations and climate change can alter natural river flow regimes. To assess impacts of climate and hydropower operations on downstream flows and energy generation, an integrated hydropower operations and catchment hydrological model is needed. The widely used hydrological model SWAT is ideal for catchment hydrology, but provides only limited reservoir operation functions. To fulfil the limitation of the SWAT and to better understand the impact of hydrological processes on hydropower operations and hydropower production, the development of the hydropower reservoir operation routine (HydROR) integrated with the SWAT was presented in Chapter 2.

In this chapter, the implementation of the HydROR to simulate hydropower reservoir operations, energy generation and their effects on flows downstream is presented. In an example application of SWAT with the HydROR, climate change impacts on energy production and hydrologic alterations due to reservoir operations were assessed for the Sesan, Srepok and Srekong (3S) subbasins of the Mekong basin. The Mekong basin is the second most biodiverse region in the world (Ziv et al. 2012), which includes 781 fish species (Baran et al. 2015). The exceptional fisheries in the basin are dependent on river flows (Thompson et al. 2014) and the annual natural flood pulse is the main driving factor of the high biodiversity (Baran et al. 2015; Junk and Wantzen 2004). The basin is undergoing rapid development and the riparian countries have been planning extensively to construct large reservoirs in the main stream, and along the tributaries of the Mekong (MRC 2019). These developments could alter the natural flow regime of the basin. Therefore, in this study, the HydROR was specifically applied to quantify hydrological alterations due to reservoir operations in the 3S basin.

3.2 Methodology

3.2.1 Study Area

The Mekong is the largest transboundary river basin in Southeast Asia with unique aquatic biodiversity (Winemiller et al. 2016; Ziv et al. 2012). The basin has a catchment area of 795,000 km² and discharges 475 km³ of water annually (MRC 2010). Originating from the Tibetan Plateau, the river flows through China, Myanmar, Laos, Thailand, Cambodia and Vietnam (Figure 3-1). The basin is undergoing rapid development and the riparian countries have been extensively planning to construct large reservoirs in the main stream, as well as along the tributaries of the Mekong (MRC 2019). The 3S rivers (Sekong, Sesan and Srepok), are the largest tributary system, thereby contributing about 20% of flow to the lower Mekong basin. The catchment area of the 3S basin is 78,650 km², of which 33% is situated in Cambodia, 29% in Lao PDR, and 38% in Vietnam. Energy demand has begun to sharply increase in the Southeast Asian region since 2000 due to growing populations, rising incomes, rapid urbanization and easy access to energy (IEA 2017). Therefore, currently hydropower reservoirs in the 3S basin are being planned and developed at a fast pace to fulfil the increasing energy demand (MRC 2010). In this study, 38 hydropower projects (Figure 3-1) were considered to investigate climate change impacts on energy production and to quantify hydrological alterations due to operation of these reservoirs. Hydropower projects were selected according to their status of progress (existing, under construction, proposed), size, location, installed capacity, development priority and data availability (Table A3-1).

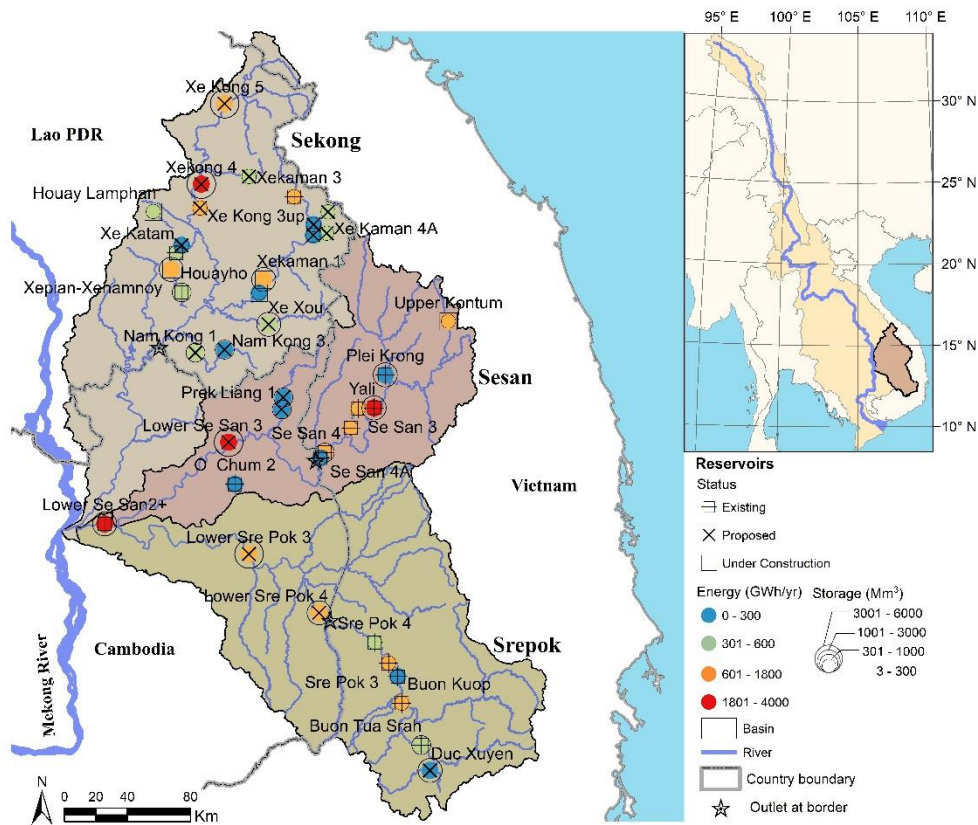


Figure 3-1: Location map showing the river network, energy production and storage capacity of each existing, proposed and under construction hydropower reservoir in the Sesan, Srepok, and Sekong (3S) river basins.

3.2.2 Hydrological Modelling

A calibrated and validated SWAT model of the 3S basin (MRC 2010; MRC 2011; Piman et al. 2013; Shrestha et al. 2016; Trang et al. 2017) was used for the HydrOR application. Input data were obtained from the Information and Knowledge Management Programme, Mekong River Commission (MRC, an inter-governmental organisation which jointly works with the governments of Cambodia, Lao PDR, Thailand and Vietnam to manage the sustainable development of the water resources of the Mekong River) (Shrestha et al. 2016). The datasets used for the SWAT model were a digital elevation model (DEM) map of 250×250 m resolution; land use types information and a land use map; and a soil map.

Meteorological data (daily maximum and minimum temperature, solar radiation, wind velocity and relative humidity data) were obtained from MRC for six stations in the 3S basin.

Temperature time series (Figure 3-2) of the 3S basin of 6 stations for 1986 - 2005 shows an annual average temperature about 23.7°C, average minimum and maximum are 20.8 °C and 26.6 °C respectively. The monthly temperature time series shows the increase in temperature from January to April and it decreases from April to July in a steeper slope than a decrease in temperature from July to December. It also reveals that the lowest temperature occurred in December and highest in April. The ranges of average annual temperature in the 3S basin were summarized in Table 3-1. The observed precipitation data provided by MRC are at the subbasin level. MRC uses the MQUAD program (Hardy 1971) to interpolate and aggregate the observed precipitation data from stations to the subbasins. The network of precipitation gauge stations in Mekong is irregularly distributed, thus MQUAD is a practical and efficient method to estimate areal rainfall by calculating a multiquadratic surface from available station data, such that the surface passes through all stations. The climate of 3S basin is monsoon-driven which is characterized by a wet season (May to October) and a dry season (November to April). The basin receives about 2600 mm of average annual rainfall, 88% of which comes during the wet season. The spatial variation of subbasin level mean annual, wet seasonal and dry seasonal precipitation shown in Figure 3-3 and Table 3-1.

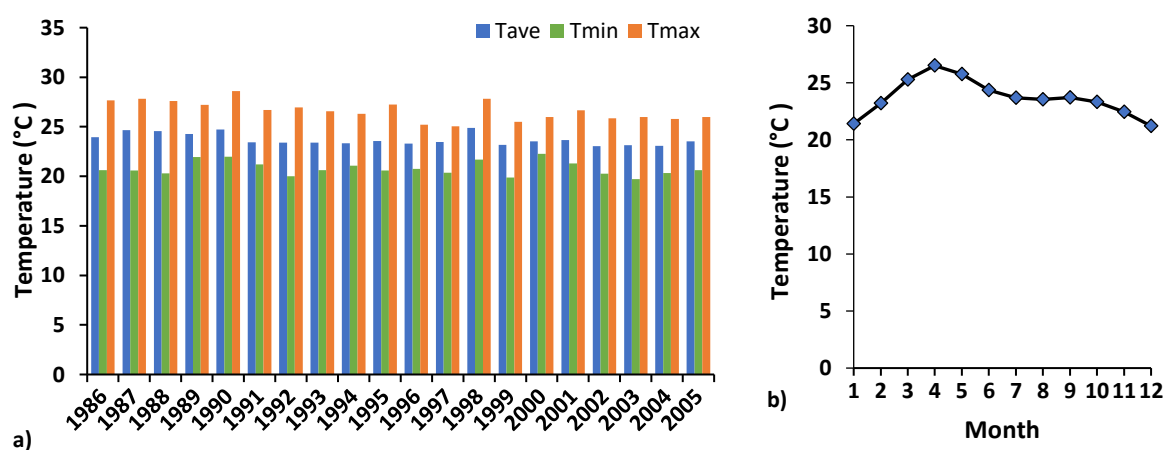


Figure 3-2: a) Average (Tave), minimum (Tmin) and maximum (Tmax) annual temperature and b) average monthly temperature for 3S basin for 1985-2005.

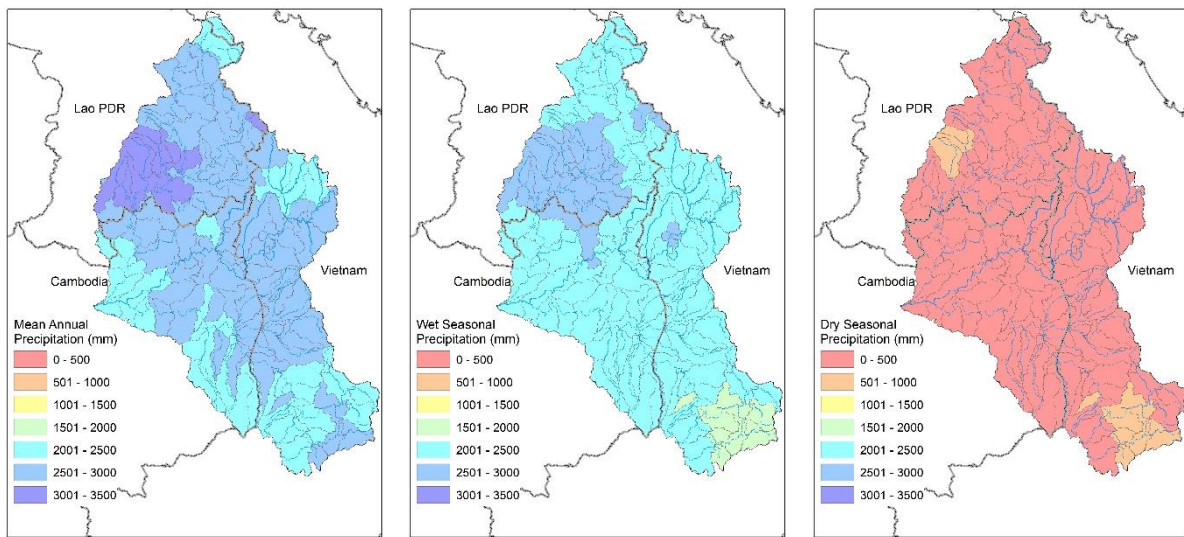


Figure 3-3: Subbasin-wise mean annual, wet seasonal and dry seasonal precipitation of the 3S basin for 1986-2005.

Table 3-1: Summary of temperature and precipitation of 3S basin

| Description | Sekong | Sesan | Srepok |
|---------------------------------------|---------|---------|---------|
| Average annual temperature range (°C) | 26 – 28 | 22 – 27 | 22 – 27 |
| Mean annual precipitation (mm) | 2774 | 2605 | 2510 |
| Wet seasonal precipitation (mm) | 2451 | 2342 | 2142 |
| Dry seasonal precipitation (mm) | 323 | 263 | 368 |

The SWAT model for 3S basin was calibrated and validated for the period 1985 to 2000 and 2001 to 2007 for observed daily discharge respectively (for details see the Appendix-3: Figure A3-1, A3-2, A3-3 and Table A3-2, A3-3, A3-4, A3-5) (Shrestha et al. 2016). The sediment load was calibrated, but not validated, because reliable and extensive measured sediment data are not available in the 3S basin (Shrestha et al. 2016). The 3S SWAT model was calibrated for monthly sediment loads with available measured total suspended solids (TSS) for the Lumphat and Bandon stations in the 3S basin. In addition, the model was calibrated for sediment loads at the 3S outlet with estimated sediment loads from the Stung Treng station nearby the 3S outlet in the Mekong River, because of the absence of measured sediment data at the 3S outlet:

$$Sed_{3S_outlet} = TSS_{Stung_Tren} \times (Flow_{Stung_Tren} - Flow_{Pakse}) \quad (3-1)$$

Where, Sed_{3S_outlet} is the sediment load at 3S outlet, TSS_{Stung_Tren} is the measured TSS at the Stung Treng station, and $Flow_{Stung_Tren}$ and $Flow_{Pakse}$ are the observed river flows at Stung Treng and Pakse stations respectively. The model calibration results have indicated that simulated flow and sediment loads were in good agreement with the observed data by resulting Nash Sutcliffe Efficiency (NSE) values of 0.66 and 0.64 for flow and sediment load for the Bandon station. The detailed results of calibration of the 3S SWAT model have been presented in Appendix-3 (Figure A3-1, A3-2, and A3-3, Table A3-2, A3-3, A3-4 and A3-5).

3.2.3 Hydropower Reservoir Simulation

HydROR has the capability to simulate complex systems of multiple hydropower reservoirs in a river basin under predefined rule curves. In this study two types of rule curves were employed: (1) the seasonal variation (SV) rule curve and (2) the full supply level (FSL) rule curve. The seasonal variation rule curve was set to optimize energy production, storing water during the wet season to allow for extended generation during the dry season. On the other hand, the FSL rule curve aims to keep the reservoir at its full supply level to simulate a more natural to ecological flow regime downstream. It allows for the release of water for generation when the water level is higher than FSL and fills the reservoir when water level is lower than FSL.

3.2.4 Climate Change Scenarios

To assess the impacts of climate change on hydropower production in the 3S basin, three general circulation models (GCMs), i.e., the Goddard Institute for Space Studies Model E2,

coupled with the Russell ocean model, with carbon cycle (GISS-E2-R-CC); the Institute Pierre-Simon Laplace Coupled Model, version 5A, coupled with NEMO, mid resolution (IPSLCM5-MR); and Geophysical Fluid Dynamics Laboratory Climate model version 3 (GFDL-CM3) were selected. Furthermore, three emissions scenarios of representative concentration pathways (RCPs), RCP2.6 (low emissions), RCP6.0 (medium emissions) and RCP8.5 (high emissions) (Table A3-6), were selected from the four resource concentration pathways developed for the IPCC 5th Assessment Report (Pachauri et al. 2014). Initially, 15 GCMs were shortlisted which were identified to be best in capturing the spatial and temporal climatic patterns of the basin and then, downsized them into three GCMs so that they still cover a wide range of uncertainty associated with plausible climate projections and the time required to do the hydrological modelling is feasible (MRC 2015). Moreover, these GCMs and emissions scenarios were selected because previous studies demonstrated that these models are reasonable for simulating the most influential climate processes in the monsoon region (MRC 2019; Shrestha et al. 2016). The period 2051–2070 was chosen for analysing the climate change impacts for the 3S basin. Previous studies (MRC 2019; Shrestha et al. 2016) indicate that this period can provide a better representation of the development of hydropower projects in the 3S basin. In this study, the climate change projections dataset of monthly change factors were applied, which are readable by SWAT model, for precipitation, temperature, solar radiation and relative humidity provided by the MRC Climate Change and Adaptation Initiative (CCAI). The method used to downscale the climate change projections dataset is described in Shrestha et al. (2016).

3.2.5 Analysing Changes Using Indicators of Hydrological Alteration (IHA Method)

The IHA (indicators of hydrological alteration) were developed by a group from The Nature Conservancy to assess impacts of human activities (e.g., reservoir operations, flow diversion or channel irrigation) on flow regimes (Richter et al. 1996). The IHA software

package computes 33 hydro-ecologically-relevant parameters based on the pre-impact and post-impact periods of streamflow data. The IHA parameters are classified into five groups characterizing the hydrologic regime with respect to magnitude of monthly flow, magnitude and duration of annual extreme events, timing of annual extremes, frequency and duration of high and low pulses and rate of change in water conditions (Table 3-2) (Richter et al. 1996; Shi et al. 2019).

Table 3-2: The 33 indicators of hydrologic alteration (IHAs) adapted from IHA Manual V7 (Richter et al. 1996; Shi et al. 2019; Timpe and Kaplan 2017; Xue et al. 2017).

| IHA Parameters Group | Hydrologic Parameters | Ecosystem Influences |
|--|--|--|
| Group 1. Magnitude of monthly water conditions (12 IHAs) | Mean or median discharge for each calendar month (m ³ /s) | Provide availability of habitat, soil moisture, water and food; access by predators to nesting sites; functional link to water temperature, oxygen levels, photosynthesis |
| Group 2. Magnitude and duration of annual extreme flows, and the base flow condition (12 IHAs) | Annual 1-, 3-, 7-, 30-, 90-day minimum flow (m ³ /s) | Creation of sites for plant colonization; structuring of river channel morphology and physical habitat conditions; nutrient exchanges between rivers and floodplains; distribution of plant communities in lakes, ponds and floodplains |
| | Annual 1-, 3-, 7-, 30-, 90-day maximum flow (m ³ /s) | |
| | Number of zero days | |
| | Base-flow index (m ³ /s) | |
| Group 3. Timing of annual extreme flow conditions (2 IHAs) | Julian date of annual 1-day minimum | Provide special habitats during reproduction or to avoid predation; influences spawning for migratory fish, evolution of life history strategies |
| | Julian date of annual 1-day maximum | |
| Group 4. Frequency and duration of high and low pulses (4 IHAs) | Number of low pulses each year | Connection to soil moisture and anaerobic stress for plants; Provide floodplain habitats; ensure nutrient and organic matter exchanges between river and floodplain, soil mineral availability Influences bedload transport, channel sediment textures and duration of substrate disturbance (high pulses) |
| | Mean duration of low pulses (days) | |
| | Number of high pulses each year | |
| | Mean duration of high pulses (days) | |
| Group 5. Rate and frequency of flow changes (3 IHAs) | Rise rate | Drought stress on plants (falling levels), Entrapment of organisms on islands, floodplains (rising levels), Desiccation stress on low-mobility stream edge (varial zone) organisms |
| | Fall rate | |
| | Number of reversals | |

Generally, observed hydrological data are used to calculate IHA parameters by dividing data period into pre-dam and post-dam periods. However, getting reliable long-term hydrological data at downstream dam sites is difficult (Shrestha et al. 2014). Using simulated data is thus the next logical choice, particularly for understanding the cumulative impacts of climate change and operation of reservoirs on hydrological alterations (Baltas 2007; Devkota and Gyawali 2015; Haguma et al. 2017; Lu et al. 2018; Middelkoop et al. 2001).

In this study, these 33 IHA parameters were used to quantify changes in the hydrologic regime due to reservoir operations and selected climate change scenarios. For every downstream dam (Figure 3-1), mean values of each IHA parameter were calculated for both pre and post-impact periods. The pre-impact flow data, which represent the natural flow regime, were obtained from SWAT simulation runs without reservoir operations using historical climate data for the period 1986–2005. The post-impact flow data were determined by simulating reservoir operations and climate change scenarios with HydROR for the period 2051–2070. The hydrological alteration (HA) values for each parameter were then calculated using the following equation (Timpe and Kaplan 2017):

$$HA\% = \frac{M_{post} - M_{pre}}{M_{pre}} \times 100 \quad (3-2)$$

Where, M_{post} is the mean for the post-impact period and M_{pre} is the mean for the pre-impact period. In addition, HA values were averaged by parameter groups and for all parameters.

3.2.6 Scenarios

Considering existing, under construction and planned hydropower reservoirs in the 3S basin, GCMs and emissions scenarios, a set of scenarios was developed to assess the impacts of climate change on hydropower production, as shown in Table 3-3. The baseline (BL) scenario does not consider reservoirs and uses the observed historical climate data for the time period from 1986–2005. Most of the existing reservoirs have been constructed after 2000 and it is assumed that by 2051 all hydropower projects selected here will be operational. Furthermore, scenarios were outlined for reservoir operations under the baseline climate (BL-R) and for three GCMs under three emissions scenarios (Table 3-3). These climate change scenarios, the GISS (“drier overall”), IPSL (“increased seasonality,” i.e., drier dry season and wetter wet season combined) and GFDL (“wetter overall”) model along with three emissions

scenarios, were specifically proposed by the MRC (MRC 2019) to assess climate change impacts on different sectors, such as domestic and industrial water consumptions, irrigation, hydropower and flood control in the Mekong basin. Therefore, these scenarios were outlined to comprehensively understand the impacts of climate change on hydropower production. Additionally, two types of rule curves were used — (1) the seasonal variation (SV) and (2) the full supply level (FSL) rule curve — for reservoir operations. The SV rule curve attempts to store water by reducing spillage during wet/flood season and release water during dry season for energy production. Thus, the main objective of the SV rule is to maximize energy production. In contrast, the FSL rule curve keeps the water level as high as the FSL of the reservoir. Thus, the reservoir acts as a run-of-the-river scheme and has the capability to maintain the downstream flow regime.

Table 3-3: Description of scenarios to assess impacts of climate change on hydropower production (where, R- simulation with reservoirs, L—low, M—medium and H—high emissions scenarios).

| Scenarios | Name | Climatic Condition | Period |
|----------------------------------|----------|---|-----------|
| Baseline (no reservoirs) | BL | Historical climate | 1986–2005 |
| Baseline (with reservoirs) | BL-R | | |
| Climate change (no reservoirs) | GISS-L | Goddard Institute for Space Studies Model | RCP2.6 |
| | GISS-M | E2, coupled with the Russell ocean model, | RCP6.0 |
| | GISS-H | with carbon cycle (GISS-E2-R-CC) | RCP8.5 |
| | IPSL-L | Institute Pierre-Simon Laplace Coupled | RCP2.6 |
| | IPSL-M | Model, version 5A, coupled with NEMO, | RCP6.0 |
| | IPSL-H | mid resolution (IPSL-CM5A-MR) | RCP8.5 |
| | GFDL-L | Geophysical Fluid Dynamics Laboratory | RCP2.6 |
| | GFDL-M | Climate model version 3 (GFDL-CM3) | RCP6.0 |
| | GFDL-H | | RCP8.5 |
| Climate change (with reservoirs) | GISS-L-R | Goddard Institute for Space Studies Model | RCP2.6 |
| | GISS-M-R | E2, coupled with the Russell ocean model, | RCP6.0 |
| | GISS-H-R | with carbon cycle (GISS-E2-R-CC) | RCP8.5 |
| | IPSL-L-R | Institute Pierre-Simon Laplace Coupled | RCP2.6 |
| | IPSL-M-R | Model, version 5A, coupled with NEMO, | RCP6.0 |
| | IPSL-H-R | mid resolution (IPSL-CM5A-MR) | RCP8.5 |
| | GFDL-L-R | Geophysical Fluid Dynamics Laboratory | RCP2.6 |
| | GFDL-M-R | Climate model version 3 (GFDL-CM3) | RCP6.0 |
| | GFDL-H-R | | RCP8.5 |

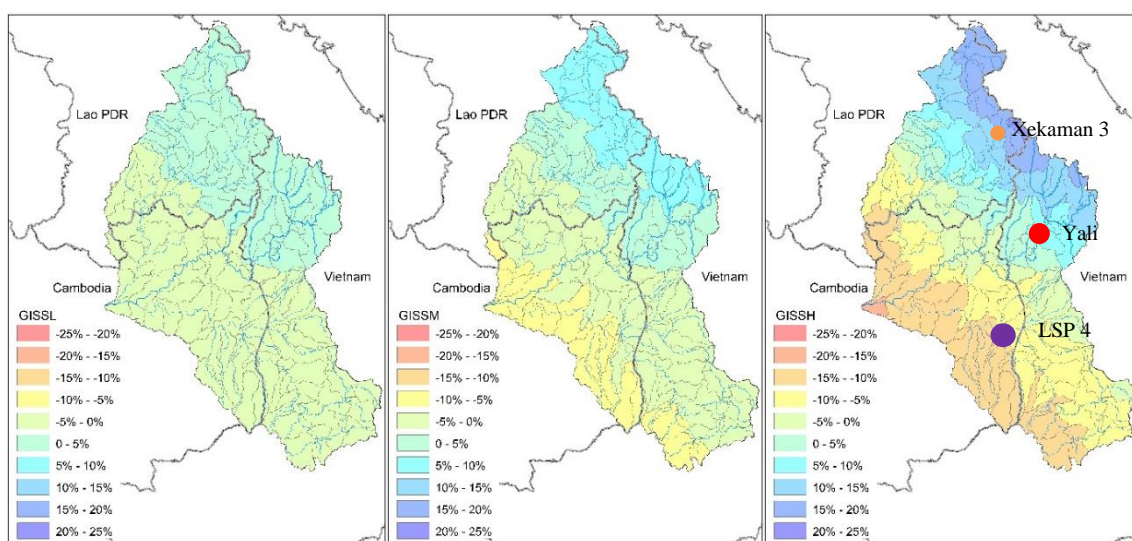
3.3 Results

3.3.1 Climate Change Impacts on Precipitation and Flow

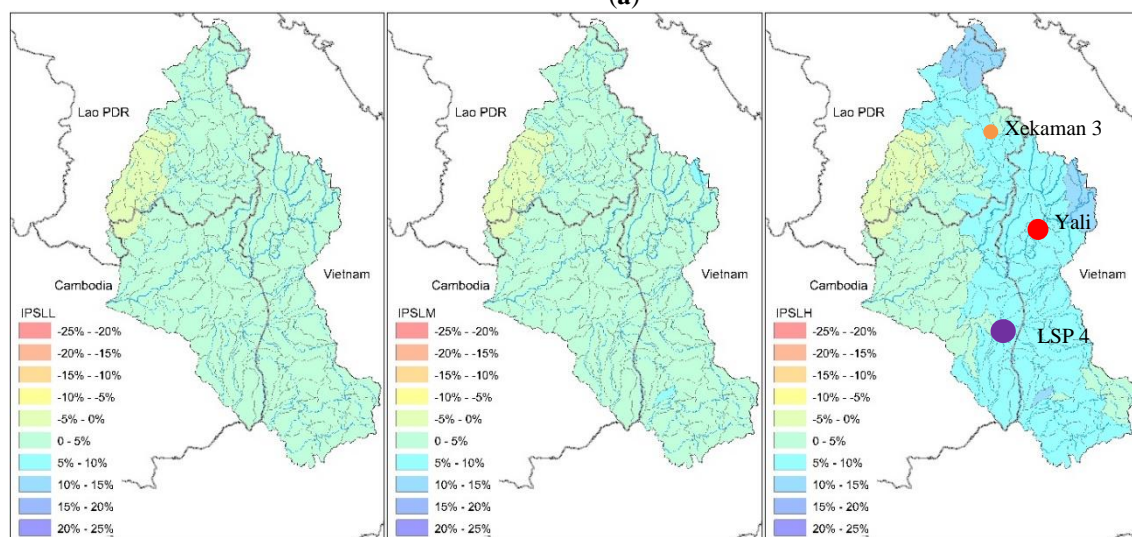
Annual average precipitation changes for the three GCMs and three emissions scenarios (L, M, H) with respect to the baseline period for the 3S basin showed significant spatial variation (Figure 3-4). According to the GISS model scenarios, annual precipitation will decrease up to 15% in the north-eastern part of the 3S basin (most of that area lies in Lao and Vietnam) and will increase up to 20% in the south-western part of the 3S basin (most of those areas lie in Cambodia). Average annual precipitation will increase up to 10% for the IPSL model scenarios, with strong spatial variations, depending on the emissions scenario. Similarly, the GFDL model scenarios also point to an increase in precipitation by 0.5–12%, yet the spatial distribution of the change in precipitation across the basin is the opposite to the distribution in the IPSL model's results. Overall average annual changes in precipitation are –0.8%, 2.8% and 4.5% under the GISS, IPSL and GFDL models for the 3S basin respectively, indicating rather low impact of climate change on the annual precipitation amount at the basin level.

The change in average annual streamflow from various GCMs (for low, medium and high emissions) at the outlet of the 3S basin is shown in Figure 3-5. The results indicate that average annual flow decreases by 6.5% for the GISS model for the high emissions scenario and increases for both IPSL and GFDL models, with a maximum increase of 6.8% at the 3S outlet.

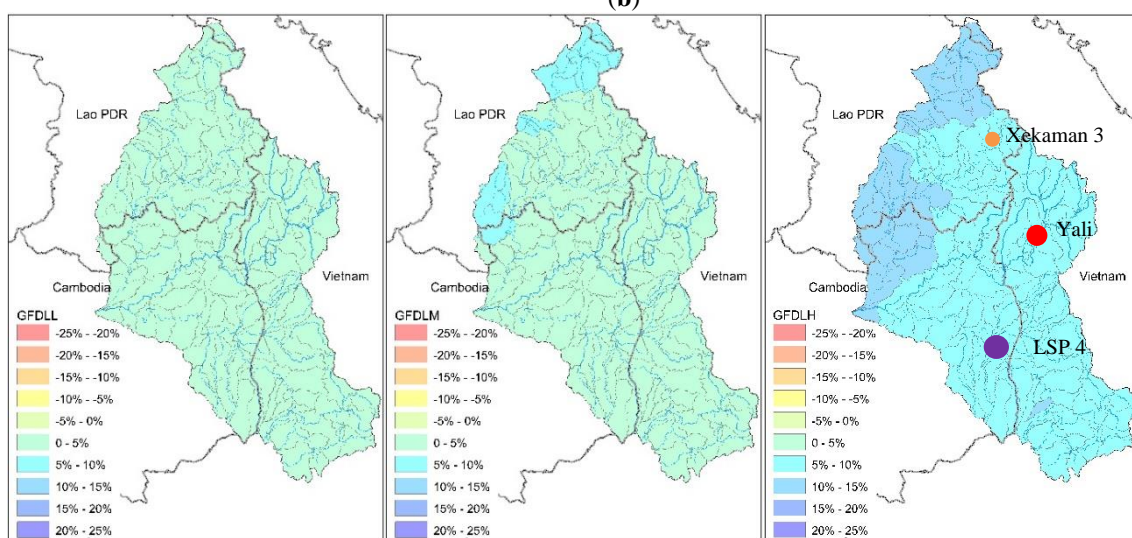
The GCMs exhibited variation in annual precipitation among the subbasins. This resulted in a predicted increases in annual flows under the IPSL and GFDL (for medium and high emissions) models and decreases in annual flows under the GISS model, which are in agreement with previous studies (Trisurat et al. 2018) of climate change projections in the lower Mekong basin. Uncertainties associated with GCMs should not be neglected (Shrestha et al. 2016).



(a)



(b)



(c)

Figure 3-4: Percentage (%) change in annual precipitation under three emissions scenarios (L—low, M—medium and H—high emissions) for GCMs: (a) GISS model, (b) IPSL model and (c) GFDL model for 2051–2070 compared to the base line climate for period 1986–2005 and location of XeKaman 3, Yali and LSP 4 for analysis of climate change impacts.

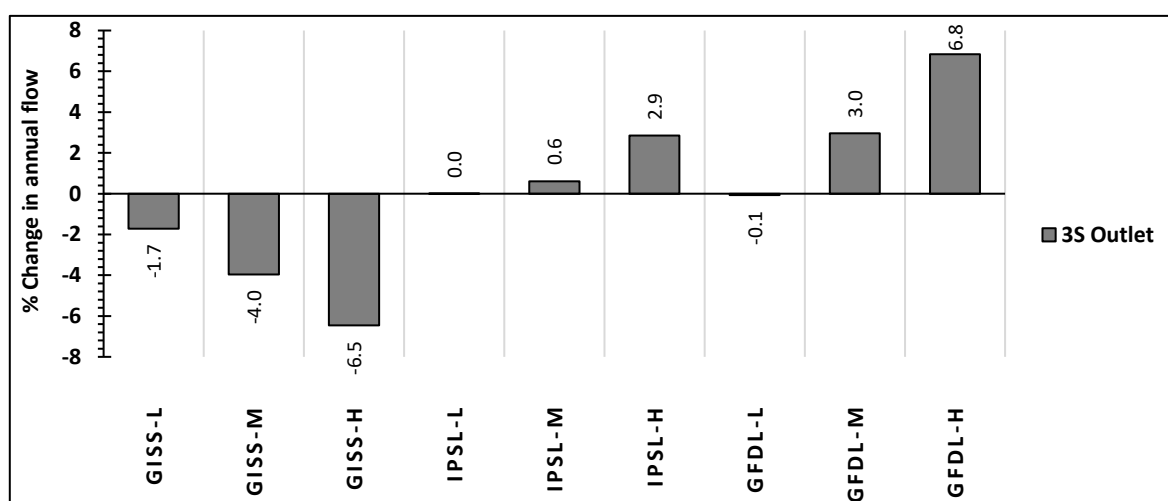


Figure 3-5: Percentage (%) change in average annual flow under three emissions scenarios (L—low, M—medium and H—high emissions) for the GISS, GFDL and IPSL models with respect to the baseline climate (BL) scenario at the 3S outlet.

3.3.2 Impacts of Operation Rules and Climate Change on Hydropower Production

The average daily hydropower production from all reservoirs for the baseline climate scenario with the seasonal variation (BL-R-SV) rule and full supply level (BL-R-FSL) rule curves are 94 and 83 GWh, respectively, i.e., an 11% difference (Figure 3-6 and Table A3-7).

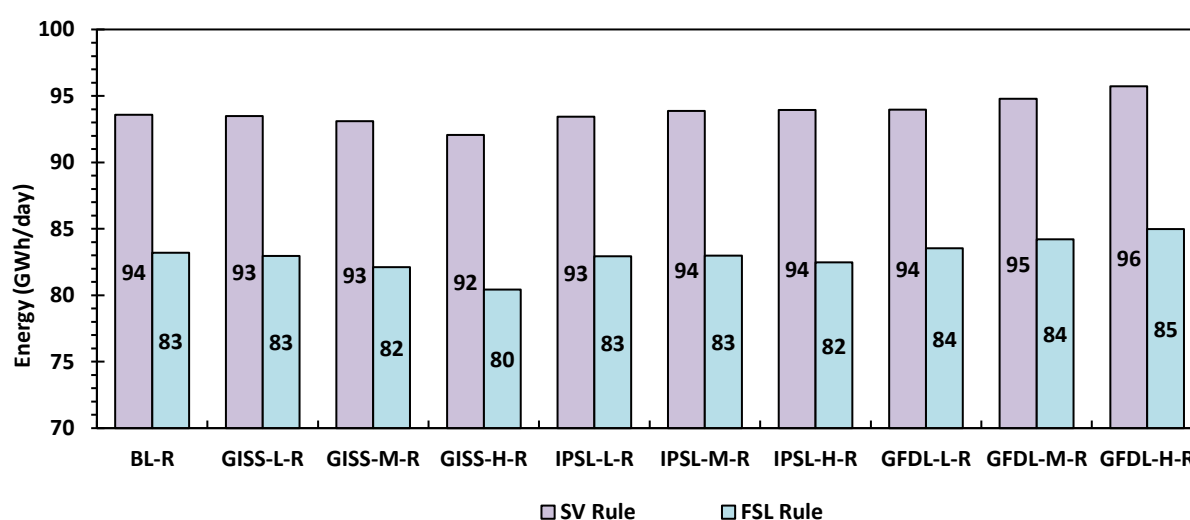


Figure 3-6: Average daily energy generation using the seasonal variation rule curve (SV rule) and full supply rule (FSL rule) curve for the baseline climate (BL-R) scenario and for each emissions scenario (L—low, M—

medium and H—high emissions) of the GISS, GFDL and IPSL models due to operation of reservoirs (R—reservoir operations).

For the climate change scenarios investigated here, the average energy production decreases slightly for the GISS model for all emission scenarios when compared with the BL-R scenario, whereas the energy production slightly increases for the GFDL model for all emissions scenarios. The energy production varies for the IPSL model for different emissions scenarios. The maximum increase in energy production is 2.3% for the GFDL model (high emissions scenario) and the maximum reduction in energy production is 1.6% for the GISS model (high emissions scenario). The average hydropower production for the 3S basin decreased 0.7% for the GISS model, and increased 0.2% and 1.3% for the IPSL and GFDL models, respectively.

The combined consideration of climate change scenarios and different rule curves revealed that energy production varies between 11% to 13% for the three GCMs, three emissions scenarios and SV and FSL rule curves (Table A3-8).

Furthermore, Laos is projected to have an up to 2% increase in energy production under the GISS model. Vietnam and Cambodia are projected to experience a maximum 3% and 6% decrease in energy production due to climate change, respectively (Figure 3-7). Considering the IPSL model, Vietnam will experience a maximum 2% increase, Cambodia will experience a maximum 1% reduction, and Laos will have an insignificant change in power production under the IPSL model. Under the GFDL model, an increase for all countries occurs except for Cambodia (low emission scenario), with the largest increase of 3% being observed in Laos (high emission scenario).

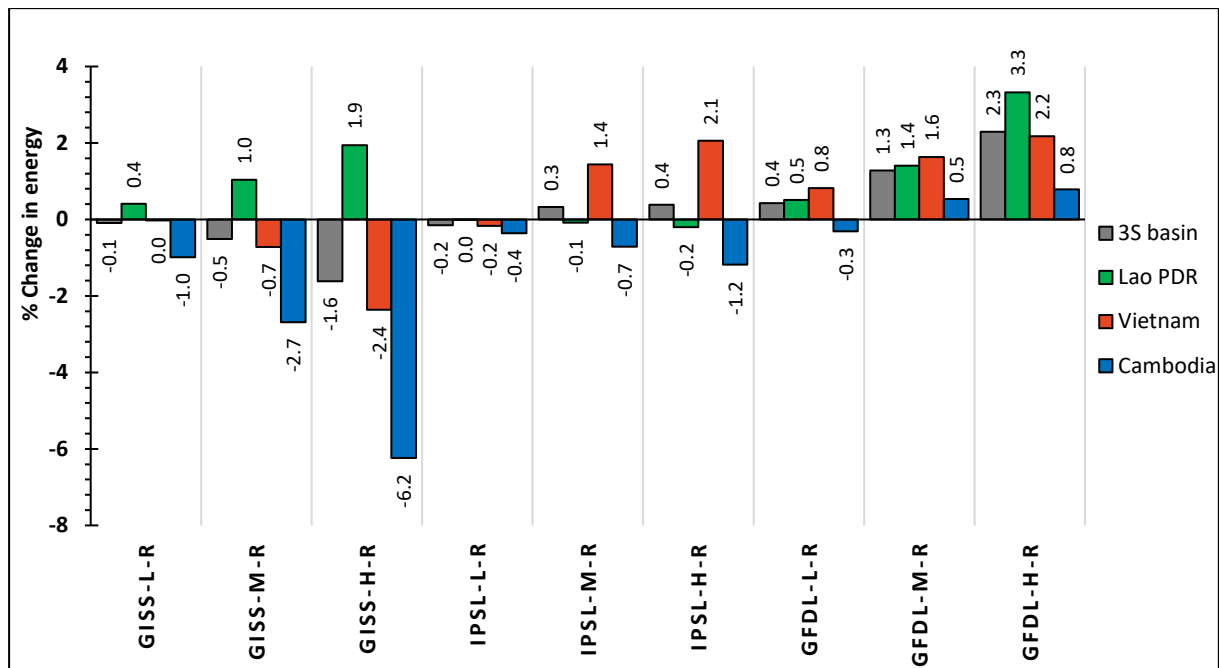


Figure 3-7: Percentage change in energy production under each emissions scenario for the GISS, GFDL and IPSL models with respect to the BL-R scenario under SV rule across the 3S basin and per country.

Furthermore, the results show that hydropower production will vary depending on the selected GCMs and the locations and size of the reservoirs (Appendix-3: Table A3-7). More detailed results of the impact of climate change on each reservoir are presented here for three reservoirs as representative reservoirs. These three reservoirs are: 1) Xekaman 3 which is a small size ($\sim 160 \text{ Mm}^3$) reservoir located in the Sekong subbasin, Laos, 2) Yali which is a medium size ($\sim 1000 \text{ Mm}^3$) reservoir located in the Sesan subbasin, Veitnam and 3) Lower Srepok 4 (LSP 4) is a large reservoir ($\sim 7500 \text{ Mm}^3$) located in the Srepok Subbasin, Cambodia (Figure 3-1 and Appendix-3: Table A3-1).

Average annual inflow and energy production are projected to increase 12% to 25% and 9% to 12% for Xekaman 3 under the GISS, IPSL and GFDL models respectively (Figure 3-6a). The results show a high increase in wet seasonal flow under all three GCMs, however, showed a very small decrease in inflow during April to May only for the IPSL model. The increase in wet seasonal flows helped to keep the reservoir water level at its FSL for a longer duration i.e. could store water during wet season (Figure 3-9a). The results revealed that the impact of

change in inflows significant for the small size Xekaman 3 reservoir. Similarly, in the case of the Yali reservoir, the impacts of climate change on inflows and energy production showed the same pattern as on Xekaman 3 but a change in energy is smaller (2% to 3%) (Figure 3-8b). This may be due to its large size and variation in seasonal flows. In the case of LSP 4, inflows and energy production will decrease significantly under the GISS model. The predicted monthly inflows in dry season are very low under the GISS model compared to the baseline climatic scenario, since the GCM forecasted a significant decrease (20% to 10%) in precipitation in LSP 4 catchment (Figure 3-3a). Although the reservoir is very large in size, the reservoir could not drawdown at the required water level to generate maximum installed capacity from May to August due to the restriction of the rule curve (Figure 3-9c). However, climate change impact can be reduced to some extent modifying the rule curve for specified GCMs and maximize the energy production. There will be a decrease in energy production from LSP 4 even if an increase in inflow under the IPSL model. This is because of a decrease in dry seasonal flow and consequently a decrease in dry seasonal energy. After all, the results showed that the impacts of climate change varies depending on the GCMs and hydropower reservoirs.

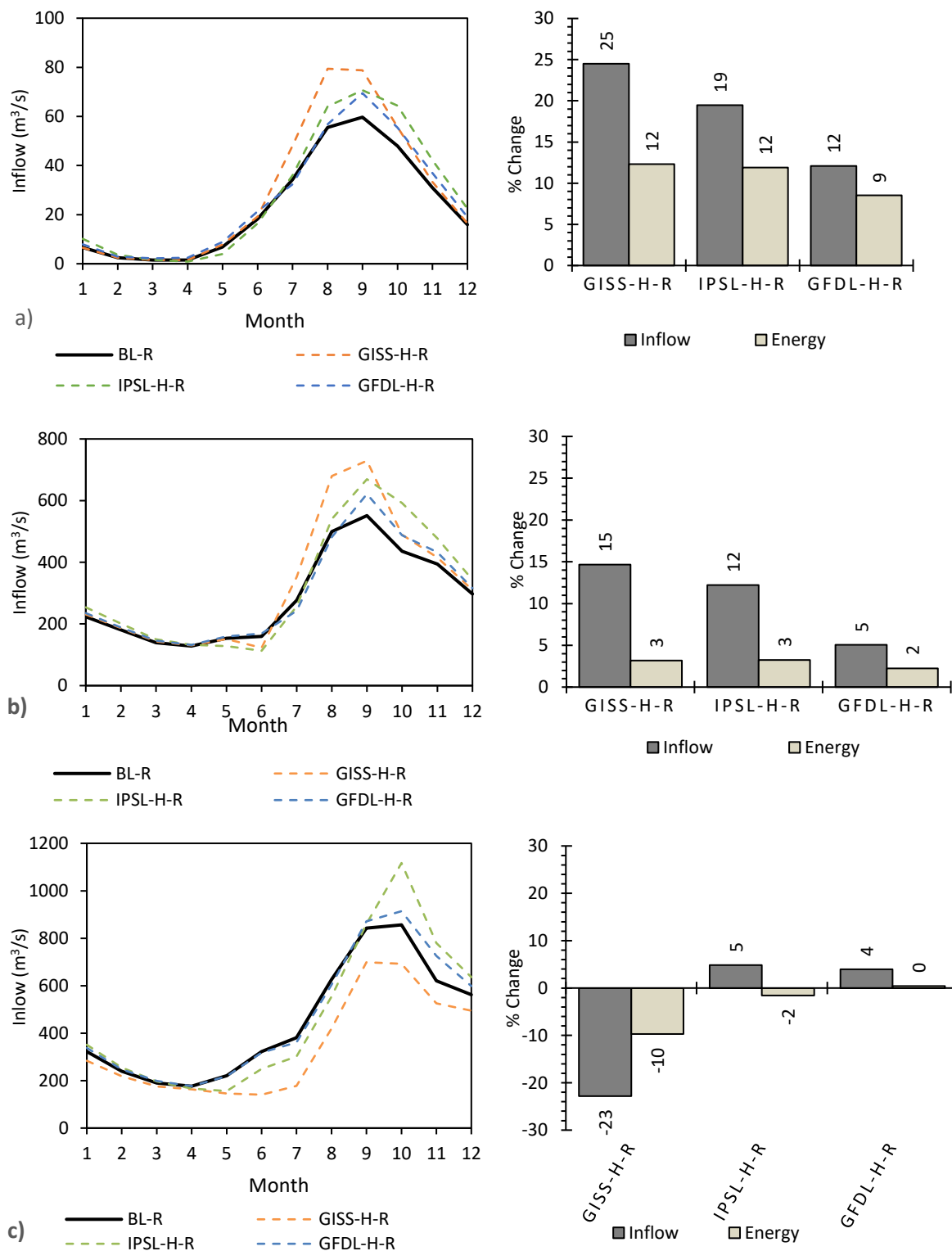


Figure 3-8: Mean monthly inflow (left), and percentage change in average annual inflow and average energy production (right) for baseline and higher emissions climate change scenarios under SV rule curves for a) Xekaman 3, b) Yali and c) LSP 4.

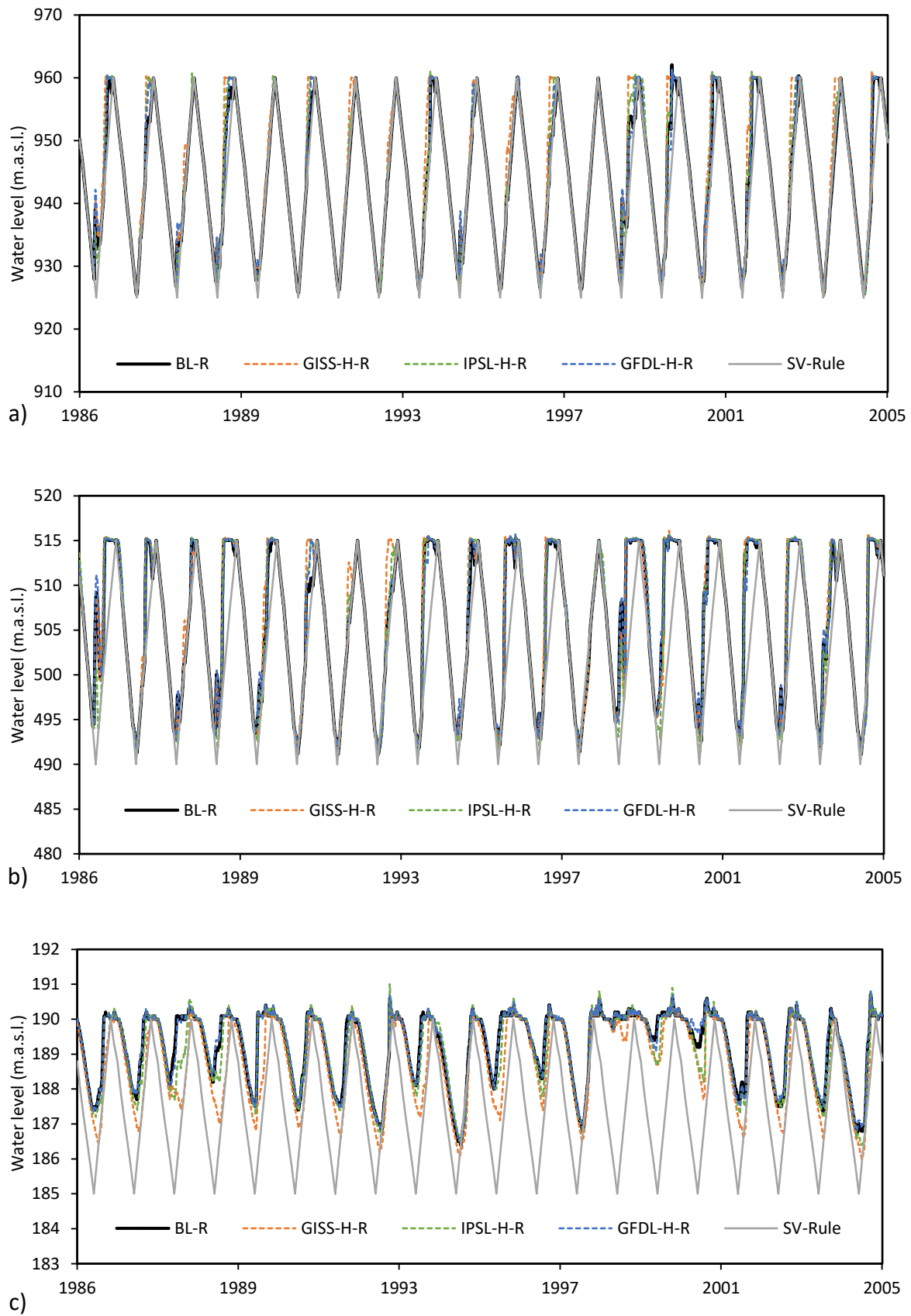
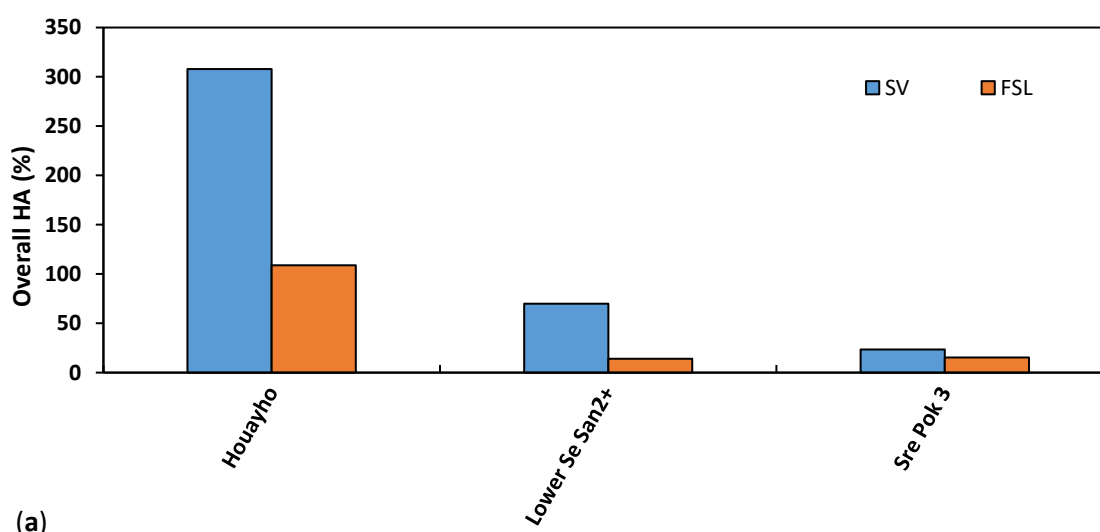
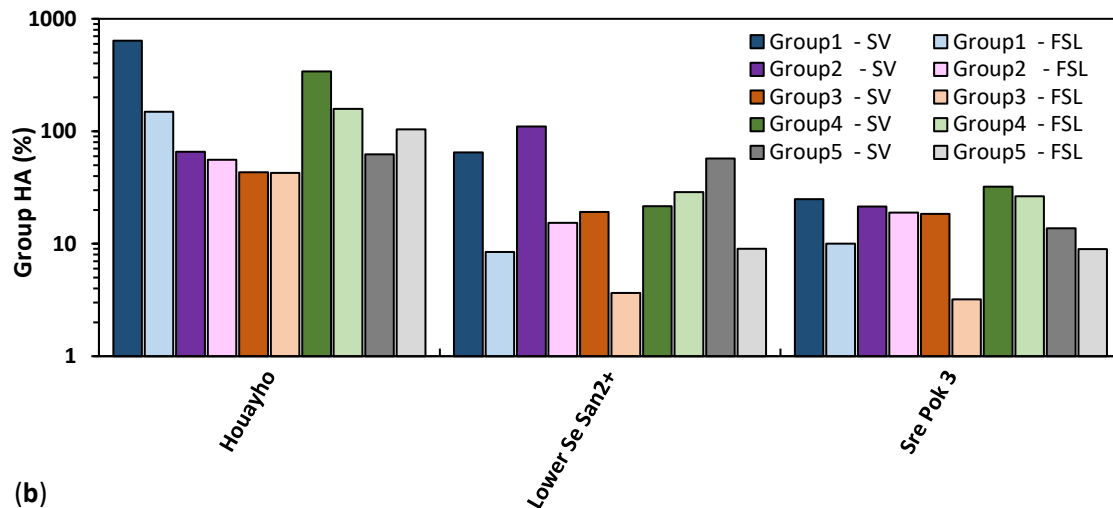


Figure 3-9: Daily water level variation for 20 years simulation period for baseline, high emissions climate change scenarios and SV-Rule curve for a) Xekaman 3, b) Yali and c) LSP 4.

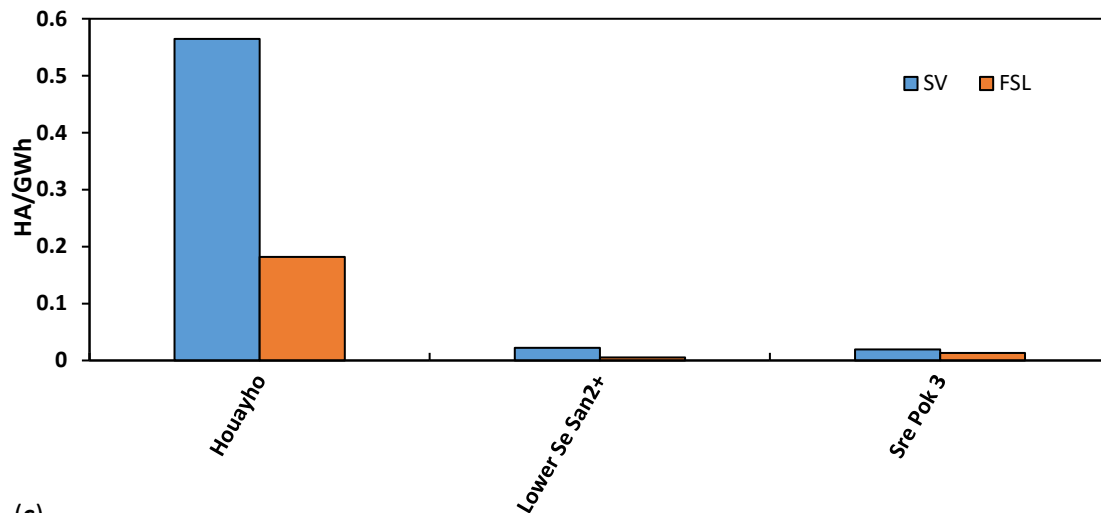
3.3.3 HA Due to Reservoir Operation and Climate Change

An alteration in the hydrologic regime can be observed downstream of all reservoirs. However, the magnitude and nature of the impact vary considerably by the reservoir, operation rule and climate change scenario. The mean overall HA from baseline conditions is 102% under the SV rule, with the highest value of 308% and the lowest value of 16% for specific reservoirs (Figure 3-10a). The reservoirs in the Xe Kong River, a tributary of the Sekong River, have high HA values (highest value for the Houayho hydropower scheme), whereas reservoirs in the Sesan subbasin (except for Upper Kontum) and the Srepok subbasin have comparably low HA values under the SV rule (Figure A3-4 and Table A3-9). The lowest impact results from the Xe Kaman 4A reservoir in the Sekong subbasin.





(b)



(c)

Figure 3-10: (a) Overall HA (%) and (b) HA for each IHA statistics group (%) in log scale) due to operation of hydropower reservoirs at downstream of each reservoir, and (c) HA per gigawatt-hour of hydropower reservoirs under the seasonal variation and full supply level rule curve (denoted by SV and FSL respectively) for the baseline climate (BL-R) scenarios.

Amongst all reservoirs, the most significant alterations of hydrologic regime occurred in groups 1 and 4 (Figure 3-10b) of HA parameters, which are related to the mean monthly flows and frequency/duration of high and low pulses.

The ratio of HA to simulated hydropower generation in GWh per year (Figure 3-10c) represents the impact of reservoirs in terms of energy production. The Xe Nam Noy 5, Namkong 3 and Xekaman-Sanxay hydropower schemes show the highest HA to energy production ratios, whereas Yali hydropower scheme shows the lowest ratio (Figure A3-4c).

The result shows that HA values due to reservoir operations under the FSL rule curve were lower than under the SV rule curve (Figure 3-10a), with overall HA values of 109%, 14% and 15% for the Houayho, LSS2 and Srepok 3 reservoir respectively. Furthermore, a maximum overall HA value of 114% for Duk E Mule and a minimum value of 1% for both the Prek Liang 2 reservoir and Xe Kaman 4A reservoir (Figure A3-5 and Table A3-10) were found. The overall HA values decrease up to 99% under the FSL rule curve compared to the overall HA value under the SV rule curve (Figure 3-11). Similarly, group HA parameters and HA/GWh values also decreased for most of the reservoirs. An increase in groups 4 and 5 HA parameters for some of the reservoirs under the FSL rule curve (Figure 3-10b) was observed. The results show an increase in HA/GWh value for the lower Sesan 3 reservoir. This was due to the significant decrease (20%) in energy production under the FSL rule curve. The mean overall HA across all reservoirs was 28% (Figure 3-12) under the FSL rule curve, which is 73% less than under the SV rule curve. Yet, the overall HA values for the Duc Xuyen reservoir increased due to the increase of group 4 HA parameters as a result of a significant increase in low flood pulse frequency. In general, HA values under the SV rule curve are higher than under the FSL rule curve due to the cumulative impact of hydropower operations, and HA values are even large when considering high emissions climate change scenarios (Figure 3-12).

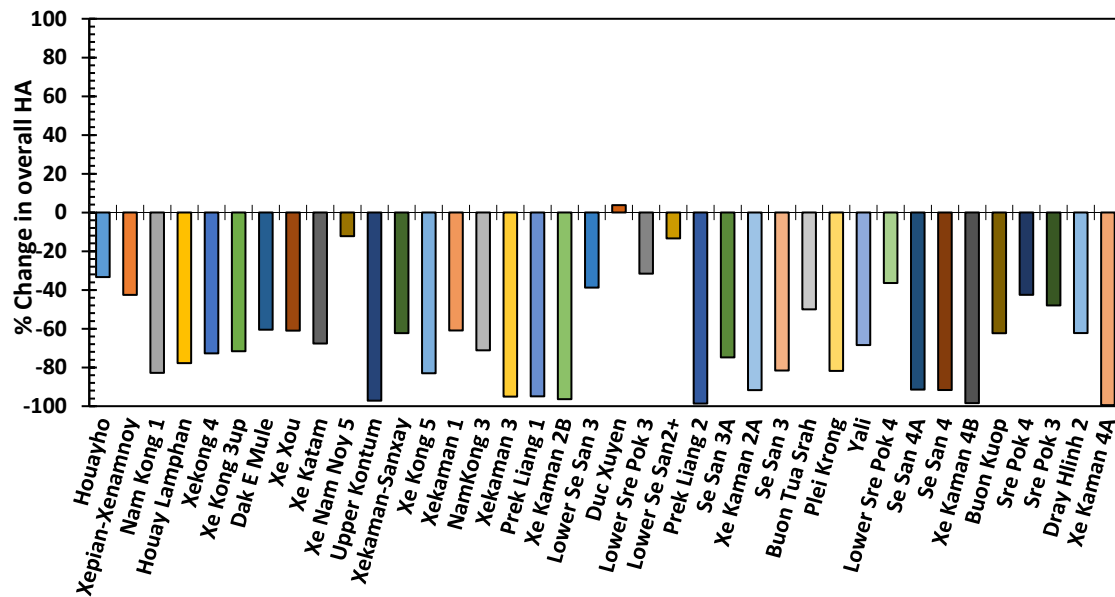


Figure 3-11: Percentage changes in overall HA due to operation of hydropower reservoirs under seasonal variation rule curves with respect to operation of reservoirs under full supply level rule curves for the baseline climate (BL-R) scenario.

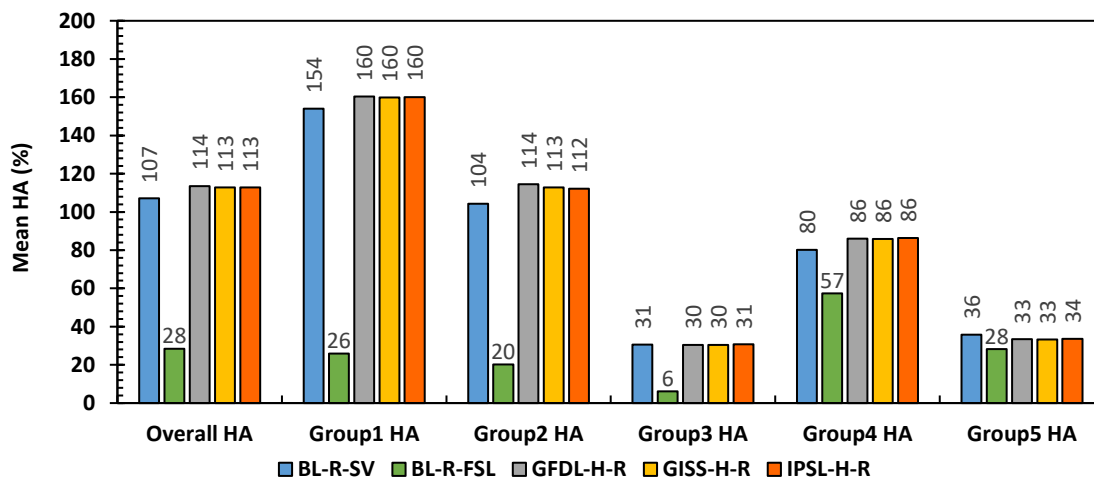


Figure 3-12: Comparison between mean HA across all reservoirs of the baseline climate using the seasonal variation rule curve (BL-R-SV scenario) and the full supply rule curve (BL-R-FSL scenario), for GFDL, GISS and IPSL models under high emissions scenarios using the seasonal variation rule (denoted as GFDL-H-R, GISS-H-R and IPSL-H-R) for overall HA and the five HA groups considered.

3.3.4 Predictors for Alteration

The design head of the hydropower plants and active storage height of the reservoirs in the 3S basin are positively correlated with HA values, whereas mean flow of the river and design discharge of hydropower schemes are negatively correlated with HA for the SV and FSL

rule curves (Table 3-4 and Table 3-5). Furthermore, the design head is a significant predictor of HA in parameter groups 1, 3 and 4 for the SV rule curve and in parameter groups 1, 3 and 5 under the FSL rule. However, reservoir surface area and storage capacity are dominant predictors of overall HA for the Sekong and Srepok subbasin for both rule curves (Figure 3-6a, c). Yet for the Sesan subbasin, HA values are significantly correlated with design head for the SV rule curve and with the reservoir surface area for the FSL rule curve. The average streamflow (Q_{mean}) is negatively correlated to the overall HA for all three subbasins, except for the Sesan subbasin when the FSL rule curve is considered. The regression analysis showed a spatial dependence of the predictors of alteration for the three subbasins. The reservoir surface area is highly correlated with alterations for the Sekong and Srepok subbasins, whereas this is not the case for the Sesan subbasin. Reasons for this may be the differing topography and hydro-climatic conditions.

Table 3-4: Pearson correlation R values for overall HA and individual IHA parameter groups (Group 1–5 IHA parameters are denoted as Gr1–5) among logarithmic predictor values for features (Energy: annual energy production; Installed: installed capacity; Storage: reservoir storage capacity at full supply level; Area: reservoir surface area at FSL; Act Ht: active storage height; FSL: full supply level; Head: design head of the scheme; Q_{mean} : mean annual flow of the river and Q_{design} : design discharge of the scheme) for the 3S basin under the SV-rule curve and FSL-rule curve (green and red indicate positive and negative correlations, bold values represent $p < 0.05$).

| Feature | SV Rule | | | | | | FSL Rule | | | | | |
|--------------|--------------|--------------|-------|--------------|--------------|-------------|--------------|--------------|-------|-------|-------|--------------|
| | Overall | Gr1 | Gr2 | Gr3 | Gr4 | Gr5 | Overall | Gr1 | Gr2 | Gr3 | Gr4 | Gr5 |
| Energy | 0.12 | 0.06 | 0.13 | -0.06 | 0.10 | 0.20 | 0.13 | 0.16 | 0.15 | 0.07 | 0.00 | 0.02 |
| Installed | 0.12 | 0.09 | 0.02 | -0.13 | 0.21 | 0.19 | 0.11 | 0.14 | 0.12 | 0.04 | -0.02 | 0.08 |
| Storage | 0.22 | 0.17 | 0.20 | -0.11 | 0.04 | 0.45 | 0.21 | 0.12 | 0.22 | 0.11 | 0.18 | 0.15 |
| Area | 0.17 | 0.17 | 0.10 | -0.09 | 0.03 | 0.49 | 0.24 | 0.10 | 0.23 | 0.13 | 0.26 | 0.15 |
| Act Ht | 0.35 | 0.33 | 0.19 | 0.21 | 0.19 | 0.07 | 0.25 | 0.24 | 0.20 | 0.24 | 0.09 | 0.40 |
| FSL | 0.27 | 0.29 | -0.07 | 0.32 | 0.44 | -0.17 | 0.24 | 0.26 | 0.11 | 0.30 | 0.08 | 0.38 |
| Head | 0.49 | 0.44 | 0.18 | 0.38 | 0.45 | 0.11 | 0.31 | 0.41 | 0.28 | 0.41 | -0.06 | 0.40 |
| Q_{mean} | -0.52 | -0.54 | -0.10 | -0.39 | -0.46 | -0.03 | -0.36 | -0.37 | -0.29 | -0.38 | -0.06 | -0.59 |
| Q_{design} | -0.27 | -0.26 | -0.10 | -0.37 | -0.18 | 0.04 | -0.12 | -0.20 | -0.10 | -0.28 | 0.10 | -0.24 |

Table 3-5: Pearson correlation R values for overall HA and IHA parameter groups (Group 1–5 IHA parameters are denoted as Gr1–5), between logarithmic predictor values for features (all notations are described in the caption of Table 3-3) for the (a) Sekong, (b) Sesan and (c) Srepok subbasin under the SV-rule curve and FSL-rule curve (green and red indicate positive and negative correlations, bold values represent $p < 0.05$).

| SV Rule | | | | | | | FSL Rule | | | | | |
|-----------|---------|-------|-------|-------|-------|-------|----------|-------|-------|-------|-------|-------|
| (a) | | | | | | | | | | | | |
| Feature | Overall | Gr1 | Gr2 | Gr3 | Gr4 | Gr5 | Overall | Gr1 | Gr2 | Gr3 | Gr4 | Gr5 |
| Energy | 0.37 | 0.22 | 0.35 | -0.22 | 0.29 | 0.10 | 0.07 | 0.13 | 0.09 | -0.06 | -0.11 | 0.05 |
| Installed | 0.26 | 0.24 | 0.08 | -0.33 | 0.35 | 0.12 | 0.06 | 0.11 | 0.03 | -0.08 | -0.09 | 0.19 |
| Storage | 0.53 | 0.47 | 0.27 | -0.10 | 0.36 | 0.47 | 0.30 | 0.14 | 0.28 | 0.13 | 0.46 | 0.30 |
| Area | 0.56 | 0.52 | 0.24 | -0.08 | 0.38 | 0.51 | 0.30 | 0.11 | 0.30 | 0.15 | 0.49 | 0.34 |
| Act Ht | 0.18 | 0.19 | 0.01 | 0.14 | 0.21 | 0.13 | 0.28 | 0.30 | 0.20 | 0.26 | 0.11 | 0.21 |
| FSL | 0.00 | 0.12 | -0.32 | 0.29 | 0.29 | -0.03 | 0.36 | 0.53 | 0.29 | 0.45 | -0.17 | 0.25 |
| Head | 0.26 | 0.31 | -0.09 | 0.33 | 0.43 | 0.02 | 0.45 | 0.59 | 0.34 | 0.48 | -0.03 | 0.33 |
| Qmean | -0.15 | -0.35 | 0.40 | -0.28 | -0.47 | -0.06 | -0.50 | -0.59 | -0.41 | -0.45 | -0.05 | -0.50 |
| Qdesign | -0.01 | -0.08 | 0.18 | -0.51 | -0.15 | 0.09 | -0.36 | -0.47 | -0.26 | -0.50 | 0.01 | -0.17 |

| (b) | | | | | | | | | | | | |
|-----------|---------|-------|-------|-------|-------|-------|---------|-------|-------|-------|-------|-------|
| Feature | Overall | Gr1 | Gr2 | Gr3 | Gr4 | Gr5 | Overall | Gr1 | Gr2 | Gr3 | Gr4 | Gr5 |
| Energy | 0.16 | 0.14 | -0.03 | 0.16 | 0.15 | 0.23 | 0.28 | 0.40 | 0.42 | 0.19 | 0.12 | -0.10 |
| Installed | 0.16 | 0.14 | -0.21 | 0.27 | 0.25 | 0.20 | 0.34 | 0.42 | 0.43 | 0.20 | 0.18 | 0.00 |
| Storage | 0.05 | 0.29 | 0.49 | 0.10 | -0.23 | 0.23 | 0.36 | 0.41 | 0.45 | 0.03 | 0.16 | 0.26 |
| Area | -0.10 | 0.14 | 0.10 | 0.44 | -0.21 | 0.55 | 0.59 | 0.77 | 0.74 | 0.60 | 0.27 | 0.23 |
| Act Ht | 0.14 | 0.28 | 0.01 | -0.07 | 0.11 | -0.30 | 0.16 | 0.19 | 0.27 | -0.36 | 0.02 | 0.35 |
| FSL | 0.58 | 0.45 | -0.21 | 0.20 | 0.67 | -0.56 | 0.08 | -0.26 | -0.20 | -0.71 | 0.17 | 0.37 |
| Head | 0.72 | 0.58 | 0.16 | 0.17 | 0.62 | -0.07 | -0.18 | 0.04 | 0.10 | -0.40 | -0.25 | -0.06 |
| Qmean | -0.77 | -0.64 | -0.17 | -0.15 | -0.68 | 0.55 | 0.34 | 0.54 | 0.49 | 0.86 | 0.16 | -0.22 |
| Qdesign | -0.21 | -0.12 | -0.21 | 0.19 | -0.12 | 0.19 | 0.55 | 0.38 | 0.36 | 0.37 | 0.44 | 0.07 |

| (c) | | | | | | | | | | | | |
|-----------|---------|-------|-------|-------|-------|-------|---------|-------|-------|-------|-------|-------|
| Feature | Overall | Gr1 | Gr2 | Gr3 | Gr4 | Gr5 | Overall | Gr1 | Gr2 | Gr3 | Gr4 | Gr5 |
| Energy | -0.01 | -0.14 | 0.43 | -0.23 | -0.44 | 0.46 | -0.52 | 0.32 | 0.28 | -0.27 | -0.53 | -0.45 |
| Installed | 0.08 | 0.14 | 0.55 | -0.13 | -0.31 | 0.46 | -0.31 | 0.05 | 0.01 | -0.13 | -0.35 | -0.27 |
| Storage | 0.76 | 0.71 | 0.72 | 0.37 | 0.26 | 0.68 | 0.28 | -0.24 | -0.22 | 0.09 | 0.29 | 0.29 |
| Area | 0.76 | 0.70 | 0.83 | 0.16 | 0.00 | 0.85 | 0.14 | -0.10 | -0.09 | 0.06 | 0.14 | 0.13 |
| Act Ht | 0.65 | 0.39 | -0.35 | 0.83 | 0.61 | -0.23 | 0.56 | -0.60 | -0.56 | -0.18 | 0.56 | 0.79 |
| FSL | -0.02 | 0.16 | -0.69 | 0.59 | 0.69 | -0.78 | 0.67 | -0.54 | -0.50 | 0.24 | 0.68 | 0.68 |
| Head | 0.04 | 0.06 | -0.16 | 0.28 | 0.27 | -0.22 | 0.18 | -0.04 | -0.03 | 0.14 | 0.18 | 0.10 |
| Qmean | -0.24 | -0.14 | 0.71 | -0.60 | -0.82 | 0.69 | -0.89 | 0.35 | 0.28 | -0.31 | -0.80 | -0.70 |
| Qdesign | -0.06 | -0.20 | 0.46 | -0.34 | -0.57 | 0.50 | -0.67 | 0.28 | 0.22 | -0.45 | -0.67 | -0.47 |

3.4 Discussion

3.4.1 Impacts of Climate Change on Hydropower Production

The focus of this investigation was to study the impacts of climate change on hydropower production due to operation of multiple reservoirs in the 3S basin, thus the results emphasize the overall impact in production rather than impact on individual or single hydropower plant. The results depict that the daily hydropower production in the 3S basin varies from 92 to 96 GWh under various climate change scenarios, which represents a -1.6% to +2.3% change from the baseline scenario. The IPSL and GFDL models projected the increase in flows

at the 3S basin outlet, while the GISS model projected slightly decrease in flows. Consequently, hydropower production was projected to increase due to the projected increase in flows under the IPSL and GFDL models. Similarly, the projected decrease in flows at 3S basin outlet due to the GISS model resulted decrease in hydropower production. The results predicted here are within agreeable range with different previous studies carried out in the Lower Mekong basin such as Piman et al. (2015), Hoang et al. (2019) and Lauri et al. (2012). However, the impact of climate change in hydropower production on each of the hydropower plants is significant depending on their location, size, operating rule curves, topography, selected GCMs and emissions scenarios. Because the projected precipitation changes are spatially varied and varied depending on the GCMs and season. Furthermore, the change in climatic variables (specifically precipitation and temperature) has projected changes in flows temporally (seasonal, annual) and geographically from subbasin to subbasin. In addition, with an increase in temperature, evaporation from the surface area of the reservoir will increase and will reduce the storage capacity of the reservoir. Further detailed analysis should be carried out to find out the impacts of climate change on evaporation and its effect on hydropower production. Therefore, the impact of such changes of flows varies from reservoir to reservoir. Yet overall, the impact of climate change on hydropower production is insignificant in the 3S basin for the 2051–2070 period, as the reservoir operations overcome the impact of climate change on the flows.

As a final point, taking into consideration of large uncertainty associated with the predictions of various GCMs, climate change in the future could have a potentially significant impact on hydropower generation (Shrestha et al. 2016). Besides, during a drought year, the impacts of climate change will significantly exacerbate the period when there is no sufficient water storage to discharge for energy generation. In contrast, the increase of peak flood flows that could increase spillway flows and may influence safety of the spillway and dam and thus the downstream areas will be at risk. Nevertheless, the impacts of climate change on

hydropower production can be reduced to some extent. In order to mitigate the loss of hydropower, adjustment of rule curves in accordance with the climate change could help to smooth operation and hydropower production (Mishra et al. 2020).

3.4.2 HA Due to Reservoir Operations and Climate Change

Analysis of the hydrological alterations parameters shows that flow regime alteration is likely due to the operation of reservoirs. However, the magnitude and intensity of the alterations vary widely based on reservoir characteristics, location and operation policies, which has also been pointed out in other studies (Lu et al. 2018; Magilligan and Nislow 2005; Shin et al. 2020; Timpe and Kaplan 2017; Xue et al. 2017; Zhang et al. 2018). The results indicated that, in addition to reservoir features, the location of the reservoir is also a significant factor for variations of the rate of hydrologic alterations, as the basin is characterized by wide variation in topography and physiography with complex climatic conditions.

It was found that the most significant changes occur for the monthly flow volume, and magnitude and duration of the extreme annual flow (IHA parameter groups 1 and 2). Reservoir volume, area and design head of the hydropower scheme showed more sensitive to IHA parameter groups 1 and 2. That was all due to the operation of the reservoirs under the SV rule, and is in agreement with previous work (Hoang et al. 2019; Li et al. 2017; Piman et al. 2013; Räsänen et al. 2017). More specifically, dry season flow (November–April) substantially increased and wet season flow (May–October) decreased due to reservoir operation, because reservoirs store water during the wet season and release water to generate hydropower energy in the dry season. Overall, alterations were observed to a lesser degree for the wet season when compared to the dry season.

The results show a significant increase in annual minimum flows and a decrease in annual maximum flows due to operation of hydropower reservoirs, which aligns with previous

findings in this region (Piman et al. 2016; Souter et al. 2020). The HA values of group 3 parameters indicate an alteration in the timing of annual extreme water conditions. The values of these group parameters were larger for reservoirs that are located on small rivers, i.e., rivers which have relatively low mean flows. This was because small-river reservoirs delayed the timing of annual maximum flows. However, HA values of group 3 are comparatively lower than the HA values of groups 1 and 2. Furthermore, impacts of reservoir operations on flood pulse dynamics, which are presented by IHA parameter group 4, are relatively lower than HA in group 1, although the Houayho, Upper-Kontum, Duc Xuyen, Se San 3A, Se San 3, Buon Tua Srah and Yali reservoirs show high HA values of group 4. HA values of groups 4 and 5 indicate dam operations where operators store water to achieve sufficient head before releasing water for generating electricity during the dry season.

In addition to reservoir operations, climate change is another factor that can alter the dry seasonal flows and the flood pulse of the 3S rivers (Hoang et al. 2019; Lauri et al. 2012; Ngo et al. 2018; Piman et al. 2015). Piman et al. (2015) (Piman et al. 2015) projected a dry seasonal flows increase of 96% and a wet seasonal flows decrease of 25% due to the operations of 41 reservoirs at the 3S basin outlet. The same authors also predicted a dry seasonal flows reduction of 6–24% and indicated uncertainty in a change of wet seasonal flows due to climate change. Ngo et al. (2018) (Ngo et al. 2018) forecasted that the annual flow might decrease by a 3–8% for the Sesan subbasin and increase by a 4–13% for the Srepok subbasin due to climate change, whereas reservoir operations alone might increase dry seasonal flow by 30% to 40% and wet seasonal flows might drop by 15% to 20% for the Sesan subbasin. In an earlier modelling attempt, Lauri et al. (2012) (Lauri et al. 2012) projected annual Mekong River discharge changes of –10% to +13% due to climate change, and a larger increase in dry seasonal flow (25–160%) and a decrease in wet seasonal flow (5–24%) due to reservoir operations. Variations in the modelled values of percentage changes relative to the results presented here

are due to differences in the extent of the study area (i.e., whole of Mekong vs. 3S basin), the selection of projected hydropower projects, GCMs, the simulation period, operation policies and simulation models.

Overall, it was found that the cumulative impacts of reservoir operations and climate change are more sensitive to the magnitude and duration of the extreme flow conditions for the 3S basin. In addition, this study confirms that reservoir operations appear to have a considerably stronger impact on the flow regime than climate change (Ngo et al. 2018; Piman et al. 2015; Yoshida et al. 2020). Furthermore, land use change plays a major role in hydrological alterations (Shrestha et al. 2018), but in this study the analysis of impacts has been limited to reservoir operations and climate change.

Operating rule curves play an essential role in enhancing power production and to reduce impacts on the ecohydrological system downstream (Zhou and Guo 2013). The FSL rule was used because previous studies (Piman et al. 2013; Yin et al. 2011) demonstrated that the application of this type rule has a low impact on the hydrological regime. In comparison with the SV rule, the application of FSL rules resulted in a significant overall decrease in HA (Figure 3-10). Additionally, decreases in HA values of groups 1 and 2 indicate that application of the FSL rule has low impacts on the flow regime. However, HA values of group 4 for Xe Xou, Duc Xuyen and Buon Tua Srah increased when using FSL rule curves, as explained by an observable increase in the low flood pulse. The designed discharges of these hydropower reservoirs are relatively larger than the mean monthly flow of the river. Thus, these reservoirs have the capacity to release larger amounts of water under the FSL rules during low flood season. Simulations under the FSL rule curve showed a decrease in energy production for all reservoirs, as expected, except for the Xe Kaman 2B, Houayho, Plei Krong, Duc Xuyen and Buon Tua Srah reservoirs which are relatively small and located uppermost of the cascades (Table A3-7).

In general, however, the operation of reservoirs applying the FSL rules minimized HA values considerably in the 3S basin.

Yet it is important to note that the SV and FSL rule curves are only representative of long-term management of the reservoirs, and are thus not optimized based on specific hydropower plant features, energy demand and detailed hydrologic conditions. Further research should be carried out on optimization of the rule curves fulfilling these criteria: (1) maximizing energy production and (2) minimizing hydrological alteration for each of the reservoirs in the complex reservoir system.

IHA parameters alone, which are only based on the analysis of pre and post-dam time series flows, cannot represent all aspects of ecological impacts due to reservoir operations. IHA parameters do not represent sediment transport, changes in geomorphology, ecological functions and floodplain connectivity. The construction of reservoirs not only alters the natural flow pattern and volume, but also impacts the sediment and nutrient transport, geomorphology of the river, and also disrupts fish passage between upstream and downstream system. Low HA values of large reservoirs may actually have relatively large ecological impacts and vice-versa for streams and rivers with greatly varying physiographies, land uses and the hydrologic regimes. For instance, the results illustrate that reservoirs with large hydropower production, such as Yali, Buon Kuop and Lower Sesan 2 + Lower Srepok (LSS 2), have low ratios of HA to hydropower production, which can be deceiving (Figure A3-4c). The LSS 2, for example, is actually ecologically critical due to its location just downstream of the confluence of the Srepok and Sesan Rivers and near the 3S rivers junction. Even though these results have shown comparatively low HA with respect to hydropower production, the LSS 2 dam will disconnect the upstream 3S ecological system from critical Mekong ecosystems (Arias et al. 2014; Binh et al. 2020) and thus could be one of the most ecologically damaging reservoirs of the basin.

However, the IHA tool does quantify the relative changes in the hydrologic regime, and therefore, quantifications of HA will help in the broader analysis of ecological impacts.

3.4.3 Possible Ecohydrological Consequences

The relatively large changes in mean monthly flows (group 1 parameters) observed in these analyses will impact habitat conditions and breeding areas for aquatic organisms (Baran et al. 2007; Richter et al. 1996). Furthermore, the decrease in wet seasonal flow is expected to reduce the sediment and nutrient load transport and will consequently affect food availability for aquatic species. In addition, rise in river water levels due to increase in dry seasonal flow may inundate fertile areas around the rivers and consequently potentially impact agricultural production. Although an increase in dry seasonal flows may prove beneficial for providing water for irrigation, creating opportunities for developing new hydropower projects in a cascade, and enhancing possibilities for navigation (Hoang et al. 2019; Räsänen et al. 2017), changes in the flow regime will have adverse effects on the ecological dynamics, biodiversity and downstream traditional agricultural production in the river margins. The alteration in extreme water conditions is likely to restrict nutrient exchange between the riverbed and floodplains. The changes in magnitude and duration of extreme flows (group 2 parameter) may change the geomorphology of river channels, which will adversely impact reproduction of certain aquatic species (Ward et al. 1999). Most fish in the 3S basin are migratory fish, and usually migrate longitudinally and laterally in the floodplain for spawning, feeding and growth (Baran et al. 2015). The alteration of timing of extreme flows will alter fish migration patterns and timing. Ecological dynamics of the 3S basin are very sensitive to changes in the frequency and duration of flood pulses (group 4) because they are responsible for availability of floodplain habitats for aquatic organisms and the exchanges of nutrients and organic matter between the river and floodplain (Richter et al. 1996). The abundant biodiversity in the basin depends on

the natural flood pulse; therefore, changes in the flood pulse may be one of the factors to compromise high biodiversity. Hence, hydrological alterations due to reservoir operations may cause great losses of biodiversity and fisheries in the 3S basin (Yoshida et al. 2020; Ziv et al. 2012).

Even though hydrological alterations due to reservoir operations cannot be completely alleviated, it is important to consider the planning, designing and operation phases of all hydropower reservoirs operating together to minimize ecological degradations. In addition to altering rule curves for moderating hydrological alterations, identifying and ensuring minimal ecological flows can help alleviate negative effects of hydropower reservoirs on the riverine ecosystem. Designing the currently proposed dams with low or mid-level outlets from the dam is essential to maintaining continuous minimum flows and to pass sediment loads. Fish passages or fish ladders in dams in this region are often ineffective, so greater emphasis on placement of new dams is important to avoid detrimental blockage of fish migration (Annandale and Kaini 2012; Wild and Loucks 2014).

3.5 Conclusions

In this chapter, SWAT with HydrOR was used to quantify hydroelectricity production under different rule curves and climate change scenarios in the 3S basin. In addition, hydrological alterations of the flow regime were assessed and their possible ecological consequences were discussed.

In this first application of the HydrOR, the hydropower production was estimated from 38 hydropower reservoirs in the 3S basin under baseline climate and different climate change scenarios using two types of rule curves simultaneously. The impact of climate change on hydropower production for 2060s in the 3S basin was found to be minimal.

Hydrological alterations in the 3S basin will be significant due to cumulative impacts of reservoir operations and climate change. However, alterations caused by climate change are comparably small. The largest alterations are changes in seasonal flows and extreme water conditions from reservoirs operated under a seasonal variation rule curve that maximizes energy production. These types of alterations are significant and are related to reservoir sizes and design heads of the hydropower schemes. The projected changes in the natural flow regime may have a serious negative impact on ecological systems. Impacts on downstream ecosystems are larger for hydropower dams with high regulation heads and reservoirs on rivers that have low mean annual flows. Hydrological alterations, however, can be minimized through adequate operation policies. The adoption of a full supply rule curve to operate dams in a more natural flow regime was found to drastically decrease impacts.

The introduction of the HydROR to SWAT allows users to establish an integrative approach to managing reservoir operations, hydropower production and hydrological alterations in complex reservoir systems under changing conditions, such as weather, climate change, land use, and policy. However, sediment inflow, deposition and outflow from the reservoir are not currently simulated. Accumulation of sediment depletes storage capacity of the reservoir, consequently affects the water release capacity of the reservoir, hydropower production and alters the downstream sediment regime. Therefore, Chapter 4 will focus on fulfilling these limitations by applying the ResSMan to assess the impacts of reservoir sedimentation and to implement various sediment management techniques.

3.6 References

- Annandale, G., and Kaini, P. (2012). "A climate resilient Mekong: Sediment pass-through at lower Se San 2." *Report submitted by Golder Associates Inc., Lakewood, CO to Natural Heritage Institute, San Francisco, CA.*
- Arias, M. E., Cochrane, T. A., Kummu, M., Lauri, H., Holtgrieve, G. W., Koponen, J., and Piman, T. (2014). "Impacts of hydropower and climate change on drivers of ecological productivity of Southeast Asia's most important wetland." *Ecological Modelling*, 272, 252-263.
- Baltas, E. A. (2007). "Impact of Climate Change on the Hydrological Regime and Water Resources in the Basin of Siatista." *International Journal of Water Resources Development*, 23(3), 501-518.
- Baran, E., Guerin, E., and Nasielski, J. (2015). *Fish, sediment and dams in the Mekong.*
- Baran, E., Starr, P., and Kura, Y. (2007). "Influence of built structures on Tonle Sap fisheries." *Cambodia National Mekong Committee and the WorldFish Center, Phnom Penh, Cambodia.*
- Binh, D. V., Kantoush, S., and Sumi, T. (2020). "Changes to long-term discharge and sediment loads in the Vietnamese Mekong Delta caused by upstream dams." *Geomorphology*, 353, 107011.
- Devkota, L. P., and Gyawali, D. R. (2015). "Impacts of climate change on hydrological regime and water resources management of the Koshi River Basin, Nepal." *Journal of Hydrology: Regional Studies*, 4, 502-515.
- Haguma, D., Leconte, R., and Krau, S. (2017). "Hydropower plant adaptation strategies for climate change impacts on hydrological regime." *Canadian Journal of Civil Engineering*, 44(11), 962-970.
- Hardy, R. L. (1971). "Multiquadric equations of topography and other irregular surfaces." *Journal of Geophysical Research (1896-1977)*, 76(8), 1905-1915.
- Hoang, L. P., van Vliet, M. T., Kummu, M., Lauri, H., Koponen, J., Supit, I., Leemans, R., Kabat, P., and Ludwig, F. (2019). "The Mekong's future flows under multiple drivers: How climate change, hydropower developments and irrigation expansions drive hydrological changes." *Science of the total environment*, 649, 601-609.
- IEA (2017). "World Energy Outlook Special Report on Southeast Asia 2017." *International Energy Agency, Paris, France.*
- Junk, W. J., and Wantzen, K. M. "The flood pulse concept: new aspects, approaches and applications-an update." *Proc., Second international symposium on the management of large rivers for fisheries*, Food and Agriculture Organization and Mekong River Commission, FAO Regional Office for Asia and the Pacific., 117-149.
- Lauri, H., De Moel, H., Ward, P., Räsänen, T., Keskinen, M., and Kummu, M. (2012). "Future changes in Mekong River hydrology: impact of climate change and reservoir operation on discharge." *Hydrol. Earth Syst. Sci. Discuss*, 9(5), 6569-6614.

- Li, D., Long, D., Zhao, J., Lu, H., and Hong, Y. (2017). "Observed changes in flow regimes in the Mekong River basin." *Journal of Hydrology*, 551, 217-232.
- Lu, W., Lei, H., Yang, D., Tang, L., and Miao, Q. (2018). "Quantifying the impacts of small dam construction on hydrological alterations in the Jiulong River basin of Southeast China." *Journal of Hydrology*, 567, 382-392.
- Magilligan, F. J., and Nislow, K. H. (2005). "Changes in hydrologic regime by dams." *Geomorphology*, 71(1-2), 61-78.
- Middelkoop, H., Daamen, K., Gellens, D., Grabs, W., Kwadijk, J. C. J., Lang, H., Parmet, B. W. A. H., Schädler, B., Schulla, J., and Wilke, K. (2001). "Impact of Climate Change on Hydrological Regimes and Water Resources Management in the Rhine Basin." *Climatic Change*, 49(1), 105-128.
- Mishra, S. K., Veselka, T. D., Prusevich, A. A., Grogan, D. S., Lammers, R. B., Rounce, D. R., Ali, S. H., and Christian, M. H. (2020). "Differential Impact of Climate Change on the Hydropower Economics of Two River Basins in High Mountain Asia." *Frontiers in Environmental Science*, 8(26).
- MRC (2010). "State of the Basin Report, Mekong River Commission." *Mekong River Commission, Vientiane, 2010*.
- MRC (2011). "Application of MRC modelling tools in the 3S basin." Mekong River Commission, Phnom Penh, Cambodia.
- MRC (2015). "1st Draft Report on Defining basin-wide climate change scenarios for the Lower Mekong Basin (LMB)." *Mekong River Commission, Phnom Penh, Cambodia*
- MRC (2019). "Basin-Wide Assessment of Climate Change Impacts on Hydropower Production." *Mekong River Commission, Vientiane, 2019*.
- MRC (2019). "State of the Basin Report 2018, Mekong River Commission." *Mekong River Commission, Vientiane, 2019*.
- Ngo, L. A., Masih, I., Jiang, Y., and Douven, W. (2018). "Impact of reservoir operation and climate change on the hydrological regime of the Sesan and Srepok Rivers in the Lower Mekong Basin." *Climatic Change*, 149(1), 107-119.
- Pachauri, R. K., Allen, M. R., Barros, V. R., Broome, J., Cramer, W., Christ, R., Church, J. A., Clarke, L., Dahe, Q., and Dasgupta, P. (2014). *Climate change 2014: synthesis report. Contribution of Working Groups I, II and III to the fifth assessment report of the Intergovernmental Panel on Climate Change*, Ipcc.
- Piman, T., Cochrane, T., Arias, M., Green, A., and Dat, N. (2013). "Assessment of flow changes from hydropower development and operations in Sekong, Sesan, and Srepok rivers of the Mekong basin." *Journal of Water Resources Planning and Management*, 139(6), 723-732.
- Piman, T., Cochrane, T. A., and Arias, M. E. (2016). "Effect of proposed large dams on water flows and hydropower production in the Sekong, Sesan and Srepok rivers of the Mekong Basin." *River Research and Applications*, 32(10), 2095-2108.

- Piman, T., Cochrane, T. A., Arias, M. E., Dat, N. D., and Vonnarart, O. (2015). "Managing Hydropower Under Climate Change in the Mekong Tributaries." *Managing Water Resources under Climate Uncertainty: Examples from Asia, Europe, Latin America, and Australia*, S. Shrestha, A. K. Anal, P. A. Salam, and M. van der Valk, eds., Springer International Publishing, Cham, 223-248.
- Räsänen, T. A., Someth, P., Lauri, H., Koponen, J., Sarkkula, J., and Kummu, M. (2017). "Observed river discharge changes due to hydropower operations in the Upper Mekong Basin." *Journal of hydrology*, 545, 28-41.
- Richter, B. D., Baumgartner, J. V., Powell, J., and Braun, D. P. (1996). "A Method for Assessing Hydrologic Alteration within Ecosystems." *Conservation Biology*, 10(4), 1163-1174.
- Shi, P., Liu, J., Yang, T., Xu, C.-Y., Feng, J., Yong, B., Cui, T., Li, Z., and Li, S. (2019). "New Methods for the Assessment of Flow Regime Alteration under Climate Change and Human Disturbance." *Water*, 11(12), 2435.
- Shin, S., Pokhrel, Y., Yamazaki, D., Huang, X., Torbick, N., Qi, J., Pattanakiat, S., Ngo-Duc, T., and Nguyen, T. D. (2020). "High Resolution Modeling of River-Floodplain-Reservoir Inundation Dynamics in the Mekong River Basin." *Water Resources Research*, 56(5), e2019WR026449.
- Shrestha, B., Cochrane, T. A., Caruso, B. S., and Arias, M. E. (2018). "Land use change uncertainty impacts on streamflow and sediment projections in areas undergoing rapid development: A case study in the Mekong Basin." *Land degradation & development*, 29(3), 835-848.
- Shrestha, B., Cochrane, T. A., Caruso, B. S., Arias, M. E., and Piman, T. (2016). "Uncertainty in flow and sediment projections due to future climate scenarios for the 3S Rivers in the Mekong Basin." *Journal of Hydrology*, 540, 1088-1104.
- Shrestha, J. P., Alfredsen, K., and Timalisina, N. (2014). "Regional Modeling for Estimation of Runoff from Ungauged Catchments: Case Study of the Saptakoshi Basin, Nepal." *2014*, 14, 8.
- Souter, N. J., Shaad, K., Vollmer, D., Regan, H. M., Farrell, T. A., Arnaiz, M., Meynell, P.-J., Cochrane, T. A., Arias, M. E., Piman, T., and Andelman, S. J. (2020). "Using the Freshwater Health Index to Assess Hydropower Development Scenarios in the Sesan, Srepok and Sekong River Basin." *Water*, 12(3), 788.
- Thompson, J., Laizé, C., Green, A., Acreman, M., and Kingston, D. (2014). "Climate change uncertainty in environmental flows for the Mekong River." *Hydrological Sciences Journal*, 59(3-4), 935-954.
- Timpe, K., and Kaplan, D. (2017). "The changing hydrology of a dammed Amazon." *Science Advances*, 3(11), e1700611.
- Trang, N. T. T., Shrestha, S., Shrestha, M., Datta, A., and Kawasaki, A. (2017). "Evaluating the impacts of climate and land-use change on the hydrology and nutrient yield in a transboundary river basin: A case study in the 3S River Basin (Sekong, Sesan, and Srepok)." *Science of the Total Environment*, 576, 586-598.

- Trisurat, Y., Aekakkararungroj, A., Ma, H.-O., and Johnston, J. M. (2018). "Basin-wide Impacts of Climate Change on Ecosystem Services in the Lower Mekong Basin." *Ecol Res*, 33(1), 73-86.
- Ward, J., Tockner, K., and Schiemer, F. (1999). "Biodiversity of floodplain river ecosystems: ecotones and connectivity1." *River Research and Applications*, 15(1 - 3), 125-139.
- Wild, T. B., and Loucks, D. P. (2014). "Managing flow, sediment, and hydropower regimes in the Sre Pok, Se San, and Se Kong Rivers of the Mekong basin." *Water Resources Research*, 50(6), 5141-5157.
- Winemiller, K. O., McIntyre, P. B., Castello, L., Fluet-Chouinard, E., Giarrizzo, T., Nam, S., Baird, I., Darwall, W., Lujan, N., and Harrison, I. (2016). "Balancing hydropower and biodiversity in the Amazon, Congo, and Mekong." *Science*, 351(6269), 128-129.
- Xue, L., Zhang, H., Yang, C., Zhang, L., and Sun, C. (2017). "Quantitative Assessment of Hydrological Alteration Caused by Irrigation Projects in the Tarim River basin, China." *Scientific Reports*, 7(1), 4291.
- Yin, X. A., Yang, Z. F., and Petts, G. E. (2011). "Reservoir operating rules to sustain environmental flows in regulated rivers." *Water Resources Research*, 47(8).
- Yoshida, Y., Lee, H. S., Trung, B. H., Tran, H.-D., Lall, M. K., Kakar, K., and Xuan, T. D. (2020). "Impacts of Mainstream Hydropower Dams on Fisheries and Agriculture in Lower Mekong Basin." *Sustainability*, 12(6), 2408.
- Zhang, Y., Zhai, X., and Zhao, T. (2018). "Annual shifts of flow regime alteration: new insights from the Chaishitan Reservoir in China." *Scientific Reports*, 8(1), 1414.
- Zhou, Y., and Guo, S. (2013). "Incorporating ecological requirement into multipurpose reservoir operating rule curves for adaptation to climate change." *Journal of Hydrology*, 498, 153-164.
- Ziv, G., Baran, E., Nam, S., Rodríguez-Iturbe, I., and Levin, S. A. (2012). "Trading-off fish biodiversity, food security, and hydropower in the Mekong River Basin." *Proceedings of the National Academy of Sciences*, 109(15), 5609-5614.

CHAPTER 4. MANAGING RESERVOIR SEDIMENTATION THROUGH COORDINATED OPERATIONS

4.1 Introduction

Sedimentation is one of the major challenges for the long-term sustainable operation of a reservoir, since trapping of sediment reduces their storage capacity and consequently diminishes hydropower production. It is estimated that 0.5–1% of the annual global storage volume is lost due to sedimentation (Basson 2009; Walling 2006). In highly regulated basins, sediment trapping efficiency is more than 50% and, half of the world's largest reservoirs are showing a local trapping efficiency of 80% or more (Kummu et al. 2010; Morris 2020; Vörösmarty et al. 2003). Sediment entering into reservoirs originates mainly due to soil and stream bed erosion and sediment deposition varies greatly between reservoir sites, depending on flow velocities and sediment loads in the rivers flowing into the reservoirs and the trapping efficiencies of the reservoirs (Heinemarm 1981; Hrissanthou 2014; Wurbs 2005). The sediment trapping not only threatens the sustainability of reservoirs, but also extend downstream sediment regime. The trapping of sediment in a reservoir decreases the release of sediment from the dam which impacts the downstream sediment regime (Hotchkiss 1990; Kantoush and Sumi 2010; Kondolf 1997; Kondolf et al. 2014). Moreover, the trapping of sediment not only alters the natural sediment regime, but also disconnect upstream-downstream ecosystems. For example, in a highly biodiverse basin such as the Mekong, blockage in sediment connectivity affects hydrological processes and habitats and diminishes river deltas, which affects valuable aquatic ecosystems (Kondolf et al. 2014; Power et al. 1996; Schmitt et al. 2018).

There are various approaches available to successfully manage reservoir sedimentation selecting suitable techniques for sustainable use of the reservoir (Palmieri et al. 2003). The techniques for reservoirs sediment management can be broadly classified as: reducing sediment inflow from upstream (catchment management, bypassing and check dams), minimizing

sediment deposition (sluicing and routing), and removal of reservoir sediment (flushing, dredging and hydrosuction) after it has been deposited (Morris 2014). The sediment delivery to the reservoir from upstream catchments can be minimized by catchment management strategies and trapping the upstream eroded sediment by constructing check dams. Flushing and sluicing are reservoir level sediment management techniques to remove sediment deposition and to minimize sediment deposition. Sediment flushing is the removal of accumulated sediment from a reservoir by passing water and sediment through low level outlets located at the bottom level of a dam. Sluicing is to route sediment inflow so as not to allowing for deposition in reservoirs (Kantoush and Sumi 2010; Palmieri et al. 2003).

However, an application of reservoir sediment management techniques can affect downstream reservoirs in terms of flow, energy production and sediment deposition in the multi-reservoir system. Sediment management of multiple reservoirs is rarely implemented on the basin scale level because of improvements needed in available modelling tools. To overcome deficiencies in current models, the development of a reservoir sediment management routine (ResSMan) and its integration into the SWAT model was presented in Chapter 2. The ResSMan routine integrated within SWAT aims to enable sediment management in multiple reservoirs through the functionality to simulate flushing and sluicing at appropriate times, duration and frequency for improved estimation of flows, energy production and sediment deposition.

Previous work on multiple reservoirs sediment management aimed to identify and evaluate alternative dam sites and operating policies to improve the downstream sediment regime (Wild and Loucks 2015; Wild et al. 2015). While it is a relevant step, that work does to date not entail coordinated operation, i.e. managing the sequence, timing and frequency of operation, of multiple reservoirs – a system of reservoirs – at the river basin scale. Furthermore, sediment management operations of the upstream reservoirs can affect the downstream

reservoirs in the cascade system by transporting and depositing large flushed sediment loads and changing inflows. A detailed analysis of these issues is necessary for sustainable operation of reservoir systems. Thus, the main objective of this chapter is to provide guidance on the coordinated operation of sediment management for effective release of sediment through multiple reservoirs to the downstream regime, as well as better management of hydropower production. The new reservoir management routine was applied to demonstrate the improved management of a coordinated operation of the implemented sediment management techniques to the multi-reservoir system in the 2S basin of the Mekong.

4.2 Methodology

4.2.1 Study area

This chapter focuses on hydropower schemes located upstream from the Lower Sesan 2+Lower Srepok (LSS 2) reservoir in the tributary of the Sesan and Srepok rivers (known as the 2S basin). The transboundary 2S basin is shared by Vietnam and Cambodia. The catchment area of Sesan is 18,800 km² and 30,900 km² of the area is occupied by the Srepok subbasin which is the largest of the 3S basin (described in Chapter 3) (Figure 4-1). The LSS 2 reservoir, one of the large reservoir in the 2S basin, is located downstream of the confluence of the Srepok and Sesan Rivers and close to the 3S rivers junction, blocking the hydro-ecological route to the critical downstream Mekong ecosystems (Arias et al. 2014; Binh et al. 2020). At present, 12 hydropower projects exist and 7 hydropower schemes are under construction and planning to fulfil the increasing energy demand in the 2S basin. To investigate the impact of trapping of sediment on storage capacity and energy production and to apply sediment management techniques for the coordinated operation of transboundary reservoirs, these 19 hydropower reservoirs were considered for simulation (Figure 4-1).

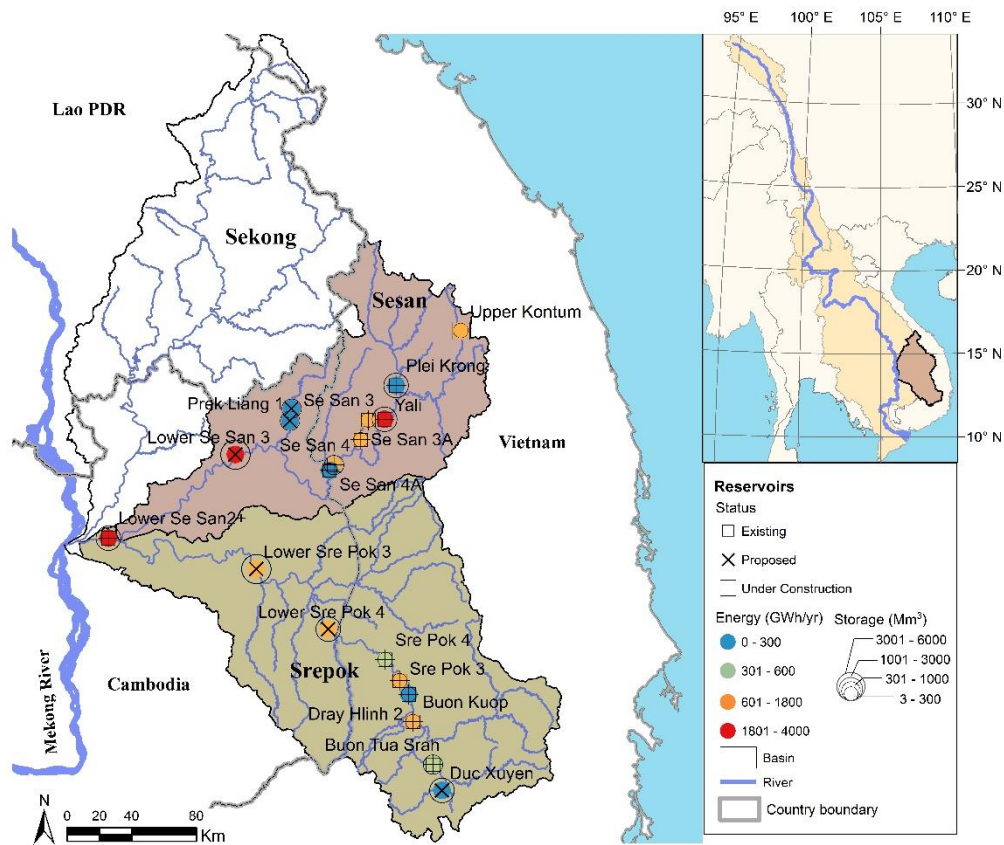


Figure 4-1: Location map of selected hydropower reservoirs (showing the river network, energy production and storage capacity of existing, proposed and under construction) in the Sesan and Srepok river basins (reproduced from Shrestha et al. (2020)).

4.2.2 Hydrological modelling

A calibrated and validated SWAT model of the 3S basin was used for the integration and application of ResSMan (Shrestha et al. 2018; Shrestha et al. 2016). The detailed methods and results of calibration and validation of the SWAT model for the 3S basin were presented in Shrestha et al. (2016) and Chapter 3.

4.2.3 Sediment management simulation

The calibrated 3S SWAT model, with an integrated ResSMan routine, was used for sediment management techniques simulations for the 2S basin. The model was simulated for a 100 year period for a realistic representation of the accumulation of sediment and its impacts on storage capacity during the typical life-span of dams. Effects of potential climate and land

use change are not considered here. However, the built-in weather generation function in SWAT was used to generate weather data for the modelling time period until 2120 (Neitsch et al. 2011; Sharpley and Williams 1990). The weather generator generates daily weather data (precipitation, temperature, solar radiation, relative humidity and wind speed) based on observed data. The 20 years (1986 - 2005) of observed weather data were used as a baseline climate data to generate required simulation period data.

ResSMan, a newly developed routine for SWAT, has capabilities to predict the accumulation of trapped sediment, its impacts on the storage capacity of a reservoir, and hydropower generation under specified operation policies. Moreover, it allows to calculate the restoration of storage capacity due to the removal of sediment by flushing (removal of sediment from a reservoir by passing water and sediment through flush gates located at the low level of a dam) and sluicing (bypassing sediment before suspended sediment solids have settled down in reservoirs). The input data (volume-area-elevation curve, hydroplant pool curve, spillway rating curve, low level outlet capacity rating curve, rule curve and hydropower plant characteristics) for simulation with ResSMan were obtained from Piman et al. (2013). Most of the reservoirs in the 2S basin that have already been constructed or are in the planning stage have no low level gates/outlets installed. As per engineering designs of these hydropower schemes, it seems that instead of applying sediment management techniques, they are designed to store sediments during their life-span providing sufficiently large storage capacity. Furthermore, most of the reservoirs are very large with respect to their inflow rates and too wide and flat for application of sediment management techniques, specifically flushing and sluicing, to be feasible (Wild and Loucks 2014). Even though reservoir sedimentation might not have significant impacts on the storage capacity and hydropower production, trapping of sediment will negatively impact on the downstream sediment regime. Thus, the theoretical case where low level gates are installed and are in operational condition for flushing and sluicing

was investigated. The RESCON model, is an excel-based tool, used to evaluate the technical and economic feasibility of sediment management techniques for particular reservoirs (Kawashima et al. 2003; Palmieri et al. 2003). The flushing specification input data such as the duration and frequency of flushing, flushing discharge, maximum flushing water level and drawdown rates were approximated using the RESCON model. Finally, ResSMan was applied to simulate flushing and sluicing operations for a complex system of multiple hydropower reservoirs in the 2S basin.

4.2.4 Scenarios

In order to quantify sedimentation and its effects on hydropower production and storage capacity, the first two scenarios were set up. Furthermore, to operate sediment management techniques individually and co-ordinately and to analyse the effects on energy production, storage capacity and sediment deposition, a sediment management scenario was formulated with three sub-scenarios.

1. Unregulated scenario: This is a scenario without any reservoirs which represents the natural flow regime. The main objective of formulation of this scenario is to assess sediment loads of the river.
2. Regulated scenario: In this scenario, 19 reservoirs were included, of which 10 reservoirs (Upper Kontum, Plei Krong, Yali, Sesan 3 (SS 3), Sesan 3A (SS 3A), Sesan 4 (SS 4), Sesan 4A (SS 4A), Prek Liang 2, Prek Liang 1, and Lower Sesan 3 (LSS 3)), are located in the Sesan cascade, 8 reservoirs (Duc Xuye, Buon Tua Srah, Buon Kuop, Dray Hlinh 1/2, Srepok 3 (SP 3), Srepok 4 (SP 4), Lower Srepok 4 (LSP 4), and Lower Srepok 3 (LSP 3)) are located in the Srepok cascade and the LSS 2 reservoir is located at the outlet of the 2S basin (Figure 4-1). Furthermore, two types were used of operation rule curves to study the impacts of operation policies on the reservoir sedimentation

(Seasonal Variation (SV) rule curve: maximizes energy production and Full Supply Level (FSL) rule curve: maintains ecological flows). All 19 reservoirs were simulated under specified rule curves however, no sediment management technique was implemented in any reservoir. This scenario was used to quantify the energy generation, reservoir sedimentation and changes in sediment regime due to the operation of hydropower reservoirs.

3. Sediment management scenarios: The Yali, SS 3, SS 3A, SS 4, SS4A (reservoirs in the Sesan cascade) (Figure 4-2a) and the SP 3, SP 4, LSP 4, and LSP 3 (reservoirs in the Srepok cascade) (Figure 4-2b) were selected as a set of reservoirs (9 reservoirs) for sediment management simulations, while the remaining reservoirs operate normally using the SV rule curves. These reservoirs were selected because sediment depositions in these reservoirs are comparably high (this has been identified with simulation runs to identify the most sensible choice of reservoirs for the purpose of this paper). Furthermore, these reservoirs are located in the main river reach and application of sediment management to the upstream reservoir significantly impacts downstream reservoirs.
 - i) Individual reservoir flushing scenario: In this scenario, total 18 (2 x 9) simulation runs were ran, one run for each reservoir flushing annually (IF-1) and 5-yearly (IF-5) for the set of reservoirs, while the other reservoirs operate under specified SV rule curves. The results of this scenario were used to analyse the impacts of flushed sediment loads on the downstream reservoirs according to their size, location and distance (Figure 4-2) and impacts on energy generation. This scenario was used to illustrate effects of flushing of upstream reservoir on the downstream reservoirs according to their size, location and hydropower production. Moreover, the IF-5

scenario was simulated specifically to investigate change in energy production by reducing the frequency of flushing.

- ii) Multiple reservoirs flushing scenario: In order to approximately optimize energy production as well as to manage reservoir sedimentation, altogether three simulation runs were ran: one run for each set of reservoirs with flushing annually (MF-1), bi-annually (MF-2) and 5-yearly (MF-5). In the case of bi-annually and 5-yearly scenarios, among the set of reservoirs, alternate reservoirs were simulated with flushing at successive flushing frequency periods according to their position in the cascade.

MF-1 is the uncoordinated operation of flushing. This scenario was simulated to quantify the sediment release downstream of the sediment regime and effects in the energy production due to the uncoordinated operation of the flushing.

MF-2 is the coordinated operation of flushing. This scenario was simulated to quantify the sediment release downstream of the sediment regime and effects in the energy production due to the coordinated operation of the flushing.

Similarly, MF-5 is the coordinated operation of flushing. In this scenario, the frequency of flushing was reduced to 5 years so that loss in energy could be reduced during flushing. This scenario was simulated to quantify sediment release downstream of the sediment regime and effects in the energy production due to coordinated operation of the flushing.

- iii) Multiple reservoirs sluicing scenario (MS-P): In this scenario, the set of selected reservoirs were simulated with sluicing during peak flood periods. This scenario was formulated to pass large sediment loads before settling in the reservoir by opening low level outlets during the flood period. The threshold maximum inflows for each of the reservoirs were defined. Sluicing begins when the inflow is above

the threshold value, and when the inflow is below this value, sluicing ends. These threshold maximum inflows were set based on the average maximum peak floods which were derived from the Regulated scenario for each of the reservoirs. These threshold values were chosen to pass the highly sediment concentrated flow during peak flood periods.

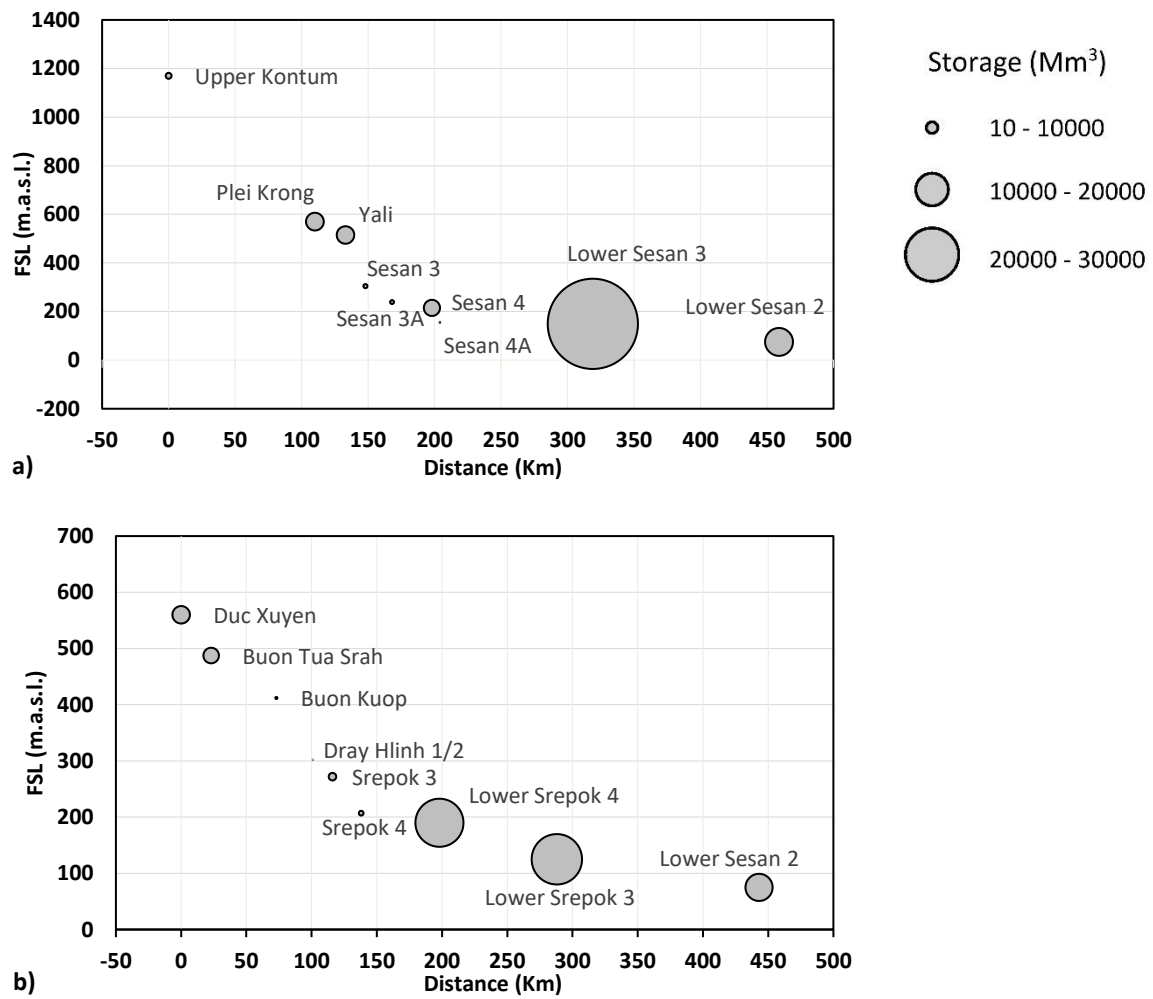


Figure 4-2: Distance (x-axis) of reservoirs from the most upstream reservoir and their full supply level (FSL on the y-axis) and storage capacity (denoted by the circle size in Mm^3) for a) Sesan cascade and b) Srepok cascade.

4.3 Results and discussion

4.3.1 Sediment load and reservoir sedimentation

The mean annual sediment load at the outlet of the LSS 2 is about 7.24 million metric tonnes per year (Mt/y) over a 100-year simulation period, of which the Sesan subbasin and Srepok subbasin contribute about 70% and 30% respectively (Figure 4-3: Unregulated scenario). As expected, the results showed a trend of an increase in sediment loads for decreasing altitude and increasing catchment area. The mean annual sediment load of the 2S rivers at the outlet of the 2S basin (i.e. at the LSS 2 reservoir) decreased significantly from the Unregulated to the Regulated-SV scenario (under the SV rule curve), resulting in a mean annual sediment inflow of 0.27 Mt/y and outflow of 0.11 Mt/y, a decrease of 96% and 98% from the Unregulated scenario, respectively. Overall it was found that reservoir operations will significantly reduce (19% to 99%) the sediment load inflow to the reservoirs.

The operation of these 19 reservoirs will trap 924 Mt of sediment over 100 years, showing that the average trapping efficiency of these reservoirs is 74%. However, the amount of sediment deposition in a particular reservoirs varies with the size of the reservoir and inflow sediment loads. The LSS 3 and the Dray Hlinh 1/2 therefore have the highest (97%) and lowest (2%) average trapping efficiencies, respectively (Figure 4-4). The Brune's trapping efficiency depends on the reservoir's residence time. The residence times are high for large reservoirs and hence the results depict high trapping efficiencies for the large reservoirs. The Dray Hlinh 1/2 showed the lowest TE because it has no significant reservoir and is operating as a run-of-river scheme, thus this result has not been considered for averaging the TE of reservoirs across the 2S basin. For reservoirs with high trapping efficiencies the impacts of sediment deposition on storage capacity are significant when compared to their original storage capacities after 100 years of operation. The results illustrated that sediment deposition will be large in the two

specific cascades considered (1. from the Plei Krong to Sesan 4A in the Sesan subbasin and 2. from the Buon Kuop to Srepok 4 in the Srepok subbasin). The reservoirs in these cascades will lose 10% to 39% of their original storage capacity. These cascades have a high reservoir density, as well as relatively high inflow sediment loads. It was found that the SS 3 reservoir will lose 39% of original storage capacity, whereas the LSS 2 will lose only 1% of its original storage capacity in 100 years of reservoir operations. Furthermore, changing the operation rule curve from the SV to FSL varies the sediment load outflows but does not significantly affect the sediment trapping efficiency and loss of storage capacity (Figure A4-1 and A4-2). The fluctuations of the storage capacity of reservoirs under the operations of these two rule curves are very small due to small changes in the residence times and trapping efficiencies.

The results showed that operation of reservoirs will significantly trap sediment loads and the most affected reservoir (SS 3) due to sedimentation can lose up-to 39% of its original capacity. This indicates that the useful life of reservoirs, particularly in the 2S basin, may be more than 100 years under the given weather conditions and land use types because a reservoir is arguably functional and efficient until 50% of its original storage capacity is depleted by sedimentation or its dead storage is completely filled with sediment (Garg and Jothiprakash 2008; Gill 1979; Issa et al. 2013). This indicates that dam owners have little interest to invest in sediment management measures for the short term period, generally 30-40 years for the Build, Own, Operate and Transfer (BOOT) contract system.

Again, the impacts of land use change and extreme events related to climate change may exacerbate the current assessment of sediment loads and increase the uncertainty of reservoir sedimentation (Lohani et al. 2020; Shrestha et al. 2018; Shrestha et al. 2018; Walling 2008). Furthermore, the uncertainty associated with the implemented operation policies, detailing of dam facilities (especially the level of hydropower intakes) and the spatial distribution of settled sediment in the reservoir bed surface makes it more difficult to predict when the reservoirs will

be non-operational and will end the useful life (Annandale 1984; Borland 1971; Michalec 2014). Whatsoever, eventually if operated without any sediment management, the reservoirs will be filled with sediment sooner or later. Hence, dam owners should analyse the impacts of potential reservoir sedimentation for sustainable use of the reservoirs.

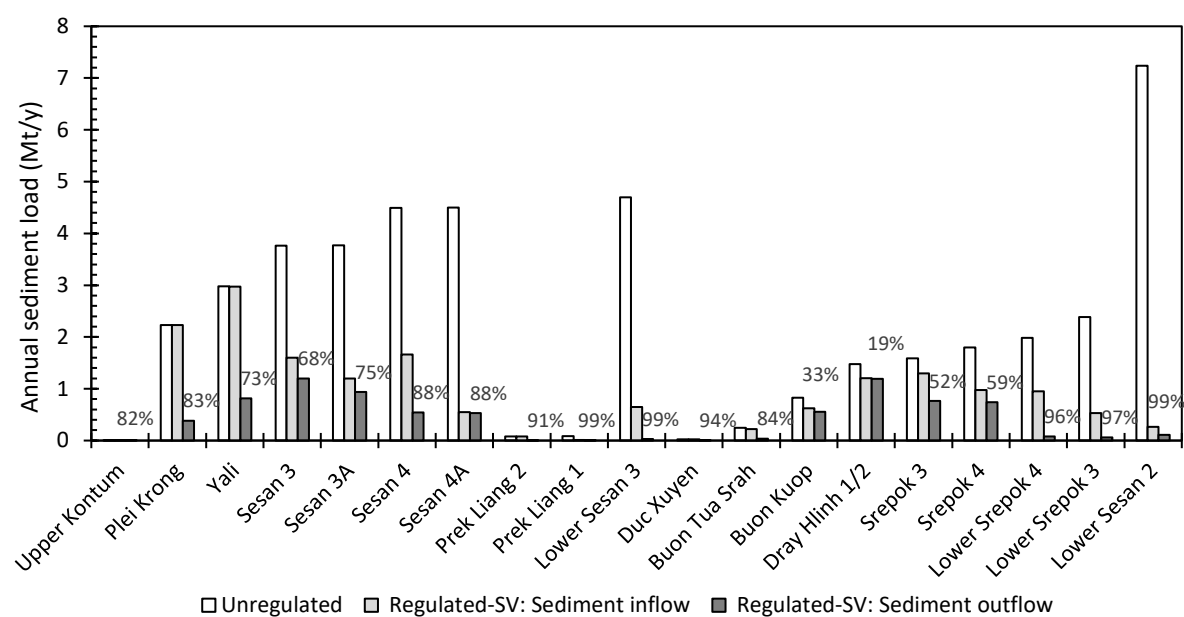


Figure 4-3: Mean annual sediment load in million ton/year (Mt/y) at the inlet of each of the reservoirs considered for the Unregulated scenario and mean annual sediment load (Mt/y) inflow and outflow for the Regulated scenario: assuming reservoirs are operating under SV rule curve but no sediment management techniques have been applied. The change in percentage between unregulated sediment load and regulated sediment outflow are shown in percentage (%) values.

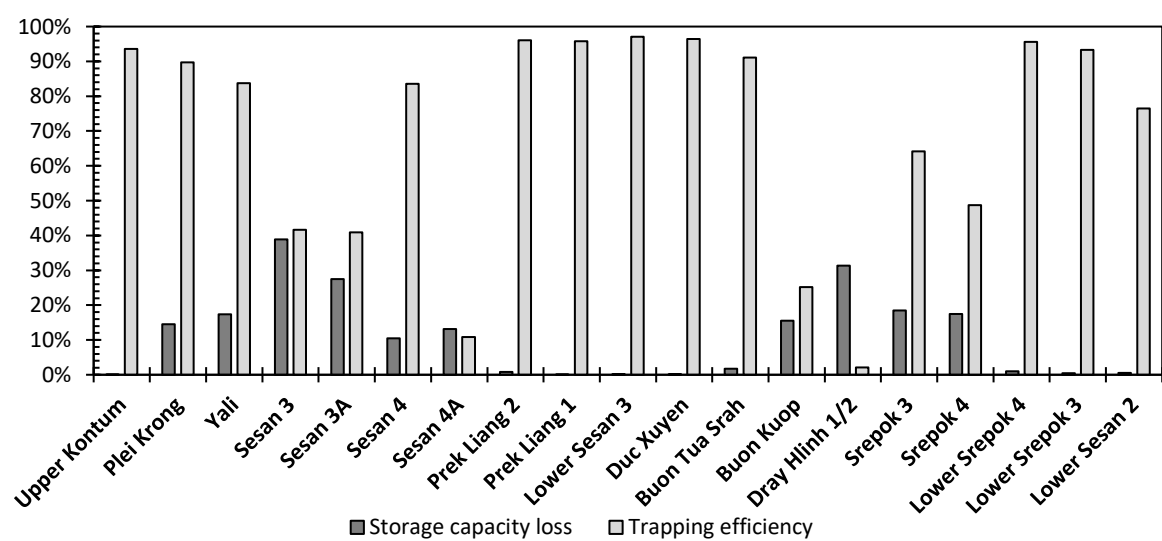


Figure 4-4: Initial storage capacity loss due to sediment deposition after 100 years of operation and average trapping efficiency of the reservoirs under the SV rule curve.

4.3.2 Sediment management simulation

4.3.2.1 *Impacts on the downstream cascade due to individual reservoir flushing*

The individual flushing of reservoirs (IF-1 scenario) were simulated to analyse the effects of flushed sediment loads on the downstream reservoirs in the cascade. Individual flushing of upstream reservoirs often resulted in varied percentages of deposition of flushed sediment loads in the downstream reservoir (Figure 4-5). In the Sesan cascade (Figure 4-5a), where flushing was simulated for the Yali reservoir, about 48% and 0.6% of flushed sediment loads will be deposited in the SS 4 and LSS 2 respectively. Furthermore, about an equal percentage (~15%) of flushed sediment loads will deposit in the SS 3 and SS 3A, and a much smaller percentage (0.8%) will accumulate in the SS 4A. This result demonstrates that the percentage of sediment deposition is strongly related to the size and position of the downstream reservoir. The SS 3 and SS 3A have the similar storage capacities, the SS 4 is larger, the SS 4A is the smallest and the LSS 3 is the largest (Figure 4-2a). Again, this analysis exhibits that a large reservoir has a higher residence time and therefore higher trapping efficiency. The results, therefore, indicated that the size of the reservoir plays a more critical role in accumulating the flushed sediment loads than the distance between the reservoirs. Similarly, large amounts of sediment deposit in the SS 4 reservoir when both the SS 3 and SS 3A are flushed. In contrast, flushing of the SS 4 and SS 4A reservoirs will largely impact the LSS 3 reservoir. In addition, the results indicated that 92% of flushing sediment loads from the SS 4 will deposit in the LSS 3, the largest reservoir in the cascade, whereas only 3.4% of flushed sediment load will deposit in the SS 4A, the smallest reservoir in the cascade (Figure 4-2a and Figure 4-5a). A large portion of sediment load is already trapped by the LSS 3 so that the percentage deposition in the relatively large LSS 2 is very low.

In the case of the Srepok cascade (Figure 4-5b), flushing of the SP 3 and SP 4 will mostly impact the LSP 4 and least impact the LSS 2. Moreover, flushing of LSP 4 and LSP 3 showed that a large portion of flushed sediment load will deposit in the adjacent downstream reservoir.

Overall the results reveal that the largest percentage of the flushed sediment loads deposits in the largest and closest downstream reservoir, while the least percentage of the flushed sediment loads deposits in a smaller reservoir, even if the adjacent downstream reservoir is at short distance from the upstream flushing reservoir.

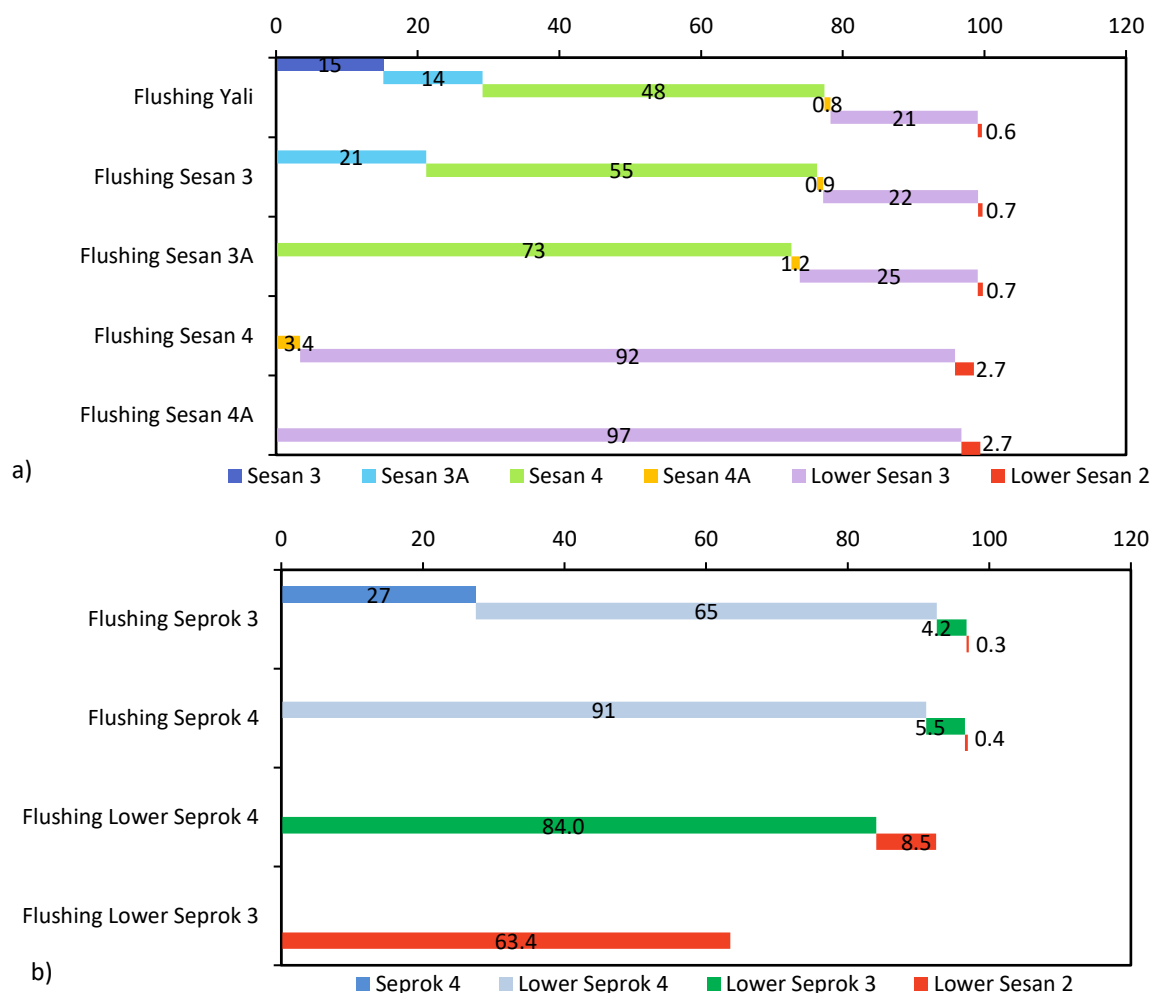


Figure 4-5: Percent (%) deposition of flushed sediment loads (x-axis) due to flushing of the upstream reservoir (y-axis) in the a) Sesan and b) Srepok cascade

4.3.2.2 Impacts on the energy production

Some amount of hydropower production will be lost during the application of sediment management measures such as flushing and sluicing because the hydropower plants will not be able to generate hydroelectric energy during the drawdown, flushing and refilling stages of the flushing process, and during the maximum drawdown of the sluicing process. The change in total energy production was analysed over the 100-year simulation period for the 2S basin and under different sediment management scenarios as compared to the regulated-SV scenario (a scenario of no sediment management) (Table 4-1). In the IF-1 scenario (individual flushing done annually), the total energy generated from the 2S basin over a 100-year simulation period will be reduced by 0.1% to 2.6%, depending on which reservoir is flushed. This indicates that the reduction in total energy production of the 2S basin due to annual flushing of any of the considered reservoirs is rather small. Conversely, if specific reservoirs are considered, the energy production loss due to annual flushing is significant. The results showed that the LSP 4 loses up to 33% of energy production and the SP 4 loses up to 4.5% of energy production. In the case of the LSP 4, the operational height (the height difference between the FSL and MOL) is smaller than the minimum possible head (the height difference between the MOL and turbine/tailwater level) of the hydropower plant (Table A3-1). Therefore, the hydropower plant is not capable of producing energy until the reservoir water level rises above the MOL in the drawdown and refilling phase. Due to the smaller operational height, the drawdown of the LSP 4 up to the MOL takes only 3-4 days, whereas emptying the reservoir takes about one month, takes about one week for actual flushing, and again about one month to refill the reservoir. As a consequence, the LSP 4 hydropower plant has to cease energy production for about two and a half months. In contrast, a complete drawdown of the SP 4 is completed within a week, and it is also likely to produce some amount of energy during the first phase of the drawdown and the final phase of refilling. Furthermore, storage capacity to mean annual inflow volume ratio

(capacity-inflow ratio, CIR) of the LSP 4 is relatively low compared to SP 4 and other reservoirs (Table 4-2). (Rooseboom and Basson 1997) indicated that the complete drawdown flushing is more effective for reservoirs with a CIR of less than 0.03. Hence, relatively large reservoirs in comparison to the mean annual inflow take considerable time to refill.

Table 4-1: Percentage (%) change in total energy production over the 100-year simulation period due to different sediment management scenarios (IF-1 and IF-5: individual reservoir flushing annually and 5-yearly respectively, MF-1, MF-2 and MF-5: multiple reservoir flushing annually, bi-annually and 5-yearly respectively and MS-P: multiple reservoir sluicing during specified threshold peak flood periods).

| Sediment Management Scenario | Reservoirs | Frequency | % change in energy production over the 100-year period | | | | | | | | | | |
|------------------------------|--------------------------------|-------------------------|--|-------|-------|-------|-------|-------|------|------|-------|-------|-------|
| | | | Overall | Yali | SS 3 | SS 3A | SS 4 | LSS 3 | SP 3 | SP 4 | LSP 4 | LSP 3 | LSS 2 |
| IF-1 | Yali | Annually | -2.6 | -13.0 | -1.8 | -1.9 | -0.4 | 0.2 | 0.0 | 0.0 | 0.0 | 0.0 | 0.2 |
| | SS 3 | | -0.8 | 0.0 | -10.9 | -0.3 | 0.1 | 0.0 | 0.0 | 0.0 | 0.0 | 0.0 | 0.0 |
| | SS 3A | | -0.1 | 0.0 | 0.0 | -4.9 | 0.0 | 0.0 | 0.0 | 0.0 | 0.0 | 0.0 | 0.0 |
| | SS 4 | | -1.3 | 0.0 | 0.0 | 0.0 | -17.3 | 0.2 | 0.0 | 0.0 | 0.0 | 0.0 | 0.3 |
| | SS 4A | | 0.0 | 0.0 | 0.0 | 0.0 | 0.0 | 0.0 | 0.0 | 0.0 | 0.0 | 0.0 | 0.0 |
| | SP 3 | | -0.5 | 0.0 | 0.0 | 0.0 | 0.0 | 0.0 | -9.3 | -0.6 | 0.2 | 0.0 | 0.0 |
| | SP 4 | | -0.1 | 0.0 | 0.0 | 0.0 | 0.0 | 0.0 | 0.0 | -4.5 | 0.1 | 0.0 | 0.0 |
| | LSP 4 | | -1.3 | 0.0 | 0.0 | 0.0 | 0.0 | 0.0 | 0.0 | 0.0 | -33.0 | 2.9 | 2.0 |
| | LSP 3 | | -0.9 | 0.0 | 0.0 | 0.0 | 0.0 | 0.0 | 0.0 | 0.0 | 0.0 | -13.5 | 0.7 |
| IF-5 | Yali | 5-yearly | -0.5 | -2.5 | -0.2 | -0.2 | 0.0 | 0.1 | 0.0 | 0.0 | 0.0 | 0.0 | 0.1 |
| | SS 3 | | -0.2 | 0.0 | -2.3 | -0.1 | 0.0 | 0.0 | 0.0 | 0.0 | 0.0 | 0.0 | 0.0 |
| | SS 3A | | 0.0 | 0.0 | 0.0 | -1.1 | 0.0 | 0.0 | 0.0 | 0.0 | 0.0 | 0.0 | 0.0 |
| | SS 4 | | -0.3 | 0.0 | 0.0 | 0.0 | -3.6 | 0.0 | 0.0 | 0.0 | 0.0 | 0.0 | 0.1 |
| | SS 4A | | 0.0 | 0.0 | 0.0 | 0.0 | 0.0 | 0.0 | 0.0 | 0.0 | 0.0 | 0.0 | 0.0 |
| | SP 3 | | -0.1 | 0.0 | 0.0 | 0.0 | 0.0 | 0.0 | -2.0 | 0.0 | 0.0 | 0.0 | 0.0 |
| | SP 4 | | 0.0 | 0.0 | 0.0 | 0.0 | 0.0 | 0.0 | 0.0 | -1.1 | 0.0 | 0.0 | 0.0 |
| | LSP 4 | | -0.3 | 0.0 | 0.0 | 0.0 | 0.0 | 0.0 | 0.0 | 0.0 | -6.7 | 0.6 | 0.4 |
| | LSP 3 | | -0.2 | 0.0 | 0.0 | 0.0 | 0.0 | 0.0 | 0.0 | 0.0 | 0.0 | -2.8 | 0.1 |
| MF-1 | A set of selected 9 reservoirs | Annually | -7.9 | -13.0 | -10.4 | -6.4 | -22.9 | 0.3 | -9.3 | -5.4 | -33.9 | -11.5 | 3.5 |
| MF-2 | | Bi-annually (alternate) | -3.8 | -6.0 | -6.4 | -2.8 | -9.2 | 0.3 | -4.5 | -3.9 | -16.9 | -5.2 | 1.2 |
| MF-5 | | 5-yearly (alternate) | -1.5 | -2.5 | -2.5 | -1.1 | -3.7 | 0.2 | -2.0 | -1.4 | -6.9 | -1.9 | 0.7 |
| MS-P | | Peak Flood Periods | -0.5 | -0.6 | -0.2 | -0.1 | -2.3 | 0.0 | 0.0 | 0.0 | -2.8 | 0.0 | 0.0 |

Table 4-2: Storage capacity (Mm³) at the full supply level, mean annual inflow (m³/s) for the Regulated-SV scenario and capacity-inflow ratio (CIR) for the considered reservoirs for sediment management

| Description | Yali | SS 3 | SS 3A | SS 4 | SS 4A | SP 3 | SP 4 | LSP 4 | LSP 3 |
|---|-------|-------|-------|-------|-------|-------|-------|-------|-------|
| Storage capacity (Mm³) | 1039 | 87 | 81 | 893 | 11 | 243 | 114 | 7471 | 8198 |
| Mean Annual Inflow (m³) | 303 | 314 | 322 | 377 | 379 | 335 | 371 | 503 | 1003 |
| CIR | 0.109 | 0.009 | 0.008 | 0.075 | 0.001 | 0.023 | 0.010 | 0.471 | 0.259 |

Alternately, in the IF-5 scenario, the loss of total energy production of the 2S basin over a 100-year simulation period will be 0.1% to 0.5%, which revealed that the loss of energy production due to flushing will be substantially reduced compared to the results of the IF-1 scenario. The largest and the least loss of energy production by the individual reservoirs are again found for the LSP 4 and SP 4 with losses of 6.7% and 1.1% respectively. However, the 2S basin has to compromise the largest amount of energy production due to flushing of the Yali because it is the largest reservoir in terms of the installed capacity.

In the case of multiple reservoirs sediment management simulations, when all the considered reservoirs for sediment management simulation are flushed annually (MF-1 scenario), the loss of energy production from the 2S basin will increase significantly. This simulation showed that the overall 2S basin will lose 7.9% of total energy production and in particular, the LSP alone will lose 33.9% of its total energy production over a 100-years period. The results showed losses of 3.8% and 1.5% in the total energy production of the 2S basin for bi-annual and 5-yearly scenarios, respectively. Alternately, the 5-yearly flushing operation is able to remove the accumulated sediment over the past five years and successfully restore the original storage capacity of the reservoirs. Thus, MF-5 scenario is more economical than the MF-1 and MF-2 scenario. In the same way, sluicing of the reservoirs during the extreme flood period (MS-P scenario) showed that a reduction of 0.5% in the total energy production and indicates the largest decrease in energy for the LSP 4.

4.3.2.3 Coordinated operations of sediment management

In order to manage transboundary reservoirs in a coordinated manner, the timing, duration and frequency of flushing and sluicing need to be accurately determined. Generally, the pre-flooding period is the period best suited for flushing because the reservoir can be emptied during low inflows and refilled during the flood season. Conversely, sluicing is more

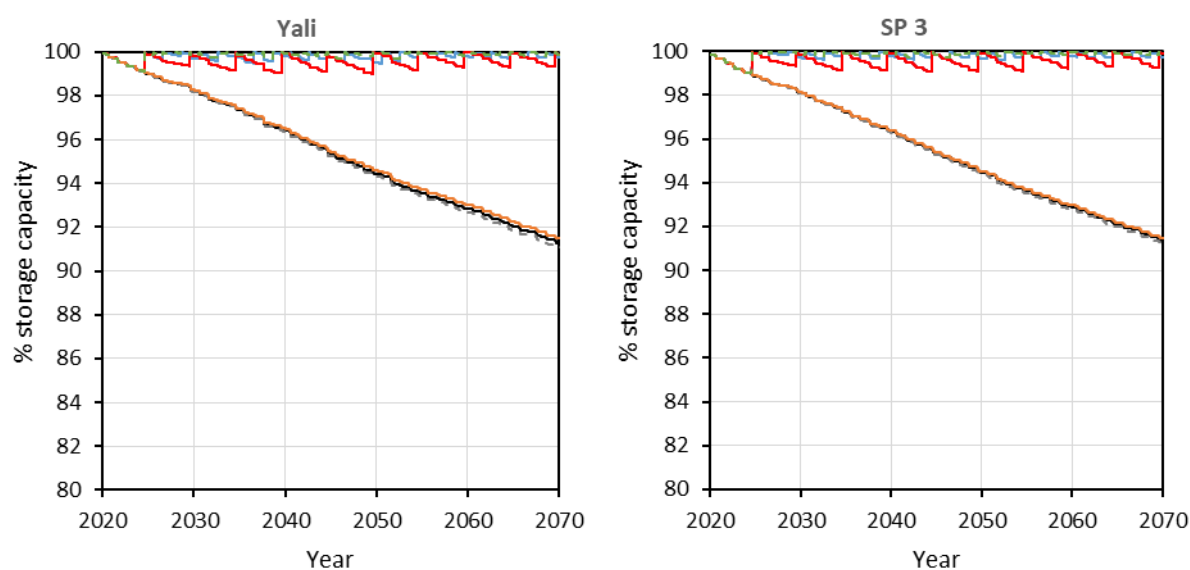
effective in the peak flood season because the conditions allow for removing the sediment in the reservoir by passing the high sediment-laden flows. As can be seen from the inflow hydrographs of reservoirs (Figure A4-3), inflow to the reservoirs usually starts to increase from late June (mid-June for LSP 3 and LSP 4) and attains peak flow in early September (early August for LSP 3 and LSP 4) under the SV rule curve operation. However, application of the FSL rule curve resulted in different hydrograph shapes. The characteristics of the inflow hydrographs indicated that June and July are favourable for flushing and August and September are favourable for sluicing under the SV operation policy.

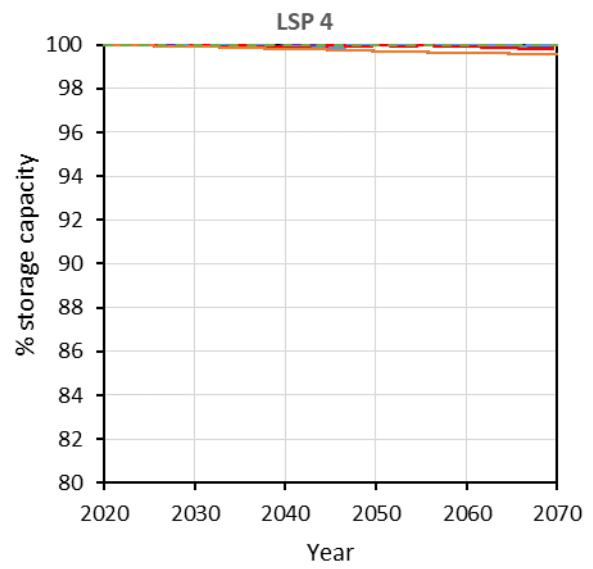
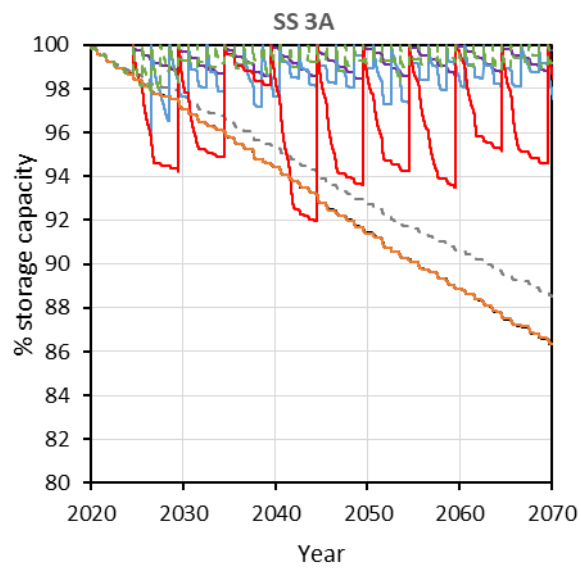
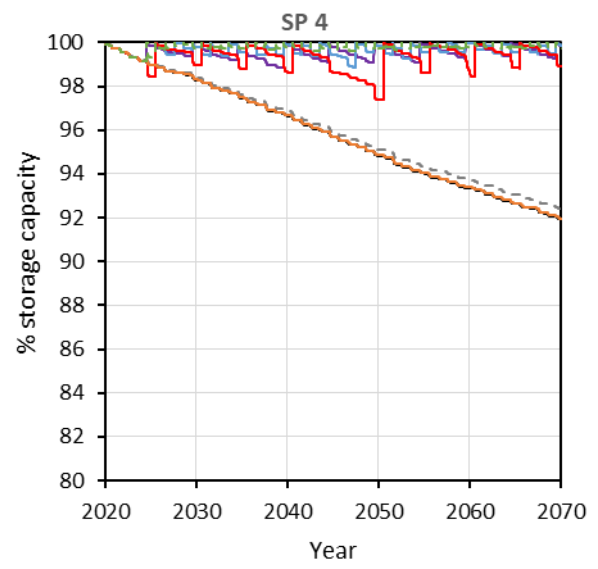
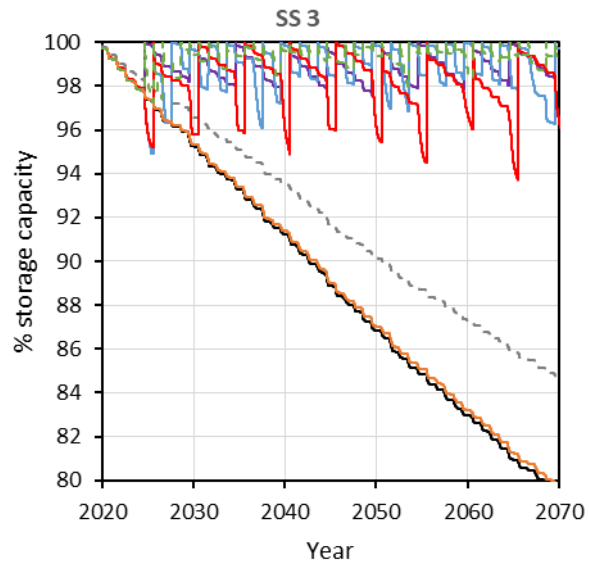
The drawdown start dates for flushing were set on the 1st June for the LSP 3 and LSP 4 and the 1st July for the remaining reservoirs. However, the results indicated that these start dates of drawdown for flushing are more effective for individual flushing scenarios (i.e. IF-1) under the specified SV rules (Figure 4-6). Initial simulations with annual flushing on those dates for the set of selected reservoirs (i.e. MF-1) showed that flushing was not successful for SS 3, SS 4, LSP 4 and LSP 3 for any given year. The inflow pattern of the Yali and SP 3 reservoirs at the top of the cascade remains the same for the particular operation policy so these reservoirs are successfully flushed in this scenario. Conversely, in the case of SS 3, SS 4 and LSP 3, flushing of large upstream reservoirs like the Yali and LSP 4 significantly increased the inflow to these reservoirs during the drawdown period. Consequently, the complete emptying of these reservoirs took comparably long and sometimes even failed to achieve a river-like flow for successful flushing. To address these issues, low-level outlets with large capacity are required to pass large floods during flushing. Installing such outlets may not always be feasible due to engineering design constraints of structures. In addition, releasing flows, larger than the natural peak floods, for a longer period can increase downstream flood hazards and can negatively impact the ecological system of the river. Furthermore, another main reason for the unsuccessful flushing of SS 3, SS 4, and LSP 4 for most of the simulation years is that they did

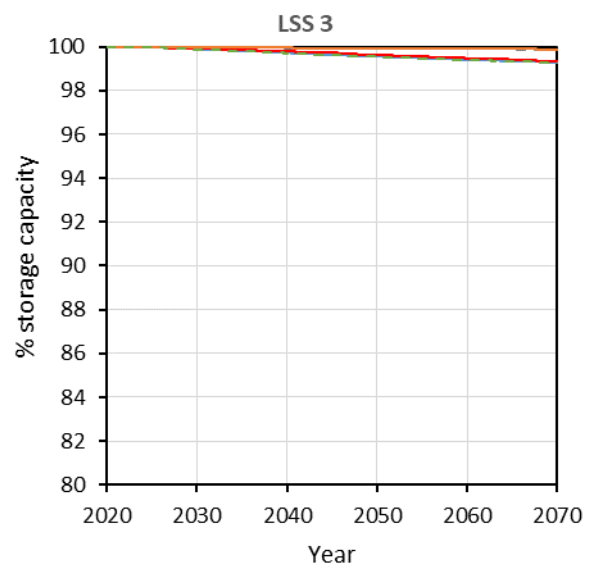
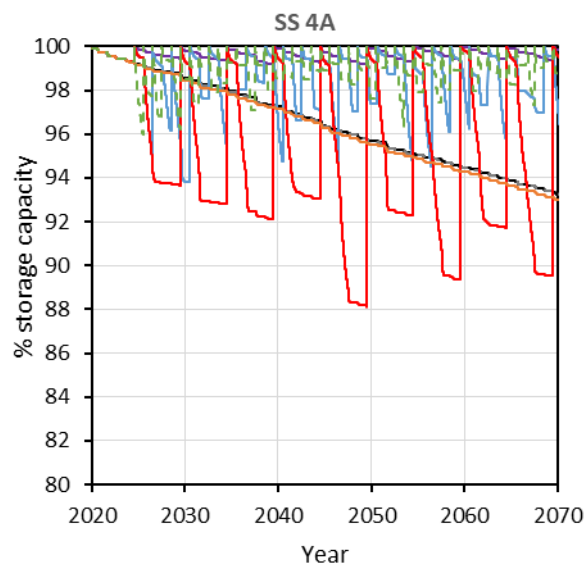
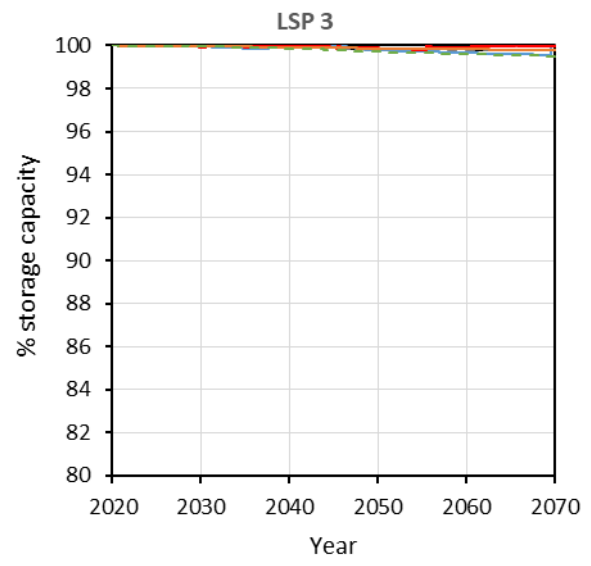
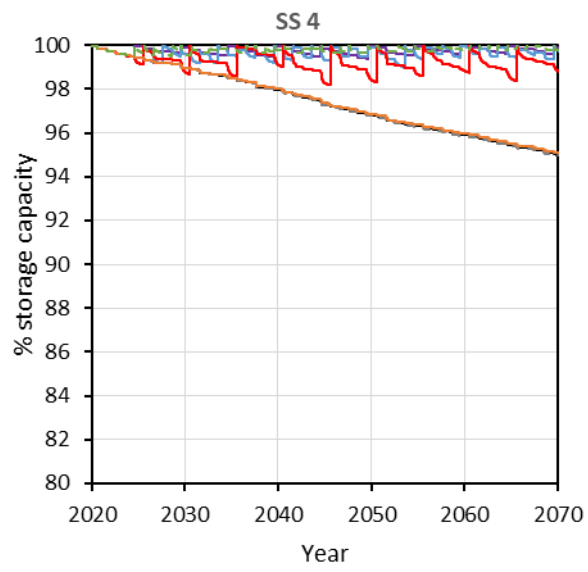
not receive sufficiently large inflows to meet the target flushing discharge. This is because the upstream reservoirs had completed flushing, were being refilled and no water was being released during that period. In the case of the LSP 3, the results revealed that the LSP 3 could not be successfully flushed because large inflows from the upstream reservoirs prevented a complete drawdown of the LSP 3. Hence, the scenarios were formulated to coordinate between the drawdown start time, flushing period and frequency of the reservoirs for effective sediment management.

To overcome the deficiencies due to uncoordinated reservoir operation, scenarios were run where the reservoirs were managed in coordination with each other for the flushing operations. The individual flushing scenario showed that depending on the size of the reservoir and the hydrological conditions, it takes on average one and a half months to complete the flushing process of these reservoirs. For this particular basin, the feasible time for flushing, i.e. duration of pre-flood, is about 2-3 months. Thus, the coordination of flushing for the set of selected reservoirs over a short duration of the pre-flood period of the same year is complex and impractical. Again, if all these reservoirs are being flushed in the same year, there will be a power deficit during that particular period and the concerned agencies will have to manage alternate sources of energy. Several possible scenarios (not all results are presented here) were analysed and two of them, the bi-annual and 5-yearly flushing of alternate reservoirs at successive flushing frequency periods (MF-2 and MF-5 scenarios), showed more effective in terms of sediment removal and energy production (Figure 4-6). The simulated scenarios were analysed not only to manage sedimentation but also with respect to energy management. The results showed that a total of 609 Mt of sediment accumulates in the considered set of reservoirs (Yali, SS 3, SS 3A, SS 4, SS 4A, SP 3, SP 4, LSP 4 and LSP 3) without sediment management in the 100-year period. When implementing uncoordinated annual flushing for these reservoirs, the total sediment deposition will be 121 Mt., whereas the bi-annual and the 5-yearly flushing

scenarios (coordinated) resulted in a total sediment deposition of 25 Mt and 37 Mt, respectively. This result indicates that the application of the 5-yearly flushing strategy can remove accumulated sediment as effectively as the bi-annual scenario, thereby losing less energy than the bi-annual scenario. Hence, the MF-5 scenario is as effective as the MF-2 scenario in terms of sediment removal. However, the amounts of the sediment loads due to flushing events are different for these scenarios and thus the impacts associated with the downstream ecology and sediment deposition in the river channel may be different. Therefore, this scenario must not be viewed as the final optimal outcome. This analysis is an initial step towards the optimization and coordination of sediment management plans and policies for multi-reservoirs system such as those in the Mekong basin.







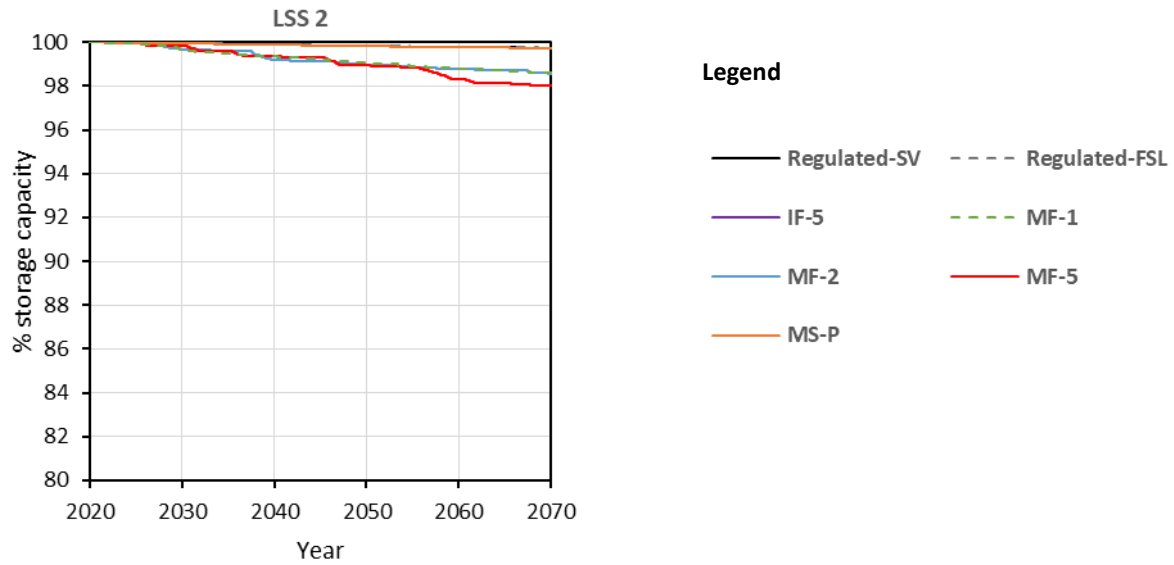


Figure 4-6: Reservoir storage capacity, expressed as a percentage of reservoir storage capacity at the full supply level, for the set of considered reservoirs over a 100-year simulation period (shown are only the first 50 years here) under the Regulated-SV (Regulated scenario under the SV rule), Regulated-FSL (Regulated scenario under the FSL rule), IF-5 (Individual reservoir 5-yearly flushing), MF-1 (Multiple reservoirs annually flushing), MF-2 (Multiple reservoirs bi-annually flushing), MF-5 (Multiple reservoirs 5-yearly flushing), and MS-P (sluicing reservoirs during extreme flood period) scenarios.

4.3.3 Possible consequences on the sediment regime

The findings illustrate that the mean monthly sediment load of the 2S basin is drastically altered by reservoir operations, in particular during high sediment load periods (June to October) (Figure 4-7). Sediment load error bars in Figure 4-7 show the variation of sediment loads due to different hydrological years and the application of different sediment management methods over the 100-year simulation period. The results show that the bi-annual and 5-yearly flushing of the considered set of reservoirs are able to increase the sediment load discharges during high sediment load periods. However, the increase in sediment load discharges due to sediment management relative to the natural sediment loads is very small. This is because sediment management techniques have been implemented only for 9 out of 19 reservoirs and have not been applied for the LSS 3 and LSS 2. While these reservoirs (LSS 3 and LSS 2) are the main barriers that prevent discharging most of the flushed sediment loads to the

downstream, flushing and sluicing is technically not feasible for these reservoirs due to their large size, wide and flat surface area and engineering design constraints. Relocation and replacement with smaller reservoirs may be the solution to overcome this challenge (Wild et al. 2015). However, LSS 2 has already been in operation since 2018 without addressing all these noted issues.

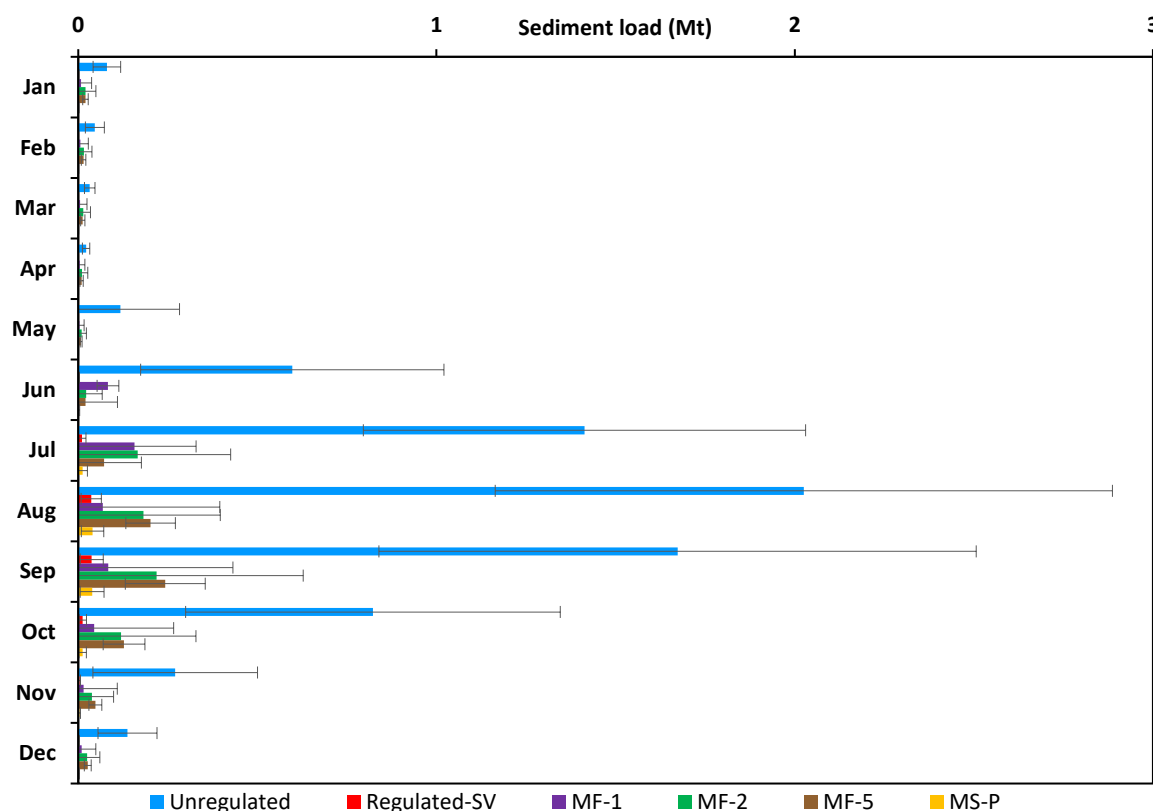


Figure 4-7: Mean monthly sediment load outflows in million tonnes at the outlet of LSS 2 over a 100-year simulation period under the Unregulated, the Regulated-SV (Regulated scenario under the SV rule), MF-1 (Multiple reservoirs annually flushing), MF-2 (Multiple reservoirs bi-annually flushing with alternate reservoirs in alternate years), MF-5 (Multiple reservoirs 5-yearly flushing with alternate reservoirs in alternate years), and MS-P (sluicing reservoirs during extreme flood periods) scenarios. The error bars represent one standard deviation of the mean.

Biodiversity in the Mekong is among the highest in the world, home to 781 fish species of which 42% (329) are found in the 3S basin (Baran et al. 2015; Ziv et al. 2012). Most of the fish species in the 3S basin are migratory fish, and at least 30 fish species migrate between the 2S basin and Tonle Sap Lake, establishing a critical hydro-ecological route (Constable 2015; Hurtle 2008). Furthermore, nutrient and minerals associated with sediment load and organic

matters are sources of food for these fish and aquatic species and also support floodplain agriculture (Manh et al. 2014). A reduction in sediment delivery to the lower Mekong, therefore, may be a great threat to the downstream ecosystems and agricultural systems. Additionally, previous studies have shown that a substantial decline in sediment supply to the Mekong delta has been triggering coastal erosion, river morphological degradation, and riverbed incision in downstream reaches (Binh et al. 2020; Kondolf et al. 2018; Syvitski et al. 2009; Tamura et al. 2020). Thus, the implications of sediment management techniques are not only important for the sustainability of reservoirs, but also to maintain the sediment budget of the downstream sediment regime.

The complete drawdown flushing method during the pre-flood period is effective to remove deposited sediment. The concentration of sediment upsurges in the downstream reaches of the river during the short period of flushing. The sudden increase in sediment concentration should not exceed the concentration that the environment can withstand (Fruchard and Camenen 2012). Discharging of large sediment loads in short time periods during the pre-flood season may have adverse impacts on the downstream ecosystems, jeopardizing fish and other aquatic lives. Furthermore, large flow release due to drawdown of reservoirs during the pre-flood season may alter the hydrological regime and shift natural hydrographs. Our previous study has shown that reservoir operations will cause large hydrological alterations in the 3S basin (Shrestha et al. 2020). While the current study provides first indications, the most suitable time for flushing and sediment load limits should be further assessed by field measurement campaigns, analysing previous flushing records (if any available) and detailed hydraulic and habitat modelling. This was also noted in the work by Moridi and Yazdi (2017).

Finally, application of frequent flushing such as annually or bi-annually may lead to a reduction in release of high sediment concentrations. Additionally, frequent flushing will facilitate to overcome downstream sediment starvation as well as help to minimize negative

environmental impact. Alternately, other available more environmentally friendly sediment management techniques such as sluicing (sediment routing) and channel bypassing (possible under favourable site conditions) can be applied to reduce reservoir sedimentation. Hence, sluicing during the peak flood periods and bypassing the fraction of sediment continuously through the bypass channel should be considered to determine the most sustainable strategy.

4.4 Conclusions

In this chapter, the ResSMan routine integrated with SWAT was applied to the 2S basin to quantify accumulated sediment and energy production. The effect of both individual and coordinated application of sediment management has been assessed, which yielded these findings:

TE of the reservoir showed dependence on the residence time and thus, the larger the reservoir the higher the TE. Sediment load inflows and loss of storage capacity of the reservoirs are significant (i.e. 10% to 39% of loss in the storage capacity) in a specific stretch of the Sesan cascade (from the Plei Krong to the SS 4A) and the Srepok cascade (from the Buon Kuop to the SP 4).

The analysis of the impacts of flushed loads on downstream reservoirs in the cascade system revealed that the largest portion (97%) of flushed sediment is deposited in the nearest largest downstream reservoir and the smallest portion (3.4%) accumulates in smaller reservoirs, even if the adjacent downstream reservoir is located at a short distance.

The loss in total energy production of the 2S basin is rather small (up-to 2.6%) due to individual flushing of any of the considered reservoirs. However, a loss of 33% of energy production occurs in the LSP 4 reservoir alone.

In the case of an individual reservoir, our simulations showed that reservoir sedimentation can be mitigated by implementing management techniques, especially flushing. The results indicated, however, that an uncoordinated operation of flushing in multiple reservoirs of the 2S basin is ineffective for removing sediment through cascades of reservoirs, thereby losing 7.9% of hydropower production. Therefore, it is recommended that sediment management, especially flushing, can be effective in a multi-reservoir system, if reservoirs are operated in a coordinated manner. Such coordinated operation can be achieved by establishing appropriate timing, frequency, and duration of flushing. For the current case favourable drawdown initiation for flushing is early June for LSP 3 and LSP 4, and early July for other reservoirs under the SV rule curve. In contrast, sluicing is favourable between August and September and the time period depends on the assigned threshold peak flood. However, these timings may vary based on the applied operation policies and the prevailing weather conditions. The application of ResSMan for coordinated operation of flushing for multiple reservoirs revealed that the bi-annually and 5-yearly flushing (alternate reservoirs in successive flushing frequency periods) scenarios could be the most effective options for efficiently releasing sediment, thereby compromising only a 1.5% of hydropower production under the 5-yearly scenario. It can be therefore concluded that coordinated energy production and sediment management of the 2S basin hydropower system will be key to achieve sustainable use of the reservoirs and improve sediment load release in the lower Mekong from the LSS 2.

The methodology presented here provides an initial step to the coordinated operation of sediment management for multiple reservoirs. The implementation of sediment management for the complex system of transboundary reservoirs in the 2S basin (Vietnam and Cambodia) is not only a technical challenge but there will also be diplomatic challenges to coordinate and collaborate between two nations and various dam owners. Moreover, an integrated power grid system should be built between these transboundary countries and a detailed power demand-

supply should be analysed to fulfil the power shortage during the operation of sediment management.

The introduction of the ResSMan routine in SWAT allows users to establish an integrative approach to managing reservoir sedimentation with the application of flushing and sluicing in complex reservoir systems at river basin scale level. Furthermore, users can take advantage of the full functionality of SWAT to assess the impacts of land use, climate change, land management practices and operation policies on reservoir sedimentation and its management. However, the major limitation of the ResSMan is that it has the capability only to simulate flushing and sluicing operations without an optimization function for coordinated sediment management of a multi-reservoir system. Therefore, ResSMan should be coupled with an optimization module to identify the most effective management strategy to remove sediment and to maximize energy production by adjusting the timing of sediment management, in particular for flushing. Moreover, further development of the ResSMan will consider integration of various other sediment management techniques such as dredging, bypassing, hydrosuction and density current venting. With such further additions planners and decision-makers will have the opportunity to select the most economic and sustainable techniques based on site conditions.

Limitations of this study are the uncertainty with regard to the capacity of low level gates to discharge floods effectively and whether site conditions are favourable for flushing and sluicing. A number of reservoirs in the 2S basin were constructed without low level gates and retrofitting of gates in existing dams may neither be economical nor feasible due to site conditions. Moreover, most of the dams are located in wider channel sections of the river. Sediment removal by means of flushing is most effective for a comparatively narrow reservoir whose cross-sectional area approximates the geometry of the incised channel evolved during flushing. Similarly, sluicing is suitable for a narrow and elongated reservoir with a relatively

steep longitudinal gradient. It is recommended that the design of reservoirs should include low level outlets so that sediment management can be implemented effectively. Moreover, from a hydraulic point of view, building smaller reservoirs instead of one single large reservoir would facilitate emptying the reservoirs quickly during flushing. Furthermore, smaller reservoirs will increase the capacity inflow ratio and can be quickly refilled after flushing has been completed.

The implementation of sediment management is important not only for the sustainability of reservoirs, but also for maintaining the downstream ecosystems. However, more detailed investigations and reliable field data will be required to evaluate the impacts on the downstream ecosystems due to sediment trapping and application of sediment management, particularly flushing. These aspects should be considered in the planning and design of future reservoirs, next to further economic, social, environmental and ecological aspects.

4.5 References

- Annandale, G. "Predicting the distribution of deposited sediment in southern African reservoirs." *Proc., Proceedings of the symposium challenges in African hydrology and water resources*, 549-558.
- Arias, M. E., Cochrane, T. A., Kumm, M., Lauri, H., Holtgrieve, G. W., Koponen, J., and Piman, T. (2014). "Impacts of hydropower and climate change on drivers of ecological productivity of Southeast Asia's most important wetland." *Ecological Modelling*, 272, 252-263.
- Baran, E., Guerin, E., and Nasielski, J. (2015). *Fish, sediment and dams in the Mekong*.
- Basson, G. "Management of siltation in existing and new reservoirs. General Report Q. 89." *Proc., 23rd Congress of the CIGB-ICOLD, Brasilia, Brazil*.
- Binh, D. V., Kantoush, S., and Sumi, T. (2020). "Changes to long-term discharge and sediment loads in the Vietnamese Mekong Delta caused by upstream dams." *Geomorphology*, 353, 107011.
- Borland, W. M. (1971). "Reservoir sedimentation." *River mechanics*, 2, 29.21-29.38.
- Constable, D. (2015). *The Sesan and Sre Pok River Basins*, IUCN Asia Regional Office.
- Fruchard, F., and Camenen, B. "Reservoir sedimentation: different type of flushing-friendly flushing example of genissiat dam flushing."
- Garg, V., and Jothiprakash, V. (2008). "Estimation of useful life of a reservoir using sediment trap efficiency." *Journal of Spatial Hydrology*, 8(2).
- Gill, M. A. (1979). "Sedimentation and useful life of reservoirs." *Journal of Hydrology*, 44(1), 89-95.
- Heinemarm, H. (1981). "A new sediment trap efficiency curve for small reservoirs." *JAWRA Journal of the American Water Resources Association*, 17(5), 825-830.
- Hortle, K. G. (2008). "Mekong River Commission." *Catch & culture*, 14(2).
- Hotchkiss, R. H. (1990). "Reservoir sedimentation and sediment sluicing: Experimental and numerical analysis."
- Hrissanthou, V. (2014). "Case studies of reservoir sedimentation as a consequence of soil erosion." *Browse's Introduction to the Symptoms & Signs of Surgical Disease*, 71.
- Issa, I. E., Al-Ansari, N., Sherwany, G., and Knutsson, S. (2013). "Sedimentation processes and useful life of Mosul Dam Reservoir, Iraq." *Engineering*, 5(10), 779-784.
- Kantoush, S. A., and Sumi, T. (2010). "River morphology and sediment management strategies for sustainable reservoir in Japan and European Alps."
- Kawashima, S., Johndrow, T., Annandale, G., and Shah, F. (2003). "Reservoir conservation, vol. II: RESCON model and user manual." *World Bank, Washington, DC*.

- Kondolf, G. (1997). "Hungry water: effects of dams and gravel mining on river channels. Department of landscape architecture and environmental planning." *University of California, Berkeley, California*, 94720, 533-551.
- Kondolf, G. M., Gao, Y., Annandale, G. W., Morris, G. L., Jiang, E., Zhang, J., Cao, Y., Carling, P., Fu, K., and Guo, Q. (2014). "Sustainable sediment management in reservoirs and regulated rivers: Experiences from five continents." *Earth's Future*, 2(5), 256-280.
- Kondolf, G. M., Rubin, Z. K., and Minear, J. T. (2014). "Dams on the Mekong: Cumulative sediment starvation." *Water Resources Research*, 50(6), 5158-5169.
- Kondolf, G. M., Schmitt, R. J. P., Carling, P., Darby, S., Arias, M., Bizzi, S., Castelletti, A., Cochrane, T. A., Gibson, S., Kumm, M., Ourng, C., Rubin, Z., and Wild, T. (2018). "Changing sediment budget of the Mekong: Cumulative threats and management strategies for a large river basin." *Science of The Total Environment*, 625, 114-134.
- Kumm, M., Lu, X. X., Wang, J. J., and Varis, O. (2010). "Basin-wide sediment trapping efficiency of emerging reservoirs along the Mekong." *Geomorphology*, 119(3), 181-197.
- Lohani, S., Dilts, T. E., Weisberg, P. J., Null, S. E., and Hogan, Z. S. (2020). "Rapidly Accelerating Deforestation in Cambodia's Mekong River Basin: A Comparative Analysis of Spatial Patterns and Drivers." *Water*, 12(8), 2191.
- Manh, N. V., Dung, N. V., Hung, N. N., Merz, B., and Apel, H. (2014). "Large-scale suspended sediment transport and sediment deposition in the Mekong Delta." *Hydrol. Earth Syst. Sci.*, 18(8), 3033-3053.
- Michalec, B. (2014). "The use of modified Annandale's method in the estimation of the sediment distribution in small reservoirs—A case study." *Water*, 6(10), 2993-3011.
- Moridi, A., and Yazdi, J. (2017). "Sediment Flushing of Reservoirs under Environmental Considerations." *Water Resources Management*, 31(6), 1899-1914.
- Morris, G. L. (2014). "Sediment Management and Sustainable Use of Reservoirs." *Modern Water Resources Engineering*, L. K. Wang, and C. T. Yang, eds., Humana Press, Totowa, NJ, 279-337.
- Morris, G. L. (2020). "Classification of Management Alternatives to Combat Reservoir Sedimentation." *Water*, 12(3), 861.
- Neitsch, S. L., Arnold, J. G., Kiniry, J. R., and Williams, J. R. (2011). "Soil and water assessment tool theoretical documentation version 2009." Texas Water Resources Institute.
- Palmieri, A., Shah, F., Annandale, G., and Dinar, A. (2003). "Reservoir conservation volume I: the RESCON approach." *Washington, DC: World Bank*.
- Piman, T., Cochrane, T., Arias, M., Green, A., and Dat, N. (2013). "Assessment of flow changes from hydropower development and operations in Sekong, Sesan, and Srepok rivers of

- the Mekong basin." *Journal of Water Resources Planning and Management*, 139(6), 723-732.
- Power, M. E., Dietrich, W. E., and Finlay, J. C. (1996). "Dams and downstream aquatic biodiversity: potential food web consequences of hydrologic and geomorphic change." *Environmental management*, 20(6), 887-895.
- Rooseboom, and Basson, G. (1997). "Dealing with reservoir sedimentation." *Water Resources Commission report*(91/97).
- Schmitt, R. J. P., Bizzi, S., Castelletti, A., and Kondolf, G. M. (2018). "Improved trade-offs of hydropower and sand connectivity by strategic dam planning in the Mekong." *Nature Sustainability*, 1(2), 96-104.
- Sharpley, A. N., and Williams, J. R. (1990). "EPIC-Erosion/Productivity Impact Calculator. I: Model Documentation. II: User Manual." *Technical Bulletin-United States Department of Agriculture*(1768).
- Shrestha, B., Cochrane, T. A., Caruso, B. S., and Arias, M. E. (2018). "Land use change uncertainty impacts on streamflow and sediment projections in areas undergoing rapid development: A case study in the Mekong Basin." *Land degradation & development*, 29(3), 835-848.
- Shrestha, B., Cochrane, T. A., Caruso, B. S., Arias, M. E., and Piman, T. (2016). "Uncertainty in flow and sediment projections due to future climate scenarios for the 3S Rivers in the Mekong Basin." *Journal of Hydrology*, 540, 1088-1104.
- Shrestha, B., Maskey, S., Babel, M. S., van Griensven, A., and Uhlenbrook, S. (2018). "Sediment related impacts of climate change and reservoir development in the Lower Mekong River Basin: a case study of the Nam Ou Basin, Lao PDR." *Climatic Change*, 149(1), 13-27.
- Shrestha, J. P., Pahlow, M., and Cochrane, T. A. (2020). "Development of a SWAT Hydropower Operation Routine and Its Application to Assessing Hydrological Alterations in the Mekong." *Water*, 12(8), 2193.
- Syvitski, J. P. M., Kettner, A. J., Overeem, I., Hutton, E. W. H., Hannon, M. T., Brakenridge, G. R., Day, J., Vörösmarty, C., Saito, Y., Giosan, L., and Nicholls, R. J. (2009). "Sinking deltas due to human activities." *Nature Geoscience*, 2(10), 681-686.
- Tamura, T., Nguyen, V. L., Ta, T. K. O., Bateman, M. D., Gugliotta, M., Anthony, E. J., Nakashima, R., and Saito, Y. (2020). "Long-term sediment decline causes ongoing shrinkage of the Mekong megadelta, Vietnam." *Scientific Reports*, 10(1), 8085.
- Vörösmarty, C. J., Meybeck, M., Fekete, B., Sharma, K., Green, P., and Syvitski, J. P. M. (2003). "Anthropogenic sediment retention: Major global impact from registered river impoundments." *Global and Planetary Change*, 39(1-2), 169-190.
- Walling, D. (2006). "Human impact on land–ocean sediment transfer by the world's rivers." *Geomorphology*, 79(3-4), 192-216.

- Walling, D. E. (2008). "The changing sediment load of the Mekong River." *AMBIO: A Journal of the Human Environment*, 37(3), 150-157.
- Wild, T., and Loucks, D. "Managing the impacts of reservoirs in the Mekong River Basin." *Proc., World Environmental and Water Resources Congress 2014*, 1070-1080.
- Wild, T. B., and Loucks, D. P. (2015). "Mitigating dam conflicts in the Mekong River Basin." *Conflict resolution in water resources and environmental management*, Springer, 25-48.
- Wild, T. B., Loucks, D. P., Annandale, G. W., and Kaini, P. (2015). "Maintaining sediment flows through hydropower dams in the Mekong River Basin." *Journal of Water Resources Planning and Management*, 142(1), 05015004.
- Wurbs, R. A. (2005). "Comparative evaluation of generalized river/reservoir system models." Texas Water Resources Institute.
- Ziv, G., Baran, E., Nam, S., Rodríguez-Iturbe, I., and Levin, S. A. (2012). "Trading-off fish biodiversity, food security, and hydropower in the Mekong River Basin." *Proceedings of the National Academy of Sciences*, 109(15), 5609-5614.

CHAPTER 5. CONCLUSIONS AND RECOMMENDATIONS

5.1 Conclusions

In this thesis, a comprehensive methodology was established to better understand the management of reservoir operations by developing a new hydropower reservoir routine for the SWAT hydrological model. This study advances the scientific understanding of hydrologic and sediment regime alterations due to reservoir operations and their management policies in a complex multi-reservoir system of the Mekong.

5.1.1 Development of a SWAT hydropower routine

A new hydropower reservoir routine (ROSMAN routine), which consists of two components: HydrOR and ResSMan, was developed and integrated into SWAT. The comparisons of the developed routine with the HEC-ResSim and SedSim models validated the capabilities of the routine. This routine enabled reservoir operation and sediment management of multiple reservoirs in a river basin scale through the ability to simulate flushing and sluicing for improved management of flows, energy production and sediment deposition.

The development of a new hydropower reservoir routine in the SWAT allows to simulate hydrological processes, hydropower reservoir operations and sediment management at a river basin level within a single modelling tool.

5.1.2 Assessing the impacts of climate change and reservoir operational policies on hydropower production and downstream hydrological regime

The impact of climate change on hydropower production for the 2060s in the 3S basin will be minimal (−1.6% to 2.3%). But, by changing the reservoir operational policies to maintaining ecological flows from maximizing energy production, hydropower generation can

be reduced by up-to 13%. However, hydrological alterations (HA) due to the combined impacts of reservoir operations and climate change will be significant. The largest alterations are changes in seasonal flows and extreme flow conditions due to reservoir operations under a seasonal variation rule curve aimed to maximize energy production. The level of alterations are significantly correlated with the reservoir size and design head of the hydropower schemes. The alterations in the natural flow regime may have serious negative effects on the ecological dynamics. Thus, hydropower dams with high regulated heads and large reservoirs on rivers that have low mean annual flows may have larger impacts on downstream ecosystems. However, hydrological alterations due to reservoir operations can be minimized through adequate operation policies. Operational policies that attempt to operate dams in a more natural flow regime will minimize flow regime alterations, but dam owners would have to compromise a considerable amount of energy production.

Climate change has a minor impact on hydropower production in the 3S basin compared to changes in operational policies. The operation of reservoirs under the maximizing energy production operational policy significantly alters the natural flow regime. Hydrological alterations can be minimized by adopting alternative operational policies that maintain ecological flows.

5.1.3 Assessing reservoir sedimentation and managing sedimentation through coordinated operation in a complex multi-reservoir system

Sediment loads are comparatively large at the inlet of specific subbasins such as at the Yali and Srepok 3 reservoir. More specifically, the sediment load inflows and storage capacity loss are significant in the specific stretch of the Sesan cascade and the Srepok cascade. Operation of 19 reservoirs in both basins (Sesan and Srepok) will accumulate 924 Mt of sediment over 100 years, resulting an average trapping efficiency of 74% for these reservoirs.

The simulation of ResSMan with flushing showed that reservoir sedimentation can be mitigated by applying the flushing technique. Additionally, the analysis of flushed loads showed that the largest amount of flushed sediment will accumulate in the nearest largest downstream reservoir and the smallest amount accumulates in smaller reservoirs, even if the adjacent downstream reservoir is in a short distance.

The drawdown initiation dates (June – July) for flushing were predetermined by analysing of inflow hydrographs, however, these dates could vary according to operation policies and weather conditions. On the other hand, sluicing is favourable between August and September and the time period depends on the assigned threshold peak flood. The uncoordinated operation of flushing in multiple reservoirs of the 2S basin was ineffective for removing sediment through the cascades of reservoirs, and resulted in the loss of 7.9% of hydropower production. System-wide sediment management coordinated operations demonstrated that flushing alternate reservoirs every 5 years can be the most effective option for efficiently releasing sediment, resulting in only a 1.5% loss of energy production.

The operation of reservoirs significantly traps sediment loads and changes the downstream sediment regime. The sediment management in the multiple reservoirs system will only be effective and efficient when sediment management techniques, particularly flushing, are operated in coordination i.e. managing the sequence, timing and frequency of operation.

5.2 Limitations

This study has several limitations related to the development of a new routine and findings of its applications. The major limitations and assumptions of the ROSMan routine (HydROR and ResSMan collectively) are that it simplifies the computation of flows and sediment trappings and distributions, which only allow it to be applied for a basin level analysis

and planning. The simulation with the routine is data extensive and can be appropriate for better representations of long-term scenarios. Additionally, the ROSMan was specifically designed for analysis of hydropower reservoirs and does not account for irrigation or water supply abstractions at present. Moreover, ROSMan only allows simulations of flushing and sluicing for sediment management and does not have capabilities to simulate other management techniques such as dredging, bypassing, hydrosuction and density current venting.

Regarding the application of the HydrOR, the study was carried out assuming that selected hydropower schemes are operational from the beginning and throughout the simulation period. Furthermore, the rule curves used are only representative of long-term management of the reservoirs, and are thus not based on daily energy demands, environmental flow requirements, and detailed hydrologic conditions. The methodology presented here to quantify the flow regime alterations only represents the broader outlook of hydro-ecological impacts and thus, does not represent all aspects of hydro-ecological impacts due to reservoir operations.

In addition to reservoir inflow, sediment loads, and storage capacity, the trapping efficiency of a reservoir depends on characteristics of sediment such as shape, size, grain size distribution and mass density. In this study, the assumptions of constant mass density and medium size sediment simplified the computation, which is intended for a basin scale level analysis for a long-term period. Furthermore, the existing and planned reservoirs in the 2S basin are relatively large and do not have low level and mid-level outlet facilities, making their feasibility for sediment management difficult. Thus, assumptions have been made for the application of the ResSMan such that the reservoirs have been fitted with low level outlets for sediment management. Therefore, the amounts of sediment release due to sediment management are only theoretical representations when these reservoirs operate under the assumptions made here. Again, the cost analysis of installation of sediment management facilities was not carried out and should be explored because that could affect the overall

economic feasibility of sediment management. The impacts of climate change and land use change were not analysed, because the intent was to emphasise the application of the routine on the coordinated operation of reservoirs, but this is something which could be explored further.

5.3 Recommendations

5.3.1 Future development of the routine

The emphasis here is on recommendations for the future development of the routine. The finding that management of flow and energy of hydropower reservoirs can be improved by changing operation policies suggests that the integration of an optimization module is required to identify the optimum sediment management plan. Operation policies should be adapted to meet energy demand by minimizing downstream hydrologic alterations.

Future developments of the routine should also focus on the addition of other sediment management techniques such as dredging, bypassing, hydrosuction and density current venting, such that planners and decision-makers will have the opportunity to identify and select the most economic and environment-friendly techniques based on site conditions. The ability to simulate other reservoir water abstractions, such as irrigation and water supply, should also be added to the routine to enable better simulations of multi-purpose reservoirs.

Moreover, the coordinated operation of flushing of hydropower reservoirs investigated here revealed that sediment can be released effectively by adjusting the timing and frequency of drawdown in accordance with hydrological conditions. Therefore, the development of an automated optimization module for adjustment of the timing of drawdown would allow for determination of the best operation for sediment management of multi-reservoir systems.

5.3.2 Future research

There is a trade-off between operating hydropower reservoirs to maximize energy production and maintaining downstream natural flows. The development of an optimisation routine is necessary to identify viable operational strategies. Thus, optimization of operational rules based on a specific hydropower schemes' features, target energy supply, environmental flow requirement and detailed hydrological conditions will further enhance sediment and flow management of specific hydropower facilities.

The scope and objective of this study were limited to quantify hydrological alterations due to hydropower operations and climate change. The quantifications of HA indicated the broader outlook of eco-hydrological consequences due to reservoir operations and climate change, therefore, detailed eco-hydrological impacts should be further assessed by observed data, detailed hydraulic and habitat modelling. Furthermore, severe and widespread HA is illustrated here and the possibility of a loss of connectivity threatens to one of the most biodiverse fish habitats, and further work is needed to adequately assess these combined ecohydrological impacts.

Several issues related to the implementation of sediment management in the 2S basin were highlighted previously which lead to the following recommendations. First, further study should be conducted on the applicability of alternative sediment management techniques such as sluicing (sediment routing) and channel bypassing and their impacts on reservoir sedimentation and downstream sediment regime. In addition, the potential downstream hydro-ecological impacts due to the release of high sediment-laden flows during flushing should be further assessed by field monitoring, analysis of historical data and detailed hydraulic modelling. Second, after the implementation of optimization modules in the routine, transboundary reservoirs can be further analysed and optimized to determine the best option for

sediment management policy in the wider catchment. Ultimately such an analysis would reveal the most economic and sustainable management techniques based on site conditions for the coordinated operation of transboundary reservoirs, including more critically located reservoirs such as LSS 2 in the 3S basin.

The study presented here has focussed on the impacts of climate change on the hydropower production and flow regime alterations. The combined effects of land use and climate change can impact the rate of soil erosion and thereby sedimentation potential. Thus, a detailed study of the impacts of climate change and land use change on reservoir sedimentation and the identification of the optimum sediment management techniques is needed.

5.3.3 Recommendations to the developers and stakeholders

Reliable and long-term sediment load data in the 3S basin are not available. The performance of the model predominantly depends upon the availability of reliable and consistent measured data. Hence, in addition to continuous monitoring of flows in the rivers, it is recommended to continuously monitor suspended sediments at critical locations in the basin and to regularly monitor sediment deposition areas in the rivers/reservoirs. More specifically, sediment load measurements including nutrient composition at the outlets of the 2S and 3S basins will improve our understanding of the detailed ecological impacts due to reservoir operations on the downstream Mekong delta.

It is recommended to the hydropower developers that reservoirs, which could be impacted by high sediment loads, should be located in the comparatively narrow river sections and their design should include low level and mid-level outlets so that sediment management can be implemented effectively. Moreover, it is suggested to consider multiple smaller reservoirs over one large reservoir because sediment trapping can be reduced by reducing the reservoir storage capacity. Additionally, sediment management techniques, especially flushing,

can be applied effectively to small reservoirs as these can be emptied and refilled quickly during flushing. From the developer's point of view, the salient features of a hydropower project and selection of appropriate sediment management techniques depend on the technical feasibility and economic viability of the project for the short-term (30-40 years) in the BOOT contract system. However, a large amount of cost is associated with the negative environmental impact due to reservoir operations and sediment trapping which are not usually considered during feasibility analysis of projects. Therefore, hydropower developers should account for the long-term (100 years) benefits due to the sustainable operations of reservoirs and the reduction in the possible environmental impacts.

Even if sediment management is implemented in the Mekong, where the construction and planning of many reservoirs have formed a complex system of multiple reservoirs, the release of sediment from upstream reservoirs will merely accumulate in downstream reservoirs. Moreover, uncoordinated operation of sediment management simulations showed ineffective and inefficient in multiple reservoirs. Therefore, coordinated operation of reservoirs is warranted to effectively release sediment through multiple reservoirs. But, the coordinated operation for the complex system of transboundary reservoirs (Vietnam and Cambodia) is not only a technical challenge but also a diplomatic challenge to implement in practice. Hence, the coordination and collaboration between the various industry professionals, stakeholders, partners and governmental bodies will enable the successful implementation of sediment management for the transboundary reservoirs.

APPENDIX - 1

A Reservoir Operation and Sediment MANagement (ROSMAN) Routine

User's Manual

TABLE OF CONTENTS

| | |
|---|------------|
| TABLE OF CONTENTS..... | I |
| LIST OF FIGURES | III |
| LIST OF TABLES | IV |
| 1. INTRODUCTION..... | 1 |
| 2. OVERVIEW OF A ROSMAN | 2 |
| 2.1 Hydropower Reservoir Operation Routine (HydROR) | 3 |
| 2.2 Reservoir Sediment Management routine (ResSMan) | 7 |
| 2.2.1 Flushing Process | 9 |
| 2.2.2 Sluicing Process | 15 |
| 3. MODIFICATION OF THE SWAT SOURCE CODE..... | 17 |
| 3.1 Read_ROSMan.f..... | 18 |
| 3.2 ResApp.f | 18 |
| 3.2.1 Subroutine Add1DAY | 18 |
| 3.2.2 Subroutine jtodate..... | 19 |
| 3.2.3 Subroutine to_date..... | 19 |
| 3.2.4 Subroutine int_date..... | 19 |
| 3.2.5 Subroutine xDAYS..... | 19 |
| 3.2.6 Subroutine rulecurve | 19 |
| 3.2.7 Subroutine interpolate_only | 19 |
| 3.2.8 Subroutine read_all_outlet | 19 |
| 3.2.9 Subroutine storage_indication..... | 19 |
| 3.2.10 Subroutine levelpool..... | 20 |
| 3.3 ResSMan.f..... | 20 |
| 4. INPUT/OUTPUT FILES | 21 |
| 4.1 Input files | 21 |
| 4.2 SWAT reservoir input file (.res) | 21 |
| 4.3 Hydroplant characteristics file (hydroplant.hpl) | 22 |
| 4.3.1 Reservoir subbasin number (integer) | 23 |
| 4.3.2 Simulate reservoir or not (integer) | 24 |
| 4.3.3 Design discharge (m ³ /s)..... | 24 |
| 4.3.4 Minimum operating level (m.a.s.l.) | 24 |
| 4.3.5 Full Supply level (m.a.s.l.) | 24 |
| 4.3.6 Installed capacity (MW) | 25 |
| 4.3.7 Turbine axis level (m.a.s.l.) and Tailwater level (m.a.s.l.)..... | 25 |
| 4.3.8 Hydropower Plant efficiency (factor)..... | 25 |
| 4.3.9 Headloss coefficient (factor) | 25 |

| | | |
|-------------------|---|-----------|
| 4.3.10 | Reservoir Length (m) | 25 |
| 4.3.11 | Initial settled sediment mass (Ton) | 26 |
| 4.3.12 | Sediment density (kg/m ³) | 26 |
| 4.3.13 | Simulate with flushing or not (integer) | 26 |
| 4.3.14 | Simulate with sluicing or not (integer) | 27 |
| 4.3.15 | Brune Curve Type (integer) | 27 |
| 4.4 | Volume-elevation-area curve (.cur) file | 27 |
| 4.5 | Rule curve (.rul) file | 28 |
| 4.6 | Spillway rating curve (.out) file | 29 |
| 4.7 | Hydroplant pool curve (.out) file | 30 |
| 4.8 | Flushing gate rating curve (.out) file | 31 |
| 4.9 | Flushing specification data (.smn) file | 31 |
| 4.9.1 | Drawdown start date (yyyymmdd) | 32 |
| 4.9.2 | Flushing duration (days) | 32 |
| 4.9.3 | Maximum water level (m.a.s.l.) | 32 |
| 4.9.4 | Minimum flushing discharge (m ³ /s) | 32 |
| 4.9.5 | Flushing channel bottom width (m) | 33 |
| 4.9.6 | Flushing channel side slope (factor) | 33 |
| 4.9.7 | Maximum drawdown rate (m) | 33 |
| 4.9.8 | Minimum flow to initiate drawdown (m ³ /s) | 33 |
| 4.9.9 | Representative reservoir bottom width (m) | 34 |
| 4.9.10 | Reservoir side slope (factor) | 34 |
| 4.9.11 | Flush gate invert level (m.a.s.l.) | 34 |
| 4.10 | Sluicing specification data (.smn) file | 34 |
| 4.10.1 | Sluicing start date (yyyymmdd) | 35 |
| 4.10.2 | Sluicing duration (days) | 35 |
| 4.10.3 | Minimum flow into reservoir to start sluicing (m ³ /s) | 35 |
| 4.10.4 | Minimum flow into reservoir to stop sluicing (m ³ /s) | 35 |
| 4.10.5 | Drawdown water surface elevation limit (m.a.s.l.) | 35 |
| 4.10.6 | Maximum drawdown rate (m) | 36 |
| 4.10.7 | Maximum refill rate (m) | 36 |
| 4.10.8 | Hydropower production during sluicing (integer) | 36 |
| 4.11 | Summary of input files | 36 |
| 4.12 | Output file | 36 |
| 5. | QUICK START GUIDE | 38 |
| 5.1 | SWAT model setup | 38 |
| 5.2 | Simulation with the ROSMan | 38 |
| 5.3 | Post-processing of the outputs | 38 |
| REFERENCES | | 39 |

LIST OF FIGURES

| | |
|---|----|
| Figure 1: Framework and capabilities of the ROSMan..... | 3 |
| Figure 2: a) Volume-Elevation Curve, b) Outflow rating curve, c) Storage Indication ($2V/\Delta t+Q$) vs outflow curve and d) Storage Indication ($2V/\Delta t+Q$) vs elevation curve for a reservoir..... | 5 |
| Figure 3: Typical features of a reservoir in the ResSMan..... | 7 |
| Figure 4: Flushing process to remove reservoir sediment deposits (a) water level drawdown, (b) flushing, (c) refilling reservoir..... | 10 |
| Figure 5: A simplified reservoir geometry and the flushing channel (inner trapezoid) cross section immediately upstream of a dam..... | 12 |
| Figure 6: The outer trapezoid is the simplified geometry of a reservoir and the inner trapezoid is the sustainable channel formed by flushing. The shaded area represents deposited sediment in the reservoir up to time period t. | 14 |
| Figure 7: An example of a SWAT reservoir input file (.res) | 21 |
| Figure 8: An example file of hydroplant.hpl..... | 22 |
| Figure 9: Hydropower plant characteristics stored in MS-Excel file..... | 23 |
| Figure 10: Reservoir ID determination using ArcSWAT | 23 |
| Figure 11: An example of volume-elevation-area curve (.cur) file..... | 28 |
| Figure 12: An example of rule curve (.rul) file | 29 |
| Figure 13: An example file of spillway rating curve (.out)..... | 30 |
| Figure 14: An example of hydroplant pool curve (.out) file | 30 |
| Figure 15: An example of flushing gate outlet rating curve (.out) file | 31 |
| Figure 16: An example of flushing specification data (.smn) file..... | 32 |
| Figure 17: An example of sluicing specification data (.smn) file | 35 |
| Figure 18: The output file for the ROSMan..... | 37 |

LIST OF TABLES

| | |
|--|----|
| Table 1: Input files and variables required for simulation with the ROSMan routine..... | 36 |
|--|----|

1. INTRODUCTION

The Reservoir Operation and Sediment MANagement (ROSMAN) routine (Shrestha et al. 2020; Shrestha et al. 2020) is a new reservoir routine implemented in SWAT (Soil and Water Assessment Tool). SWAT is a physically-based hydrological model initially developed for large complex catchments (Arnold et al. 1998) by the U.S. Department of Agriculture, Agricultural Research Service (USDA-ARS), and used to assess impacts of impoundments, best management practices (BMPs), climate change, or land use change on streamflow and/or pollutant and sediment transport of catchments world-wide.

The SWAT has capabilities to simulate and predict inflow and sediment yields to the reservoirs under various climatic conditions and land use changes. Even though the SWAT model has been successfully applied in many studies for different purposes such as for predicting sediment yields, assessing climate change impacts on surface runoff, and simulating hydrology in different catchments, hydropower reservoir operation methods and sediment management techniques have not yet been implemented within the framework of the SWAT. Therefore, the ROSMAN routine has been introduced into the SWAT to simulate reservoir operations and sediment management techniques under different operation policies.

2. OVERVIEW OF A ROSMan

The ROSMan has fundamentally two capabilities: 1) hydropower reservoir operations without considering sedimentation (HydROR) (Shrestha et al. 2020) and 2) accumulation and removal of sediment under hydropower reservoir operations and sediment management techniques (ResSMan) (Shrestha et al. 2020) (Figure 1). Thus, the user can choose between the HydROR and ResSMan. If the main purpose of simulation is to predict energy generation and impacts on the hydrologic regime of a river due to operation of hydropower reservoirs under different policies at the river basin scale, then it is suggested to simulate with the HydROR. The HydROR calculates the water balance of a reservoir and energy generation of a hydropower plant using predefined rule curves and plant efficiency without considering the impacts of sedimentation on the storage capacity. On the other hand, if the main objective of the study is to assess the accumulation of sediment and its impact on reservoir storage capacity, then the user must simulate with the ResSMan. The ResSMan routine has capabilities to predict the accumulation of trapped sediment, its impacts on the storage-capacity of a reservoir, and losses in hydropower generation under user-specified operation policies. Furthermore, it allows to compute the restoration of storage volume due to the removal of sediment by flushing (removal of sediment from a reservoir by passing water and sediment through flush gates located at the low level of a dam) and sluicing (passing sediment before suspended sediment solids have settled down in reservoirs).

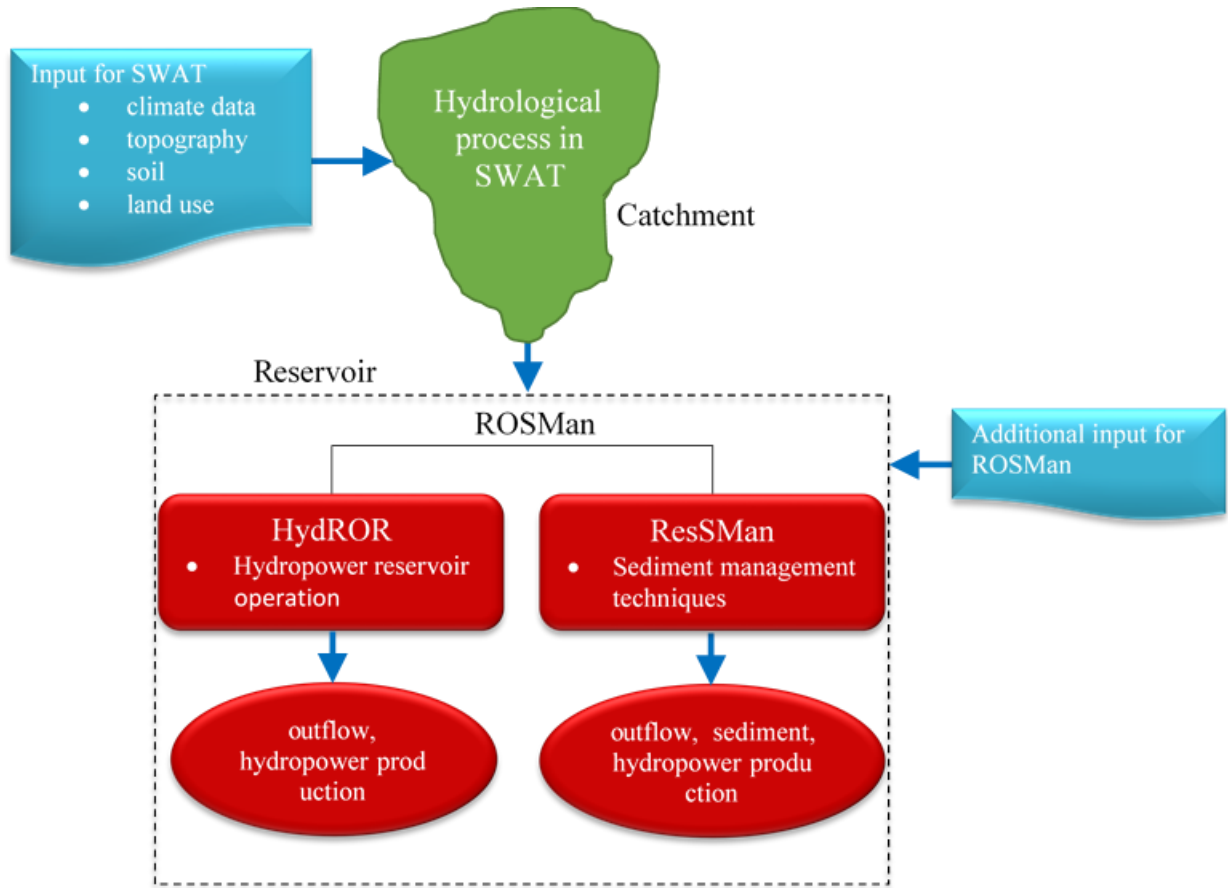


Figure 1: Framework and capabilities of the ROSMan

2.1 Hydropower Reservoir Operation Routine (HydROR)

The HydROR has capabilities to operate hydropower reservoirs, to compute water balance of a reservoir and energy generation using the predefined rule curves. The HydROR neglects the effect of sedimentation on storage capacity of reservoirs, however, it uses the existing sediment routing method of the SWAT to compute sediment in and out from the reservoir. The water inflow to the reservoir, precipitation on the reservoir surface area and potential evapotranspiration from the reservoir surface area are generated by a hydrologic component of the SWAT model. Additional data are needed to estimate hydropower production and to operate the reservoir under the predefined operational policy. These additional data such as area-elevation, volume-elevation curve, maximum/minimum operating level, rule/guide curves, plant efficiency, and design flow of plant are separately entered.

The reservoir routing is accomplished by the following steps in the HyDROR. Firstly, the volume of the total outflow ($V_{flowout}$) of a reservoir is estimated using the level pool routing method (Modified Puls Method), which calculates outflows by solving the continuity equation (eq. 1-4) of mass balance (Chow 1964) for every time step of the simulation. The right hand side (unknown) term of equation 3 can be found by interpolation of the Storage Indication ($2V/\Delta t + Q$) vs Outflow curve (Figure 2c)), which is created by combining the Outflow curve and the Volume-Elevation curve. Hence, additional data such as Volume-Elevation curve and Outflow curve (spillway rating curve) for a reservoir must be entered separately for every reservoir in the basin. The relationship between water level and reservoir volume can be derived by using a topographic map of the reservoir. The outflow rating curve of the spillway is derived from hydraulic equations relating discharge and head of the spillways.

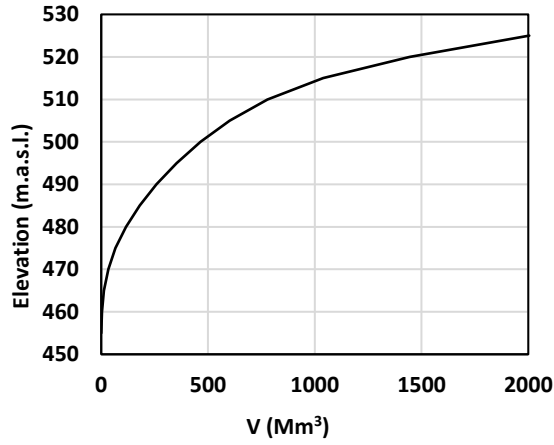
$$I - Q = \frac{\Delta V}{\Delta t} \quad (1)$$

$$\frac{I_{t-1} - I_t}{2} - \frac{Q_{t-1} - Q_t}{2} = \frac{V_{t-1} - V_t}{2} \quad (2)$$

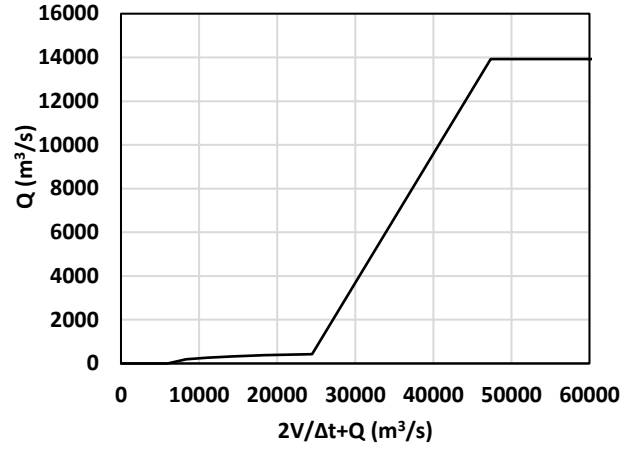
$$[i_{t-1} - i_t] + \left[\frac{2V_{t-1}}{\Delta t} - q_{t-1} \right] = \left[\frac{2V_t}{\Delta t} - q_t \right] \quad (3)$$

$$V_{flowout} = Q_t \times \Delta t \quad (4)$$

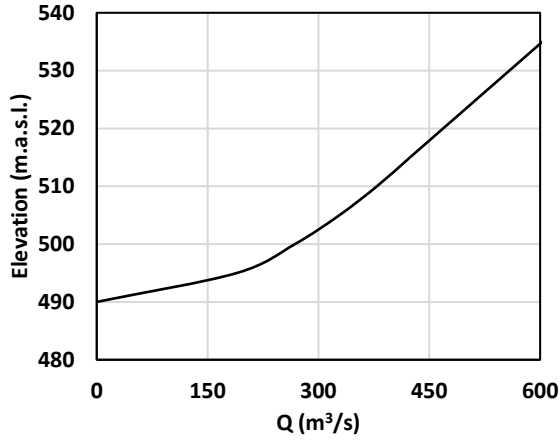
Where, I and Q are average inflow and outflow in m^3/s , i_{t-1} and i_t are inflows to the reservoir at simulation time steps $t-1$ and t in m^3/s , Q_{t-1} and Q_t are outflows from the reservoir for simulation time steps $t-1$ and t in m^3/s , ΔV is change in storage capacity in the reservoir in m^3 , and $V_{flowout}$ is the volume of outflow at time t in m^3 .



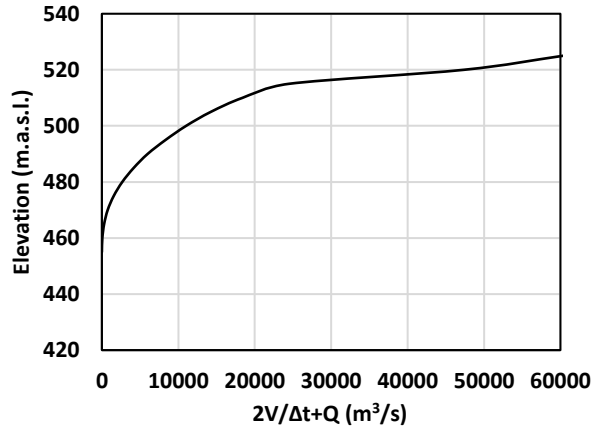
a)



c)



b)



d)

Figure 2: a) Volume-Elevation Curve, b) Outflow rating curve, c) Storage Indication ($2V/\Delta t+Q$) vs outflow curve and d) Storage Indication ($2V/\Delta t+Q$) vs elevation curve for a reservoir

Secondly, the final outflow (Equations (5)–(8)) of the reservoir is determined based on the operating policy using a user-defined rule curve of the reservoir. In HydrOR, the rule curve is defined by specifying a target water level for the first day of each month and the routine calculates daily target water levels by linear interpolation.

$$V_t = V_{t-1} + V_{flowin} - V_{outflow} + V_{pcp} - V_{evap} - V_{seep} \quad (5)$$

$$V_{check} = V_{t-1} + V_{flowin} + V_{pcp} - V_{evap} - V_{seep} - V_{rule} \quad (6)$$

$$\text{IF } (V_{check} \leq 0), \text{ then } V_{final_outflow} = 0 \quad (7)$$

$$\text{IF } (V_{check} \leq V_{outflow}), \text{ then } V_{final_outflow} = V_{check} \quad (8)$$

$$\text{IF}(V_{check} > V_{outflow}), \text{ then } V_{final_outflow} = V_{outflow} \quad (9)$$

Where, V_t is the volume of water in the reservoir at the simulation time step t (m^3), V_{t-1} is the volume of water stored in the reservoir at the simulation time step $t-1$ (m^3), V_{flowin} is volume of water entering the reservoir (m^3), $V_{outflow}$ is volume of water flowing out of the reservoir (m^3), V_{pcp} is volume of precipitation falling on the reservoir (m^3), V_{evap} is volume of evaporated water from the reservoir (m^3) and V_{seep} is volume of water lost from the reservoir by seepage (m^3), V_{rule} is volume of the reservoir as indicated by the rule curve for a simulation time step and V_{check} is the difference in total water volume (V) and V_{rule} . $V_{final_outflow}$ is the final outflow from the reservoir. This final outflow includes the outflows from different outlets of a reservoir:

$$V_{final_outflow} = V_{spill} + V_{tur} \quad (10)$$

Where, V_{spill} is the volume of water spilling from the spillway (m^3) and V_{tur} is the volume of water flowing through a turbine (or turbines) for power generation (m^3). The discharge through a spillway is allocated using the outflow rating curve of the spillway. The turbine flow for hydropower generation depends on the design discharge for hydropower plants and operation rules.

Thirdly, power generation from the hydropower plant for every time step of simulation is calculated as in Equations (11) and (12).

$$P = \frac{\eta \times \gamma \times Q_{tur} \times H_{net}}{1000} \quad (11)$$

$$E = \frac{P \times hr}{1000} \quad (12)$$

where Q_{tur} is the flow through turbine in m^3/s , η is the efficiency of power plant, γ is the specific gravity of water in KN/m^3 , H_{net} is net head for power plant in m , hr is time in hour, P is power production in MW and E is energy generation in GWh . The net head is calculated by

taking the difference between reservoir water level and the tailrace level/turbine level of the power plant, which should be entered by a user.

Lastly, the HyDROR updates reservoir water volume using the mass balance equation and updates water level and surface area from the volume-area-elevation curve of the reservoir and writes the results (reservoir volume, level, outflow and power generation) to an output file.

2.2 Reservoir Sediment Management routine (ResSMan)

The REServoir Sediment MANagement routine (ResSMan) is a hydropower reservoir routine specifically developed for integration into the SWAT. The main functions of the ResSMan are to simulate reservoir routing and sediment management techniques such as flushing and sluicing. Typical features of a reservoir to be assessed with ResSMan contains a spillway at the dam crest level, hydropower intakes to divert flow for hydropower generation, low level outlets for sediment management purposes and the storage capacity is divided into two parts by the full supply level (FSL) and minimum operating level (MOL) into the active and dead storage (Figure 3).

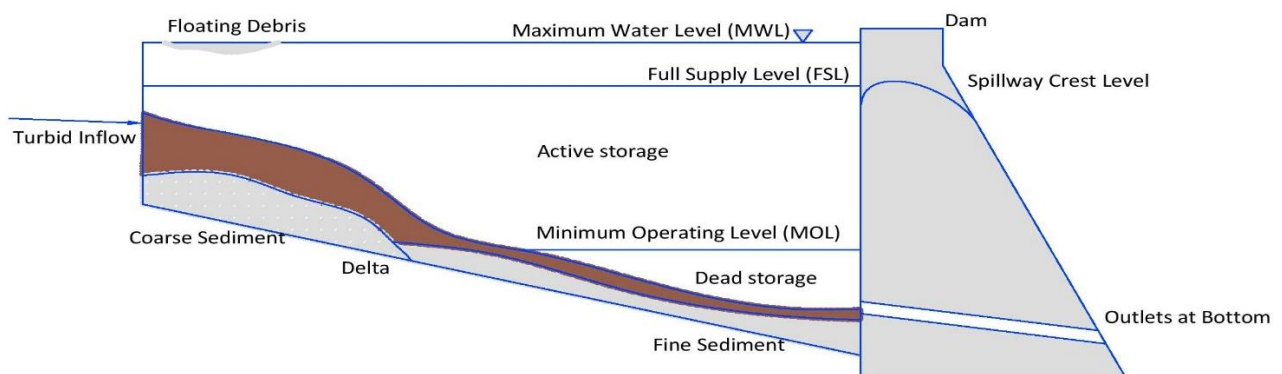


Figure 3: Typical features of a reservoir in the ResSMan

The water and sediment inflow to the reservoir, precipitation onto the reservoir surface area, seepage loss from the reservoir bottom and evapotranspiration from the reservoir surface area are computed by a hydrologic module of the SWAT model. Furthermore, the ResSMan

predicts the accumulation of trapped sediment using the Brune curve (Brune 1953), its impacts on the storage capacity of a reservoir, and hydropower generation under user-specified operation policies. When the user specifies to simulate with sediment management techniques, the routine computes the outflow of the removed sediment, restoration of storage capacity and energy production. The ResSMan uses the following empirical equations to estimate the trapping efficiency as proposed by Gill (1979) for coarse-grained, medium and fine-grained sediments:

$$TE = \frac{\Delta T^2}{(0.994701 \times \Delta T^2 + 0.006297 \times \Delta T + 0.3 \times 10^{-5})} \quad (13)$$

$$TE = \frac{\Delta T}{(0.012 + 1.02 \times \Delta T)} \quad (14)$$

$$TE = \frac{\Delta T^3}{(1.02655 \times \Delta T^3 + 0.02621 \times \Delta T^2 - 0.133 \times 10^{-3} \times \Delta T + 0.1 \times 10^{-5})} \quad (15)$$

$$\Delta T = \left(\frac{V}{I}\right) / 365 \quad (16)$$

Where, TE is trapping efficiency, ΔT is the residence time in days, V is storage capacity of the reservoir in m^3 , I is average daily inflow volume in $m^3/s/day$. Furthermore, the ResSMan computes the settled sediment mass using the sediment mass balance equation.

$$Set_t = Sed_{flowin} \times TE \quad (17)$$

$$Conc_t = \frac{(Conc_{t-1} \times V_{t-1} + (Sed_{flowin} - Set_t)/\rho)}{(V_{t-1} + V_{flowin})} \quad (18)$$

$$Sed_{outflow} = (Conc_t) \times V_{final_outflow} + Sed_{flushed} \quad (19)$$

$$dep_t = dep_{t-1} + Set_t - Sed_{flushed} \quad (20)$$

Where, $Conc_{t-1}$ and $Conc_t$ are the sediment concentration of suspended solids (ton/m^3) at time step $t-1$ and t respectively; Sed_{flowin} , $Sed_{outflow}$, Set_t and $Sed_{flushed}$ are sediment mass inflow, outflow, settled sediment mass and sediment mass removed due to flushing (ton) respectively; dep_{t-1} and dep_t are deposited sediment mass (ton) at the time step $t-1$ and t ; ρ is

the density of sediment mass (ton/m³) and the other symbols are as described above. The final reservoir outflow ($V_{final_outflow}$) and final reservoir storage volume is calculated by using the mass balance equation of water (Eq. 23) of a reservoir.

$$V_{check} = V_{t-1} + V_{flowin} + V_{pcp} - V_{evap} - V_{seep} - V_{rule} - Set_t/\rho \quad (21)$$

$$V_{final_outflow} = Min[Max(V_{check}, 0), V_{tot_outlet}, Max\{(V_{t-1} + V_{flowin} + V_{pcp} - V_{evap} - V_{seep}), 0\}] \quad (22)$$

$$V_t = V_{t-1} + V_{flowin} - V_{final_outflow} + V_{pcp} - V_{evap} - V_{seep} - Set_t/\rho \quad (23)$$

Where, V_{rule} is the volume of the reservoir (m³) as indicated by the rule curve for the simulation time step, V_{check} is the initial estimate of the volume (m³) to meet the storage target according to the specified rule curve and V_{tot_outlet} is the sum of outflow capacities of all the outlets (m³) which is determined on the basis of the water surface level, storage volume and outlet capacity rating curve.

2.2.1 Flushing Process

The process of flushing in the ResSMan routine comprises three phases: drawdown of water surface level, removal of sediment due to occurrence of the flushing, and refilling the reservoir (Figure 4). The drawdown initiates on or after the user specified initiation date of drawdown and meets the criterion of minimum reservoir inflow. The flushing gates, which are usually installed at the bottom of a dam, are opened at their full capacity to achieve the complete drawdown of the reservoir. The routine assumes the gates are opened as soon as drawdown is initiated and closed once flushing is completed. Further, during the flushing process, there is no energy generation from the hydropower plants. Thus, water flow to the turbines is considered nil. However, other outlets such as spillways are in full function to release the water. The operation policy of reservoir routing during the drawdown phase is to achieve river-like flow emptying the reservoir. The total water release from a given reservoir results from reservoir

inflow, water storage during drawdown, the maximum drawdown capacity and sum of release capacity of all opened outlets.

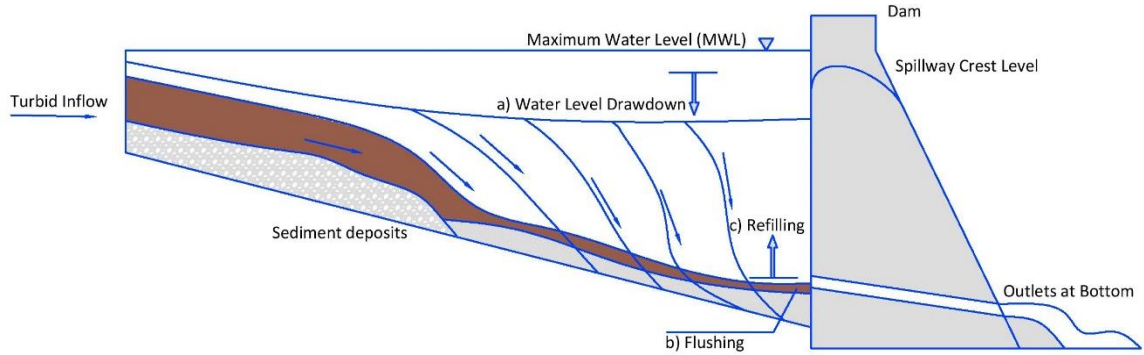


Figure 4: Flushing process to remove reservoir sediment deposits (a) water level drawdown, (b) flushing, (c) refilling reservoir.

It is considered that all the sediment entering the reservoir to remain in suspension during the flushing process. So, the trapping of sediment equals zero and concentration of the suspension sediment rises. Thus, flow with high sediment concentration is passed during release of water through outlets. However, previously deposited sediment mass cannot be removed until the criteria for occurrence of flushing have been satisfied. The following two criteria should be satisfied for successful flushing to take place, as mention in the SedSim model user manual (Wild and Loucks 2012):

- i) The water surface level should not exceed the maximum flushing water surface elevation as specified by the user.
- ii) The water release from flushing gates should be greater than the required minimum flushing flow.

The first criterion suggests to maintain the water surface level as low as possible, and to achieve the river-like flow and in order to increase the efficiency of the flushing (Lai and Shen 1996; Wen Shen 1999). Furthermore, Wen Shen (1999) suggested that the drawdown water level should not exceed the original river normal flow level. Yet in the ResSMan, it is

assumed that the water level can drop up to the original river bed level at the time of flushing. After the complete drawdown of the reservoir, the outflow through the flushing gates equals the runoff of the river and it depends on hydrological condition of the catchment and time of operation of flushing. Thus, the user can define the required minimum flushing flow by analysing the historical hydrological data of the river flow.

After fulfilling both criteria, there will be occurrence of flushing on a particular day and if one of these criteria is not satisfied then the routine waits one more day to achieve successful flushing. Once flushing has successfully taken place for a specified duration, the flushing phase is completed, flushing gates will be closed and refilling of the reservoir begins. The outflow from the reservoir is zero until the water level rises above the MOL of the reservoir. Once the reservoir water level rises above MOL, the reservoir runs in the normal operating policy using the specified rule curve.

During the flushing process, the trapping efficiency of the reservoir is assumed to be zero, thus increases the concentration of suspended sediment of the reservoir. The amount of removed sediment during drawdown phase is equal to the concentration of sediment multiplied by the volume of water outflow. During the flushing phase, deposited sediment is assumed to be removed from portions of the volume-area-elevation curve in the same way in which the distribution of sediment deposition in the reservoir was assumed. The steps of estimating volume of sediment removed during the flushing phase is outlined as below (Wild and Loucks 2012):

1. Determine the original (initial) long term capacity ratio (LTCR) as explained in the 'The feasibility of flushing sediment from reservoirs' (Atkinson 1996). LTCR is defined as the ratio of the sustainable reservoir capacity to the original capacity of a reservoir. The sustainable reservoir capacity is the storage capacity of a reservoir that can be sustained due to flushing in the long term.

The calculation of LTCR can be described by a simplified geometry of a reservoir. Figure 5 represents the simplified cross section of a reservoir immediately upstream of a dam. In the figure, the outer trapezoid (A_r) represents the cross section of the reservoir and the inner trapezoid represents the cross-sectional area (A_f) of the flushing channel that can be sustained by flushing. Using these definitions, the initial LTCR is expressed by the following equation:

$$LTCR_o = \frac{A_f}{A_r} \quad (24)$$

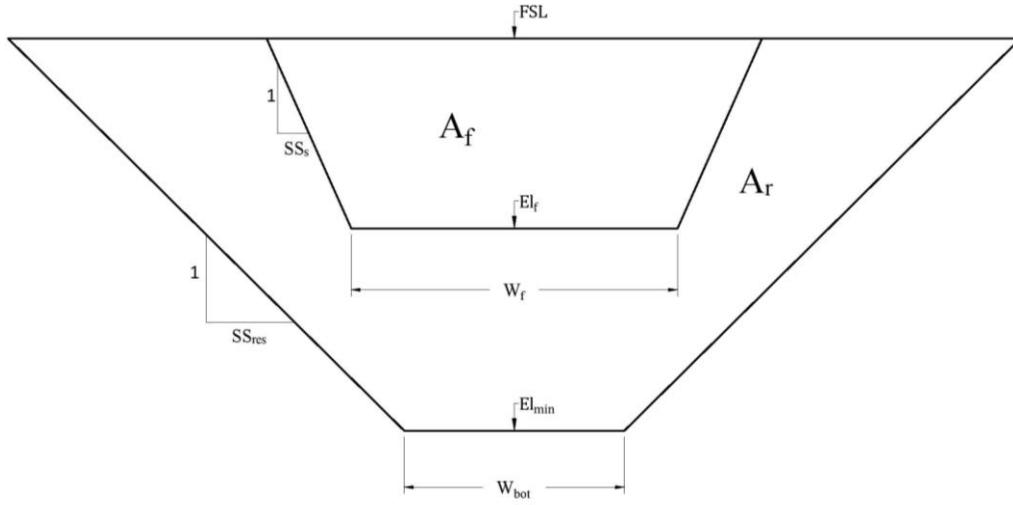


Figure 5: A simplified reservoir geometry and the flushing channel (inner trapezoid) cross section immediately upstream of a dam.

Depending on the combination of different side slopes of the reservoir and the flushing channel, the formation of different cross sectional configurations of the reservoir are possible. For instance, if the flushing channel side slope is steeper than reservoir side slope, then the flushing channel sides will meet the top of the reservoir as shown in Figure 5. The flushing channel side slopes depend on the sediment properties, the degree of consolidation, the depth of deposits and water level fluctuation during flushing (Atkinson 1996). The flushing channel side slope (SS_s) is predicted by using the following simplified equation:

$$SS_s = \frac{10 \times 5}{31.5 \times \rho^{4.7}} \quad (25)$$

Further, the areas of A_r and A_f for the above case are calculated as follows:

$$W_f = 12.8 \times \sqrt{Q_f} \quad (26)$$

$$W_f = \text{Min}(W_f, W_{bot}) \quad (27)$$

$$W_{res} = W_{bot} + 2 \times SS_{res} \times (El_f - El_{min}) \quad (28)$$

$$W = \text{Min}(W_f, W_{res}) \quad (29)$$

$$W_{tf} = W + 2 \times SS_s \times (FSL - El_f) \quad (30)$$

$$W_l = W_{bot} + 2 \times SS_{res} \times (FSL - El_{min}) \quad (31)$$

$$A_r = 0.5 \times (W_l + W_{bot}) \times (FSL - El_{min}) \quad (32)$$

$$A_f = 0.5 \times (W_{tf} + W) \times (FSL - El_f) \quad (33)$$

Where, Q_f is minimum discharge for flushing (m^3/s), W_f is flushing channel bottom width (m), W_{bot} is representative bottom width of the reservoir (m), SS_{res} is reservoir side slope, El_f is invert level of the bottom outlet (m.a.s.l.), El_{min} is original river bed level immediately upstream from the dam (m.a.s.l.), W_{res} is representative width of the reservoir in the reach upstream from the dam at the flushing water surface elevation (m), W is the representative width of flow for flushing conditions (m), W_{tf} is top width of flushing channel at the top water level (m) and W_l is reservoir width at the top water level (m).

2. Determine the average depth of the settled sediment for every time step (t) of simulation:

$$ressa = \frac{V_o}{FSL - El_{min}} \quad (34)$$

$$D_t = \frac{(Set_t/\rho)}{ressa} \quad (35)$$

Where, V_o is the initial storage capacity of the reservoir at the FSL, and El_{min} is the reservoir bottom level, D_t is average depth of the settled sediment layer (m) and Set_t is settled sediment mass in ton (derived from eq. 17) due to trapping at the time t .

3. The routine assumes that sediment deposits uniformly within the reservoir cross section. When the ratio (eq. 36) of the sustainable long-term storage capacity (V_t), which can be maintained due to successful flushing, to the initial storage capacity (V_o) is equal to

its initial LTCR (*i.e.* $LTCR_o = LTCR_t$), all deposited sediment can be removed by flushing.

$$LTCR_t = \frac{V_o}{V_t} \quad (36)$$

Where, $LTCR_t$ is LTCR at time step t , V_t is the sustainable reservoir storage capacity at time step t and V_o is the initial storage capacity.

4. If a reservoir has not reached its sustainable storage capacity, the amount of removed sediment is equal to the settled sediment multiplied by the ratio of the flushing channel top width (FCT_t) to the top width of deposited sediment in the reservoir (RST_t) at simulation time step t can be given by the equations (see also Figure 6):

$$FCL_t = FCL_{t-1} + D_t \quad (37)$$

$$FCT_t = \text{Min}[W_{tf}, \{W_f + 2 \times SS_s \times (FCL_t - El_f)\}] \quad (38)$$

$$RST_t = \text{Min}[W_t, \{W_{bot} + 2 \times SS_{res} \times (FCL_t - El_{min})\}] \quad (39)$$

$$Sed_{flushed} = Sed_t \times \frac{FCT_t}{RST_t} \quad (40)$$

Where, FCL_t and FCL_{t-1} are the flushing channel top level at the sediment deposit at the t and $t-1$ simulation time steps (m.a.s.l.), FCT_t is flushing channel top width at t , RST_t is the top width of deposited sediment in the reservoir at t , and $Sed_{flushed}$ is sediment removal volume (m^3) at t .

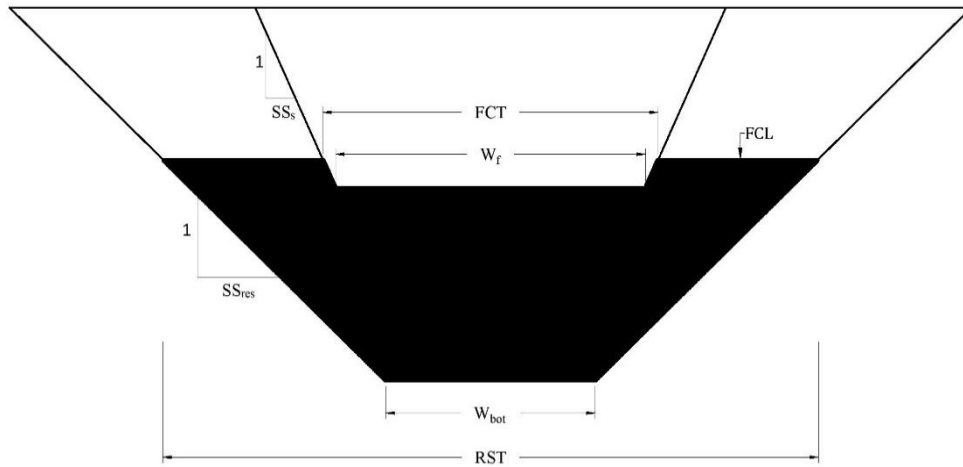


Figure 6: The outer trapezoid is the simplified geometry of a reservoir and the inner trapezoid is the sustainable channel formed by flushing. The shaded area represents deposited sediment in the reservoir up to time period t .

2.2.2 Sluicing Process

Sluicing is the process of passing suspended sediment solids before they settle in reservoirs. In the ResSMan, the drawdown for sluicing initiates either on the user specified initiation date of drawdown or when the criterion of minimum reservoir inflow is met. Thus, the initiation of drawdown depends on which criterion has been specified by the user. Once the drawdown is started, the routine will try to achieve and keep the reservoir water level at target sluicing level releasing water through the low level outlets. However, drawdown on a day should not exceed the user-specified maximum drawdown rate. This criterion is implemented to maintain downstream floods to be lower than peak floods. During the sluicing period, sediment trapping efficiency is estimated by the Churchill Curve. Daily trapping efficiency values are computed using the equations 41 and 42. During reservoir drawdown process, reservoirs are hydrologically smaller than during normal operations. Therefore, the Churchill Curve can approximate more accurately passing of sediments for this condition than the Brune Curve method. Normally, hydropower is generated during sluicing, however a user can specify whether to generate hydropower or not during this time period. Sluicing will end either if the duration of sluicing has been completed or if the reservoir inflow is less than the user-specified minimum reservoir inflow. After the completion of sluicing, the reservoir begins to refill and returns back to its normal operation. But the refilling rate per day is restricted to the user-specified maximum refill rate.

$$SI = \frac{(V/I)^2}{L} \quad (41)$$

$$TE = 112 - 800 \times (0.3048 \times SI)^{-0.2} \quad (42)$$

Where, SI is Sedimentation Index, V is storage capacity of the reservoir (m^3), I is average daily inflow in m^3/s , L is the length of the reservoir measured from the dam wall to the most upstream impounded water at dam storage capacity (m).

3. MODIFICATION OF THE SWAT SOURCE CODE

The ROSMan is programmed in the Fortran programming language in order to seamlessly integrate the code into the SWAT. To introduce the ROSMan into the official SWAT model version SWAT2012 Rev. 670 (released on the 1st October, 2018), several modifications to the source code were carried out. In the source code files, a comment "!! edited by JPS" has been mentioned wherever the original code lines have been modified; therefore, the code changes can be found by searching for the text "JPS". However, the ROSMan does not affect the original other simulation processes of the SWAT and if desired a user can still simulate reservoirs using the existing original reservoir simulation methods in the SWAT. The following SWAT source code files have been modified:

- i. modparm.f
- ii. allocate_parms.f
- iii. readfile.f
- iv. header.f
- v. headout.f
- vi. readfig.f
- vii. routres.f
- viii. res.f
- ix. writem.f
- x. stdaa.f
- xi. std1.f
- xii. std2.f
- xiii. std3.f
- xiv. subaa.f
- xv. biofilm.f

- xvi. writea.f
- xvii. writed.f
- xviii. writem.f
- xix. pestw.f
- xx. print_hyd.f
- xxi. rchday.f
- xxii. rchaa.f
- xxiii. rchmon.f
- xxiv. rchyr.f

The following additional subroutines and modules of source code files have been added to simulate with the ROSMan:

3.1 Read_ROSMan.f

This subroutine reads input data from additional input files (described detail in sections below), stores and initializes variables to simulate with the ROSMan.

3.2 ResApp.f

This Fortran module contains several other subroutines and functions which allows for interpolation, simple computation and date conversion. These functions and subroutines are called by the main ROSMan subroutine whenever required for these applications. The ResApp module contains the following functions:

3.2.1 Subroutine Add1DAY

This subroutine is used to add a one day to a given date1 and computes date2 in yyyyymmdd format.

3.2.2 Subroutine jtodate

This subroutine converts Julian day (1 to 365/366 days) of a given year (yyyy) into a date in the form of yyyyymmdd.

3.2.3 Subroutine to_date

This subroutine converts year (yyyy), month (mm) and day (dd) into a date in the form of yyyyymmdd.

3.2.4 Subroutine int_date

This subroutine is opposite to the subroutine to_date, so that it segregates date into year, month and day.

3.2.5 Subroutine xDAYS

To calculate the number of days between two dates, this subroutine is used.

3.2.6 Subroutine rulecurve

This subroutine is used to interpolate daily reservoir water elevation and volume using monthly rule curve and volume-elevation-area curve data provided by the user at specified date (according to given year, month and day) for the given reservoir.

3.2.7 Subroutine interpolate_only

This subroutine gives the interpolated value (y) for the given value (x) from its location array (a) and respective value array (b) using the method of two point formula.

3.2.8 Subroutine read_all_outlet

This subroutine is called whenever it required data of outlet rating curves (spillway, hydropool and low level outlet rating curves). It extracts data from these outlet curves for the specified reservoir.

3.2.9 Subroutine storage_indication

This subroutine is only called by the HyDROR routine. This subroutine generates values of the array for the Storage Indication ($2 \times \text{volume/time} + \text{outflow}$) vs outflow curve, combining

the outlet capacity curve and Volume-Elevation-Area Curve. This array is used to estimate the outflow of the reservoir using the Modified Puls Method.

3.2.10 Subroutine levelpool

This is the main subroutine is used by the HydROR routine. This subroutine estimates the reservoir outflow using the Modified Puls Method (Level Pool Routing) for the specified reservoir.

3.3 ResSMan.f

This is the main subroutine for simulation with the ResSMan. This routine will be executed for simulation of every reservoir which is specified by the user to simulate with the ResSMan (IRESCO = 7). This routine outputs reservoir storage capacity, water level, water outflow, sediment outflow accumulated sediment and energy generation of the hydropower scheme.

4.1 Input files

4.2 SWAT reservoir input file (.res)

```

C:\000020000.res - Notepad
File Edit Format View Help

Reservoir data:      .res file Subbasin: 2 24/10/2019 12:00:00 AM ArcSWAT 2012.10_4.21
2      | RES_SUB : Number of the subbasin the reservoir is in
0      | MORES : Month the reservoir became operational (1-12)
1980   | IYRES : Year of the simulation the reservoir became operational
0      | RES_ESA : Reservoir surface area when the reservoir is filled to the emergency spillway [ha]
0.0    | RES_EVOL : Volume of water needed to fill the reservoir to the emergency spillway [104 m3]
0.0    | RES_PSA : Reservoir surface area when the reservoir is filled to the principal spillway [ha]
0.0    | RES_PVOL : Volume of water needed to fill the reservoir to the principal spillway [104 m3]
0.0    | RES_VOL : Initial reservoir volume [104 m3]
4000.0 | RES_SED : Initial sediment concentration in the reservoir [mg/l]
4000.0 | RES_NSED : Normal sediment concentration in the reservoir [mg/l]
10.0   | RES_D50 : Median particle diameter of sediment [um]
0.0    | RES_K : Hydraulic conductivity of the reservoir bottom [mm/hr]
6      | TRESKO : Outflow simulation code

OFLOWMX: maximum daily outflow for January - June [m3/s]
0.0    0.0    0.0    0.0    0.0    0.0
OFLOWMX: maximum daily outflow for July - December [m3/s]
0.0    0.0    0.0    0.0    0.0    0.0
OFLOWMN: minimum daily outflow for January - June [m3/s]
0.0    0.0    0.0    0.0    0.0    0.0
OFLOWMN: minimum daily outflow for July - December [m3/s]
0.0    0.0    0.0    0.0    0.0    0.0

0.0    | RES_RR : Average daily principal spillway release rate [m3/s]
RESMONO : Name of monthly reservoir outflow file

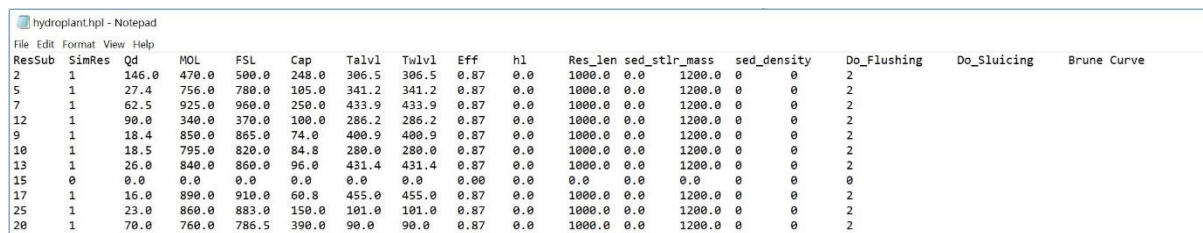
```

21

4.3 Hydroplant characteristics file (hydroplant.hpl)

The hydroplant characteristics input file “hydroplant.hpl” is the main input file which stores the properties of hydropower plants and reservoirs in the catchment. The name of this file must be the same as described above with extension of “.hpl” in the text file format. Each row of this file corresponds to the reservoir assigned in the SWAT model at the time of catchment delineation. In this file, the user have to include all the assigned reservoirs in the study catchment, even the reservoir is not used for simulation. As shown in Figure 8, for the ResSub 15 is not used for simulation, thus the most of properties can be filled with 0 and assigned the “SimRes” column with 0.

The first line of the file is used for a header or user comments. From 2nd line, it contains 16 columns with data values and each column is spaced by a single tab. The format of the file should match as described and shown in figures here, any distortions in file format may cause errors in simulation. To easily prepare input files, one can store all the data in Excel (Figure 9) and then paste into the text file (Figure 8).



| ResSub | SimRes | Qd | MOL | FSL | Cap | Talvl | Twlvl | Eff | h1 | Res_len | sed_stlr | mass | sed_density | Do_Flushing | Do_Sluicing | Brune Curve |
|--------|--------|-------|-------|-------|-------|-------|-------|------|-----|---------|----------|--------|-------------|-------------|-------------|-------------|
| 2 | 1 | 146.0 | 470.0 | 590.0 | 248.0 | 306.5 | 306.5 | 0.87 | 0.0 | 1000.0 | 0.0 | 1200.0 | 0 | 0 | 2 | |
| 5 | 1 | 27.4 | 756.0 | 780.0 | 105.0 | 341.2 | 341.2 | 0.87 | 0.0 | 1000.0 | 0.0 | 1200.0 | 0 | 0 | 2 | |
| 7 | 1 | 62.5 | 925.0 | 960.0 | 250.0 | 433.9 | 433.9 | 0.87 | 0.0 | 1000.0 | 0.0 | 1200.0 | 0 | 0 | 2 | |
| 12 | 1 | 90.0 | 340.0 | 370.0 | 100.0 | 286.2 | 286.2 | 0.87 | 0.0 | 1000.0 | 0.0 | 1200.0 | 0 | 0 | 2 | |
| 9 | 1 | 18.4 | 850.0 | 865.0 | 74.0 | 400.9 | 400.9 | 0.87 | 0.0 | 1000.0 | 0.0 | 1200.0 | 0 | 0 | 2 | |
| 10 | 1 | 18.5 | 795.0 | 820.0 | 84.8 | 280.0 | 280.0 | 0.87 | 0.0 | 1000.0 | 0.0 | 1200.0 | 0 | 0 | 2 | |
| 13 | 1 | 26.0 | 840.0 | 860.0 | 96.0 | 431.4 | 431.4 | 0.87 | 0.0 | 1000.0 | 0.0 | 1200.0 | 0 | 0 | 2 | |
| 15 | 0 | 0.0 | 0.0 | 0.0 | 0.0 | 0.0 | 0.0 | 0.00 | 0.0 | 0.0 | 0.0 | 0.0 | 0 | 0 | 0 | |
| 17 | 1 | 16.0 | 890.0 | 910.0 | 60.8 | 455.0 | 455.0 | 0.87 | 0.0 | 1000.0 | 0.0 | 1200.0 | 0 | 0 | 2 | |
| 25 | 1 | 23.0 | 860.0 | 883.0 | 150.0 | 101.0 | 101.0 | 0.87 | 0.0 | 1000.0 | 0.0 | 1200.0 | 0 | 0 | 2 | |
| 20 | 1 | 70.0 | 760.0 | 786.5 | 390.0 | 90.0 | 90.0 | 0.87 | 0.0 | 1000.0 | 0.0 | 1200.0 | 0 | 0 | 2 | |

Figure 8: An example file of hydroplant.hpl

| | A | B | C | D | E | F | G | H | I | J | K | L | M | N | O | P | Q |
|----|--------|--------|-------|-------|-------|-------|-------|--------|------|-----|---------|---------------|-------------|-------------|------------|-------------|---|
| 1 | ResSub | SimRes | Qd | MOL | FSL | Cap | Talvl | Twlavl | Eff | hl | Res_len | sed_stlr_mass | sed_density | Do_Flushing | Do_Sluicin | Brune Curve | |
| 2 | 2 | 1 | 146.0 | 470.0 | 500.0 | 248.0 | 306.5 | 306.5 | 0.87 | 0.0 | 1000.0 | 0.0 | 1200.0 | 0 | 0 | 2 | |
| 3 | 5 | 1 | 27.4 | 756.0 | 780.0 | 105.0 | 341.2 | 341.2 | 0.87 | 0.0 | 1000.0 | 0.0 | 1200.0 | 0 | 0 | 2 | |
| 4 | 7 | 1 | 62.5 | 925.0 | 960.0 | 250.0 | 433.9 | 433.9 | 0.87 | 0.0 | 1000.0 | 0.0 | 1200.0 | 0 | 0 | 2 | |
| 5 | 12 | 1 | 90.0 | 340.0 | 370.0 | 100.0 | 286.2 | 286.2 | 0.87 | 0.0 | 1000.0 | 0.0 | 1200.0 | 0 | 0 | 2 | |
| 6 | 9 | 1 | 18.4 | 850.0 | 865.0 | 74.0 | 400.9 | 400.9 | 0.87 | 0.0 | 1000.0 | 0.0 | 1200.0 | 0 | 0 | 2 | |
| 7 | 10 | 1 | 18.5 | 795.0 | 820.0 | 84.8 | 280.0 | 280.0 | 0.87 | 0.0 | 1000.0 | 0.0 | 1200.0 | 0 | 0 | 2 | |
| 8 | 13 | 1 | 26.0 | 840.0 | 860.0 | 96.0 | 431.4 | 431.4 | 0.87 | 0.0 | 1000.0 | 0.0 | 1200.0 | 0 | 0 | 2 | |
| 9 | 15 | 0 | 0.0 | 0.0 | 0.0 | 0.0 | 0.0 | 0.0 | 0.00 | 0.0 | 0.0 | 0.0 | 0.0 | 0 | 0 | 0 | |
| 10 | 17 | 1 | 16.0 | 890.0 | 910.0 | 60.8 | 455.0 | 455.0 | 0.87 | 0.0 | 1000.0 | 0.0 | 1200.0 | 0 | 0 | 2 | |
| 11 | 25 | 1 | 23.0 | 860.0 | 883.0 | 150.0 | 101.0 | 101.0 | 0.87 | 0.0 | 1000.0 | 0.0 | 1200.0 | 0 | 0 | 2 | |
| 12 | 20 | 1 | 70.0 | 760.0 | 786.5 | 390.0 | 90.0 | 90.0 | 0.87 | 0.0 | 1000.0 | 0.0 | 1200.0 | 0 | 0 | 2 | |

Figure 9: Hydropower plant characteristics stored in MS-Excel file

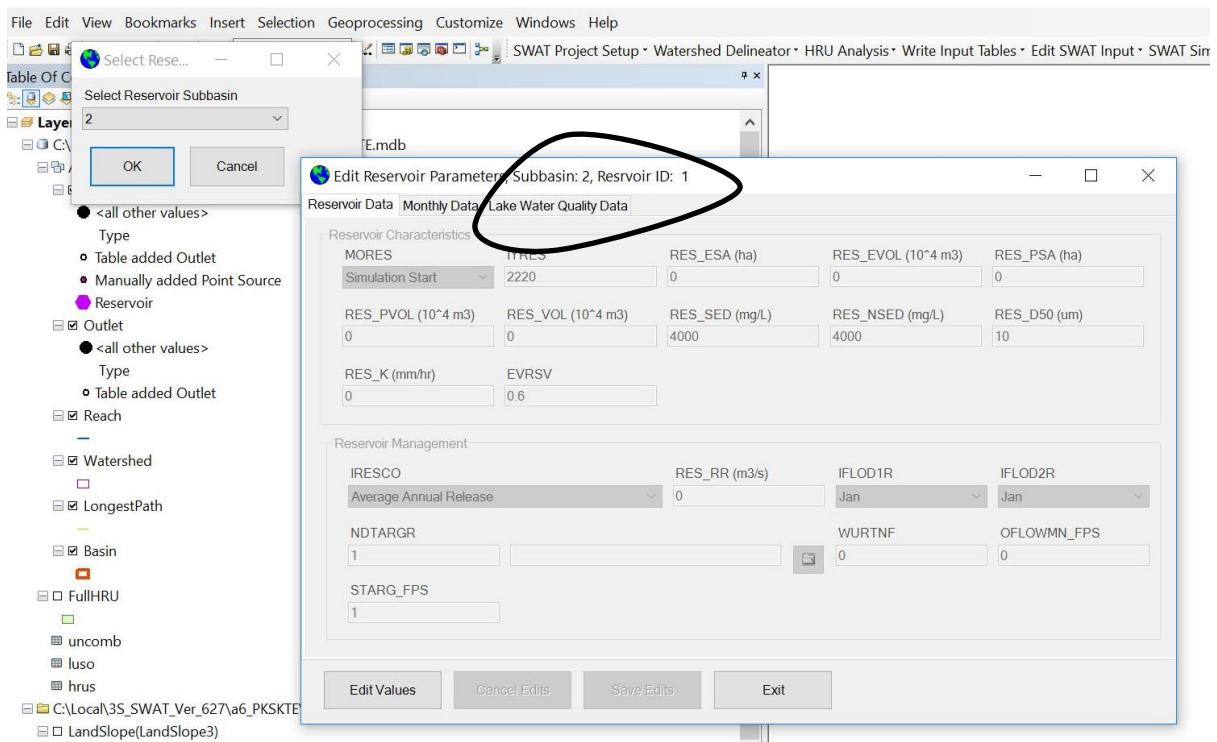


Figure 10: Reservoir ID determination using ArcSWAT

4.3.1 Reservoir subbasin number (integer)

The first column of “.hpl” file stores the subbasin number (integer) of the reservoir. The subbasin number stored in each row must be identical to the subbasin as defined in the “.res” reservoir input file. Again, the sequence of each reservoir must be according to the Reservoir

ID (Figure 10), because the SWAT simulate the reservoir in the order of this unique ID. The Reservoir ID (Figure 10) can be found from ArcSWAT model setup as shown in Figure 10. In the given example, the reservoir ID with 1 is located in the subbasin number 2 and thus it is stored in the 1st row of the data. The simulation sequence of reservoirs is very critical information.

4.3.2 Simulate reservoir or not (integer)

The user must enter 1 in the 2nd column if the specific reservoir is simulating. If the user has specified 0 for any reservoirs, then these reservoirs will not be simulated and any values of other columns will not be used for any purposes and respective other files also will not be read.

4.3.3 Design discharge (m^3/s)

The 3rd column of this file is the design discharge in m^3/s of corresponding hydropower plant of the reservoir. The user must provide this data in the real format, if the information is not known then must leave with 0.0.

4.3.4 Minimum operating level (m.a.s.l.)

This column represents the minimum operating water level (MOL) in meter above sea level (m.a.s.l.) of the active storage of the reservoir. The ResSMan uses this level to compute the dead and active storage volume of the reservoir. The model assumes that dead storage and active storage volume is separated by this level and dead storage is below this level. The dead storage zone is only used for storing settled sediment mass and the storage capacity within this zone cannot be used for hydropower generation.

4.3.5 Full Supply level (m.a.s.l.)

The 5th column of this file stores the information of the full supply level (FSL) of the reservoir. The FSL represents the upper limit of the active storage volume of the reservoir and used to compute the dead and active storage volume of the reservoir (Figure 3). The active

storage volume fluctuates between FSL and MOL and specifically used for hydropower generation.

4.3.6 Installed capacity (MW)

This column represents the installed capacity (MW) of the hydropower plant for each reservoir. This is the maximum capacity that the hydropower plant can produce at simulation period. If the reservoir has not facility to generate hydropower, then the user must assign to 0.

4.3.7 Turbine axis level (m.a.s.l.) and Tailwater level (m.a.s.l.)

The information in 7th and 8th column is stored with turbine axis level and Tailwater level of the hydropower plant. These data are used to compute the head of hydropower plant to estimate the power production. The model assumes constant Tailwater level during the simulation period. The user must provide these information. If one of these information is not known, then can be assigned as equal values but assigning 0.0 will effect on computation of hydropower production.

4.3.8 Hydropower Plant efficiency (factor)

The 9th column specifies the combined efficiency of the hydropower plant in the form of a factor. This efficiency is combination of turbines and generators and assumes to be constant during simulation period.

4.3.9 Headloss coefficient (factor)

In this column, specify headloss coefficient (fraction) of the hydropower plant. This headloss coefficient includes all possible losses such as frictional loss, entry loss and exit loss of hydropower plant and assumes constant during simulation period. If user assigns this column with 0.0, then model ignores headloss.

4.3.10 Reservoir Length (m)

This column represents the reservoir length at the FSL. This input is used only to simulate with the sluicing technique. During sluicing, the ResSMan computes reservoir

trapping efficiency using the Churchill Method (1948). Thus, reservoir length is required to compute the Sedimentation Index (SI), ultimately this index is used to estimate trapping efficiency. If the user is not simulating with sluicing, then this value can be assigned with 0.0.

4.3.11 Initial settled sediment mass (Ton)

The 12th column represents the amount of sediment mass in metric tonne (Ton) deposited in the bottom of the reservoir at the beginning of the simulation period. This value accounts only quantity of deposit sediment and can be assigned as 0.0, if the initial reservoir volume is 0. The initial suspended sediment concentration (mg/l) is assigned in .res file which is represented as RES_SED. The sediment outflow depends on the concentration of suspended sediment at the beginning of the simulation. If the initial volume of reservoir is zero then, it can be assigned as 0.0. The variable RES_NSED (mg/l) is the equilibrium sediment concentration in the reservoir which is required to simulate with existing SWAT reservoir routine. The SWAT assumes that suspended sediment will be settled when the concentration of suspend sediment exceeds this value. However, the ResSMan predicts the settle sediment implementing the Brune Curve method. Hence, whatever value assigned for the RES_NSED, the ResSMan will not use this value for any calculations.

4.3.12 Sediment density (kg/m³)

The 13th column represents the density of sediment in kg/m³. The volume of settled sediment mass is calculated using this value. This value must provide if the particular reservoir is simulated with the ResSMan.

4.3.13 Simulate with flushing or not (integer)

The 14th column is used to specify whether the reservoir is simulating with flushing or not. The value of this column must be “1” or “0”. If the specific reservoir is simulating with the flushing technique, then the user must assign 1, if not then the user must assign 0.

4.3.14 Simulate with sluicing or not (integer)

Same as column 15th, if the specific reservoir is simulating with the sluicing technique, then the user must assign 1, if not then the user must assign 0.

4.3.15 Brune Curve Type (integer)

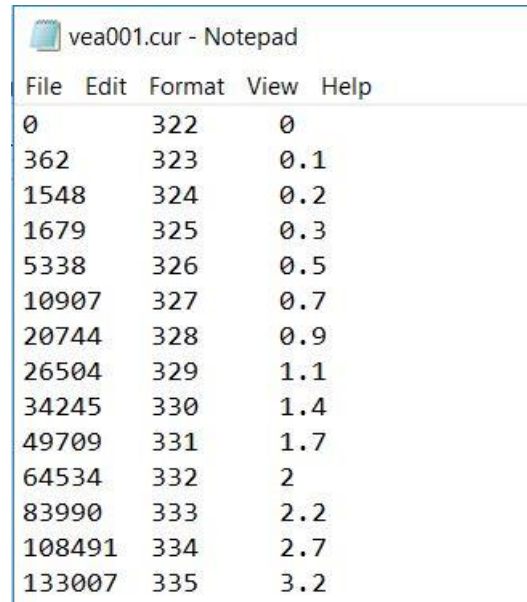
In the ResSMan, the sediment trapping efficiency is calculated by Brune Curve method. Brune (1953) developed a trapping efficiency curve as related to reservoir capacity-inflow ratio by using data of 40 normally ponded reservoirs and 4 other types of reservoirs in the USA. Brune has classified these curves into three category: 1) lower trapping efficiency curve for fine grained sediment; 2) original median trap curve for median grained sediment and 3) higher trapping efficiency curve for coarse sediment. In this column, the user can specify one of these curves assigning 1 for lower curve, 2 for median curve and 3 for higher curve.

4.4 Volume-elevation-area curve (.cur) file

The “.cur” file contains volume (m^3), elevation (m.a.s.l.) and surface area (ha) of a reservoir (Figure 11). The data start from 1st line of the file without any headers and comments. The 1st row of volume and surface area data should be 0 and its respective elevation. This file should be created for each of the reservoirs which will be simulated with the ROSMan (both HyDROR and ResSMan). The name of file should be in “vea001.cur”, “vea002.cur”, “vea015.cur”. Where, the corresponding file of reservoir ID 1 is vea001.cur, corresponding file of reservoir ID 2 is vea002.cur and corresponding file of reservoir ID 15 is vea015.cur respectively. The naming order of other input files must be also in the same order as described here.

The volume-elevation-area curve of the reservoir can be obtained from the topographic map of the reservoir. This curve is used to estimate active and dead storage volume, water surface level and surface area. The hydropower production capacity and accumulation of sediment on the bottom of reservoir depend on the active and dead storage volume. The water

surface elevation is used to calculate the head of the hydropower plant, while the surface area is used to estimate the amount of precipitation and evaporation on and from the reservoir surface area respectively.



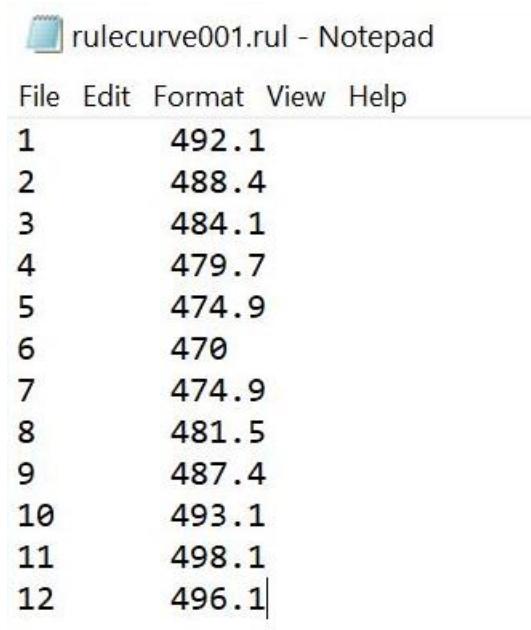
| File | Edit | Format | View | Help |
|--------|------|--------|------|------|
| 0 | | 322 | 0 | |
| 362 | | 323 | 0.1 | |
| 1548 | | 324 | 0.2 | |
| 1679 | | 325 | 0.3 | |
| 5338 | | 326 | 0.5 | |
| 10907 | | 327 | 0.7 | |
| 20744 | | 328 | 0.9 | |
| 26504 | | 329 | 1.1 | |
| 34245 | | 330 | 1.4 | |
| 49709 | | 331 | 1.7 | |
| 64534 | | 332 | 2 | |
| 83990 | | 333 | 2.2 | |
| 108491 | | 334 | 2.7 | |
| 133007 | | 335 | 3.2 | |

Figure 11: An example of volume-elevation-area curve (.cur) file

4.5 Rule curve (.rul) file

Reservoir operation is accomplished by a predefined rule curve in the ROSMan. The rule curves can be generated on the basis of maximum hydropower production, flood control, and environmental criteria such as water quality for fish and wildlife preservation, and downstream flow regulation.

The “.rul” file of 1st column contains month number (integer) and 2nd column contains water surface elevation (m.a.s.l.) corresponding to the 1st day of respective month (Figure 12). The data start from 1st line of the file without any headers and comments. The names of files should be as rulecurve001.rul, rulecurve002.rul.....in the order of reservoirs as in the hydroplant.hpl file. Using this monthly rule curve, the ROSMan interpolates water elevation and storage volume for each day of simulation.



| File | Edit | Format | View | Help |
|------|------|--------|------|------|
| 1 | | 492.1 | | |
| 2 | | 488.4 | | |
| 3 | | 484.1 | | |
| 4 | | 479.7 | | |
| 5 | | 474.9 | | |
| 6 | | 470 | | |
| 7 | | 474.9 | | |
| 8 | | 481.5 | | |
| 9 | | 487.4 | | |
| 10 | | 493.1 | | |
| 11 | | 498.1 | | |
| 12 | | 496.1 | | |

Figure 12: An example of rule curve (.rul) file

4.6 Spillway rating curve (.out) file

The file names for spillway rating curves should be as spillway001.out, spillway002.out.....in the order of reservoirs as in the hydroplant.hpl file. This file contains water surface level (m.a.s.l.) in the 1st column and respective discharge capacity in m^3/s in the 2nd column (Figure 13).

The spillway outlet is used to spill the excess volume of water when the water level is higher than the active storage level of the reservoir. It is assumed that the spillway crest level is located at the top of the active storage level. Thus, this outlet does not allow for hydropower generation. Hence, this outlet is used to release excess flood storage water. However, even if the water surface level of the reservoir is higher than the active storage level, the spillway does not release any water until the rule curve for the reservoir dictates a release is required.

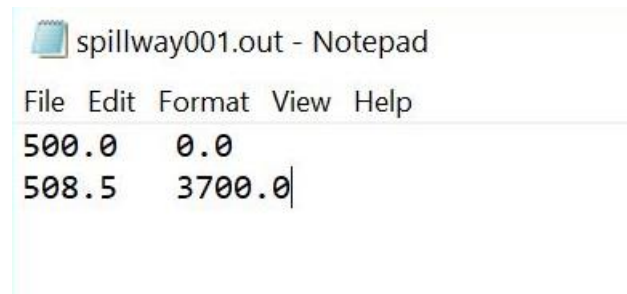


Figure 13: An example file of spillway rating curve (.out)

4.7 Hydroplant pool curve (.out) file

Water discharge capacity of a hydropower intake with respect to water elevation is provided by this hydroplant pool curve. Discharge through the hydropower intake is solely used to generate hydropower energy and is discharged to immediate downstream channel of the basin after passing through turbines.

The file names for hydroplant pool curves should be as hydropool001.out, hydropool002.out.....in the order of reservoirs as in the hydroplant.hpl file. This file contains water surface level (m.a.s.l.) in the 1st column and respective discharge capacity in m³/s in the 2nd column (Figure 14). The water elevation at the first line should be minimum operating level (MOL) and water level at the last line should be full supply level (FSL) and their respective discharge capacities.

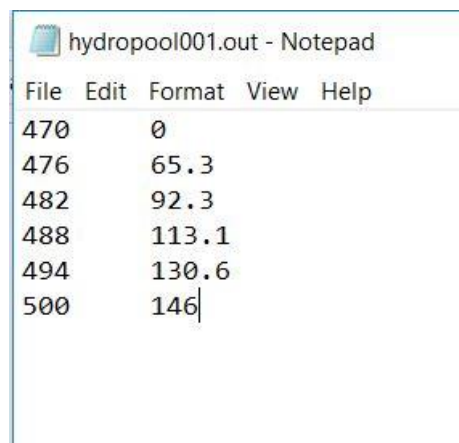


Figure 14: An example of hydroplant pool curve (.out) file

4.8 Flushing gate rating curve (.out) file

Flushing gate or low level outlet gates are located at the bottom of the dam. This flushing gates are used to release water and sediment into the downstream channel for during simulation with flushing and sluicing management techniques and discharge through these gates do not result hydropower generation. It is assumed that these gates are only operable during flushing and sluicing and remain closed at normal condition operation.

The file names for flushing gate rating curves should be as flushoutlet001.out, flushoutlet 002.out.....in the order of reservoirs as in the hydroplant.hpl file. This file contains water surface level (m.a.s.l.) in the 1st column and respective discharge capacity of gates in m^3/s in the 2nd column (Figure 15). The water elevation at the first line should be original river bed elevation (i.e. the first elevation of “.cur” file).


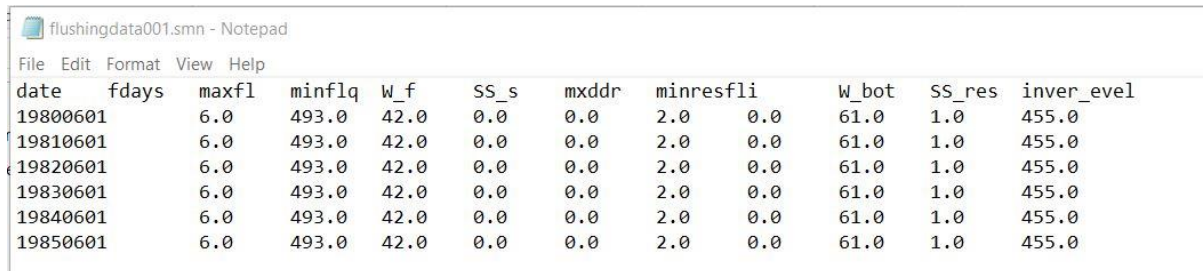
 flushoutlet001.out - Notepad
File Edit Format View Help
322.0 0.0
325.0 25.0
328.0 50.0|

Figure 15: An example of flushing gate outlet rating curve (.out) file

4.9 Flushing specification data (.smn) file

This file is needed to simulate the reservoir with flushing sediment management technique. When the user has assigned 1 for “Simulate with flushing or not (integer)” in the “.hpl” file, this file must be provided for each of the reservoirs. The file names should be as flushingdata001.smn, flushingdata002.smnin the order of reservoirs as in the hydroplant.hpl file. The first line of the file is specified for the header or comments and data

begins from the 2nd line of the file. The data should be entered in the order as described below and columns should be delimited by tabs.



| date | fdays | maxfl | minflq | W_f | SS_s | mxddr | minresfli | W_bot | SS_res | inver_evel |
|----------|-------|-------|--------|-----|------|-------|-----------|-------|--------|------------|
| 19800601 | 6.0 | 493.0 | 42.0 | 0.0 | 0.0 | 2.0 | 0.0 | 61.0 | 1.0 | 455.0 |
| 19810601 | 6.0 | 493.0 | 42.0 | 0.0 | 0.0 | 2.0 | 0.0 | 61.0 | 1.0 | 455.0 |
| 19820601 | 6.0 | 493.0 | 42.0 | 0.0 | 0.0 | 2.0 | 0.0 | 61.0 | 1.0 | 455.0 |
| 19830601 | 6.0 | 493.0 | 42.0 | 0.0 | 0.0 | 2.0 | 0.0 | 61.0 | 1.0 | 455.0 |
| 19840601 | 6.0 | 493.0 | 42.0 | 0.0 | 0.0 | 2.0 | 0.0 | 61.0 | 1.0 | 455.0 |
| 19850601 | 6.0 | 493.0 | 42.0 | 0.0 | 0.0 | 2.0 | 0.0 | 61.0 | 1.0 | 455.0 |

Figure 16: An example of flushing specification data (.smn) file

4.9.1 Drawdown start date (yyyymmdd)

The first column of this file is the drawdown start date in yyyymmdd format. Drawdown will be started at this date when the inflow rate criterion (defined in the 3rd column) is satisfied. If the flushing is simulated more than once during the overall SWAT simulation period, then the user must provide each data line with all required parameters for each drawdown start date (Figure 16).

4.9.2 Flushing duration (days)

The 2nd column is number of days required to remove deposit sediment due to flushing after flushing criteria have met. This duration does not include drawdown duration.

4.9.3 Maximum water level (m.a.s.l.)

The 3rd column of this file is maximum water level (m.a.s.l.) of the reservoir. When reservoir water level is higher than this level, the reservoir will not be able remove sediment due to flushing. To achieve successful flushing, this criterion should be met. The user must provide this information.

4.9.4 Minimum flushing discharge (m^3/s)

The 4th column in the flushing data file is the minimum flushing discharge through the flushing gates. When the water release through the flushing gates is greater than the required minimum flushing discharge, the deposit sediment will be removed successfully due to flushing

process. After the complete drawdown of the reservoir, the outflow through the flushing gates equals about to the runoff of the river and it depends on hydrological condition of the catchment and time of operation of the flushing. Thus, the model user can define the required minimum flushing flow analyzing the historical hydrological data of the river flow.

4.9.5 Flushing channel bottom width (m)

The 5th column of this file is bottom width (m) of the flushing channel. The ResSMan assumes that trapezoidal flushing channel will be formed during the flushing process. The cross sectional area of flushing channel is used to estimate quantity of sediment removal by flushing process. If the user assigned this column with 0.0, then the model will estimate by itself as described in the section 2 (Atkinson 1996).

4.9.6 Flushing channel side slope (factor)

The user should enter side slope (m/m, vertical/horizontal) of the flushing channel in the 6th column of this file. The user can allow to determine the flushing channel side slope by entering 0.0 for this variable as described in the section 2.

4.9.7 Maximum drawdown rate (m)

The 7th column of this file is maximum drawdown rate (m). This criterion controls the rapid drawdown of water level and thus controls downstream flash floods.

4.9.8 Minimum flow to initiate drawdown (m^3/s)

The 8th column of the file is the minimum flow into the reservoir which controls the drawdown start date. The user must enter the drawdown start date at 1st column. The ResSMan checks inflow to the reservoir on and after specified drawdown start date, but drawdown will actually initiate after the reservoir inflow exceeds this value. If the user wants to initiate drawdown at exact specified date in the 1st column, then the user should enter this column with 0.

4.9.9 Representative reservoir bottom width (m)

In the 9th column of this file, the user should provide the representative reservoir bottom width. This value is used to compute the cross sectional area of the reservoir. This value can be assumed the bottom length of the dam. This value should be constant for the reservoir and so should enter same value for different dates of flushing.

4.9.10 Reservoir side slope (factor)

The user should enter side slope (m/m, vertical/horizontal) of the reservoir side banks in the 10th column of this file. This value is also constant for the reservoir and so should be entered the same value for different dates of flushing. This value is also used to estimate cross sectional area of the reservoir during flushing process.

4.9.11 Flush gate invert level (m.a.s.l.)

The 10th column of this input file is the invert level of the flush gate or low level outlet. The user must provide this elevation. This value must be equal to the first elevation value of the flushoutlet.out file.

4.10 Sluicing specification data (.smn) file

This file is needed to simulate the reservoir with sluicing sediment management technique. When the user has assigned 1 for “Simulate with sluicing or not (integer)” in the “.hpl” file, this file must be provided for each of the reservoirs. The file names should be as sluicingdata001.smn, sluicingdata 002.smnin the order of reservoirs as in the hydroplant.hpl file. The first line of the file is specified for the header or comments and data begins from the 2nd line of the file. The data should be entered in the order as described below and columns should be delaminated by tabs (Figure 17).

| start_date | duration | slminflq | slminfli | slmaxlvl | slmxddr | mxrefil | slpower |
|------------|----------|----------|----------|----------|---------|---------|---------|
| 20200601 | 20 | 37.6 | 37.6 520 | 2 0.5 | 1 | | |
| 20210601 | 20 | 37.6 | 37.6 520 | 2 0.5 | 1 | | |
| 20220601 | 20 | 37.6 | 37.6 520 | 2 0.5 | 1 | | |

Figure 17: An example of sluicing specification data (.smn) file

4.10.1 Sluicing start date (yyyymmdd)

The 1st column of the sluicing specification data (.smn) file is the starting date of the sluicing for the specified year. This column can be filled with 0, if the user wish to start sluicing after meeting the criteria of 3rd column.

4.10.2 Sluicing duration (days)

The 2nd column is the duration of sluicing in days. The sluicing will continue for this duration period after the starting date of the sluicing and then simulation will continue according to the defined rule curve. This value can be assigned with 0, if the user wishes to stop the sluicing after meeting the 4th column criterion.

4.10.3 Minimum flow into reservoir to start sluicing (m³/s)

The 3rd column of this file is an optional and can be filled with 0.0. If sluicing starting date is not specified, the ResSMan will start sluicing when the reservoir inflow is greater than this value and sluicing will be delayed until this criterion is fulfil.

4.10.4 Minimum flow into reservoir to stop sluicing (m³/s)

The value on the 4th column is also an option if the user has assigned the sluicing start date and duration. If 1st and 2nd column values are 0, then this column must be enter with proper value. The sluicing will be stopped when the reservoir inflow is lower than this value. The sluicing will be continue until this criterion has met.

4.10.5 Drawdown water surface elevation limit (m.a.s.l.)

In this column, the user must provide the water surface elevation of the reservoir. The ResMan attempts to maintain the water level at this limit by releasing the water and sediment through flushing gates. The value of this limit could be assign nearly equal to MOL.

4.10.6 Maximum drawdown rate (m)

The 6th column of this file is the maximum drawdown rate of the reservoir. This value controls the abrupt drop in water surface level.

4.10.7 Maximum refill rate (m)

In this column, the user should specify the maximum rate of refilling per day the reservoir after the sluicing process.

4.10.8 Hydropower production during sluicing (integer)

In this column, the user should specify with value 1, if hydropower generation is allowed during sluicing or specify with value 0, if hydropower generation is not allowed during sluicing.

4.11 Summary of input files

Table 1: Input files and variables required for simulation with the ROSMan routine

| File/variable | HydROR | ResSMan | Remarks |
|--------------------|---------------------------|------------------------|--|
| IRESKO (.res file) | 6 | 7 | Must provide |
| hydroplant.hpl | Applicable columns (1-10) | All columns applicable | Not applicable columns can be assigned with 0. |
| vea.cur | Applicable | Applicable | Must provide |
| rulecurve.rul | Applicable | Applicable | Must provide |
| spillway.out | Applicable | Applicable | Must provide |
| hydropool.out | Applicable | Applicable | Must provide |
| flushoutlet.out | Not applicable | Applicable | Must provide |
| flushingdata.smn | Not applicable | Applicable | Optional |
| sluicingdata.smn | Not applicable | Applicable | Optional |

4.12 Output file

In addition to all other output files of the SWAT, there is a one separate output file for ROSMan routine, called output_rosman.rsv. This file contains the reservoir ID number (not the subbasin number), Julian day of simulation period, reservoir volume in m^3 , water elevation (m.a.s.l.), reservoir inflow (m^3/s), outflow (m^3/s), precipitation (m^3), evaporation (m^3), seepage (m^3), power (MW), energy generation (GWh), sediment inflow (ton), sediment outflow (ton), sediment concentration (ppm), trapping efficiency (factor), accumulated sediment (ton) (N/A for the HydROR) and simulation year.

Figure 18: The output file for the ROSMan

5. QUICK START GUIDE

This guide briefly explains the steps that are obligatory to run the ROSMan. Regarding the preparation of input data to the routine, the user must strictly follow the previous sections.

5.1 SWAT model setup

Before simulation with the ROSMan, a SWAT model for the study area needs to be set up. The detailed process and theory on the SWAT are explained in SWAT I/O manual (Arnold et al. 2013) and SWAT Theoretical Documentation (Neitsch et al. 2011).

5.2 Simulation with the ROSMan

The user must load all the required input files for the ROSMan, as described above, in the SWAT “TxtInOut” folder. Furthermore, an executable file of the ROSMan (ROSMan.exe) also must be placed in the “TxtInOut” folder. Finally, the simulation can be run by clicking the ROSMan.exe file.

5.3 Post-processing of the outputs

After completion of the simulation, the outputs of the ROSMan will be printed in the “output_rosman.rsv” file as explained in the previous section. The user can export the output file into the MS-Excel to plot graphs and to further analyse the results or can use any other data processing tools. The user must evaluate the outputs of the ROSMan whether the outputs are reasonable or not. The performance of the ROSMan solely depend on user defined physical properties of hydropower plants, outlet capacities, reservoir geometry and operation policies such as rule curves. Thus, the user must provide accurate and realistic input data to obtain reasonable results.

REFERENCES

- Arnold, J., Kiniry, J., Srinivasan, R., Williams, J., Haney, E., and Neitsch, S. (2013). "SWAT 2012 Input/Output Documentation." Texas Water Resources Institute.
- Arnold, J. G., Srinivasan, R., Muttiah, R. S., and Williams, J. R. (1998). "Large area hydrologic modeling and assessment part I: model development." *JAWRA Journal of the American Water Resources Association*, 34(1), 73-89.
- Atkinson, E. (1996). "The feasibility of flushing sediment from reservoirs." *TDR Project R5839*, Report 0D137, HR Wallingford, UK.
- Brune, G. M. (1953). "Trap efficiency of reservoirs." *Eos, Transactions American Geophysical Union*, 34(3), 407-418.
- Chow, V. T. (1964). *Handbook of Applied Hydrology*, McGraw-Hill, New York, N.Y.
- Gill, M. A. (1979). "Sedimentation and useful life of reservoirs." *Journal of Hydrology*, 44(1), 89-95.
- Lai, J.-S., and Shen, H. W. (1996). "Flushing sediment through reservoirs." *Journal of Hydraulic Research*, 34(2), 237-255.
- Neitsch, S. L., Arnold, J. G., Kiniry, J. R., and Williams, J. R. (2011). "Soil and water assessment tool theoretical documentation version 2009." Texas Water Resources Institute.
- Shrestha, J. P., Pahlow, M., and Cochrane, T. A. (2020). "Development of a SWAT Hydropower Operation Routine and Its Application to Assessing Hydrological Alterations in the Mekong." *Water*, 12(8), 2193.
- Shrestha, J. P., Pahlow, M., and Cochrane, T. A. (2020). "Managing Reservoir Sedimentation through Coordinated Operation of Transboundary Reservoirs in the Mekong " *Manuscript submitted for publication*.
- Wen Shen, H. (1999). "Flushing sediment through reservoirs." *Journal of Hydraulic Research*, 37(6), 743-757.
- Wild, T., and Loucks, D. (2012). "SedSim model: a simulation model for the preliminary screening of sediment transport and management in river basins, version 3.0: documentation and users manual." *Department of Civil and Environmental Engineering, Cornell University, Ithaca, NY USA*

APPENDIX - 2

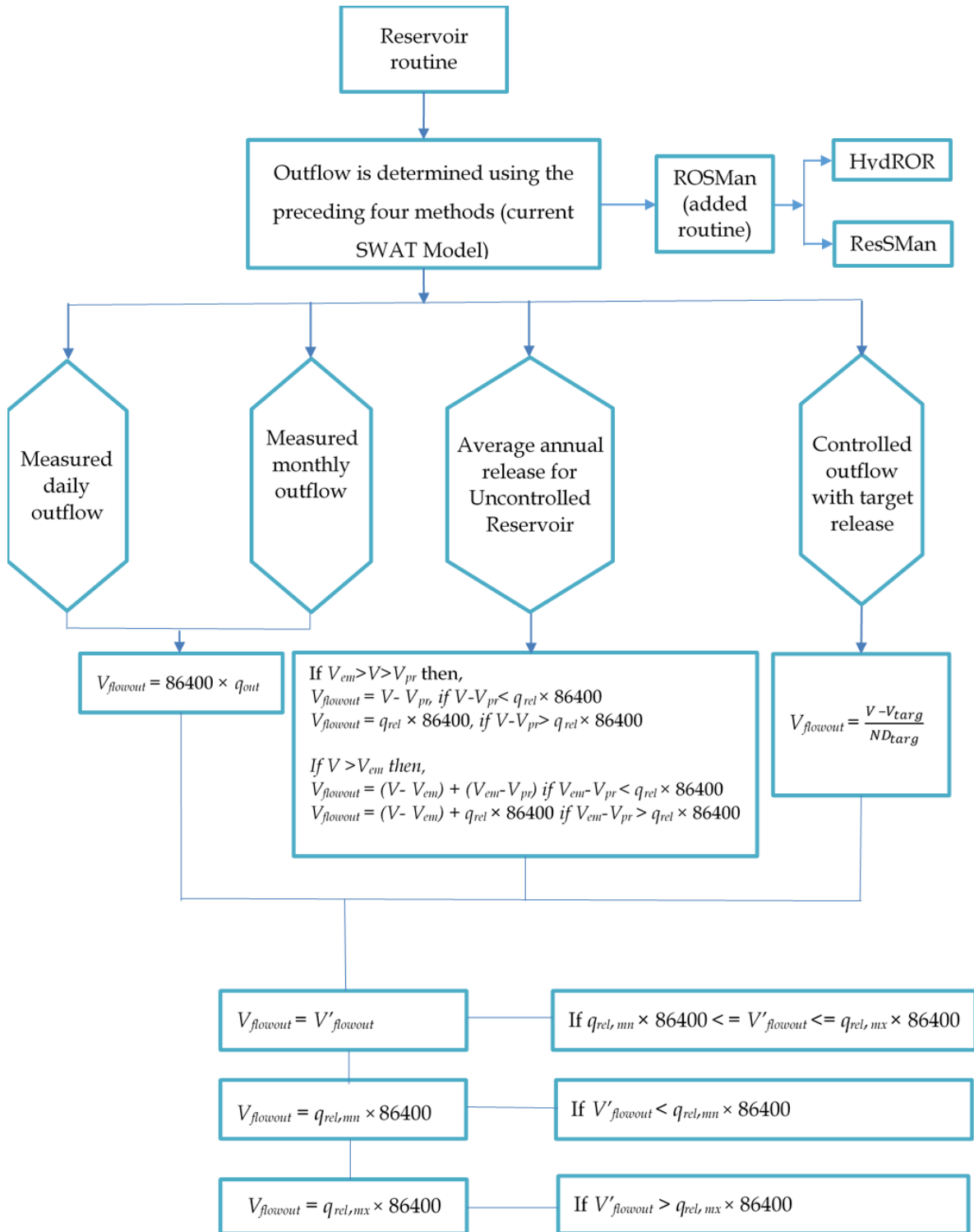


Figure A2-1: Flow chart for calculation of outflow from reservoir in the SWAT Model and added new routines.

Where,

$V_{flowout}$ = the volume of water flowing out of the water body during the day or month (m^3)

q_{out} = outflow rate (m^3/s)

q_{rel} = average daily principal spillway release rate (m^3/s)

V_{em} = volume of water held in the reservoir when filled to the emergency spillway (m^3),

V_{pr} = volume of water held in the reservoir when filled to the principal spillway (m^3),

V_{targ} = target reservoir volume for a given day (m^3),

ND_{targ} = the number of days required for the reservoir to reach target storage

$V_{flowout}$ = volume of water flowing out of the reservoir (m^3),

$V'_{flowout}$ = initial estimate volume of water flowing out of the reservoir (m^3),

$q_{rel,mn}$ = minimum average daily outflow for the month (m^3/s),

$q_{rel,mx}$ = maximum average daily outflow for the month (m^3/s).

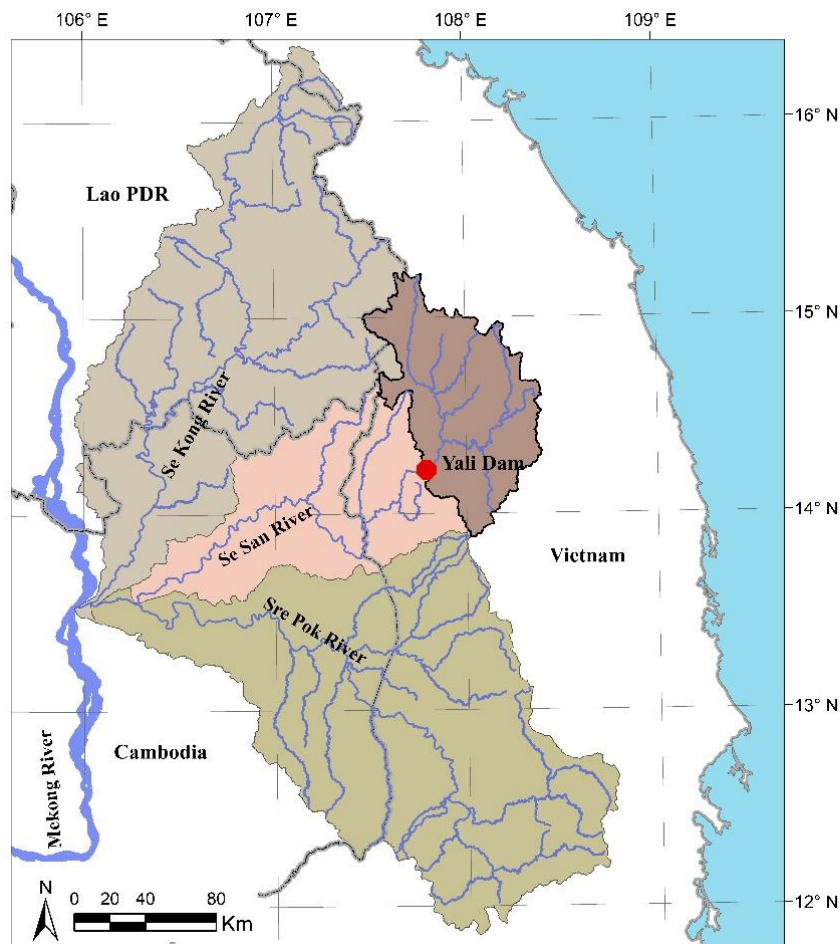
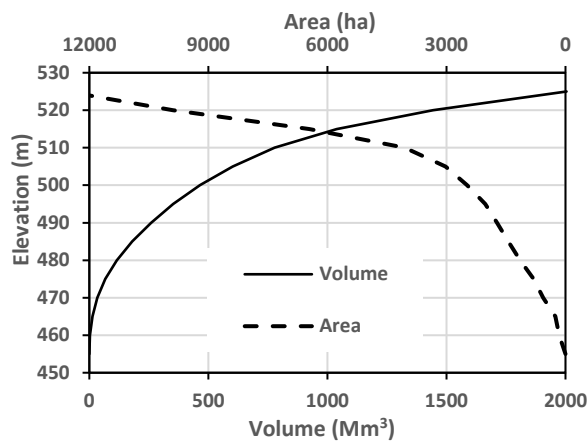
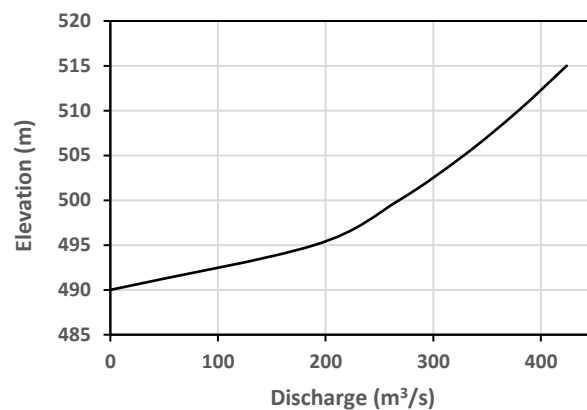


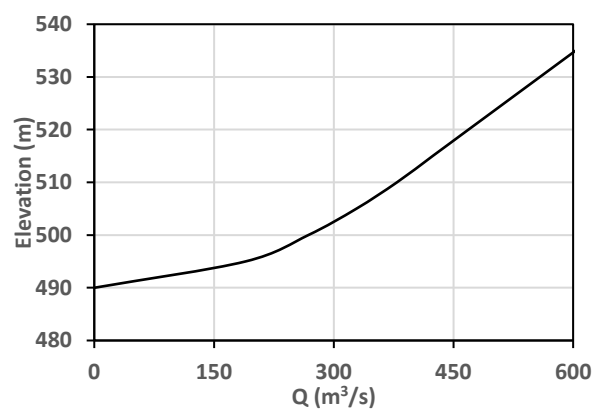
Figure A2-2: Catchment at Yali reservoir.



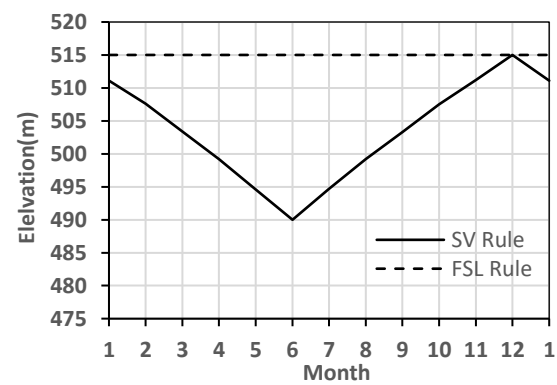
(a)



(b)



(c)



(d)

Figure A2-3: (a) Volume-Area-Elevation Curve, (b) Hydropower pool curve, (c) Spillway outflow curve and (d) Rule curves for the Yali reservoir.

Table A2-1: Yali hydropower plant characteristics.

| Characteristics | Unit | Quantity |
|-------------------------|-------------------|----------|
| Design Flow | m ³ /s | 424 |
| Minimum Operating Level | m.a.s.l | 490.0 |
| Full Supply Level | m.a.s.l | 515.0 |
| Installed Capacity | MW | 720 |
| Tailwater/turbine level | m.a.s.l | 300.0 |
| Plant Efficiency | - | 0.87 |
| Headloss coefficient | - | 0.05 |

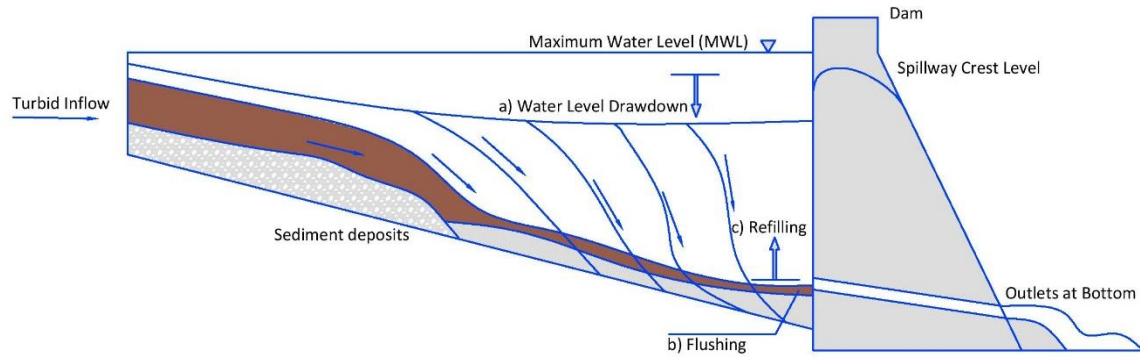


Figure A2-4: Flushing process to remove reservoir sediment deposits (a) water level drawdown, (b) flushing, (c) refilling reservoir.

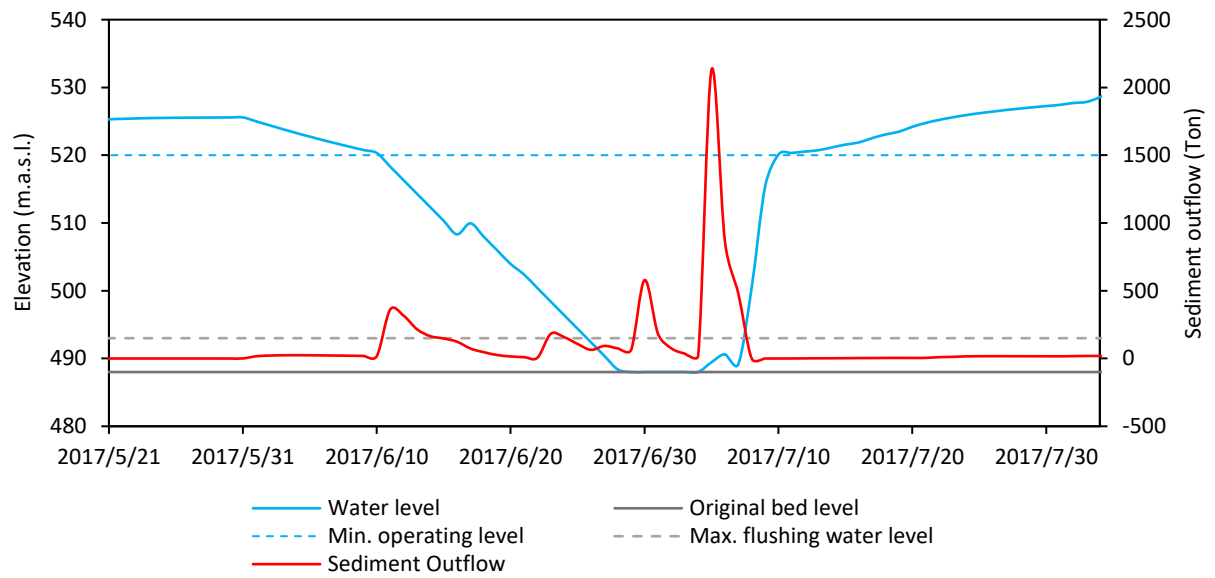


Figure A2-5: Drawdown process and removal of deposited sediment due to flushing from the Nam Kong 3 reservoir

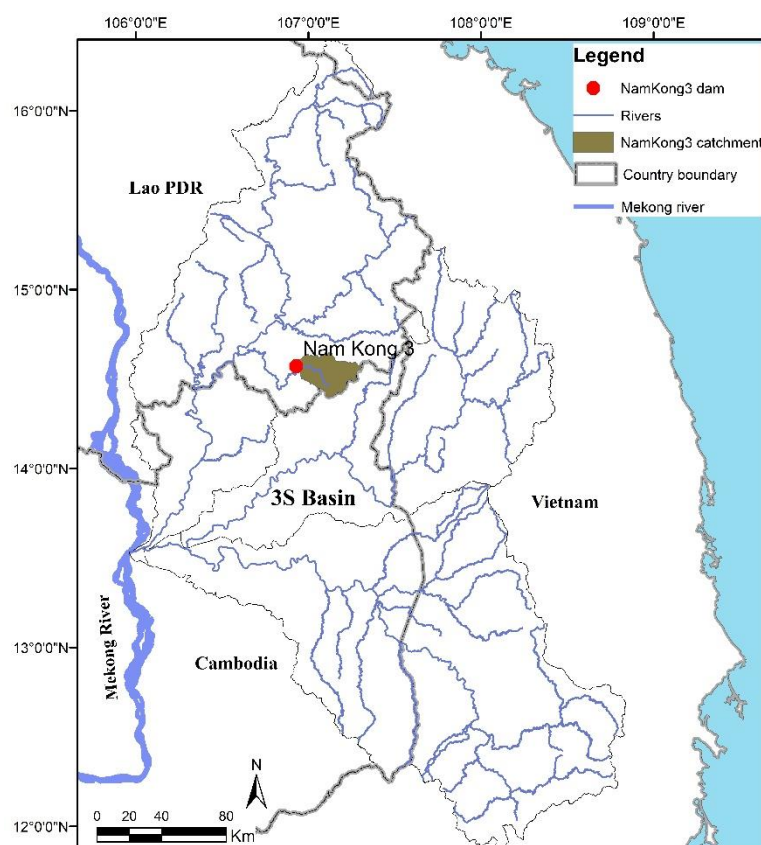


Figure A2-6: Location map and catchment of Nam Kong 3

Table A2-2: Nam Kong 3 hydropower plant characteristics.

| Characteristics | Unit | Quantity |
|-------------------------|-------------------|----------|
| Design Flow | m ³ /s | 100 |
| Minimum Operating Level | m.a.s.l | 520.0 |
| Full Supply Level | m.a.s.l | 540.0 |
| Installed Capacity | MW | 28 |
| Tailwater/turbine level | m.a.s.l | 455.0 |
| Plant Efficiency | - | 0.87 |
| Headloss coefficient | - | 0.05 |

Table A2-3: Flushing specification inputs for Nam Kong 3

| Flushing specification | Value |
|---|--------------|
| Start date | 2021/06/01 |
| Duration (days) | 6 |
| Max. Flushing Water Level (m.a.s.l.) | 493 |
| Min. Flushing discharge (m ³ /s) | 42 |
| Max. drawdown rate (m) | 2 |
| Reservoir bottom width (m) | 61 |
| Reservoir side slope (m/m) | 1 |
| Reservoir bed level (m.a.s.l.) | 488 |

Table A2-4: Sluicing specification inputs for Nam Kong 3

| Sluicing specification | Value |
|-------------------------------|--------------|
| Start date | 2021/07/01 |
| Duration (days) | 60 |
| Target water level (m.a.s.l.) | 520 |
| Max. drawdown rate (m) | 2 |
| Max. refill rate (m) | 0.5 |

APPENDIX - 3

Table A3-1: Features of considered hydropower reservoirs for simulation in the 3S basin.

| Reservoirs | Latitude | Longitude | Design Discharge (m ³ /s) | Full Supply Level (m.a.s.l.) | Min. Operating Level (m.a.s.l.) | Installed Capacity (MW) | Tailwater Level (m.a.s.l.) | Volume at FSL (m ³) | Status | Remarks |
|-----------------|----------|-----------|--------------------------------------|------------------------------|---------------------------------|-------------------------|----------------------------|---------------------------------|--------------------|--------------|
| Xe Kong 5 | 15.98 | 106.93 | 146 | 470 | 500 | 248 | 306.5 | 3.30E+09 | Proposed | |
| Dak E Mule | 15.56 | 107.07 | 27.4 | 756 | 780 | 105 | 341.2 | 2.43E+08 | Proposed | |
| Xekaman 3 | 15.44 | 107.33 | 62.5 | 925 | 960 | 250 | 433.9 | 1.64E+08 | Existing | |
| Xe Kaman 2B | 15.28 | 107.45 | 90 | 340 | 370 | 100 | 286.2 | 2.68E+08 | Proposed | |
| Xe Kaman 4B | 15.35 | 107.53 | 18.4 | 850 | 865 | 74 | 400.9 | 3.42E+07 | Proposed | |
| Houay Lamphan | 15.36 | 106.50 | 18.5 | 795 | 820 | 84.8 | 280 | 1.48E+08 | Under Construction | |
| Xe Kaman 4A | 15.23 | 107.52 | 26 | 840 | 860 | 96 | 431.4 | 1.88E+07 | Proposed | |
| Xe Katam | 15.12 | 106.63 | 16 | 890 | 910 | 60.8 | 455 | 1.19E+08 | Existing | |
| Houayho | 14.89 | 106.66 | 23 | 860 | 883 | 150 | 101 | 8.09E+08 | Existing | |
| Xepian-Xenamnoy | 15.03 | 106.60 | 70 | 760 | 786.5 | 390 | 90 | 1.13E+09 | Under Construction | |
| Plei Krong | 14.41 | 107.86 | 367.6 | 537 | 570 | 100 | 534 | 1.07E+09 | Existing | |
| Xe Xou | 14.71 | 107.17 | 131.3 | 160 | 180 | 63.4 | 123.2 | 2.42E+09 | Proposed | |
| Upper Kontum | 14.71 | 108.23 | 30.5 | 1146 | 1170 | 250 | 260.9 | 1.53E+08 | Under Construction | |
| NamKong 3 | 14.56 | 106.91 | 37.6 | 520 | 540 | 28 | 455 | 3.11E+08 | Proposed | |
| Nam Kong 1 | 14.55 | 106.74 | 44.5 | 287 | 320 | 75 | 132 | 5.98E+08 | Proposed | |
| Prek Liang 2 | 14.29 | 107.26 | 17.7 | 496 | 515 | 25 | 342 | 7.38E+08 | Proposed | |
| Prek Liang 1 | 14.22 | 107.25 | 27.2 | 310 | 330 | 35 | 172 | 7.10E+08 | Proposed | |
| O Chum 2 | 13.79 | 106.97 | 3.8 | 254 | 251 | 1 | 219 | 1.00E+05 | Existing | not modelled |
| Duc Xuyen | 12.14 | 108.09 | 81 | 551 | 560 | 49 | 490 | 1.09E+09 | Proposed | |
| Buon Tua Srah | 12.28 | 108.04 | 204.9 | 465 | 487.5 | 86 | 436 | 8.79E+08 | Existing | |
| Xe Nam Noy 5 | 15.17 | 106.66 | 3.9 | 780 | 800 | 20 | 222.7 | 9.80E+06 | Proposed | |
| Xe Kaman 2A | 15.22 | 107.44 | 155 | 275 | 280 | 64 | 231 | 8.80E+06 | Proposed | |
| Xekaman 1 | 14.97 | 107.15 | 336.6 | 218 | 230 | 290 | 123.4 | 4.62E+09 | Under Construction | |
| Xekaman-Sanxay | 14.89 | 107.12 | 378 | 122 | 123 | 32 | 111.2 | 1.25E+07 | Under Construction | |

| | | | | | | | | | | |
|-----------------------------|-------|--------|--------|-------|-------|-------|-------|----------|----------|---------------|
| Xekong 4 | 15.52 | 106.78 | 240 | 270 | 290 | 300 | 145 | 6.71E+09 | Proposed | |
| Xe Kong 3up | 15.38 | 106.78 | 460 | 155 | 160 | 144.6 | 121.3 | 2.79E+08 | Proposed | |
| Yali | 14.22 | 107.79 | 424 | 280 | 515 | 720 | 306.9 | 1.04E+09 | Existing | |
| Se San 3 | 14.22 | 107.70 | 486 | 303.2 | 304.5 | 260 | 239 | 8.67E+07 | Existing | |
| Se San 3A | 14.11 | 107.65 | 500 | 238.5 | 239 | 96 | 207.5 | 8.06E+07 | Existing | |
| Se San 4 | 13.97 | 107.50 | 719 | 210 | 215 | 360 | 150 | 8.93E+08 | Existing | |
| Se San 4A | 13.94 | 107.47 | - | 150 | 155.2 | - | - | 1.13E+07 | Existing | no hydropower |
| Buon Kuop | 12.53 | 107.93 | 316 | 409 | 412 | 280 | 313.5 | 3.65E+07 | Existing | |
| Dray Hlinh 2 | 12.68 | 107.91 | 101 | 299 | 302 | 16 | 278.5 | 2.90E+06 | Existing | |
| Sre Pok 3 | 12.76 | 107.86 | 412.8 | 268 | 272 | 220 | 207 | 2.43E+08 | Existing | |
| Sre Pok 4 | 12.87 | 107.78 | 468.9 | 204 | 207 | 70 | 184.9 | 1.14E+08 | Existing | |
| Lower Sre Pok 4 | 13.05 | 107.45 | 327 | 185 | 190 | 143 | 137.8 | 7.47E+09 | Proposed | |
| Lower Se San 3 | 14.03 | 106.93 | 500 | 147 | 149.4 | 243 | 83.5 | 2.44E+10 | Proposed | |
| Lower Sre Pok 3 | 13.39 | 107.05 | 775 | 118 | 125 | 204 | 88.5 | 8.20E+09 | Proposed | |
| Lower Se San2+ Lower Srepok | 13.57 | 106.20 | 2119.2 | 74 | 75 | 400 | 44.8 | 2.48E+09 | Existing | |

Note: highlighted
colour

| | |
|------------------------|--|
| Reservoirs in Laos | |
| Reservoirs in Cambodia | |
| Reservoirs in Viet Nam | |

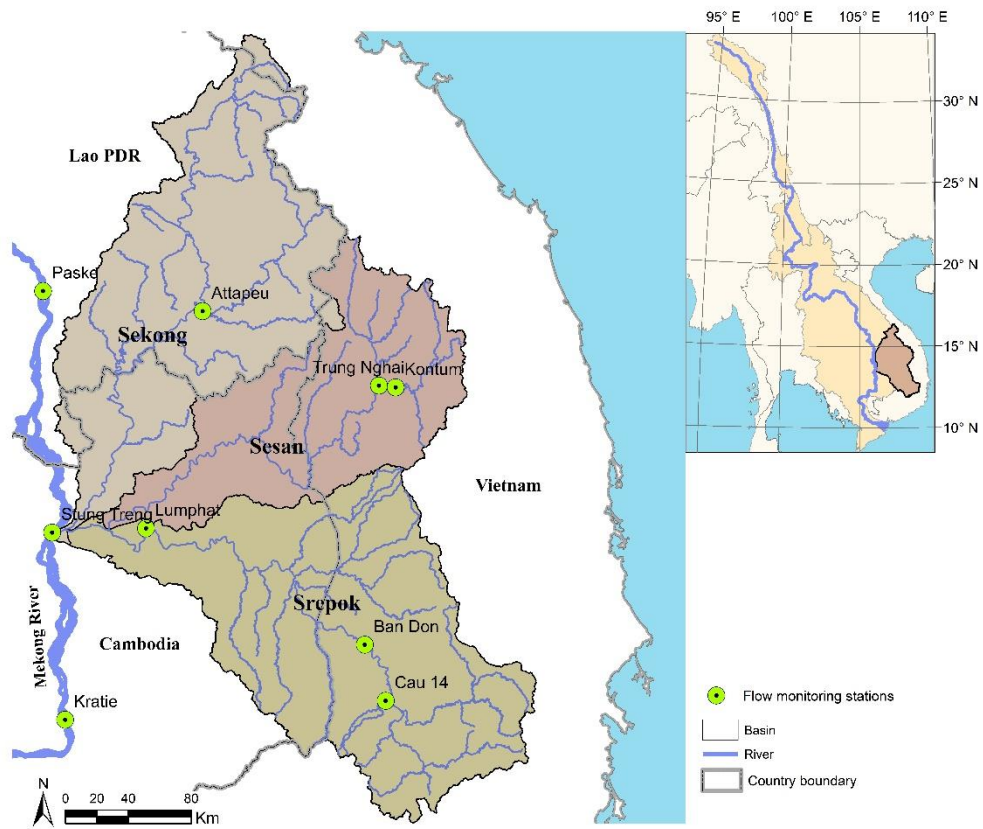


Figure A3-1: Location map of the study area and flow monitoring stations.

Table A3-2: Calibrated parameters and their initial range for the 3S SWAT model adopted from (Shrestha et al. 2016).

| Parameter Name | Description and Units | Initial Range | | Fitted Parameter Value | | | | | |
|-----------------------------|--|---------------|---------|------------------------|-------------|---------|---------|---------|---------|
| | | Minimum | Maximum | Attapeu | Trung Nghai | Kontum | Cau 14 | Ban Don | Lumphat |
| v__GW_DELAY.gw ^a | Groundwater delay time (days) | 0 | 100 | 0.251 | 60.197 | 87.007 | 40.842 | 6.500 | 4.505 |
| v__ALPHA_BF.gw | Baseflow alpha factor (1/days) | 0 | 1 | 0.421 | 0.965 | 0.609 | 0.511 | 0.899 | 0.388 |
| v__GWQMN.gwb | Threshold depth of water in the shallow aquifer required to return flow to occur (mm) | 0 | 1000 | 804.170 | 273.934 | 733.549 | 602.734 | 579.000 | 726.015 |
| v__GW_REVAP.gw | Groundwater "revap" coefficient (-) | 0.02 | 0.2 | 0.180 | 0.148 | 0.188 | 0.190 | 0.196 | 0.199 |
| v__REVAPMN.gw | Threshold depth of water in the shallow aquifer for "revap" or percolation to the deep aquifer to occur (mm) | 0 | 2000 | 382.083 | 1107.332 | 424.352 | 402.142 | 326.000 | 540.646 |
| v__RCHRG_DP.gw | Deep aquifer percolation fraction (-) | 0 | 0.5 | 0.460 | 0.206 | 0.310 | 0.163 | 0.451 | 0.277 |
| v__LAT_TTIME.hru | Lateral flow travel time (days) | 0 | 180 | 157.255 | 105.691 | 12.924 | 145.942 | 122.580 | 103.472 |
| v__SLSOIL.hru ^b | Slope length for lateral subsurface flow (m) | 0 | 100 | 91.697 | 49.821 | 23.955 | 1.840 | 30.100 | 83.285 |
| v__CANMX.hru | Maximum canopy storage (mm) | 0 | 20 | 15.857 | 0.092 | 12.565 | 13.797 | 15.500 | 17.196 |
| v__ESCO.hru | Soil evaporation compensation factor (-) | 0 | 1 | 0.070 | 0.712 | 0.949 | 0.460 | 0.541 | 0.344 |
| v__CH_N2.rte | Mannings "n" value for the main channel | 0.014 | 0.15 | 0.133 | 0.102 | 0.064 | 0.123 | 0.124 | 0.129 |
| v__CH_K2.rte | Effective hydraulic conductivity in main channel alluvium (mm/hr) | 0 | 25 | 2.775 | 19.565 | 11.268 | 3.507 | 12.425 | 5.184 |
| v__ALPHA_BNK.rte | Baseflow alpha factor for bank storage (days) | 0 | 1 | 0.090 | 0.618 | 0.762 | 0.859 | 0.593 | 0.176 |
| v__CH_N1.sub | Maning's "n" value for the tributary channels | 0.014 | 0.15 | 0.033 | 0.082 | 0.059 | 0.137 | 0.121 | 0.016 |
| v__CH_K1.sub | Effective hydraulic conductivity in triutary channel alluvium (mm/hr) | 0 | 25 | 4.657 | 17.025 | 23.471 | 3.519 | 11.775 | 19.111 |
| r__SOL_AWC(1).sol | Avialble water capacity in the soil layer (mm/mm soil) | -0.3 | 0.3 | -0.017 | 0.138 | -0.061 | 0.010 | 0.208 | -0.105 |
| r__CN2.mgt ^c | Initial SCS runoff curve number for mositure condition II (-) | -0.15 | 0.15 | 0.134 | -0.054 | -0.078 | -0.010 | 0.029 | 0.027 |

Note: ^a The extension (e.g., .gw) refers to the SWAT input file where the parameter occurs; ^b The qualifier (v) refers to the substitution of a parameter by a value from the given range; ^c The qualifier (r) refers to relative change in the parameter where the value from the SWAT database is multiplied by 1 plus a factor in the given range.

Table A3-3: Calibrated parameters and their initial range for sediment loads

| Parameter Name | Description | Initial Range | | Fitted Parameter Value | SWAT Input Files |
|----------------|--|---------------|---------|------------------------------|------------------------|
| | | Minimum | Maximum | | |
| SPCON | Linear parameter for calculating the maximum amount of sediment that can be re-entrained during channel sediment routing | 0.001 | 0.01 | 0.0015 | .bsn |
| SPEXP | Exponent parameter for calculating sediment re-entrained in channel sediment routing | 1 | 1.5 | 1.1 | |
| PRF | Peak rate adjustment factor for sediment routing in the main channel | 0 | 2 | 0.6 | .rte |
| CH_COV1 | Channel erodibility factor | -0.05 | 0.6 | 0.761 | |
| CH_COV2 | Channel cover factor | -0.001 | 1 | 0.015 | |
| CH_ERODMO | Monthly channel erodability factor | 0 | 1 | 0.48 | |
| USLE_K_B_CLAY | USLE equation soil erodibility (K) factor | 0 | 0.65 | 0.65 | .sol |
| USLE_K_C_CLAY | | | | | |
| USLE_K_D_CLAY | | | | | |
| USLE_K_B_LOAMY | | | | | |
| USLE_K_D_LOAMY | | | | | |
| USLE_C_DECD | Min. value of USLE_C factor applicable to the land cover/plant. | 0.001 | 0.02 | 0.001 | plant.dat |
| USLE_C_UDFR | | | | | |
| USLE_C_DTFR | | | | | |
| USLE_C_PRNL | | | | | |

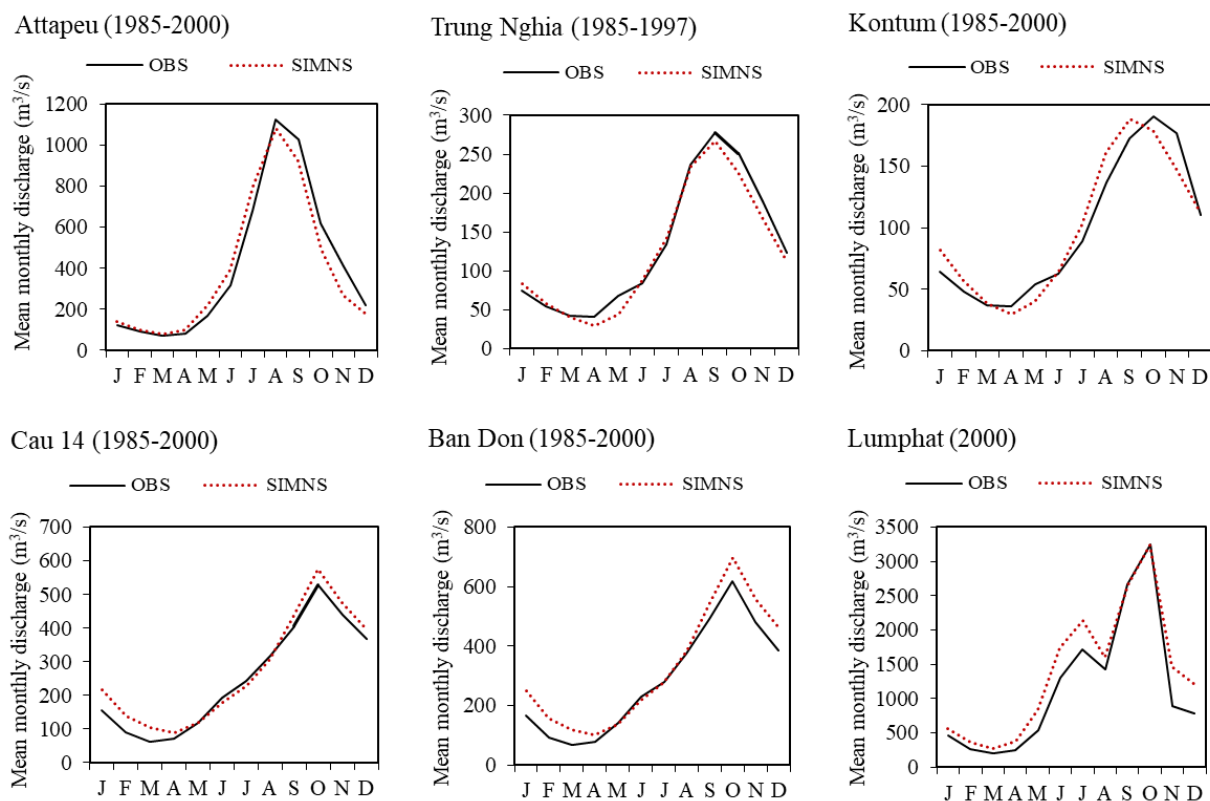


Figure A3-2: Observed (OBS) and simulated (SIMNS) flow for six gauging stations within the 3S basin for the calibration period (adopted from (Shrestha et al. 2016)).

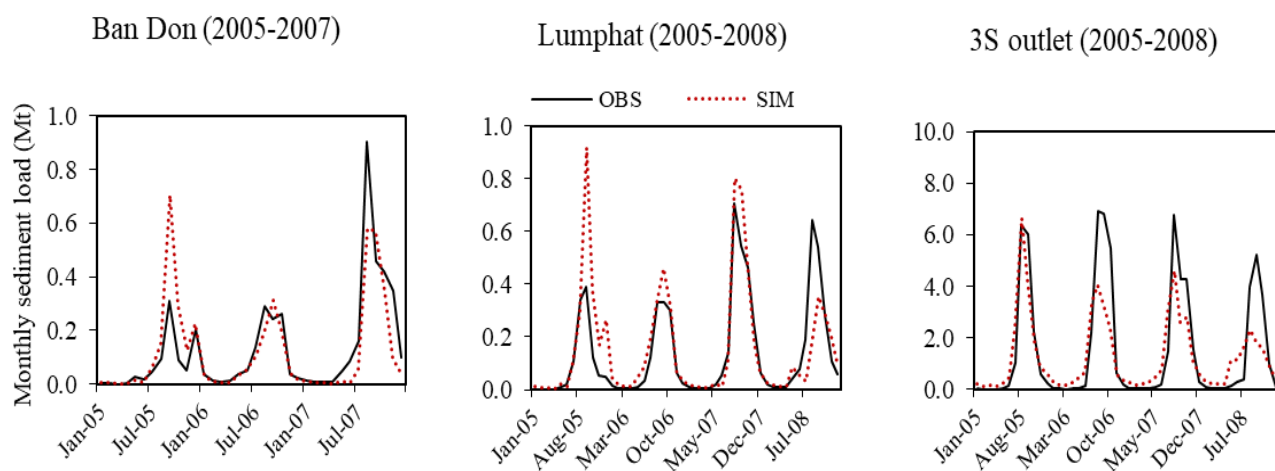


Figure A3-3: Observed (OBS) and simulated (SIM) sediment loads for two gauging stations and 3S outlet for the calibration period (adopted from (Shrestha et al. 2016)).

Table A3-4: SWAT model performance for daily flow in the calibration and validation periods for the 3S basin (adopted from (Shrestha et al. 2016)).

| Stations | Calibration | | | | Validation | | | |
|-------------|-------------|-----------------------|----------------|---------|------------|-----------------------|----------------|---------|
| | Period | Performance Indicator | | | Period | Performance Indicator | | |
| | | NSE | R ² | PBIAS | | NSE | R ² | PBIAS |
| Attapeu | 1985–2000 | 0.57 | 0.57 | 3.01% | 2001–2005 | 0.68 | 0.69 | 6.32% |
| Trung Nghai | 1985–1997 | 0.51 | 0.51 | 4.93% | - | - | - | - |
| Kontum | 1985–2000 | 0.42 | 0.44 | -1.96% | 2001–2006 | 0.48 | 0.54 | -20.27% |
| Cau 14 | 1985–2000 | 0.67 | 0.68 | -9.14% | - | - | - | - |
| Ban Don | 1985–2000 | 0.66 | 0.70 | -14.51% | 2001–2007 | 0.53 | 0.66 | -26.28% |
| Lumphat | 2000 | 0.73 | 0.76 | -19.81% | 2001–2007 | 0.58 | 0.7 | -38.89% |
| Stung Treng | 1985–2000 | 0.96 | 0.97 | -4.69% | 2001–2007 | 0.97 | 0.97 | -5.33% |
| Kratie | 1985–2000 | 0.96 | 0.97 | -9.46% | 2001–2007 | 0.97 | 0.98 | -8.70% |

Table A3-5: SWAT model performance for monthly sediment loads in the calibration periods for the 3S basin

| Stations | Calibration | | | |
|-----------|-------------|-----------------------|----------------|---------|
| | Period | Performance Indicator | | |
| | | NSE | R ² | PBIAS |
| Ban Don | 2005–2007 | 0.64 | 0.66 | 4.94% |
| Lumphat | 2005–2008 | 0.54 | 0.66 | -15.41% |
| 3S outlet | 2005–2008 | 0.71 | 0.76 | 14.90% |

Table A3-6: Climate change data used for the study.

| GCM (Model ID) | Emission scenario | Spatial resolution (longitude x latitude) |
|--|---------------------------|---|
| Goddard Institute for Space Studies Model E2, coupled with the Russell ocean model, with carbon cycle (GISS-E2-R-CC) | RCP2.6, RCP6.0, RCP8.5 | 2.5° × 2° |
| Institute Pierre-Simon Laplace Coupled Model, version 5A, coupled with NEMO, mid resolution (IPSL-CM5A-MR) | RCP2.6, RCP6.0, RCP8.5 | 2.5° × 1.27° |
| Geophysical Fluid Dynamics Laboratory Climate model version 3 (GFDL-CM3) | RCP2.6, RCP6.0, RCP8.5 | 2.5° × 2° |

Table A3-7: Annual average energy (GWh) production for each of hydropower plants under different scenarios.

| Reservoir | BL-R-SV | BL-R-FSL | GISS-H-R-SV | IPSL-H-R-SV | GFDL-H-R-SV |
|-----------------|---------|----------|-------------|-------------|-------------|
| Xe Kong 5 | 1408 | 1234 | 1496 | 1448 | 1464 |
| Dak E Mule | 508 | 443 | 513 | 502 | 512 |
| Xekaman 3 | 884 | 855 | 992 | 989 | 959 |
| Xe Kaman 2B | 262 | 282 | 314 | 293 | 285 |
| Xe Kaman 4B | 372 | 361 | 383 | 346 | 383 |
| Houay Lamphan | 389 | 310 | 389 | 400 | 416 |
| Xe Kaman 4A | 395 | 388 | 410 | 395 | 415 |
| Xe Katam | 458 | 380 | 448 | 438 | 463 |
| Houayho | 545 | 599 | 510 | 506 | 569 |
| Xepian-Xenamnoy | 1731 | 1546 | 1629 | 1595 | 1785 |
| Plei Krong | 269 | 340 | 314 | 297 | 282 |
| Xe Xou | 322 | 288 | 344 | 338 | 347 |
| Upper Kontum | 722 | 711 | 919 | 807 | 756 |
| NamKong 3 | 151 | 130 | 146 | 149 | 155 |
| Nam Kong 1 | 574 | 411 | 556 | 565 | 581 |
| Prek Liang 2 | 195 | 155 | 193 | 194 | 199 |
| Prek Liang 1 | 248 | 197 | 243 | 246 | 254 |
| Duc Xuyen | 201 | 207 | 143 | 203 | 209 |
| Buon Tua Srah | 350 | 389 | 267 | 351 | 359 |
| Xe Nam Noy 5 | 175 | 175 | 175 | 175 | 175 |
| Xe Kaman 2A | 295 | 277 | 308 | 295 | 309 |
| Xekaman 1 | 1284 | 1156 | 1393 | 1317 | 1355 |
| Xekaman-Sanxay | 173 | 145 | 179 | 169 | 179 |
| Xekong 4 | 2531 | 2027 | 2536 | 2526 | 2540 |
| Xe Kong 3up | 931 | 830 | 930 | 916 | 942 |
| Yali | 3883 | 3550 | 4007 | 4009 | 3971 |
| Se San 3 | 1423 | 1260 | 1463 | 1470 | 1457 |
| Se San 3A | 611 | 531 | 617 | 616 | 621 |
| Se San 4 | 1623 | 1515 | 1662 | 1704 | 1674 |
| Buon Kuop | 1629 | 1547 | 1332 | 1569 | 1642 |
| Dray Hlinh 2 | 140 | 138 | 137 | 139 | 140 |
| Sre Pok 3 | 1217 | 1173 | 984 | 1176 | 1228 |
| Sre Pok 4 | 446 | 420 | 374 | 429 | 448 |
| Lower Sre Pok 4 | 1122 | 932 | 1012 | 1104 | 1126 |
| Lower Se San 3 | 1986 | 1585 | 1952 | 1973 | 2003 |
| Lower Sre Pok 3 | 1571 | 1235 | 1434 | 1549 | 1582 |
| Lower Se San2+ | 3153 | 2665 | 2923 | 3110 | 3175 |

Table A3-8: Annual average energy production for 3S basin and countrywide for different scenarios.

| Scenario | Annual energy (GWh) | | | | | | | |
|------------|---------------------|---------|---------|----------|----------|---------|---------|----------|
| | SV-Rule | | | | FSL-Rule | | | |
| | 3S Basin | Lao PDR | Vietnam | Cambodia | 3S Basin | Lao PDR | Vietnam | Cambodia |
| BL-R | 34,176 | 13,389 | 12,514 | 8274 | 30,388 | 11,828 | 11,773 | 6763 |
| GISS-L-R | 34,146 | 13,444 | 12,510 | 8192 | 30,297 | 11,841 | 11,750 | 6681 |
| GISS-M-R | 34,003 | 13,528 | 12,423 | 8051 | 29,992 | 11,838 | 11,625 | 6503 |
| GISS-H-R | 33,625 | 13,649 | 12,219 | 7758 | 29,377 | 11,826 | 11,346 | 6181 |
| IPSL-L-R | 34,124 | 13,387 | 12,493 | 8244 | 30,287 | 11,800 | 11,735 | 6727 |
| IPSL-M-R | 34,287 | 13,378 | 12,694 | 8215 | 30,307 | 11,724 | 11,881 | 6677 |
| IPSL-H-R | 34,309 | 13,362 | 12,771 | 8176 | 30,128 | 11,617 | 11,883 | 6603 |
| GFDL-L-L-R | 34,321 | 13,457 | 12,616 | 8248 | 30,510 | 11,877 | 11,855 | 6753 |
| GFDL-M-R | 34,616 | 13,580 | 12,721 | 8316 | 30,757 | 11,877 | 11,855 | 6753 |
| GFDL-H-R | 34,959 | 13,834 | 12,786 | 8338 | 31,038 | 12,151 | 11,997 | 6863 |

Table A3-9: Overall HA and HA for each IHA statistics group due to operation of hydropower reservoirs under seasonal variation rule curve under BL-R scenario at downstream of each reservoir and country boundaries and HA per gigawatt-hour of hydropower reservoirs.

| Reservoir | Overall HA | Group1 HA | Group2 HA | Group3 HA | Group4 HA | Group5 HA | HA/GWh |
|------------------|-------------------|------------------|------------------|------------------|------------------|------------------|---------------|
| Houayho | 308 | 639 | 66 | 43 | 341 | 62 | 0.56 |
| Xepian-Xenamnoy | 290 | 648 | 60 | 55 | 220 | 69 | 0.17 |
| Nam Kong 1 | 256 | 256 | 455 | 33 | 37 | 47 | 0.45 |
| Houay Lamphan | 240 | 445 | 160 | 87 | 135 | 56 | 0.62 |
| Xekong 4 | 215 | 236 | 335 | 4 | 90 | 36 | 0.08 |
| Xe Kong 3up | 205 | 227 | 316 | 2 | 103 | 17 | 0.22 |
| Dak E Mule | 195 | 334 | 159 | 72 | 111 | 29 | 0.38 |
| Xe Xou | 174 | 334 | 118 | 69 | 60 | 57 | 0.54 |
| Xe Katam | 163 | 171 | 236 | 153 | 70 | 32 | 0.36 |
| Xe Nam Noy 5 | 153 | 215 | 175 | 121 | 55 | 34 | 0.87 |
| Upper Kontum | 148 | 89 | 39 | 18 | 588 | 25 | 0.20 |
| Xekaman-Sanxay | 142 | 222 | 155 | 46 | 33 | 53 | 0.82 |
| Xe Kong 5 | 136 | 176 | 165 | 40 | 62 | 73 | 0.10 |
| Xekaman 1 | 133 | 235 | 121 | 45 | 29 | 41 | 0.10 |
| NamKong 3 | 128 | 288 | 48 | 13 | 40 | 58 | 0.85 |
| Xekaman 3 | 97 | 98 | 156 | 16 | 39 | 34 | 0.11 |
| Prek Liang 1 | 82 | 85 | 129 | 11 | 34 | 20 | 0.33 |
| Xe Kaman 2B | 79 | 137 | 62 | 23 | 42 | 33 | 0.30 |
| Lower Se San 3 | 77 | 74 | 123 | 16 | 25 | 57 | 0.04 |
| Duc Xuyen | 72 | 83 | 37 | 25 | 164 | 18 | 0.36 |
| Lower Sre Pok 3 | 72 | 72 | 92 | 22 | 49 | 69 | 0.05 |
| Lower Se San2+ | 70 | 65 | 110 | 19 | 22 | 57 | 0.02 |
| Prek Liang 2 | 67 | 57 | 114 | 5 | 34 | 26 | 0.34 |
| Se San 3A | 56 | 55 | 37 | 11 | 129 | 26 | 0.09 |
| Xe Kaman 2A | 54 | 69 | 66 | 19 | 22 | 38 | 0.18 |
| Se San 3 | 49 | 56 | 33 | 11 | 87 | 31 | 0.03 |
| Buon Tua Srah | 48 | 63 | 23 | 31 | 93 | 7 | 0.14 |
| Plei Krong | 47 | 70 | 45 | 15 | 35 | 13 | 0.18 |
| Yali | 44 | 57 | 29 | 9 | 68 | 33 | 0.01 |
| Lower Sre Pok 4 | 44 | 42 | 62 | 21 | 12 | 56 | 0.04 |
| Se San 4A | 41 | 54 | 46 | 10 | 21 | 31 | - |
| Se San 4 | 41 | 54 | 45 | 10 | 21 | 32 | 0.03 |
| Xe Kaman 4B | 30 | 24 | 50 | 3 | 10 | 30 | 0.08 |
| Buon Kuop | 27 | 26 | 19 | 22 | 55 | 6 | 0.02 |
| Sre Pok 4 | 24 | 23 | 22 | 18 | 38 | 14 | 0.05 |
| Sre Pok 3 | 24 | 25 | 21 | 18 | 32 | 14 | 0.02 |
| Dray Hlinh 2 | 23 | 25 | 21 | 19 | 29 | 11 | 0.16 |
| Xe Kaman 4A | 16 | 23 | 14 | 7 | 12 | 14 | 0.04 |
| Lao-Cam | 170 | 166 | 295 | 6 | 54 | 30 | 0.01 |
| Viet-Cam1 | 41 | 54 | 46 | 10 | 21 | 31 | 0.00 |
| Viet-Cam2 | 23 | 21 | 23 | 12 | 34 | 13 | 0.00 |

Table A3-10: Overall HA and HA for each IHA statistics group due to operation of hydropower reservoirs under full supply rule curve under BL-R scenario at downstream of each reservoir and country boundaries and HA per gigawatt-hour of hydropower reservoirs.

| Reservoir | Overall HA | Group1 HA | Group2 HA | Group3 HA | Group4 HA | Group5 HA | HA/GWh |
|---------------------|---------------|--------------|--------------|--------------|--------------|--------------|--------|
| Houayho | 109 | 149 | 56 | 43 | 158 | 104 | 0.18 |
| Xepian- Xenamnoy | 88 | 142 | 49 | 18 | 76 | 96 | 0.06 |
| Nam Kong 1 | 22 | 7 | 22 | 1 | 52 | 35 | 0.05 |
| Houay Lamphan | 46 | 68 | 29 | 11 | 47 | 44 | 0.15 |
| Xekong 4 | 15 | 10 | 19 | 3 | 26 | 9 | 0.01 |
| Xe Kong 3up | 15 | 10 | 19 | 3 | 26 | 9 | 0.02 |
| Dak E Mule | 114 | 176 | 105 | 14 | 59 | 82 | 0.26 |
| Xe Xou | 55 | 9 | 23 | 5 | 227 | 63 | 0.19 |
| Xe Katam | 56 | 85 | 55 | 13 | 35 | 19 | 0.15 |
| Xe Nam Noy 5 | 63 | 106 | 34 | 28 | 64 | 32 | 0.36 |
| Upper Kontum | 4 | 2 | 2 | 1 | 4 | 18 | 0.01 |
| Xekaman-Sanxay | 25 | 8 | 24 | 1 | 62 | 42 | 0.17 |
| Xe Kong 5 | 52 | 71 | 44 | 13 | 55 | 30 | 0.04 |
| Xekaman 1 | 27 | 8 | 25 | 6 | 69 | 42 | 0.02 |
| NamKong 3 | 38 | 13 | 40 | 16 | 92 | 40 | 0.29 |
| Xekaman 3 | 13 | 2 | 7 | 1 | 33 | 45 | 0.01 |
| Prek Liang 1 | 4 | 1 | 1 | 1 | 12 | 14 | 0.02 |
| Xe Kaman 2B | 9 | 2 | 6 | 1 | 18 | 32 | 0.03 |
| Lower Se San 3 | 14 | 10 | 18 | 4 | 21 | 12 | 0.01 |
| Duc Xuyen | 82 | 9 | 17 | 6 | 411 | 33 | 0.40 |
| Lower Sre Pok 3 | 15 | 10 | 19 | 3 | 26 | 9 | 0.01 |
| Lower Se San2+ | 14 | 8 | 15 | 4 | 29 | 9 | 0.01 |
| Prek Liang 2 | 1 | 0 | 0 | 1 | 2 | 9 | 0.01 |
| Se San 3A | 12 | 2 | 3 | 3 | 55 | 7 | 0.02 |
| Xe Kaman 2A | 6 | 2 | 4 | 3 | 11 | 26 | 0.02 |
| Se San 3 | 9 | 2 | 2 | 3 | 38 | 7 | 0.01 |
| Buon Tua Srah | 39 | 4 | 6 | 2 | 181 | 48 | 0.10 |
| Plei Krong | 27 | 2 | 2 | 1 | 127 | 42 | 0.08 |
| Yali | 15 | 10 | 19 | 3 | 26 | 9 | 0.00 |
| Lower Sre Pok 4 | 15 | 10 | 19 | 3 | 26 | 9 | 0.02 |
| Se San 4A | 4 | 3 | 3 | 3 | 2 | 12 | - |
| Se San 4 | 4 | 3 | 3 | 2 | 2 | 11 | 0.00 |
| Xe Kaman 4B | 3 | 0 | 1 | 0 | 2 | 29 | 0.01 |
| Buon Kuop | 15 | 10 | 19 | 3 | 26 | 9 | 0.01 |
| Sre Pok 4 | 15 | 10 | 19 | 3 | 26 | 9 | 0.04 |
| Sre Pok 3 | 15 | 10 | 19 | 3 | 26 | 9 | 0.01 |
| Dray Hlinh 2 | 15 | 10 | 19 | 3 | 26 | 9 | 0.11 |
| Xe Kaman 4A | 1 | 0 | 0 | 0 | 2 | 8 | 0.00 |
| Lao-Cam | 55 | 73 | 42 | 10 | 71 | 30 | 0.00 |
| Viet-Cam1 | 4 | 3 | 3 | 3 | 2 | 12 | 0.00 |
| Viet-Cam2 | 17 | 1 | 2 | 2 | 91 | 5 | 0.00 |

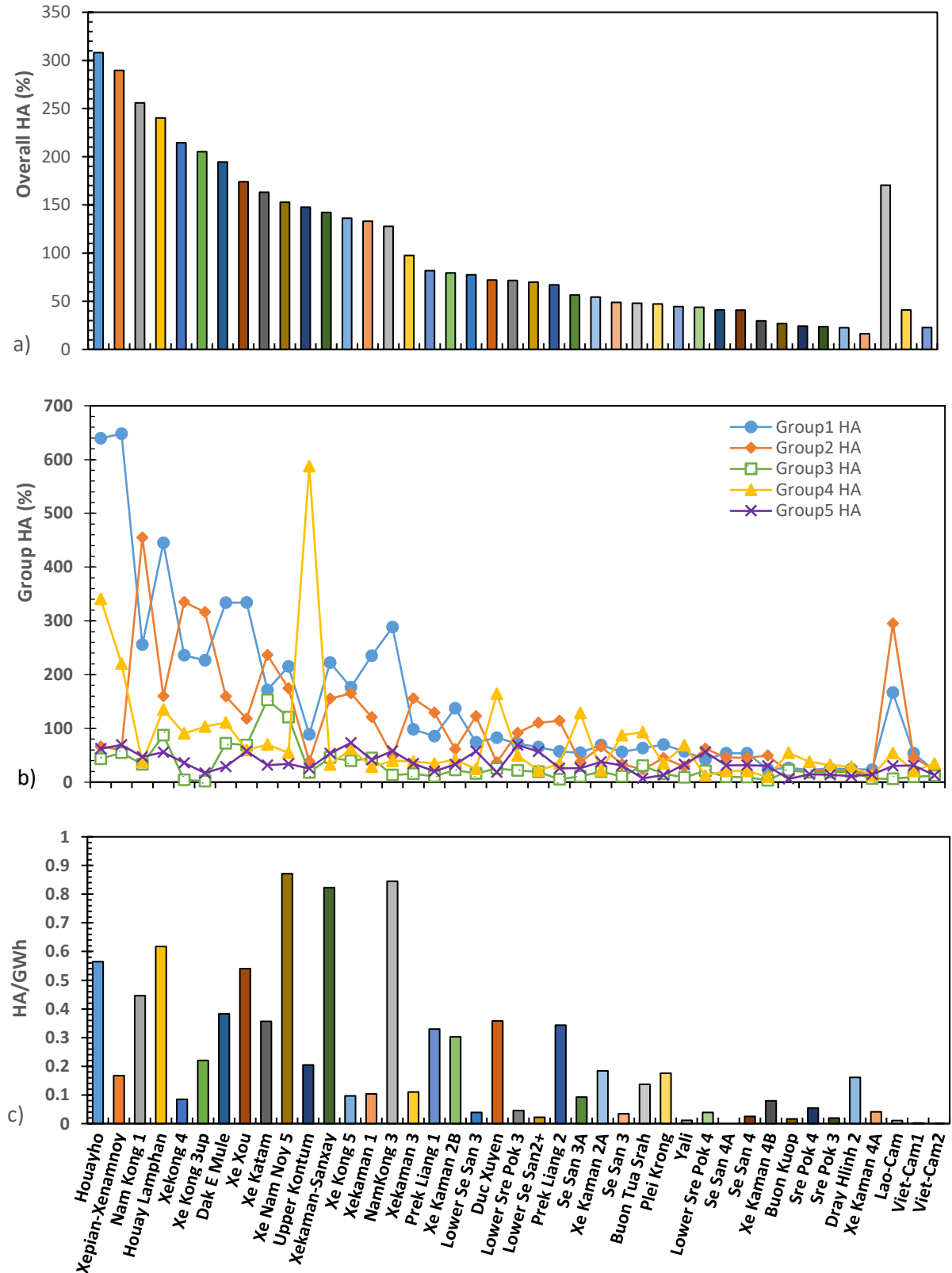


Figure A3-4: (a) Overall HA and (b) HA for each IHA statistics group due to operation of hydropower reservoirs under seasonal variation rule curve under BL-R scenario at downstream of each reservoir and country boundaries and (c) HA per gigawatt-hour of hydropower reservoirs.

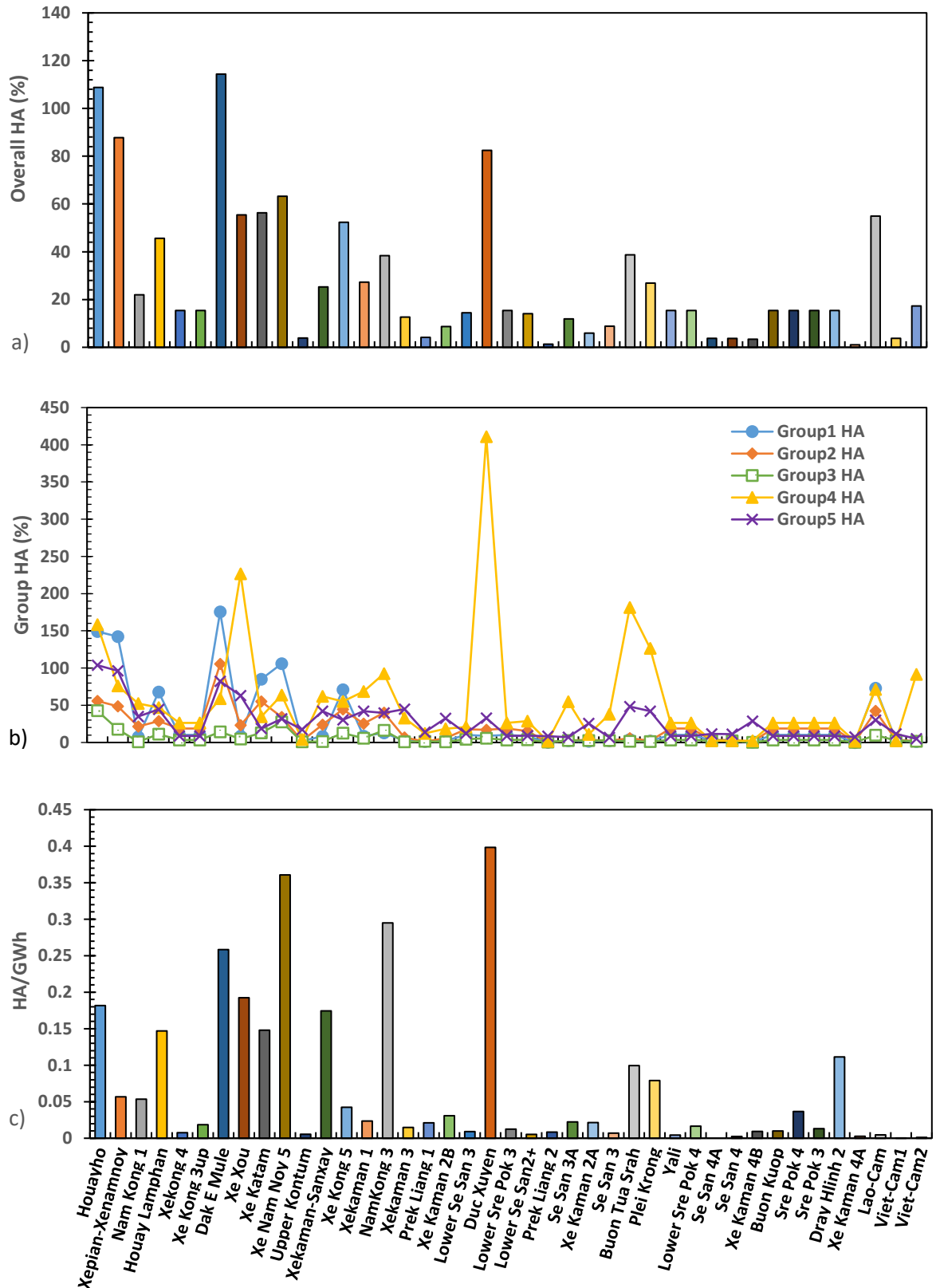


Figure A3-5: (a) Overall HA and (b) HA for each IHA statistics group due to operation of hydropower reservoirs under full supply rule curve under BL-R scenario at downstream of each reservoir and country boundaries and (c) HA per gigawatt-hour of hydropower reservoirs.

References

Shrestha, B., Cochrane, T. A., Caruso, B. S., Arias, M. E., and Piman, T. (2016). "Uncertainty in flow and sediment projections due to future climate scenarios for the 3S Rivers in the Mekong Basin." *Journal of Hydrology*, 540, 1088-1104.

APPENDIX - 4

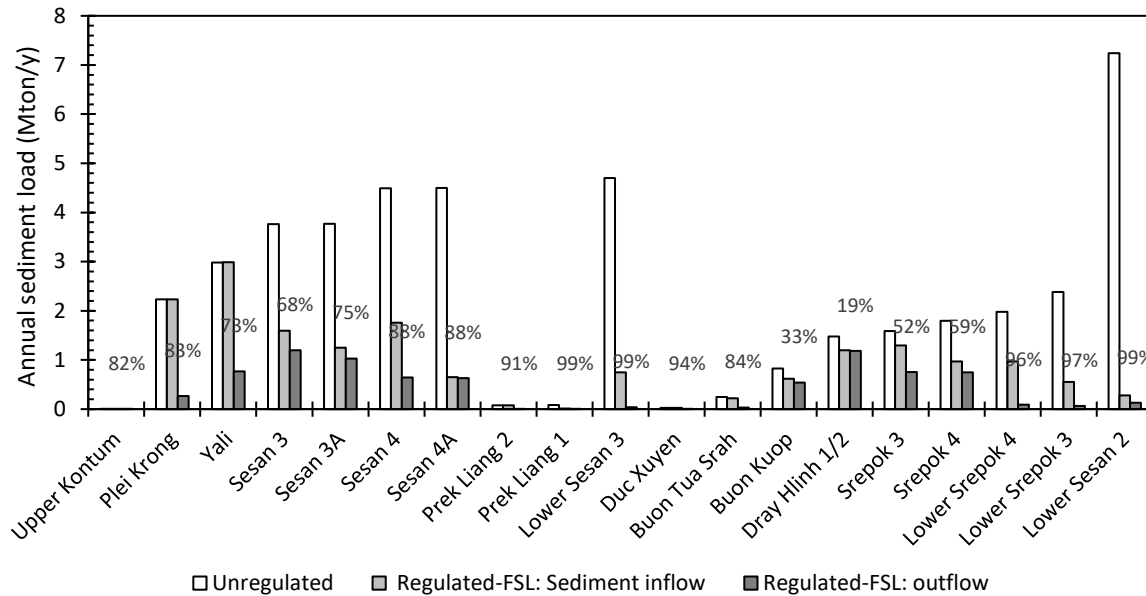


Figure A4-1: Mean annual sediment load in million ton/year (Mt/y) at inlet location of each of the reservoir for the Unregulated scenario and mean annual sediment load (Mt/y) inflow and outflow for the Regulated-FSL scenario: assuming reservoirs are operating under FSL rule curve but not any sediment management techniques have been applied. The change in percentage between the Unregulated sediment load and Regulated-FSL sediment outflow are shown in percentage (%) values.

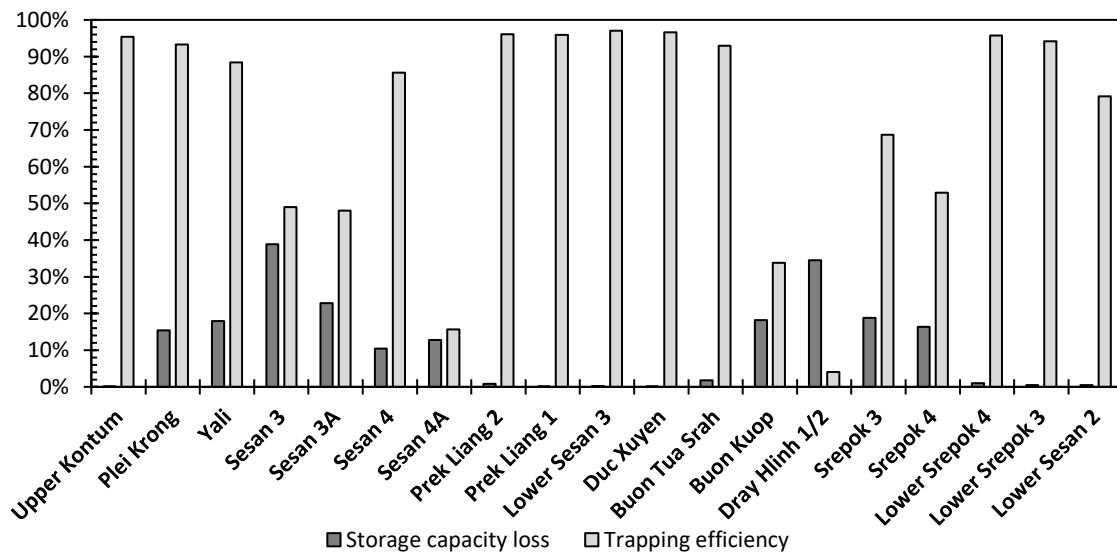


Figure A4-2: Initial storage capacity loss due to sediment deposition after 100 years of operation and average trapping efficiency of the reservoirs under the FSL rule curve.

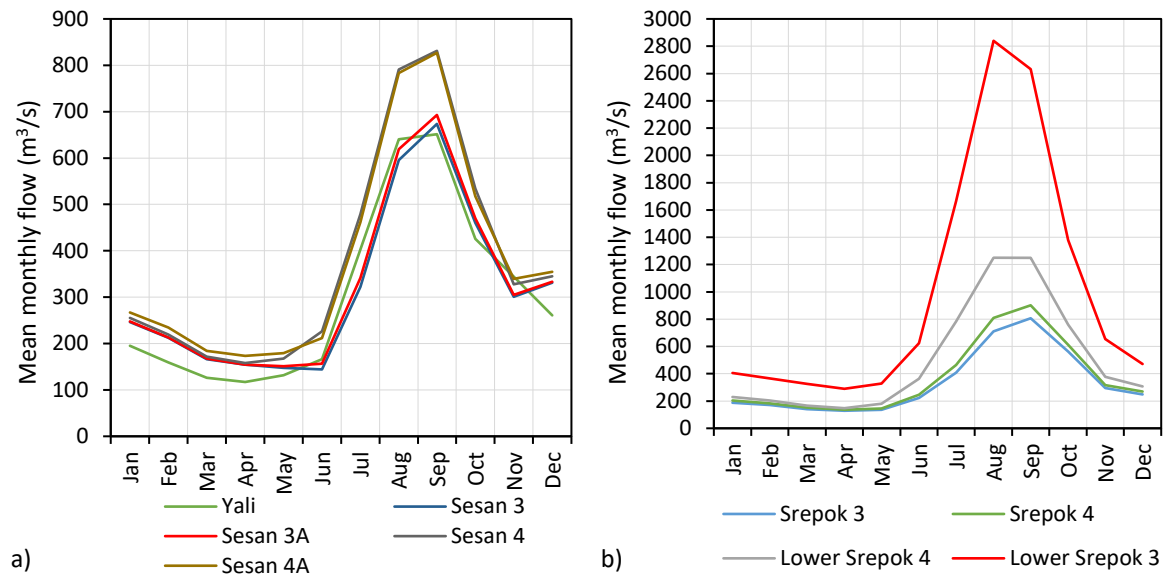


Figure A4-3: Mean monthly inflows to the reservoirs under the SV rule curve for a) Sesan cascade and b) Srepok cascade.